Swaying of trees in relation to wind and forestry practices

Iain G Turnbull

MPhil

1993

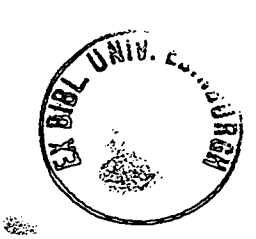

Declaration

I hearby declare that the work described in this thesis is entirely my own unless otherwise stated and that it has not been submitted for any other examination.

Iain Turnbull 31 May 1993

Acknowledgements

I would like to thank everyone who has helped during the period of study which has led to this thesis, particularly my wife who has consistantly encouraged me to continue, especially when writing up, without that encouragement I doubt if this document would ever have been completed. Special mention is also due to John Grace and Ronnie Milne for their invaluable advice and support, and to Morna for her assistance in the field where she sufferred constant abuse from the midges and rain.

Finally, I would like to dedicate this thesis to my parents for all their support throughout the apparently unending period of my university career.

TABLE OF CONTENTS

LIST OF SYMBOLS AND ABBREVIATIONS

Symbols

A	area (m^2)
A_o	basal area (m^2)
a	Galinski's windthrow risk constant (approximately 2.5)
b_i	length of branches in the i^{th} whorl (m)
C	height of winch cable attachment (m)
C_d	aerodynamic drag coefficient
D	diameter (m)
d	zero-plane displacement (m)
d_m	diameter at the mid point of a stem section
$d_{1.3}$	diameter at breast height (1.3 metres above the ground) (m)
E	Young's modulus of elasticity (Pa)
f	frequency (Hz)
F_1	Natural frequency assuming non-linear taper (Hz)
F_2	Natural frequency assuming linear taper and a truncated end (Hz)
F_3	Natural frequency assuming no taper and a concentrated mass (whole crown) (Hz)
F_4	Natural frequency assuming no taper and a concentrated mass (live crown) (Hz)
F_m	Measured natural frequency of tree with branches (Hz)
F_{m1}	Measured natural frequency of tree without branches (Hz)
g	gravitational acceleration ($m\ s^{-2}$)
h	stem height (m)
h_i	height of the i^{th} whorl
I	2^{nd} area moment of inertia (m^4)
I_o	2^{nd} area moment of inertia at the base of the stem/beam (m^4)
i_u	turbulence intensity of the horizontal wind speed
K	coefficient of eddy diffusion ($kg\ m\ s^{-1}$)
k	von Karman's constant (approximately 0.41)
K_m	eddy viscosity ($m^2\ s^{-1}$)
L	average foliage density ($kg\ m^{-3}$)
l	length (m)
M	bending moment ($kg\ m^2\ s^{-2}$)

m	mass (kg)
m_b	mass of the stem/beam (kg)
m_c	mass of the crown (kg)
n	power law factor describing stem shape assuming non-linear taper
P	force (N)
r	radius (m)
r_o	basal radius (m)
s	spring constant (N m^{-1})
$S(f)_{TF}$	mechanical transfer function (m^4 s^4 kg^{-2})
$S(f)_{rr}$	power spectrum of the Reynold's stress (kg^2 m^{-2} s^{-4})
$S(f)_u$	power spectrum of the u component of the wind speed (m^2 s^{-2})
$S(f)_w$	power spectrum of the w component of the wind speed(m^2 s^{-2})
$S(f)_x$	power spectrum of the x coordinate of stem displacement (m^2)
$S(f)_y$	power spectrum of the y coordinate of stem displacement (m^2)
T	height to point of truncation of stem (m)
t	constant describing the linear taper of the stem
u	wind speed (m s^{-1})
$\overline{u}$	mean wind speed (m s^{-1})
u^*	friction velocity (m s^{-1})
u'	instantaneous deviation from $\overline{u}$ (m s^{-1})
V	volume (m^3)
v	cross component of the wind speed (m s^{-1})
$\overline{v}$	mean of the cross component of the wind speed (m s^{-1})
v'	instantaneous deviation from $\overline{v}$ (m s^{-1})
w	vertical component of the wind speed (m s^{-1})
$\overline{w}$	mean vertical wind speed (m s^{-1})
w'	instantaneous deviation from $\overline{w}$ (m s^{-1})
z	height above the ground (m)
z_o	roughness length (m)
λ	taper parameter
λ_1	taper parameter for a non-linearly tapered stem/beam
λ_2	taper parameter for a linearly tapered, truncated stem/beam

μ	stem density (kg m^{-3})
μ_a	air density (kg m^{-3})
μ_1	stem density for complete stem (kg m^{-3})
μ_2	stem density for truncated stem (kg m^{-3})
σ_u	standard deviation of the fluctuating part of the wind speed (m s^{-1})
τ	shearing stress (kg m^{-1} s^{-2})
τ_r	Reynold's stress (kg m^{-1} s^{-2})
π	3.14159
ω	rotational velocity (m s^{-1})

Abbreviations

dbh	diameter at breast height (1.3 m above ground) (m)
o.b. diameter	over-bark stem diameter (m)
u.b. diameter	under-bark stem diameter (m)
PST	position sensing transducer
WHC	Windthrow Hazard Classification

LIST OF TABLES

LIST OF FIGURES

CHAPTER 1 INTRODUCTION

Wind damage occurs in forests throughout the world, in many cases to such an extent that it is of great economic importance to the industry. Forests suffer widespread destruction from exceptionally violent storms, but these events are rare. Recent examples of catastrophic damage include the storms of November 1972 and April 1973, which caused damage to about 7,000 ha of broadleaved woodland and 65,000 ha of conifers in Lower Saxony and surrounding areas of West Germany (Savill 1983). The more recent storm experienced in November 1985 in southern Britain also caused severe damage to many older trees as well as to substantial areas of commercial forest (Grayson 1989). These catastrophic events are clearly of great significance to the industry but little can be done to prevent this damage, due to the very high windspeeds. However, the common 'endemic' windthrow of tall trees is caused by gusts during periods of lower windspeed and is therefore of greater economic importance (Grayson 1989) and it is this area where research has been concentrated.

There may be important links between the canopy shape and stem form, as influenced by silvicultural practices and the turbulent wind structure in the region of the upper canopy. This interaction influences momentum transfer and the dynamic forces acting on individual trees, and also affects the resistive/flexural responses of the trees under wind loading (Miller 1986).

As a result of such events a great deal of research has been carried out in an attempt to clarify the processes involved in the windthrow of trees, and hence, to isolate the major factors causing some trees to be unstable and fall over, while others remain standing, with the general objective of alleviating this problem. The product of this research is a large amount of literature, some of which merely outlines the problems and gives examples of storm damage (Curtis 1943, Holtham 1971, Oliver and Mayhead 1974, Savill 1983, Grayson 1989). Other authors refer to experiments in the field and in wind tunnels which investigate various aspects of windthrow (Day 1950, Fraser 1962a, 1962b, 1964, Landsberg and Thom 1971,

Armstrong *et al* 1976, Boyd and Webb 1981, Cremer *et al* 1982, Blackburn 1986, Gardiner 1989, 1990, Milne 1986, 1990), while others take a more general overview (Savill 1983, Milne 1992). In addition to this, there is much material dealing with the mechanics of structures in general, some of which is relevant to the windthrow problem (Bisshopp and Drucker 1945, Timoshenko and Gere 1961, Coutts 1983, 1986, Putz *et al* 1983, Mayer 1987, 1989, Milne 1991).

This project is involved with both field measurements and mechanical modelling of stem swaying, and the relationship between the wind and how a tree responds to it. The main emphasis is on the forestry aspects of the problem but there is a certain amount of engineering and mechanical theory used in an attempt to quantify some of the processes involved. However, it is intended that the results of such analysis should be applicable to the forest situation which differs greatly from the standard conditions usually applied to theoretical approaches. This introduction primarily looks at the work which has been done in the past relating to forestry aspects of windthrow, including stem form, species choice, establishment techniques and silvicultural management. The following chapter deals specifically with the more theoretical approaches used to look at wind and stem movement.

1.1 Forestry aspects of the problem

1.1.1 Rooting, soils and cultivation

For any slender structure, such as a tree, to be stable it must be firmly anchored in the ground. In the case of trees this is achieved by the roots, and where windthrow is a serious problem it has frequently been shown to be the result of shallow or uneven rooting, in many cases caused by the soil type or cultivation techniques used for establishment (Armstrong *et al* 1976). Therefore, when considering the forestry aspects of tree stability the roots, soil and cultivation methods must be examined at some stage. Some people consider soil conditions to be the most limiting factor with regard to tree stability (Savill 1976).

Pyatt (1970) described the main soil groups of upland forests in Britain with respect to their suitability for planting.

BROWN EARTHS (STABLE)
Frequently the best soils, freely draining.

PODZOLS (STABLE)
Free drainage, good conditions for rooting.

IRON PAN SOILS (POOR STABILITY)
Peaty accumulation and mineral horizons above the iron pan are often waterlogged and anaerobic.

SURFACE WATER GLEYS (POOR STABILITY)
Seasonal perched water-table, anaerobic upper layer in wet periods.

GROUND WATER GLEYS (POOR STABILITY)
Permanent high water-table.

DEEP PEATS (POOR STABILITY)
Require intensive drainage for stability.

It is difficult to rank soils in terms of tree stability in any way as they vary so much from site to site. However, in Ireland surface water gleys are commonly thought to be the most vulnerable to windthrow (Hendrick 1986), while in Canterbury, New Zealand, frequently-saturated shingle soils (15-36 cm deep) are considered very susceptible (Prior 1959). Regardless of which soil group is being considered, there are certain physical features of the soil which will determine its strength, and hence, how stable a tree crop might be if grown on it, due mainly to the root structure able to develop. Pyatt (1970) went on to describe these features

HIGH BULK DENSITIES
As density increases so does root growth, up to a limit.

VARIABLE NUTRIENT LEVELS
Roots near nutrient accumulations grow well, but less favoured ones suffer.

WATERLOGGING
Few tree species have roots which can tolerate the anaerobic conditions associated with waterlogging.

Having looked briefly at the soil groups in question and the important aspects of these soils, it is now worth considering how roots prevent a tree from falling over, and what form of rooting is most likely to be successful. Very little has been definitely resolved in any quantitative manner. Most of the literature deals in a descriptive way with the habits and functions of tree roots.

The important components of root anchorage can be separated into the dimensions and mass of the root-soil plate levered from the ground by the displaced stem; soil resistance; the resistance of the roots under tension on the windward side of the tree; and, the resistance to bending at the hinge on the leeward side of the tree (Coutts 1983, 1986). Thus, safety in anchorage can be considered as a mechanical matter determined by the resistance at the root-soil interface to the force which is transmitted to the roots from the crown (Day 1950). This latter point suggests that windthrow will be more serious on shallow soils as there will be less root-soil interface.

The root-plate oscillates continuously throughout the life of a tree, accumulating damage in the process. This will eventually lead to soil breakage resulting in a reduction in the resistance to bending, which in turn leads to a greater amount of sway, and hence, more damage to the root system, and so on until the tree falls over (Blackburn 1986). This idea has lead to the 'critical rooting density' concept of Coutts (1983, 1986) which is defined as the point at which root development is such that root resistance is greater than soil strength, hence, if the tree is to fall over failure of the soil is necessary (Figure 1.1).

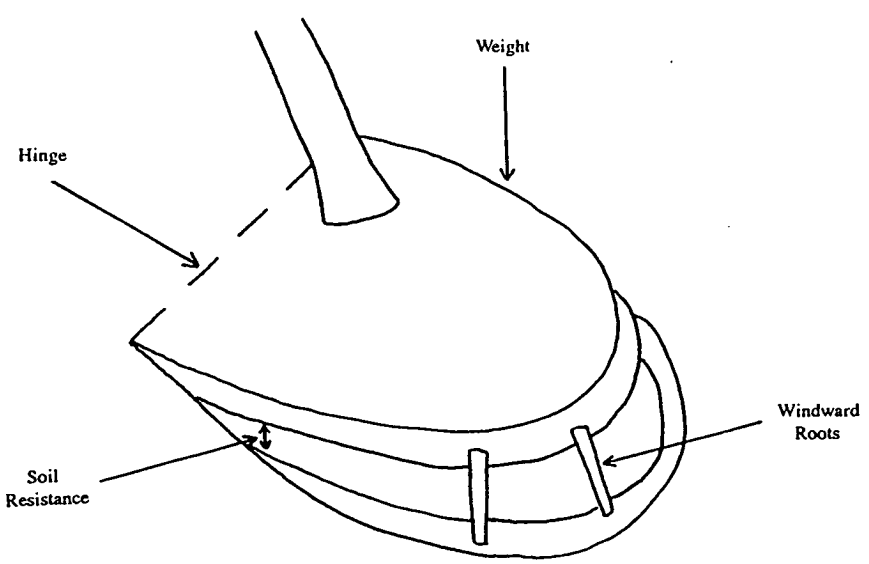

Figure 1.1 Diagrammatic view of a shallowly rooted tree showing four components of the anchorage which resist the horizontal force acting on the stem
viz. the weight of the root-soil plate, resistance of the soil to mainly tensile failure, resistance of the roots placed under tension on the windward side of the tree, and resistance to bending at the hinge. (Blackwell *et al* 1990)

Returning to the subject of cultivation and drainage, it is necessary to use some form of ground preparation to establish a forest successfully on upland sites (Savill 1976), but this can have serious effects on the stability of the crop in its later life. The main reason why cultivation is needed is that establishment requires dry conditions and most upland soils are unstable for forests due to fluctuating water-tables or permanent high water-tables, which lead to anaerobic conditions and the death of the deeper roots. This can also occur at the growing point of pine roots near an ironpan, causing a flattened root-plate which is less stable (Goss 1960). There have been various techniques of ploughing and drainage used in the past to overcome this problem of waterlogged sites. Changes in cultivation have recently been suggested aiming more at stability of the crop than at maximising stocking density, as was the priority in the past. The main problem caused by ploughing is that trees are planted on the ridges, and the furrows are frequently full of water. Hence, the roots fail to cross the furrows to interlink with those of neighbouring trees, and in some cases the simple physical shape of the furrow may impede root growth. Where roots encounter furrows or ditches they tend to fork with a proportional loss of diameter. Therefore, few thick roots will cross such ditches (Deans 1983). This leads to an asymmetric development of the root-plate, aligned along the ridge which makes the trees susceptible to windthrow (Hendrick 1986).

In the past in the British Isles turf planting was used with four lines of trees between the ditches which were produced by digging the turfs. Thus, some root linkage was possible between ditches. However, spaced furrow ploughing is used more now, so only one or two lines of trees can be planted between the furrows (depending on whether single- or double-mouldboard ploughing is used) (Savill 1976, Thompson 1984). The result is a reduction in stability of the older trees (Figure 1.2). In Ireland mole drainage has been used since 1971 and has reduced this problem slightly due to a reduction in the water-table, and hence, more roots are able to cross the furrows (Hendrick 1986). Therefore, drainage clearly offers some respite from this problem, but the extent to which drains will lower the water-table is very dependent on the soil type. For example, rooting depth of Sitka spruce on surface water gleys is unlikely to be increased to any great extent

by intensive deep drainage due to the small particle size of the soil (Savill 1976).

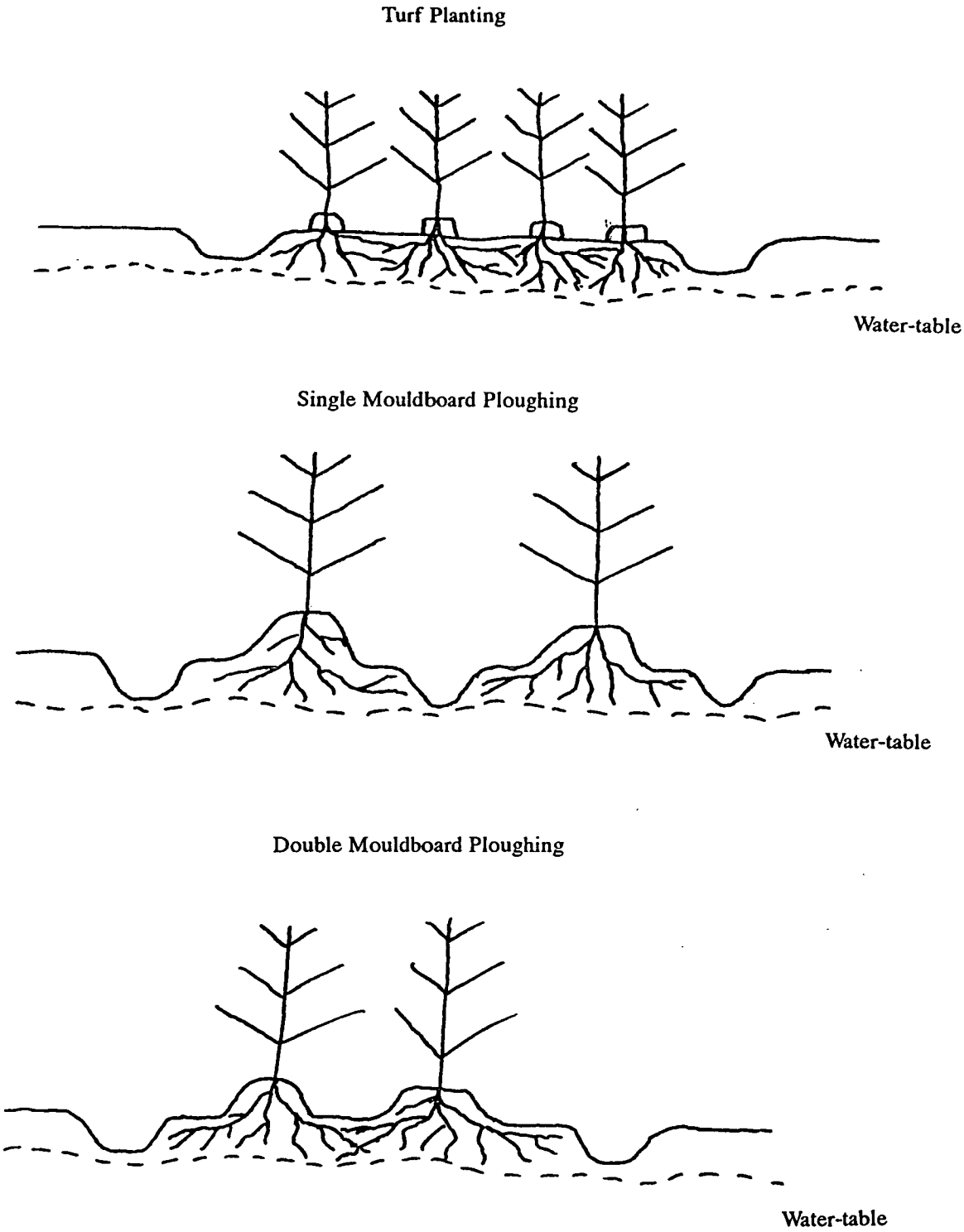

Figure 1.2 Schematic diagram illustrating some forms of cultivation used to establish commercial forests and their effects on the root system

The current recommendations for establishing trees on such sites are, the creation of a weed-free planting site on imperfectly drained soils (i.e. ploughing with planting on the ridge); and for impeded drainage, ploughing with soil disturbance to, or beyond, 60 cm depth to induce water movement from the upper layers. However, these recommendations may improve establishment but they also severely restrict root development. So it has been suggested that wider spacings, or even a return to turf planting should be adopted on soils such as gleys (Savill 1976), which would result in a greater number of roots linking up with their neighbours, and a more symmetrical development of the root-plate.

1.1.2 Planting spacing, thinning and forest design

It is commonly thought that thinning a stand of Sitka spruce planted at about 2 m spacing is likely to cause a severe risk of windthrow on upland sites in Britain. Some research has been carried out looking at the reasons behind this theory, resulting in some ideas about the mechanics of the process. Trees in a newly thinned stand will sway more because of reduced damping in the crown due to the space which the thinning has created (White, White and Mayhead 1976, Milne 1991). Also the rate of diameter increment will increase in the trees, leading to the timber in the outer layers being less dense. A similar situation can be seen in trees grown at wider spacings, in that the timber density is lower, knot size is greater and the volume of 'juvenile core' (weak timber) is increased. Therefore, the modulus of elasticity (resistance to bending, described in more detail in Chapter 2) drops and swaying increases (Blackburn 1986). Jacobs (1954) also pointed out that the swaying tended to be greater in a heavily thinned stand. In New Zealand there have been reports of an increase in the risk of windthrow after heavy thinning of *Pinus radiata* (Cremer *et al* 1982). As a result of this increased risk it has been suggested by some (Day 1950) that where windthrow is likely, thinning practice should favour deep crowns and irregular canopies, while others think smoother canopies would reduce momentum transfer to the trees from the wind, and hence, reduce the damage (Mayhead *et al* 1975).

In the case of choosing a suitable planting spacing, or stocking density, maximising timber production has always been the priority. However, now we are beginning to consider alternative objectives for a variety of reasons including stability. Cremer *et al* (1982) showed that for *P. radiata* in New Zealand, except on sites where root growth was severely restricted, plantations raised at lower stocking rates generally experienced less wind damage. Thus, they suggested that trees should be given as much space to grow in as economics will allow, from as early an age as possible.

Mayhead *et al* (1975) calculated that on unstable soils a symmetrical root-plate of at least 2.5 m diameter is required for a 16 m tall tree to stand up in a lightly thinned crop. Deans (1983) assumed this relationship to be linear and predicted that a symmetrical root-plate of 3.6 m diameter would be required to support a tree of sawlog dimensions. This would mean that all trees would have to be planted at least 1.8 m from the nearest ditch or furrow on a spaced furrow scheme. If this relationship holds true for larger trees such as this, present cultivation and drainage practices would need to be drastically altered for such spacings to be implemented.

Forest design and treatment of forest margins are also of interest when considering wind damage. It is noticeable that when damage occurs in a stand it is usually concentrated in the middle, with the edges remaining fairly well intact. This is thought to be due to these edge trees being 'acclimatized' to the wind exposure, and therefore being more resistant. However, Fraser (1964) showed in the wind tunnel that there was an area in the centre of a model stand which experienced greater force from the wind as a result of small scale turbulence. He went on to investigate the effect of various margin designs (heavily thinned, dense, wedge shaped and convex into the wind), plus the effect of roads or an irregular structure, with the aim of streamlining the forest. The result was that all the margins (except the convex one) reduced, or eliminated the zone of greater force. Fraser (1964) concluded that no roads should cut exposed edges, or bend abruptly, or end after long runs in one direction. The irregular structure also removed the

zone of high forces, but it did produce some points throughout the forest which experienced even higher forces.

More recently Priest *et al* (1991) reported signs of windblow in Kielder forest, Northumberland, where Sitka spruce trees had been planted on the lee-side of old stumps. These old stumps appeared to be curtailing the development of new roots. This is obviously an important feature as we move into an era of second rotation forestry in Britain.

Neckelmann (1986) also looked at the treatment of recent internal edges in Denmark. The effects of removing tree tops and high pruning were looked at as methods of reducing turbulence. Topping resulted in a gradually rising edge up to canopy height. This was very effective in terms of reducing turbulence, but the topped trees tended to die within one to two years of being topped. However, the high pruned stand margins, which allowed more wind to penetrate the stand, had a similar effect but the trees remained alive if the top 20% of the stem was left untouched.

Therefore, it appears that high pruning of margins to allow more wind into the stand should reduce the risk of wind damage in the remainder of the forest. However, regardless of the edge treatment, areas of restricted rooting should be avoided for internal edges. It is clear that by increasing spacings, reducing thinning intensities, and by treating forest margins and internal edges more intensively the risk of windthrow should be reduced in our forests.

1.1.3 Species selection

Species selection also has an impact on the stability of a forest, in that on wet sites certain species are more stable than others. In a November storm in 1982 in Central France, about 12 million hectares of Norway spruce and Scots pine fell, but Douglas fir and larch were very resistant (Bouchon 1986). Goss (1960) had earlier stated that larch was more resistant to windthrow than some other species because of the adventitious nature of its roots and its deciduous character. Thus

the root-plate of larch is generally wider, and less energy is transferred from the wind to the trees due to the lack of foliage in winter.

It is possible that careful choice of species, or even the adoption of intricate mixtures, or self-thinning mixtures, might alleviate the windthrow problem somewhat. If larch is used in a mixture the other trees will be exposed to more wind during the winter, and thus might develop greater resistance. Neckelmann (1986) proposed that the use of more stable species at the edge of the forest might also reduce damage to some extent. However, very little work has been done on variations in species and the use of mixtures in relation to tree stability.

1.1.4 Tree form and stability

One important aspect of tree stability not yet discussed is that of the relative resistance to windthrow of the various forms of stem and crown which can be found in a forest plantation. There are a number of attributes of a tree which might be expected to influence its stability by affecting the absorption of energy from the wind, or by regulating the sway period or amplitude. Such characteristics include crown size and density, stem taper, stem diameter and flexibility, tree height, and buttress or root collar development.

Firstly, the crown of a tree obviously determines how much energy is transferred to the stem from the wind. Curtis (1943) explained that open crowned trees often escaped wind damage, and described the length of green crown in relation to total height of a tree as being a very important factor of stability. Takahashi and Wakabayashi (1981) also stated that in larger crowns non-synchronous motion of the branches would cancel out the bending moment arising from other branches to some extent, thus producing a smaller bending moment on the stem. This would suggest that larger crowned trees are more stable, but they will also exert more drag on the wind, so perhaps some compromise is required.

One of the most useful indices for risk of damage for a tree is the height to diameter at breast height ratio (height:dbh) (Cremer *et al* 1982). The smaller this parameter is the more stable the tree (Holbo *et al* 1980), i.e. short fat trees are

more stable than tall slender ones. Reduced stocking will lead to a smaller height:dbh ratio and should therefore improve stability. Kuiper (1986) found a good correlation between maximum turning moment and stem volume and growing space for Douglas fir. The maximum turning moment occurs at the instant of overturning of the stem. Blackburn (1986) also derived a good relationship between maximum turning moment and dbh^3, and went on to say that if the correct regression coefficient for soil type was known, then the maximum turning moment could be determined for any tree from its dbh measurement.

Of course swaying is not only affected by stem form, but also affects stem form (Jacobs 1954). Swaying results in an increase in diameter growth at the point of anchorage, and a similar increase in diameter of the roots near the trunk, as well as eccentric stem development along the line of the main winds (Jacobs 1954). Thus trees which are exposed to swaying from an early stage of development will develop accordingly and are likely to be more suited to windy conditions.

Petty and Swain (1985) described conifer stems of paraboloidal form as bending along curves which produce uniform strain in the outer wood. However, the bending of the stem is strongly influenced by taper. A tapered stem deflects more, which reduces the moment arm and thus lowers the maximum stress in a tapered stem (Leiser and Kemper 1973). Generally trees with larger crowns are more heavily tapered, and exposure to wind causes a shift of growth increment towards the base of the stem (Larson 1965), so wider spaced trees should be more stable.

From a mechanical point of view the optimum structural member is one in which there is the most uniform distribution of stress. From a biological viewpoint stress should however be distributed uniformly in the region of the stem where wood development is most advanced, i.e. at the base of the stem (Leiser and Kemper 1973). The resistance to bending depends on the modulus of elasticity of the wood (E), discussed in the following chapter, and the tree diameter and taper, so open grown trees will offer less resistance to swaying because of their greater degree of taper and their less dense wood. Hence, the force on the upper parts will be less,

with more force being concentrated at the base (Blackburn 1986).

So generally, trees with low height:dbh ratios and a large degree of taper and large crowns should be more stable, in that the force exerted on the root-plate will be less than that exerted by a densely grown, slender stem. This might offer a basis for some ideas for improving the stability of our forests, but as always other factors, such as economics, are important too.

1.2 Current ideas for reducing wind damage

When considering methods of alleviating the problem of wind damage it is first necessary to classify the forest area in relation to the risk of windthrow occurring. For windfirm sites standard silvicultural practices are acceptable, but on areas of greater risk alterations need to be made. Fraser (1965) stated that the onset of windthrow on wet or poorly drained soils is often associated with a slowing down of height increment in the trees due to death or damage of roots, and an increase in exposure of the remaining trees after some have fallen. This idea is useful in predicting when to clear any given area at risk, but the Forestry Commission's Windthrow Hazard Classification (WHC) (Booth 1977, Miller 1985) is perhaps the best, and certainly the most commonly used technique currently available of classifying areas at risk in Britain.

The WHC is based on the risk of damage being closely related to the following features of the site:

1. Windiness of the regional climate;
2. Elevation;
3. Topography;
4. Soil conditions.

However useful this system might be, it does have some limitations in that it is only really workable over large areas (about 500 ha or more), so no great resolution or accuracy of risk is possible. Also, the original data-base was derived from out-dated silvicultural practices, so relationships may not be valid for today's systems (Miller 1985).

Therefore it is necessary for more research to be done on the effects of wider spacings, pre-commercial thinning and chemical thinning, and various alternative forms of ground preparation, along with a more detailed study of site features to improve the accuracy of the WHC system.

Another method of estimating windthrow risk has been developed in Poland by Galinski (1989) using stem bending theory. Galinski has produced a formula which produces a risk index from tree height, length of branches and dbh

$$R = [\, b_i h_i^{[-a(1-hi/h)]}]/d_{1.3} \qquad (1.1)$$

where, R = risk index

b_i = length of branches in the i^{th} whorl (m)

h_i = height of the i^{th} whorl (m)

h = height of the stem (m)

$d_{1.3}$ = diameter at breast height (1.3 m) (m)

a = constant (approx. 2.5)

This process lends itself to practical use and could be very helpful in comparing the effects of different silvicultural techniques on the risk of wind damage. However, due to the intensity of survey work which would be required to classify any area by this method it is unlikely to have a very widespread use except for experimental purposes, such as the effects of different spacings, thinning and forest design on the risk of wind damage for an area.

Papesch (1983) listed some possible ways to reduce wind damage, which included:

1. Improved ground preparation;
2. Improved rooting qualities of the planting stock;
3. Altering spacing, pruning and thinning practices;
4. Improved forest design, including species selection, harvesting coupes and road construction;
5. Improved classification of risk.

Kuiper (1986) proposed an alternative approach using a mixture of 'plus trees' for

timber quality, and stability trees. The stability trees should be given space to develop large stems with low height:dbh ratios and optimal rooting, and thus provide a backbone for the 'plus trees' which would eventually form the main timber crop.

Most of the above ideas concentrate on reducing wind turbulence or swaying of the trees, but cultivation should also offer some ways of increasing stability, or reducing risk. Deep drainage is unlikely to help rooting much on surface water gleys, which form the majority of British forest soils, due to the small particle size, so we should concentrate on developing more widely spaced root systems (Savill 1976). Ploughing developments should be aimed at increasing the space between ditches or furrows, or removing these obstructions completely (Thompson 1984). Until then single mouldboard ploughing should be replaced by double mouldboard or turf planting on susceptible sites (Savill 1976).

By the use of thinning and spacing it is possible to alter the damping ratios, drag coefficients, sway periods, crown areas, and size of the trees in a forest, and thus it should be possible to reduce the risk of wind damage. Management should allow thinning of firm areas with risk areas left unthinned or selectively thinned to maintain smooth canopy profiles (Papesch 1974).

Mergen (1954) suggested three major ways to protect trees against the stress applied by the wind:

1. Modifying the distribution of the wind, by special treatment of the forest edges;
2. Improving anchorage, by drainage or cultivation and spacing improvements;
3. Altering the shape and size of the crown, by selecting the best spacing.

Thus there is potential for reducing the risk of damage to our forests from wind, most of which is based on more careful and slightly more intensive management techniques, but more research is required on the responses of the trees to different cultivation systems and thinning regimes with respect to swaying and stability. This work concentrates on the sway response of the trees to the wind, the natural frequency of the stems and their resistance to bending. Various models were used

to attempt a prediction of the natural sway period of the trees according to their physical characteristics, and spectral analysis techniques were applied to investigate the dynamic response of the trees to the wind. These areas of research are described in detail in the following chapters and are discussed in relation to windthrow risk in the final chapter which attempts to put the results into a silvicultural context.

1.3 Aims of this study

The objectives of this work were two-fold. Firstly, it was intended to simultaneously measure wind speed above the canopy of a Sitka spruce (*Picea sitchensis* (Bong.) Carr) plantation and the stem displacement of constituent trees. From this it was intended to investigate the dynamic processes involved in tree sway. The second major aim was to attempt to estimate the natural sway period of trees in the same plantation of Sitka spruce, using a variety of models which incorporate the physical features of the trees. It was intended to carry out both of the above objectives in a range of different plots covering a variety of spacings and thinning regimes. However, due to lack of time it was only possible to look at two plots, one unthinned and the other thinned.

From these measurements and calculations it was considered that some light could be shed on the problems involved in windthrow of trees. At worst, if no actual definite conclusions could be drawn as how best to reduce this problem then at least some techniques by which further investigation could be carried out would be possible.

It was understood that this work would involve using various theoretical approaches to estimating natural frequency of beams of similar shape to tree stems and that a number of engineering and mathematical concepts would be employed in the analysis of the data collected. However, it was not felt that it was the place for this work to undertake to derive these theorems from first principles as those used are readily accepted in the engineering fraternity as being applicable to

cantilever beams satisfying certain conditions. The formulae used were chosen because they applied to beams which were the most similar to tree stems in external appearance, and it was felt un-necessary to develop new formulae which might take into consideration the more complex nature of the wood which formed the tree stems. Therefore, it was the intention of this work to use commonly accepted engineering formulae and analytical techniques, as explained in the following chapters, to attempt to throw some light on the dynamic nature of tree sway and the processes involved in windthrow.

1.4 Methodology

The methods used in this work are given in the following chapters, with chapter 2 concentrating on all the theoretical background. It might, however, be useful to briefly draw attention to some of the major forms of measurement and analysis used. To look at the dynamic response of trees to stimulation by wind, the wind speed was measured about 1 m above the canopy using a 3-dimensional anemometer, while the stem movement was measured using two position sensing transducers situated at 90° to each other. These instruments were all linked to a data logger which dumped the results onto tape cassette as required. The main form of analysis used was spectral analysis (Chatfield 1984, Stull 1989) to produce a mechanical transfer function (Mayer 1987,1989) between the turbulent component of the wind and the resultant stem displacement.

With regard to the estimation of natural frequency a number of physical characteristics were simply measured in the field from a number of sample trees. In addition to this the stems were bent by a winch and the displacement and force were recorded. By this method the spring constant (s) was determined, which was subsequently used to determine Young's modulus of elasticity (E). The stem shape was measured, stem mass and crown mass were measured in 1 m sections up the stem. From these measurements the natural frequency was estimated using three models (Blevins 1979) and compared with measurements of actual natural sway period taken in the field.

1.5 The site

One site was used for fieldwork in this study. The forest was located off the A74 road, three miles north of Moffat (NT 018048, Figure 1.3). It belongs to and is managed by the Forestry Commission (now Forest Enterprise) and the two stands which were used were planted in 1963 with Sitka spruce at approximately 1.6 m spacing on a spaced furrow basis. One of the plots was unthinned and had undergone no silvicultural management while the other plot had been thinned in 1983 with one in three trees being removed. The two plots were separated by a track and the sample trees were about 200 m apart. The unthinned plot was located on a slightly steeper slope than the thinned plot and was also better drained. The soil was a peaty podzol with tendencies towards ground water gleying in the thinned plot where the organic layer was thicker. Some drainage work had been carried out but this was irregular throughout the area.

There was a Hiway Walk-Up Tower in the unthinned plot (16 m high) which was used to attach instruments for the wind and tree sway measurements described above. In the thinned plot this was replaced by a hydraulic mast (15 m high) which simply held the anemometer. The position-sensing transducers were mounted on separate poles (Chapter 4). Diagrams showing the positions of the eleven sample trees with respect to their immediate neighbours are given in Appendix I. The distance to each neighbouring tree and its diameter at breast height (dbh) was measured to provide some picture of the relative space in which each tree had to sway.

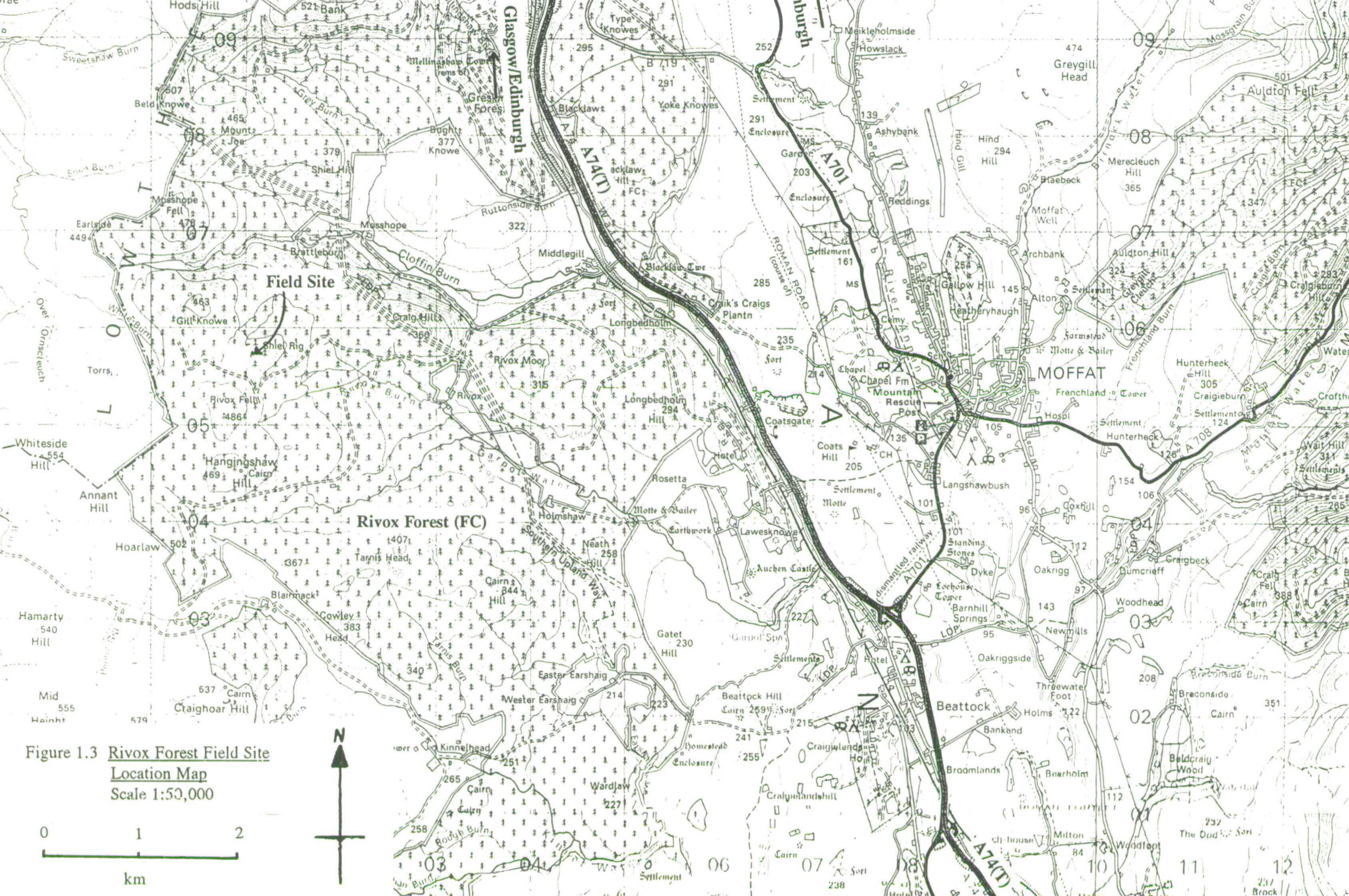

Figure 1.3 Rivox Forest Field Site Location Map

Scale 1:50,000

CHAPTER 2 THEORETICAL BACKGROUND

This chapter explains briefly the analysis of wind speed with respect to turbulent transfer of momentum to surfaces and how this relates to trees and stem bending. A description of various techniques which quantify the dynamic processes involved is also made, concentrating on those which are subsequently used for this work.

2.1 Classical Micrometeorology

The classical approach to the analysis of wind speed in relation to turbulent transfer of entities such as heat, mass and momentum to vegetation surfaces was developed during the 1960's and relies on certain conditions and assumptions being met. The most important condition is that the crop is uniform and sufficiently extensive to allow the turbulent airflow to become completely adjusted to the roughness of the vegetation and the influence of any geographical or morphological sinks or sources of energy. A second condition is that observations are made over a suitably long time interval, typically 30 minutes, so that a large sample of individual events are averaged out, and the net process can be regarded as diffusion, analogous to molecular diffusion, but involving movement of air parcels instead of molecules. This type of transfer of entities is called turbulent diffusion, and the flux of the entity is proportional to the concentration gradient.

$$F = -K.\mathrm{d} \quad /\mathrm{d}z \tag{2.1}$$

where F is the flux, d /dz is the vertical concentration gradient and K is known as the coefficient of eddy diffusion. The meaning of these terms depends on the entity being considered, but the K has the same units, reflecting the fact that all entities, momentum, water, carbon dioxide and heat, are transferred between vegetation and the atmosphere in the same parcels of air, and in proportion to the gradient of concentration of that entity.

In order to relate this equation to momentum transfer in a practical way some information about the wind speed is required. It has frequently been observed that mean horizontal wind speed increases with height above the ground in a logarithmic fashion, and such data can be represented by

$$u_z = (u_*/k)\ln[(z-d)/z_o] \qquad (2.2)$$

where u_z is the mean horizontal wind speed at height z; u_* is the friction velocity which may be regarded as the velocity at which turbulent eddies at the top of the canopy rotate; k is von Karman's constant (approximately 0.41); d is the zero-plane displacement which is a measure of the height of the momentum sink above the ground; and, z_o is the roughness length which describes the effectiveness of the vegetation at absorbing momentum from the wind.

Since there are three unknowns (u_*, d and z_o) some iteration of d around its expected value of 0.6 - 0.7h (where h is the vegetational height) is required (Legg *et al.* 1981) and plotting $\ln(z-d)$ against u_z at each iteration until the graph becomes a straight line (Figure 2.1).

$$\ln(z-d) = k/u_*(u_z) + \ln z_o \qquad (2.3)$$

The slope of this line gives an estimate of (k/u_*) and therefore of u_*, while the intercept ($\ln z_o$) gives the roughness length z_o. Values of d and z_o have been determined on a large number of occasions and empirical relationships relating these to canopy height (h) have been suggested. For a wide variety of crops, d falls in the range 0.6 - 0.7h and z_o is about 0.1h (Legg *et al.* 1981, Grace 1983) (Figure 2.2).

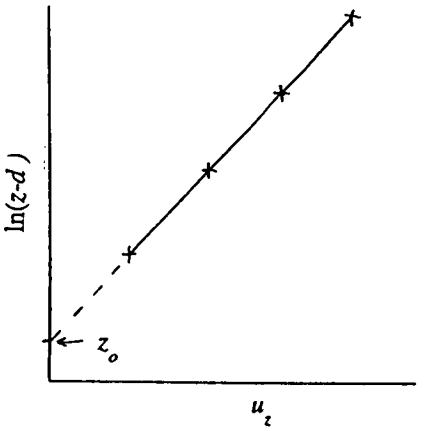

Figure 2.1 Determination of d and z_o using the logarithmic wind speed profile

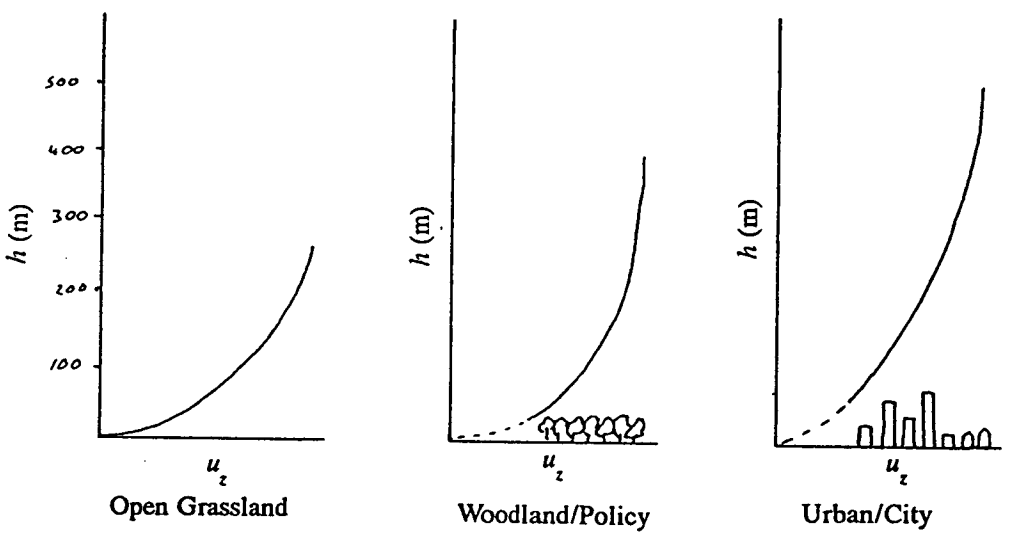

Figure 2.2 Logarithmic wind speed profiles above a variety of surfaces

The determination of d and z_o is very sensitive to measurement errors and a variety of other limitations also apply. The mean wind speeds must be determined over time periods of sufficient length to cover small scale variations in the flow. A large fetch is required to ensure that the air flow has properly developed, Grace (1983) suggests a minimum of 200 m for a logarithmic profile of 1 m depth. The logarithmic profile is only found in conditions of neutral stability. If the air is stable (i.e. air temperature increasing with height) higher wind speeds than

otherwise recorded will occur, and if conditions are unstable (i.e. air temperature rapidly decreases with height) bouyancy results and lower windspeeds will be measured. When the lapse rate of temperature is known it is possible to apply correction factors (Monteith and Unsworth 1990) but these are unreliable for forests.

Equation 2.1 can be used to determine the momentum flux to the surface by using u as the entity (Thom 1975). Thus, the momentum flux can be calculated from

$$\tau = -K_m . \, du/dz \qquad (2.4)$$

K_m is the turbulent transfer coefficient for momentum and can also be determined from u_*

$$K_m = ku_*(z-d) \qquad (2.5)$$

This equation also requires modification when dealing with non-neutral stability conditions.

This classical approach to micrometeorology, known as flux-gradient analysis, helps us to understand *mean* transfer rates of momentum and it has been successfully used for the case of short crops such as grass and for cereals. However, this approach deals only with mean values and tells us nothing about fluctuations in the wind speed pattern. Catastrophic damage to forests may be more closely associated with turbulence and extreme values than with mean wind speeds. Most non-cultivated vegetation does not meet the requirements for this form of analysis and it is therefore impossible to predict accurately what region of the boundary layer is characteristic of the vegetation type. However, the stability correction factors for tall vegetation are not well founded. Finally, turbulent diffusion is really only useful when the eddies are small in relation to the gradient or the distance over which the transfer is being considered. In forests the eddies are usually very large, and a very large part of the momentum, mass and heat that

is transferred can be ascribed to a small number of 'sweeps' of air that penetrate the canopy through gaps (van Gardingen and Grace 1991). So for forests, it is found that the flux gradient approach is limited.

As a result of these limitations various other forms of analysis have been developed to study atmosphere-canopy exchanges in a more fundamental way, assisted by the technological advances in wind speed measurement. In the last ten years attention has been turned away from consideration of mean values, towards the analysis of turbulence. Some of these alternative approaches were used in this work and are therefore described in the following section.

2.2 Fluctuating Winds

With the advent of light-weight propellor anemometers and sonic anemometers, associated with suitable data loggers or signal processing equipment it has become possible to measure rapid fluctuations in wind speed in the field. More importantly, it has also been made possible to resolve the wind speed vector into the three directional components (u, v and w) which correspond to the horizontal streamwise, horizontal lateral and vertical components. As a result of these advances in technology a variety of mathematical approaches can be used to look at the turbulent character of the air flow over vegetation surfaces.

The instantaneous wind speed vector can be split into the three directional components and each of these can then be considered as two parts, a mean part ($\overline{u}$, $\overline{v}$ and $\overline{w}$) and a fluctuating part (u', v' and w') so

$$\begin{aligned} u &= \overline{u} + u' \\ v &= \overline{v} + v' \\ w &= \overline{w} + w' \end{aligned} \qquad (2.6)$$

and a measure of the spread of values obtained is given by the standard deviation of the fluctuating part

$$\sigma_u = \overline{(u'^2)}^{0.5} \qquad (2.7)$$

where $\overline{(u'^2)}$ is the mean of the sum of the squares of all the u' values. From this it is then possible to obtain a measure of, for example, the horizontal turbulence intensity

$$i_u = \sigma_u / \bar{u} \qquad (2.8)$$

This turbulence intensity has been measured inside canopies and usually lies in the range 0.2 - 0.8 for the horizontal components and 0.1 - 0.5 for the vertical component (Cionco 1972, Shaw *et al* 1974, Finnigan 1979). It is possible to relate the profile of turbulence intensity within the canopy to the distribution of the branches and foliage (roughness elements) with some of this turbulence resulting from gusts over the canopy penetrating into the lower layers. Other sources of turbulence may include moving of tree parts, such as branches, and the disturbance of the air flow which this causes.

The turbulence intensity statistic gives no information about the frequency of the fluctuations. In this study it was deemed necessary to study the frequency distribution of wind energy to see how it related to the frequency of swaying of the trees. Power spectra were thus utilised to study the simultaneous fluctuations of the wind and the stem movement. With regard to wind speed the turbulence spectrum can be defined as the relative strengths of different scale eddies, or irregular swirls of motion (Stull 1989). Power spectra are determined from continuous series of measurements of wind speeds using a sensor which responds fast enough to trace the pattern of turbulent flow, using a type of data processing referred to as spectral analysis.

Spectral analysis is essentially concerned with estimating how much of the variation in time series data comes from different frequency bands. This analysis is basically a modification of Fourier analysis to suit random rather than deterministic functions of time. A function is approximated by the sum of sine and cosine terms which describe the time series. This is described in detail in

Chatfield (1984). In effect this form of analysis transfers the time series into the frequency domain producing a series of components corresponding to frequencies which are determined by the length of the original time series and the variability of that series. The longer the time series the greater the number of frequencies which are obtained. The maximum frequency is equivalent to 1/2N, where N is the number of data points in the original time series. This is known as the Nyquist Frequency.

These spectral energies, $S(f)$, characteristically peak at the lower frequencies (Stull 1989) with a decrease as the frequency increases. There are a number of ways of presenting these patterns but in this work a simple linear presentation was used where the frequency range was limited to below 1.0 Hz, as this was the maximum frequency at which the anemometer could be assumed to be accurate. This simple technique of plotting $S(f)$ vs. f produced spectra with peaks corresponding to periodicities for both wind speed and stem displacement.

For a stochastic signal, such as wind speed, the spectra produced is more-or-less similar to Figures 2.4a and 2.4b. However, if there is some cyclical nature to the signal a peak will appear corresponding to the frequency of the cycle (Figures 2.4c and 2.4d).

A useful extension of this analysis was used to convert the spectra of the wind speed components into spectra of the stress exerted by that wind speed on to the trees below. This stress is known as Reynolds stress (τ_r) (simply the drag force described earlier) and is derived from the turbulent components of the horizontal and vertical wind speed vectors

$$\tau_r = -\mu_a \overline{u'.w'} \qquad (2.9)$$

where τ_r is the Reynolds stress, or force acting on the surface, and μ_a is the air density. One assumption in determining τ_r is that the mean lateral component of the wind speed, v, is zero. Therefore, prior to determining τ_r the raw wind speed

data undergoes a coordinate rotation so that the u component faces directly into the mean wind direction.

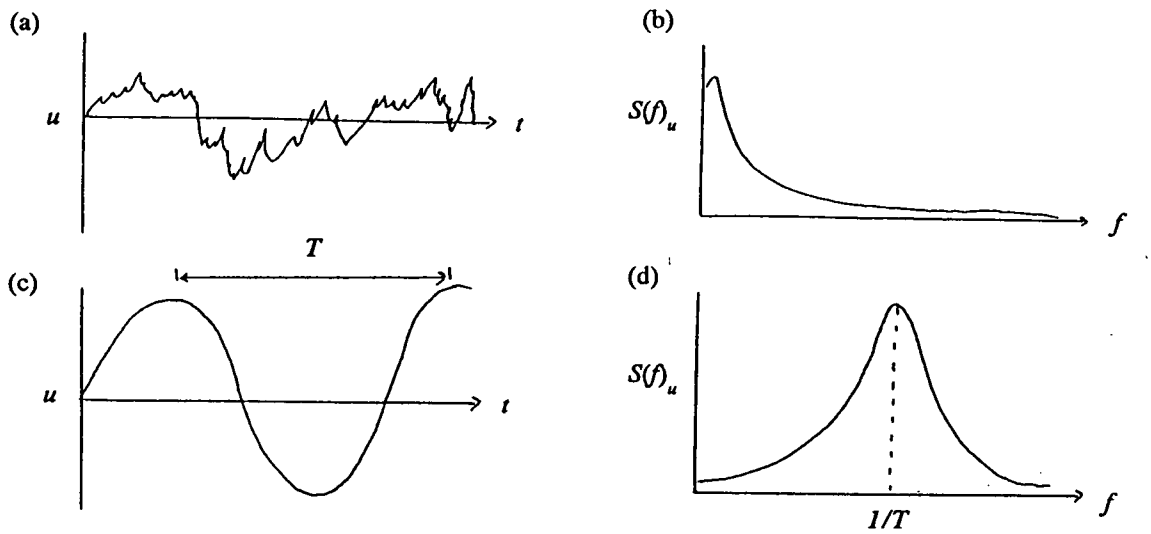

Figure 2.3 Spectral shapes resulting from time series signals

To produce a spectrum for τ_r it is necessary to carry out a cross-spectrum analysis, whereby two time series, u' and w' are used to produce a single frequency domain output of stress. The shape of the spectrum is very similar to that of u or of w.

This spectrum can be used as an input into mechanical transfer function analysis, which is explained later in this chapter (section 2.4), which links the Reynolds stress spectra to the stem displacement spectra. However, before attempting to explain the dynamic processes going on between the trees and the wind it is worth looking briefly at the mechanical nature of trees with respect to stem bending and swaying.

2.3 Stem Swaying

Stem bending under static loading has been looked at by a number of authors (Fraser 1964, Petty and Swain 1985, Milne and Blackburn 1989) and the effects of snow loading have been studied by King and Loucks (1978), Petty and Worrell (1981) and King (1986). These studies have used various methods of determining mechanical parameters of trees, such as Young's modulus of elasticity (E) which can be defined as the resistance to bending of the stemwood. However, in the case of windthrow the damage is normally done by the gusting nature of the wind. Therefore, a dynamic approach is also required when looking at stem bending (Mayhead 1973, Holbo *et al* 1980, Milne 1986, Mayer 1987, Blackburn *et al* 1988, Milne 1991).

A tree stem can be likened to a tapered cantilever beam, and stem sway is a periodic motion which is constantly being affected by variable input of energy from the wind. The most important parameters of a tree stem which relate to its mechanical behaviour while swaying are: its resistance to bending (EI) (dependent on the nature of the wood); its physical shape, described in this case by a variety of equations and the use of a parameter called the 2nd Area Moment of Inertia (I) which varies according to the shape and scale of the horizontal cross-section of the stem; its length, as this will affect its natural frequency which in turn is possibly the most important feature, certainly in the dynamic process of windthrow; and finally, the amount of damping, as this has an effect on how quickly sways will die away and the magnitude of displacement likely to occur.

There are many engineering formulae describing how cantilever beams and similar structures bend and sway including many ways of predicting their natural frequency (Bisshopp and Drucker 1945, MacDonald and Morgan Unpubl., MacMahon and Kronauer 1976, Blevins 1979, Simiu and Scanlan 1986, Thomson 1988). However, these theoretical approaches are based on well accepted engineering principles which assume certain conditions which clearly do not apply to forests. Engineering beams are usually of uniform or predictable form and construction and can therfore easily be modelled mathematically, while tree stems

vary according to their surroundings and a whole range of biological functions. Thus trees are less predictable in form and are therefore not so easy to model or predict. In addition to this is the variable nature of the energy input to the forest system, which is related to wind speed but is also affected to a certain extent by the way trees down-wind of any given point react to the wind and the consequent effect of this reaction upon the wind.

However, these engineering approaches do shed some light on the dynamic processes which are occurring in forests and with some adaptation could perhaps provide good models for use in forests. If we assume that the force applied to a stem is regular then that tree will oscillate in a periodic motion. The frequency of this motion will depend upon the length of the stem, the rigidity of that stem and its shape and composition. The simplest form of periodic motion is Simple Harmonic Motion where the movement is described by equation 2.10.

$$x_t = A\sin \omega t \qquad (2.10)$$

where x_t is the stem displacement at time t, A is the maximum amplitude of the displacement, and ω represents the frequency of the oscillation (Figure 2.5).

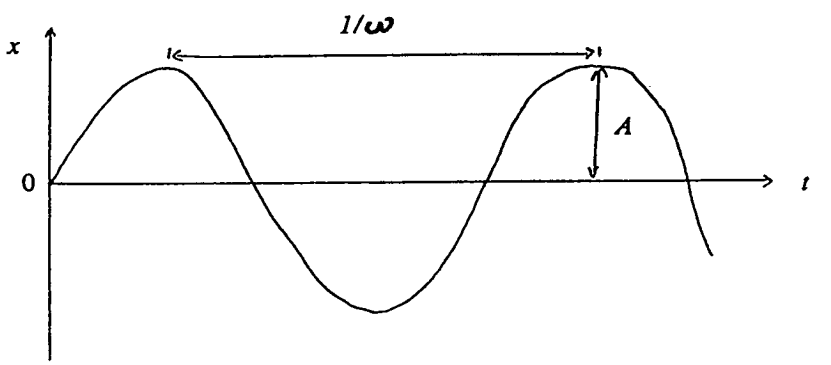

Figure 2.4 Simple Harmonic Motion

The velocity and acceleration of harmonic motion can be simply determined by differentiation of equation 2.10

$$x = A\cos t \qquad (2.11)$$

$$x = -\ ^2A\sin t \qquad (2.12)$$

Motion of structures is generally not this simple and more complex formulae are required to describe it. In many cases there is no obvious periodicity to the motion of a structure but spectral analysis can be used to determine the movement as the sum of many separate periodicities. Stem swaying in the forest situation falls into this category, except over short periods of time where some form of simple periodic swaying is visible, but these events are very short lived. Therefore, spectral analysis was used here to investigate the variations of the stem movement in a Sitka spruce forest. This is explained in more detail in the following section.

Although the dynamic processes are of vital importance here it is essential to understand some of the static responses to applied force in order to be able to attempt to explain why a tree responds dynamically the way it does. As outlined earlier the most important static features of the beam, or tree stem, are its 2nd Area Moment of Inertia (I), and the resistance to bending of the wood (E). I describes the shape of the beam or stem and depends on the horizontal cross-section. In the case of tree stems we will assume that the cross-section is circular and therefore I can be determined by equation 2.13

$$I = \tfrac{1}{4}\pi r^4 \qquad (2.13)$$

where r is the radius of the tree stem of circular cross-section. I is used in the relationship

$$E = sl^3/3I = (F/x)(l^3/3I) \qquad (2.14)$$

where s is the Spring Constant of the tree stem which can be defined as the force (F) required to obtain a given amount of stem bending (x), and l is the length of

the tree stem, i.e. tree height.

Young's modulus is an important parameter as it directly affects the extent of bending which a given force will cause. A number of estimates of E have been made for timber (USDA 1974) and more recently there have been estimates for whole stems or parts of stems or branches (Cannell and Morgan 1987, Blackburn *et al* 1988, Gardiner 1989, Milne and Blackburn 1989). The values for whole stems have been consistently lower than those obtained for dry or green timber, possibly as a result of the presence of bark which is of lower density than the other timber.

The standard engineering technique outlined above for relating E to the spring constant assumes that there is no variation in diameter along the length of the stem and that the stem is of uniform composition. This is clearly not the case for trees and a number of attempts have been made to compensate for the taper which exists in tree stems (Gardiner 1989, Milne 1990). The method used here was that of Gardiner (1989) which is based on equation 2.14 but additional terms are included to allow for stem taper. Gardiner (1989) applied a force to tree stems using a winch and measured the resultant deflection in order to determine the spring constant (s). From this value it is possible to determine E

$$E = (G/B)(sl^3/I_o) \qquad (2.15)$$

where, $G = [1-4n(x/l)^{(3-4n)} - R(3-4n)(x/l)^{(2-4n)} + R(2-4n)(3-4n)(x/l)$
$-(1-4n)(3-4n)(x/l) + (1-4n)(2-4n) - R(1-4n)(3-4n)]$

and, $R = (l - C)/l = x/l$

and, $B = (1-4n)(2-4n)(3-4n)$

and, C = height of cable attachment

I_o = 2nd Area Moment of Inertia at the base of the stem

n = power law factor describing beam taper where,

$y = r_o(x/l)^n \qquad (2.16)$

and, x = distance of cable attachment from the free end of the stem
$= l - C$

There are various forms of damping which all combine to restrict the speed of stem movement. Damping includes inter-crown contact between neighbouring trees, aerodynamic damping caused by the drag effect of the crown moving through the air, and the resistance to movement of the root-soil interface as well as energy absorption within the stem. There is also a physical limit to the extent of movement due to major branches causing obstructions. The complex relationships between all these factors makes it difficult to visualise but there are ways of estimating the total extent of damping occurring in the forest situation, but not to allocate proportions to each of the above sources.

Damping will affect stem swaying through its effect on the extent of stem displacement. Increased damping will restrict the amplitude of displacement due to the slowing of motion from greater crown contact between neighbouring trees as well as the direct reduction of the extent of stem movement. High levels of damping will reduce the risk of large deflections developing and therefore there should be less chance of stem damage or windthrow.

The remaining parameter still to be discussed is the natural frequency of tree stems (f). Any beam or similar structure will vibrate at a given frequency on excitation depending on its composition and size given that it is allowed to vibrate freely. This frequency is known as the natural frequency of the stem or beam. A great deal of work has been done on the natural frequencies of structures by engineers and Blevins (1979) described a wide variety of formulae for predicting the natural frequency of beams of various forms. A tree stem most closely approximates to a tapered cantilever beam anchored at the ground.

Three models were used to estimate natural frequency (f) of trees in a Sitka spruce plantation. Figure 2.7 illustrates the schematic shapes of the model stems used to determine natural frequency.

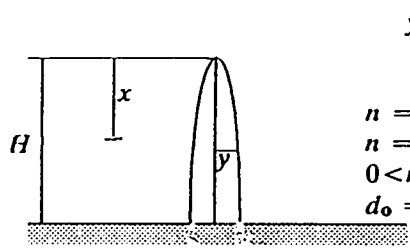

Assumption 1: Non-linear taper

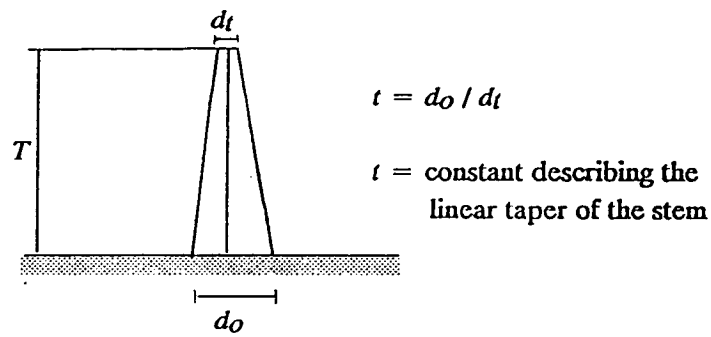

Assumption 2: Linear taper with a truncated end

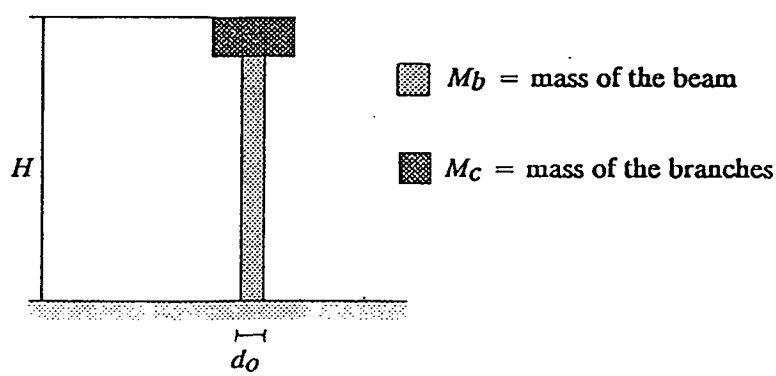

Assumption 3: No taper and a concentrated mass at the free end

Figure 2.5 Stem form models used to determine natural frequency

Model 1

This model assumes that the tree is of uniform composition and has a shape which can be described by the power law function in equation 2.16. There is no allowance for the tree canopy and the mass contained therein and there is no allowance for insecure anchorage in the soil. The parameters required to use this formula are the length of the stem (l), Young's modulus of elasticity (E), the basal 2nd Area Moment of Inertia (I_o), the stem density (μ_l), the stem's basal area (A_o) and the diameter profile of the stem. The last parameter, the diameter profile is used to determine n using equation 2.16. This value of n is then used in conjunction with empirical data relating to n and the stem shape to produce another parameter known as the dimensionless taper parameter (λ_1) (Figure 2.8).

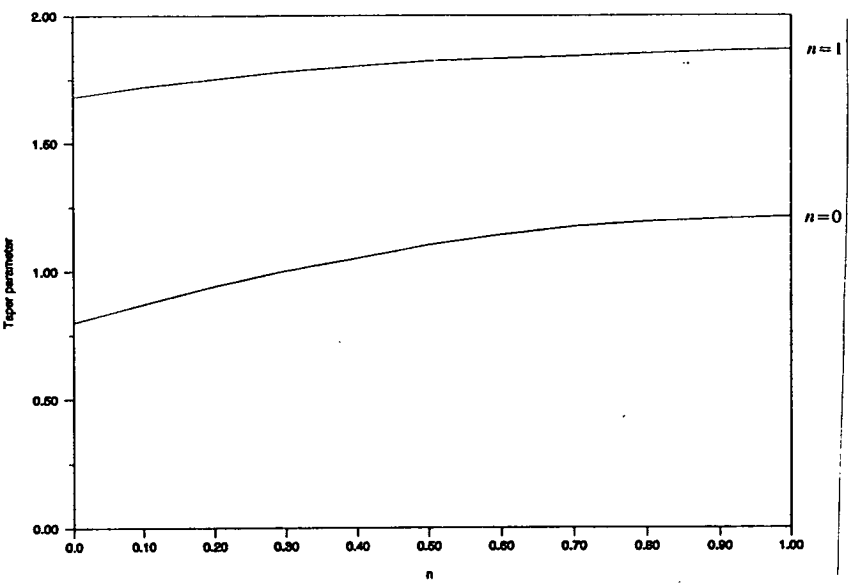

Figure 2.6 Illustration of how λ_1 varies with n for a non-linearly tapered stem

These parameters are combined in equation 2.18 to determine the natural frequency of a stem on non-linear taper

$$F_1 = [\lambda_1^2/(2\pi l^2)][(EI_o)/(\mu_1 A_o)]^{1/2} \qquad (2.18)$$

Model 2

This model uses the same approach as Model 1 but λ_1 is replaced by λ_2 which describes the shape and boundary conditions of a stem of uniform taper which would taper to a point but is truncated at some height, T. This value T replaces l

in equation 2.18. Figure 2.9 illustrates the relationship between λ_2 and the degree of uniform taper which is described by

$$t = d_o/d_t \qquad (2.19)$$

Where d_o is the basal diameter and d_t is the diameter at the truncated end, and equation 2.20 is used to determine frequency (F_2) using Model 2

$$F_2 = [\lambda_2^2/(2\pi T^2)][(EI_o)/(\mu_2 A_o)]^{1/2} \qquad (2.20)$$

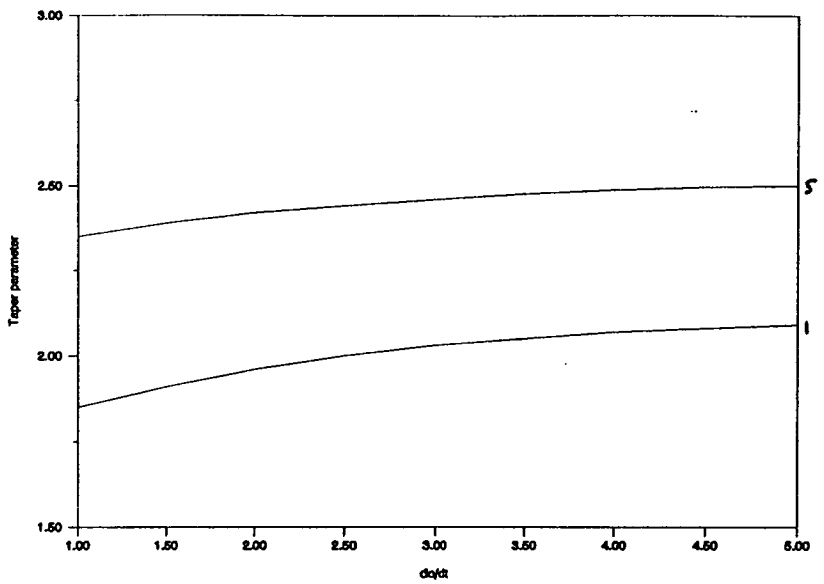

Figure 2.7 Illustration of how λ_2 varies with t for a stem with linear taper

This model assumes that the taper of the stem is better estimated by linear taper and that the top part of the stem has no effect on the natural frequency of the stem but its length would alter the answer coming out of these computations.

Model 3

The third model uses a slightly different approach which attempts to take into account the effect of branch mass on the natural frequency of the stem. This model assumes that the stem does not taper significantly but does apply a given mass to the free end of the stem which corresponds to the mass of the crown. There is no need for a taper parameter but the mass of the stem (m_b) and the crown (m_c) are needed.

$$F_3 = (1/2\pi)[(3EI_o)/(l^3(m_c+0.24m_b))]^{1/2} \quad (2.21)$$

None of these three models takes all the parameters of the tree into consideration and therefore there is likely to be some error in the estimates which result from them. However, in the absence of better models which look more closely at the shape and composition of trees in particular, these models are the most likely to be applicable to tree stems.

The following section details the techniques used to quantify the dynamic processes going on in the forest system and illustrates an attempt to relate the dynamic input from the wind to the equally dynamic output in the form of the stem displacement. The estimates of natural frequency obtained by the methods described above are of relevance to these dynamic processes and will be discussed further at the appropriate time.

2.4 The Mechanical Transfer Function

If simultaneous time series of wind speed (or Reynold's stress) and stem displacement are compared there is usually no clear simple relationship between them, except perhaps over very short time periods where large sways have obviously resulted from large gusts of wind. However, there is clearly some form of dynamic relationship between the wind and stem displacement and one way of describing this is by the use of the mechanical transfer function. This technique has been used recently by Mayer (1987) and Milne (1991) for forest trees with some success, and forms the basis of a large part of this work (Chapter 6).

The mechanical transfer function is based on spectral analysis of the time series of the wind speed and the stem displacement (Figure 2.10)

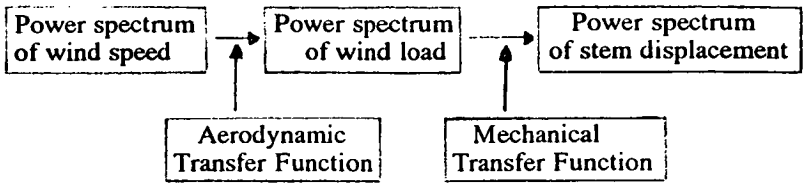

Figure 2.8 Schematic illustration of the transfer function concept (After Mayer 1987)

Power spectra have already been explained with respect to wind speed in section 2.2 and the same calculation is carried out to determine the spectrum of the stem displacement. The aerodynamic transfer function between the wind speed spectrum and the wind load spectrum is simply the calculation of the cross-spectrum of the instantaneous deviations from the mean horizontal and vertical wind speeds, i.e. Reynold's stress as described earlier. The determination of the mechanical transfer function is somewhat different.

To determine the mechanical transfer function the stem displacement spectrum is simply divided by the wind load spectrum (or Reynold's Stress)

$$S(f)_{TF} = S(f)_x / S(f)\tau_r \qquad (2.22)$$

Therefore, the mechanical transfer function is also in the frequency domain and takes the form of a power spectrum (Figure 2.9).

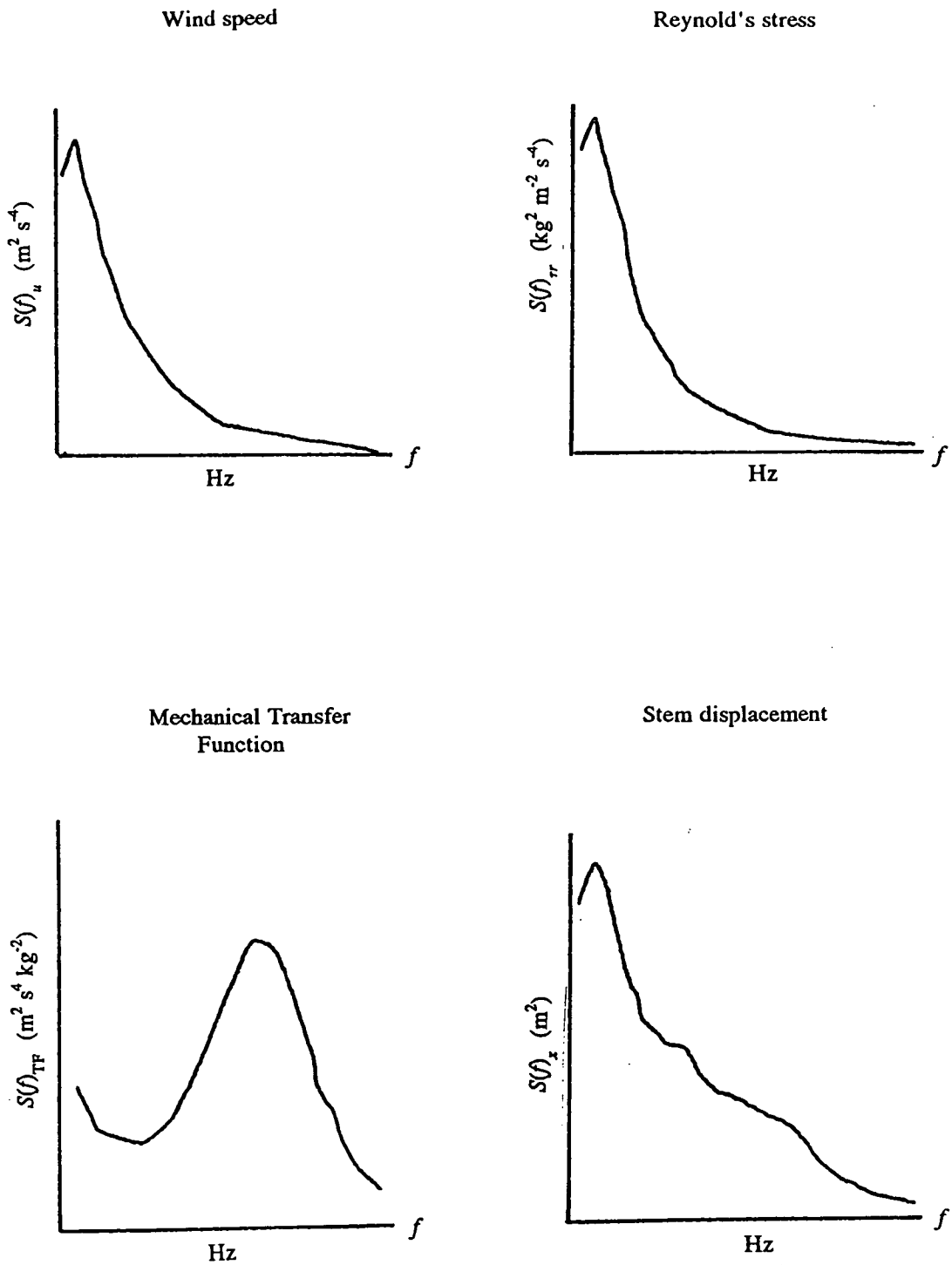

Figure 2.9 Illustration of a mechanical transfer function and its derivation

Certain characteristics of these spectra are of significance here. Firstly, the existence of any peaks which would suggest that the tree will respond more to gusts of wind at that frequency. Thus the position of any peaks over the frequency range is important. Secondly, the height of any peaks on the spectra generally illustrates the efficiency of energy transfer between the two components, i.e. the wind and the trees. The higher the peak, or the greater the area under the spectrum, the greater the energy transfer. And thirdly, the width of any peaks is also important as this illustrates the frequency band over which large deflections might arise from any given wind speed, and can also be used as an indicator of the amount of damping in the system. The broader the peak the greater the damping. The width of a power spectrum peak is measured as the width of the peak at half its maximum amplitude (Stull 1988) in order to apply a standard approach for comparison between spectra.

With respect to trees and windthrow risk these transfer function spectra could be very useful. It is possible to compare the location on the frequency axis of any peaks with the natural frequency of trees as either measured or estimated using the formulae described in the preceding section. This will give us an idea of the likelihood of resonant vibration occurring. The two frequencies should correspond exactly if the tree were in an open location with no neighbouring trees to interrupt its sway. However, in practice this is unlikely, due to damping, which spreads the peak of the spectrum over a wider range of frequencies; and to neighbouring trees interrupting sways part-way through their cycle by banging into the sample tree and therefore giving the impression of a shorter cycle, i.e. raising the frequency of the peak.

This forms the basis of the work carried out here. The measurement methods are described in the following chapters and the results are discussed with a view to explaining the processes involved in windthrow of trees.

CHAPTER 3 STEM FORM

3.1 Introduction

The engineering theory described in Chapter 2 has shown that the period of oscillation of a beam can be calculated from a knowledge of certain physical characteristics of that beam. The relevant beam theory has already been explained in some detail and will therefore not be repeated here, however, some specific details will be given as they are of particular relevance. In this work the theory is applied to the swaying of large trees, with the object of investigating the manner in which variations in the form of the stems, brought about by alterations in silvicultural practice, might influence the sway period and possibly the risk of the tree being blown over.

Estimation of the natural frequency of sway for the stems requires certain assumptions to be made about their structure, as explained in Chapter 2. For the purposes of this work three sets of assumptions were made associated with the three models described in the preceding chapter (Figure 2.5). These models require a knowledge of a variety of physical parameters and this chapter explains the methods used to obtain this physical data and presents that data for use in the subsequent chapters as necessary. The parameters of concern here are the tree height; stem shape and taper; stem density; stem and crown mass; and, some impression of the uniformity of radial and longitudinal growth.

3.2 Methods

The methodology can be split into three stages: the selection of the trees; the measurements taken in the field; and, the measurements taken in the laboratory. The measurement of tree height, diameter, stem and crown mass for Trees 1 to 6 in the unthinned plot, and the stem bending data and swaying data (Chapters 5 and 6) were obtained in collaboration with Dr. R. Milne. All the laboratory measurements for the unthinned plot and all the field and laboratory measurements for the thinned plot were made by the author alone.

3.2.1 Selection of the sample trees

The selection of the trees in the unthinned plot was based on the following criteria:

1. Obtaining a representative range of diameters at breast height (dbh);
2. Straight, unforked stems;
3. Uniform crowns;
4. Ease of measurement and instrumentation.

A range of diameters at breast height (1.3 m above ground level) was required to ensure that variation within the plot was covered, so 180 trees in a block adjacent to the experimental site, which had undergone similar management, were measured to estimate the range of diameters which could be expected over the plot. Straight, unforked stems with uniform crowns were desirable as these trees would provide a better approximation to the engineering beams that the model formulae were designed for. However, there is an argument against this in as much as the sample should be completely representative of the entire plot. Six trees were finally chosen according to these criteria, although the ease of instrumentation was in some cases an over-riding factor.

In the thinned plot a similar preliminary method was adopted which resulted in the selection of 10 trees initially, of which only four were used for measurements. This excess number of trees allowed for any disturbance in the trees, or their neighbours, during the fieldwork. Such a disturbance occurred, for example, when a neighbouring tree blew over and came to rest against one of the 10 originally selected, thus rendering it useless for swaying experiments. Three of the trees studied in this plot were treated as explained below, but the fourth tree was also used to obtain data on wind induced swaying (Chapter 6). This tree was treated in a similar fashion except that no measurements of natural sway period or stem bending using a winch were made as a result of instrument failure. The same applies to Tree 7 which was used for wind induced sway measurements in the unthinned plot.

3.2.2 Field measurements

The following measurements were made in both the unthinned and thinned plots on each of the sample trees, unless otherwise stated.

Each stem was marked off into 1 m sections up to a height of 9 m above the ground. This was done by climbing up the tree and measuring with a tape measure attached to the base of the tree, hence these measurements were only approximate. In the unthinned plot paint was used to mark the stems, while insulating tape was used in the thinned plot and on Tree 7 in the unthinned plot. The trees were split into 1 m sections more accurately after the tree had been felled at the end of the fieldwork. The remainder of the stem above 9 m was also marked off into 1 m sections at this later stage.

The stem diameter was measured at approximately 0.5 m intervals up the stem. This was done using a diameter tape while marking the stem as outlined above. These measurements allowed an approximate determination of the stem shape to be made. The diameter measurements were made to the nearest 1 mm and were once again confirmed after felling.

In the thinned plot the total height of the tree was estimated using a hypsometer at the time of initial selection. This reading was verified, by tape measure, and altered if required, once the tree had been felled. In the unthinned plot the height was determined only after felling. The hypsometer reading was only accurate to about the nearest 1 to 2 m because of visibility problems caused by branches. The tape measure readings were more accurate, being accurate to the nearest 1 cm, although an accuracy of 0.5 m was considered sufficient for analysis purposes.

All the branches were removed as part of the swaying procedure (Chapter 5) and were weighed in the process, according to the initial 1 m sections on the stem. The point where the live crown began was also noted. The measurement of branch mass was carried out using a spring balance suspended from a metal rod supported between two trees, the branches were held in a bucket for weighing.

These measurements were made to the nearest 0.1 kg.

The tree was then felled, after which the stem was cut into the more accurate 1 m sections and each was weighed using the same apparatus to the nearest 0.1 kg. A cross-sectional slice approximately 10 cm thick was removed from the top end of each section. If a knot was visible in the cut face a thicker slice was removed to present an unblemished face. These slices were taken for analysis in the laboratory, as explained in section 3.2.3, to describe the degree of uniformity of radial growth, and to see if there were any structural abnormalities present in the stem which might cause either a greater or lesser resistance to bending.

The locations of any neighbouring trees were noted to provide an image of how much crown interaction would be likely, and thus to compare the area in which each tree was able to sway. This was done using a prismatic compass and a tape measure with the distances being taken to the nearest 5 mm from the centre of the felled sample tree to the nearest edge of the neighbour. If a stem was forked or split then the largest limb was measured.

3.2.3 Laboratory procedure

The following procedure was followed for all the stem slices taken from both the unthinned and thinned plots.

The slices were kept in polythene bags prior to analysis to reduce drying out which would induce shrinkage or cracking. The main aim was to measure the annual under-bark diameter increment at 1 m intervals up the stem. This would give a good indication of how each stem had developed. To do this it was necessary to polish the cut surface and highlight the annual rings. The polishing was done using a belt sander which involved letting the slices dry slightly producing a minimal amount of shrinkage. The degree of shrinkage was estimated for each slice simply by measuring the diameter, using a ruler, across the largest part of each slice and repeating this after drying. In all cases, except where a split

or crack developed, the difference between these measurements was less than 3 % of the original diameter, with the larger percentage differences occurring on the smaller sections.

After polishing, the rings were highlighted using a black indelible ink pen with a 0.3 mm diameter nib. The slices were then suitable for photocopying on to white paper and the copies were checked for an accurate and clear reproduction as well as for shrinkage or enlargement.

The photocopies were now used for measurement thus preventing damage to the original slices in case any further measurements were required in the future. The measurement process involved a Delta-T Area Meter (Δ-T Area Meter, Delta-T Devices, Cambridge, England) linked to a closed-circuit monochrome video camera (RCA Hi-Pot TV Camera, RCA, Lancaster, England) and a television screen. The area meter was set to measure the light area on a dark background, i.e. the stem slice area (under-bark). These area values were later converted into diameters assuming that the cross-section was circular. Starting from the outer ring, each ring was successively darkened using a black felt-tipped pen, and the new area measured with the decrease in area corresponding to the area of the annual ring just blackened out. In some cases the rings were so close together that it was impossible to measure the diameter in this way. In such cases the average annual diameter increment was used for the section of the slice where this applied. These average diameter increments were always less than 1 mm. The area meter was calibrated using a number of different sized pieces of white paper.

This technique had two main advantages over the simpler method of taking readings direct from the slices along the two major axes. Firstly, as explained earlier, the over-bark diameter measurements and the engineering beam theory used to estimate natural frequency both assume a circular cross-section. Secondly, if any cracks did develop in the slices they simply showed up as dark areas on the photocopies, and therefore there would be no significant change in the area measured by this method, where the alternative method would be inaccurate

The main disadvantages of this technique were that the annual rings showed up as dark lines on the photocopies, so the area measured would be slightly low. However, after removing these lines to measure this effect it was found to be insignificant and in some cases not even detectable. The procedure used here was, however, very time consuming.

The areas were converted to diameter values assuming a circular cross-section

$$A = \pi r_x^2 \qquad (3.1)$$

so,
$$r_x = (A/\pi)^{1/2}$$

therefore,
$$d_x = 2(A/\pi)^{1/2} \qquad (3.2)$$

where A is the area of rings remaining after a ring has been blackened out, and r_x and d_x are the radius and diameter of the area left. Thus, the diameter increment of each ring is the difference between the value of d_x before and after it has been blackened out. In this way the history of stem diameter was developed for each slice, or 1 m section of the stem, with the intention of detecting changes in growth rate or form.

3.3 Results and Discussion

The analysis and presentation of the results produced by the work outlined in the preceding section can be split into four parts. For each of these parts the raw data are presented, in summary form where appropriate, followed by a description of any analysis applied and the results of that analysis. Each part is treated separately at this stage and is discussed as such, with a more general discussion and conclusions forming the final section of this chapter. The four sub-sections are:

1. Stem height and dbh;
2. Over-bark diameter and stem shape;
3. Stem and crown mass;
4. Under-bark diameter.

3.3.1 Stem height and dbh

There was a wide range of stem heights covered by the eleven sample trees but the trees from the unthinned plot were generally taller than those from the thinned plot (Table 3.1). The tallest tree was 15.5 m in the unthinned plot as compared with 12.7 m in the thinned plot. While the shortest tree in the unthinned plot was 13.0 m as compared to 9.9 m in the thinned plot.

There was also a wide range of dbh values recorded. In this case the larger values were obtained from the thinned plot where the range was from 25.8 cm to 34.1 cm while the range in the unthinned plot was from 11.3 cm to 22.3 cm (Table 3.1). The reason for taller slender trees in the unthinned plot and shorter broader stems in the thinned plot is the reduced level of competition for light between the remaining stems in the thinned plot. Therefore, the trees no longer require to grow upwards at the maximum rate possible to obtain this light. Instead, the trees put on more foliage, which increases the amount of photosynthesis which is possible, and so the stems can grow more quickly in terms of diameter.

	Tree No.	Height (m)	dbh (m)	*h*/dbh
	1	13.0	0.113	113.0
	2	14.0	0.155	90.3
	3	15.5	0.183	84.7
A	4	13.5	0.106	127.4
	5	13.5	0.167	79.9
	6	13.0	0.140	92.9
	7	14.6	0.157	93.0
	8	12.7	0.242	52.5
B	9	11.9	0.180	66.1
	10	11.7	0.191	61.3
	11	9.9	0.161	61.5

Table 3.1 Stem height and dbh values for eleven sample Sitka spruce trees
A = Unthinned plot; B = thinned plot

Several authors (Kilpatrick *et al* 1981, Stuhr 1981, Savill 1983) have used height/dbh as an indicator of stability for trees. A low value suggests that a stem will be stable while a high value corresponds with an unstable tree. Therefore, a broad short stem should be more stable than a tall thin one. The value of this ratio

for each tree used here is also presented in Table 3.1.

These results clearly show lower values of height/dbh for trees from the thinned plot compared to those from the unthinned plot. This suggests that trees from the thinned stand should be less susceptible to windthrow due to their wider base and shorter stems. Savill (1983) gave figures for height/dbh in unthinned Sitka spruce of between 64 and 104 depending on the original stocking density. He quoted a value of 96 for an original stocking density of 2,500 stems per hectare which is now the normal stocking level for this country. The results presented in Table 3.1 are within 20% of this value in the unthinned plot with the exception of Tree 4 which, due to its high value for height/dbh might be assumed to be very unstable. In the thinned plot all four trees provided values substantially below 96. However, it is more common for trees to blow over once a stand is thinned, especially soon after the thinning procedure (Savill 1983, Blackburn 1986). This may be due more to alterations in crown damping than in the intrinsic stability of individual stems.

The possibility of the effects of swaying are not incorporated into this simple concept of a wide base leading to a more stable structure, nor is the influence of rooting. Dynamics may in fact alter the stability of stems according to other factors such as stem flexibility, crown mass and crown damping. Some of these possibilities are investigated and discussed further in the following chapters. The effects of poor rooting are not studied in this work but the thinned plot was noticeably wetter than the unthinned plot and therefore it can be assumed that the rooting of the trees has been damaged. Hence, the trees may be less stable. This is a common feature after a stand has been thinned, due to less water being required by the stand since there are fewer stems, and so the water-table rises accordingly.

3.3.2 Over-bark diameter and stem shape

The over-bark (o.b.) diameter results are given in Table 3.2 which shows how o.b. diameter changed with height above ground for each of the eleven sample trees. These results are also presented in graphical form in Figure 3.1 as an example, and in Appendix II for all eleven trees.

Height (m)	Over-bark Diameter (cm) Tree										
	1	2	3	4	5	6	7	8	9	10	11
0.0	18.0	22.5	22.5	14.1	23.0	18.0	22.3	34.1	25.8	30.6	26.1
0.5	13.3	16.8	19.7	11.3	19.7	15.5	17.3	26.4	19.4	21.8	20.4
1.0	12.0	16.6	18.6	10.6	16.9	14.4	16.2	25.3	18.1	19.3	17.5
1.5	11.5	15.9	17.8	10.4	16.3	13.7	15.3	23.6	17.5	18.9	15.9
2.0	11.3	15.4	17.3	10.6	16.3	12.4	15.0	22.3	17.2	17.5	15.3
2.5	11.0	15.1	17.3	9.6	16.4	12.6	14.6	21.6	16.6	16.6	14.0
3.0	10.2	15.0	17.0	9.5	15.8	11.8	14.3	21.3	16.2	16.6	13.7
3.5	9.9	14.7	16.8	9.2	15.3	12.1	13.7	20.4	15.9	15.4	13.4
4.0	10.4	14.1	16.3	8.8	15.1	11.2	13.5	20.1	15.3	15.3	12.9
4.5	9.5	13.7	16.1	8.6	14.7	10.5	13.1	19.4	14.3	14.3	12.1
5.0	9.1	13.3	15.6	8.5	14.9	9.9	12.7	18.3	14.3	14.0	11.8
5.5	9.0	13.0	15.1	8.2	14.3	9.5	12.4	16.7	13.7	13.1	10.8
6.0	8.5	12.3	14.6	8.1	13.7	9.7	12.1	16.4	13.1	11.9	9.9
6.5	8.0	12.1	14.0	7.7	13.6	8.9	11.6	15.3	12.3	11.1	8.9
7.0	7.9	11.6	13.8	7.5	12.6	8.6	11.3	14.0	11.8	10.5	8.6
7.5	7.7	10.9	12.8	7.1	12.2	8.2	11.1	12.4	11.0	9.2	7.3
8.0	7.2	10.8	12.3	6.9	11.5	7.7	10.5	11.6	9.7	8.1	5.7
8.5	6.8	9.7	11.7	6.5	11.0	7.1	9.5	9.9	9.2	7.0	
9.0	6.3	9.4	11.0	6.2	10.7	6.9	9.2	8.6	8.0	6.7	
9.5	5.7	7.5	10.0	5.9	9.8	6.1	8.6	7.6	6.4	5.1	
10.0	4.9	6.6	9.4	5.3	8.5	5.3	8.0	6.2	5.1		
10.5	4.0	6.2	9.2	5.0	8.0	4.7	7.2				
11.0	3.3	5.8	8.8	4.5	6.6	3.8	6.7				
11.5	2.4	4.3	7.8	3.6	5.9	2.9	5.7				
12.0	1.9	3.9	5.9	2.0	4.5	2.0	5.4				
12.5	1.7	2.9	5.1	2.2	2.9	1.3					
13.0	1.2	2.5	4.4	1.6	2.3	0.9					
13.5		2.0	2.9	1.2	1.5						
14.0		1.5	2.5								
14.5			1.8								
15.0			1.2								
15.5			1.2								

Table 3.2 Over-bark diameter against height for the eleven sample Sitka spruce trees
Trees 1-7 Unthinned plot; 8-11 Thinned plot

The diameter data outlined in Table 3.2 are the values taken in the field after the trees had been felled. These data were used to determine the taper for each stem. This estimate of taper was required for Blevins' (1979) models predicting natural frequency (Chapter 5) to be used. Therefore, two calculations were carried out as described below.

First, for the determination of natural frequency assuming non-linear taper of the stem (Model 1 in Chapter 2) a power law was applied to predict values for diameter at various points on the stem (equation 2.16). The product of this calculation was the value n which was required to determine the dimensionless taper parameter as explained in the previous chapter. Using an iterative process the best solution to equation 2.16 was determined for each tree. This was carried out using a computer programme (Appendix III) and entering various values of n until the best solution was achieved, i.e. the value which produced estimated diameters with the smallest difference from those measured in the field. The values of n are presented in Table 3.3.

Tree	n	λ_1	t	λ_2
1	0.71	2.62	1.69	2.05
2	0.64	2.50	1.64	2.00
3	0.72	2.65	1.52	1.90
A 4	0.58	2.42	1.60	1.97
5	0.63	2.50	1.48	1.85
6	0.77	2.74	1.78	2.09
7	0.69	2.59	1.41	1.78
8	0.86	2.85	3.13	2.25
9	0.61	2.48	2.42	2.20
B 10	0.86	2.85	3.52	2.28
11	1.00	2.90	4.08	2.30

Table 3.3 Taper values for eleven sample Sitka spruce trees
A = Unthinned plot; B = Thinned plot

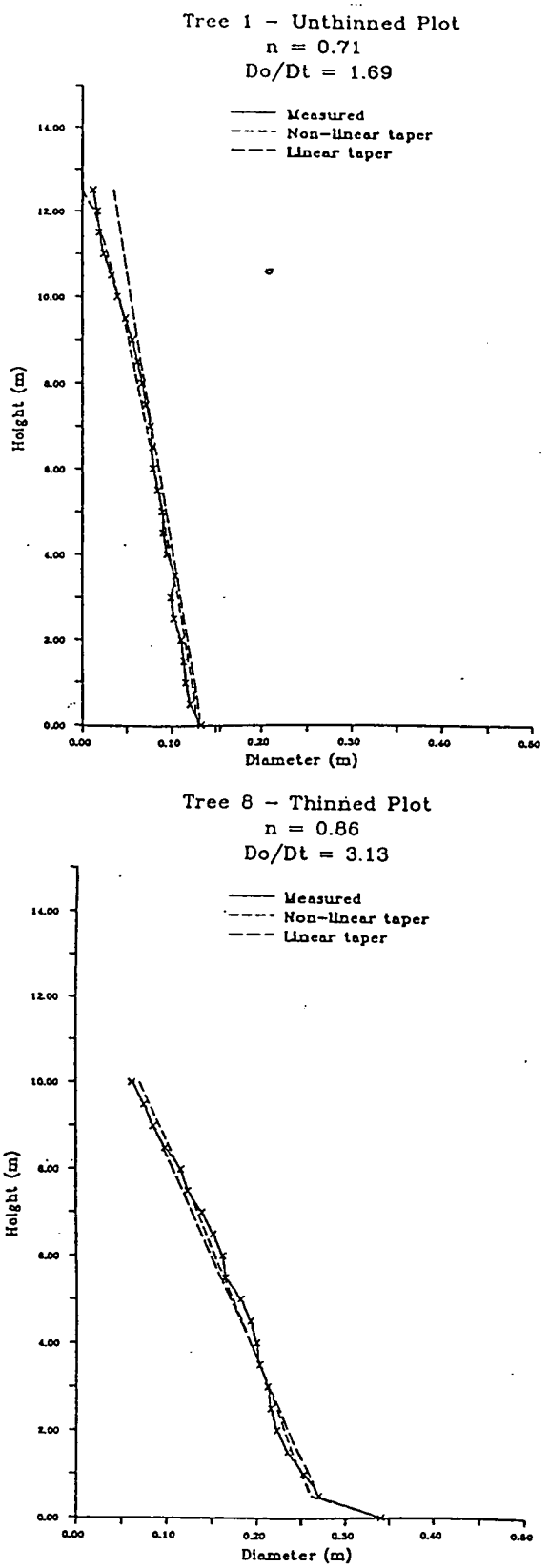

Figure 3.1 Measured and estimated over-bark diameters against height for Tree 1 (unthinned plot) and Tree 8 (thinned plot)

Secondly, when assuming that the stem is linearly tapered up to a point of truncation (Model 2) it was also necessary to determine taper. In this case equation 2.19 was used producing a value of t for each tree. Once again the results of this calculation are presented in Figure 3.1 and Appendix II with the values of t are given in Table 3.3.

Both n and t were used to determine values for λ_1 and λ_2 respectively for each tree (Blevins 1979). This determination was based on the two sets of curves given in Chapter 2 (Figures 2.6 and 2.7 respectively) which assume that the trees were vibrating in the first mode and that all other assumptions previously described apply. Values for λ_1 and λ_2 are presented in Table 3.3 according to these relationships.

The values quoted for d_o in Table 3.2 were not the ones used in either Figure 3.1 or for the above calculations of n and t. In these cases the values of $d_{0.5}$ were used for the basal diameter to remove the effect of buttressing which would have led to widely inaccurate predictions in stem form. It is also worth noting that a value of $n = 0$ corresponds to a stem of constant thickness, or zero taper, while a value of $n = 1$ corresponds to linear taper as illustrated by Tree 11. However, in this case neither model appears to predict diameter very well, due to the extent of buttressing.

In most cases both models match the measured values quite accurately, but the linear taper model only does so up to the point of truncation and where buttressing is not a major feature of the stem. This latter point also applies to the non-linear taper model. It is also clear from the graphs (Appendix II) that the non-linear taper model is better in the unthinned plot than it is in the thinned plot. Hence, when applying this method of analysis a careful consideration of buttressing should be carried out, and any estimate of natural frequency for stems with significant buttressing may be less accurate than for more uniformly shaped stems.

3.3.3 Stem and crown mass

The mass of stem sections, each 1 m long, along with the mass of branches for these sections are illustrated in Figure 3.2 for Trees 1 and 8 and in Appendix IV for all eleven stems. These values are also tabulated in Tables 3.4 and 3.5 respectively. Total mass for both stem and foliage for each tree is also given in the tables. Note that these data were obtained as fresh weights. Values for stem mass ranged from 61.5 kg to 160.9 kg in the unthinned plot, while in the thinned plot the range was from 122.4 kg to 254.9 kg. The stem mass is generally greater in the trees from the thinned plot even though they have shorter stems.

Height Section (m)	Stem mass (kg) Tree 1	2	3	4	5	6	7	8	9	10	11
1	15.2	23.2	29.0	10.7	26.5	18.0	24.4	52.7	31.0	34.2	30.0
2	10.6	21.0	22.9	8.5	19.5	12.7	20.9	43.8	24.0	28.8	25.5
3	9.8	18.9	21.2	6.7	17.8	11.1	16.5	37.2	17.8	22.7	15.4
4	8.2	17.1	20.6	6.3	16.2	8.8	13.2	31.6	18.6	19.5	17.0
5	8.0	16.4	18.4	5.5	16.2	7.6	14.8	29.3	17.4	19.7	11.8
6	6.4	14.3	16.7	5.1	14.4	6.9	11.8	24.2	15.0	16.0	12.2
7	6.1	13.6	14.8	4.8	13.4	6.0	11.3	17.9	13.5	11.8	5.9
8	5.0	11.1	13.0	3.8	11.4	5.3	9.1	13.2	9.5	8.7	4.6
9	4.0	6.6	11.1	3.1	9.6	4.5	8.0	9.5	6.9	4.9	
10	2.8	4.1	8.4	2.6	7.5	3.3	7.4	5.0	4.0	2.3	
11	1.7	2.4	6.3	2.8	4.9	2.2	4.8				
12	0.7	1.4	4.2	1.1	2.6	1.2	3.2				
13	0.2	0.4	3.0	0.4	0.9	0.4					
14		0.1	0.9	0.1	0.2	0.1					
15			0.3								
Total	78.7	159.7	190.8	61.5	160.9	88.1	145.4	254.9	157.8	168.6	122.4

Table 3.4 Stem mass (kg) for 1 m sections of the eleven sample Sitka spruce trees (Trees 1-7 Unthinned plot; 8-11 Thinned plot)

Height Section (m)	Foliage mass (kg) Tree 1	2	3	4	5	6	7	8	9	10	11
1	0.5	0.6	3.1	0.8	0.5	1.2	1.0	3.0	1.0	2.5	2.3
2	1.1	1.4	2.5	1.3	1.3	1.0	6.0	7.5	5.0	5.6	4.3
3	1.3	1.3	2.9	0.7	0.9	1.4	4.0	9.6	3.0	7.0	4.6
4	0.8	1.0	2.3	1.1	1.0	0.6	2.0	7.3	6.0	10.5	6.5
5	1.1	2.9	2.2	0.8	1.4	0.9	1.5	18.3	5.0	13.7	6.7
6	0.4	1.5	2.1	0.9	1.1	0.8	3.0	17.5	15.0	0.6	13.2
7	4.0	3.9	2.2	1.8	2.4	0.9	6.0	29.0	14.0	18.8	8.7
8	3.6	4.4	4.8	1.0	5.6	0.9	5.0	19.1	33.0	11.7	14.9
9	4.5	8.4	8.8	1.2	6.3	2.2	10.0	29.5	15.0	12.9	10.5
10	4.6	19.5	10.7	2.6	10.4	2.7	13.0	10.5	19.0	5.4	7.9
11	4.3	2.8	7.0	0.9	6.5	3.3	10.0		13.0	11.3	
12	1.9	1.8	4.2	1.3	4.9	2.7	11.0		6.0	8.2	
13	0.1	0.9	2.0	1.0	3.3	0.9	9.0				
14			0.7	0.1	0.6	0.1	7.0				
Total	28.4	55.8	65.0	15.5	46.2	19.6	88.5	161.5	135.0	97.6	96.6

Table 3.5 Foliage mass (kg) for 1 m section of the eleven Sitka spruce trees (Trees 1-7 Unthinned plot; 8-11 Thinned plot)

The results for foliage mass show a very significant variation between the two plots. The range in the unthinned plot is from 15.5 kg to 88.5 kg while it is from 96.9 kg to 161.5 kg in the thinned plot. Both these sets of data agree with the concept of a tree putting on more foliage and increased radial growth after thinning. The average stem and foliage mass were determined for both plots and are given in Table 3.6.

Plot	Unthinned	Thinned
Stem mass (kg)	126.4	175.9
Foliage mass (kg)	45.6	122.8

Table 3.6 Average values for stem and foliage mass in unthinned and thinned stands of Sitka spruce

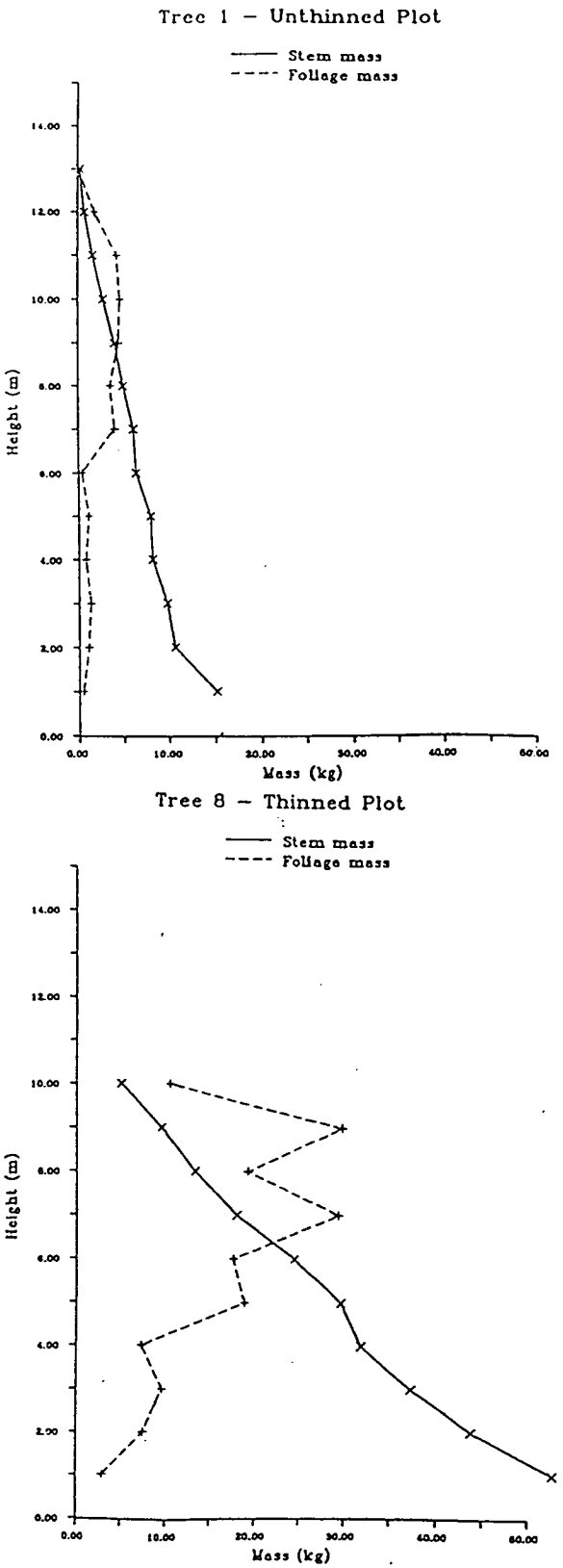

Figure 3.2 Stem and foliage mass against height for Tree 1 (unthinned plot) and Tree 8 (thinned plot).

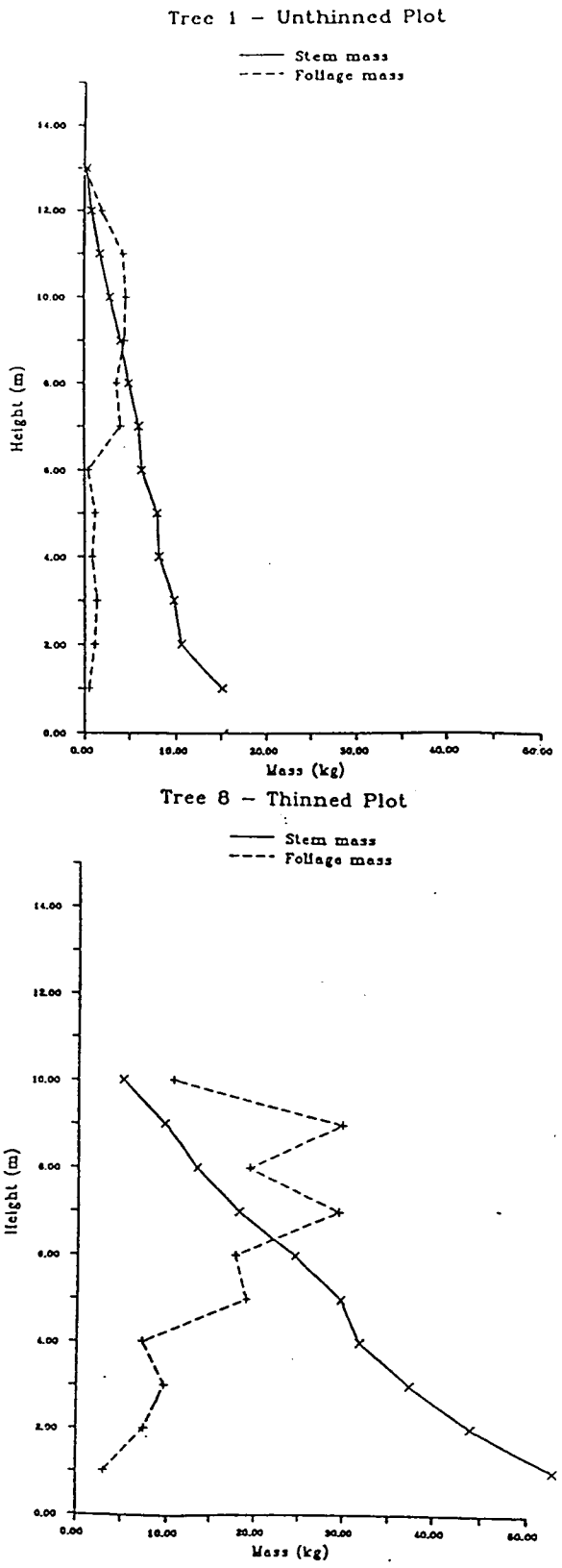

Figure 3.2 Stem and foliage mass against height for Tree 1 (unthinned plot) and Tree 8 (thinned plot).

The only analysis which was required using this data was the determination of average density for each stem. This parameter was required for the estimation of natural frequency of the stems as outlined in Chapter 2.

The average density of each stem was determined in two ways according to which of the two frequency estimation Models (1 or 2) was being applied. For Model 1 (non-linear taper) the volume of each 1 m stem section was calculated by

$$V_i = \pi(d_m/2)^2 l \qquad (3.3)$$

where, V_i = volume of the ith section of the stem (m)

d_m = mid diameter of the ith section of the stem (m)

l = length of the ith section of the stem (assumed to be 1 m except for the top section of each tree) (m)

Then a density value (μ_i) was calculated for each section

$$\mu_i = m_i/V_i \qquad (3.4)$$

where, μ_i = density of the i^{th} section of the stem (kg m^{-3})

m_i = mass of the i^{th} section of the stem (kg)

The average value of these densities over the whole tree was then used as the stem density for each tree (μ_1 for Model 1). For Model 2 (linear taper to a point of truncation) the same approach was used but only the stem sections up to 9.0 m (i.e. the point of truncation) were used to determine the average stem density (μ_2), except for Tree 11 where the truncation point was 8.0 m. The results of this analysis are presented in Table 3.7.

The average values for μ_1 and μ_2 for the unthinned plot were 1026.1 kg m^{-3} and 982.0 kg m^{-3} respectively and for the thinned plot they were 1082.1 kg m^{-3} and 1065.1 kg m^3. Again the values were slightly higher in the thinned plot which is most likely due to the time of year in which the samples were taken from the field. The stem sections were taken for the unthinned plot in late autumn/winter while they were removed from the thinned plot during the summer. Therefore the

sections which were taken during the summer would be expected to have a higher water content and hence a greater density.

Tree No.	μ_1 (kg m^{-3})	μ_2 (kg m^{-3})
1	1112.3	1061.1
2	898.6	1045.6
3	992.5	942.2
A 4	1005.4	951.1
5	969.3	918.9
6	1144.6	928.9
7	1059.8	1026.5
8	1051.0	1027.5
B 9	1025.1	991.8
10	1128.1	1117.1
11	1124.1	1124.1

Table 3.7 Stem density values for eleven sample Sitka spruce trees
(μ_1 = whole stem; μ_2 = truncated stem)
(A = Unthinned plot; B = Thinned plot)

The total mass of the stem and the foliage for each tree, as presented earlier were used in the determination of natural frequency using Model 3 (Blevins 1979) but no further analysis was required at this stage.

3.3.4 Under-bark diameter

The under-bark diameter results presented here were obtained by ring analysis as described in section 3.2.3. The under-bark diameters are presented for each tree in graphical form against age for various points on the stem in Appendix V. An example of one of these graphs for each of the plots is given in Figure 3.3 (Trees 1 and 8). This figure gives an impression of how uniformly the stems grew in radial terms at a number of heights above the ground. It was considered that these data were too numerous to present in tabular form. Hence, the average annual under-bark diameter increment (i.e. averaged over the various heights) was determined for each tree. These results are presented in Table 3.8.

The very low values sometimes shown in row 1 (i.e. year 1) and in the last value for each tree are most likely due to incomplete growing seasons. As these values are derived from averaging increments at different points on the stem it is possible that a tree may have reached a certain height, say 7 m for example, half way through a growing season. Therefore, the first year's increment at 7 m will not be as high as expected when compared with values from lower down the stem.

The values presented for each tree in Table 3.8 are also illustrated in graphical form in Figure 3.4. These graphs show that the general trend is very similar for all eleven trees, rising initially, then levelling off with some variation, and finally declining. However, there is some evidence that the thinned trees show signs of increased diameter increment after year 18, although this is very slight in the case of Tree 9, and is very short lived, about 3 to 4 years. This increase corresponds to 1983 when the thinning took place.

Year of	Unthinned								Thinned				
Growth	1	2	3	4	5	6	7	Ave	8	9	10	11	Ave
1	0.70	1.20	0.10	0.10	0.70	0.30	0.30	0.49	0.30	0.60	0.20	0.20	0.32
2	0.70	1.30	0.70	0.60	1.10	0.80	0.60	0.83	0.50	0.50	0.50	0.70	0.55
3	.065	1.30	0.80	1.00	1.20	0.90	1.60	1.06	0.70	0.80	0.70	1.00	0.80
4	1.05	1.20	0.60	0.95	1.05	0.85	1.30	1.00	1.00	0.70	0.90	1.10	0.92
5	1.27	1.07	1.05	0.67	1.05	1.07	1.20	1.05	1.05	0.95	0.90	0.90	0.95
6	0.83	1.50	1.00	0.83	1.03	1.13	1.40	1.10	1.45	0.87	1.05	0.85	1.06
7	0.95	1.22	1.17	0.78	1.10	1.10	1.10	1.06	1.00	1.03	0.87	0.85	0.94
8	0.85	1.11	1.08	0.85	1.00	0.98	1.40	1.04	1.28	0.90	0.90	1.03	1.03
9	0.90	1.10	0.96	0.80	1.02	1.00	1.32	1.01	1.18	1.08	0.80	1.07	1.03
10	0.86	0.99	1.10	0.72	1.03	0.90	1.12	0.96	1.14	0.94	0.72	0.85	0.91
11	0.60	0.98	0.92	0.67	1.09	0.83	1.05	0.88	1.30	0.90	0.70	0.80	0.92
12	0.70	1.02	0.85	0.58	0.89	0.79	0.97	0.83	1.10	0.77	0.80	0.84	0.88
13	0.63	0.97	0.84	0.48	0.82	0.65	0.81	0.74	1.18	0.80	0.80	0.85	0.91
14	0.59	0.88	1.00	0.44	0.84	0.65	0.78	0.74	1.10	0.75	0.73	0.82	0.85
15	0.56	0.89	0.98	0.45	0.86	0.56	0.71	0.72	1.32	0.69	0.86	0.76	0.91
16	0.60	0.79	0.91	0.56	0.70	0.57	0.71	0.69	1.14	0.82	0.81	0.74	0.88
17	0.53	0.79	0.92	0.42	0.68	0.57	0.64	0.65	0.89	0.71	0.66	0.55	0.70
18	0.45	0.74	0.94	0.41	0.75	0.46	0.63	0.63	0.76	0.59	0.72	0.44	0.63
19	0.33	0.87	0.64	0.33	0.67	0.42	0.48	0.53	0.87	0.61	0.76	0.59	0.71
20	0.27	0.79	0.63	0.30	0.84	0.32	0.58	0.53	1.16	0.80	0.98	0.75	0.92
21	0.22		0.68	0.38	0.75	0.23	0.58	0.47	1.43	0.76	1.06	0.84	1.02
22	0.24		0.62	0.32		0.28	0.41	0.37	1.11	0.68	0.79	0.60	0.80
23	0.25		0.76			0.29	0.61	0.48	0.68	0.45	0.80	0.48	0.60
24			0.64							0.39			

Table 3.8 Average annual under-bark diameter increments (cm) for eleven sample Sitka spruce trees
(Trees 1-7 Unthinned plot; Trees 8-11 Thinned plot)

The average under-bark diameter increment figures for the thinned and unthinned plots shown in Table 3.8 are also presented in graphical form in Figure 3.5. This once again shows the trend described above, but it also illustrates more clearly the rise in diameter increment which occurred in the thinned plot from year 18. Both sets of data reach similar values by year 23, so the period of increased radial growth lasted five years which should correspond with the time required to achieve canopy closure again. However, the thinned plot had not reached canopy closure by the time of this fieldwork so the return to more normal growth rates can be explained by the fact that when a stand is thinned the water level in the soil rises and causes stress in the trees due to root damage. This in turn results in reduced growth rates as appears to have happened here.

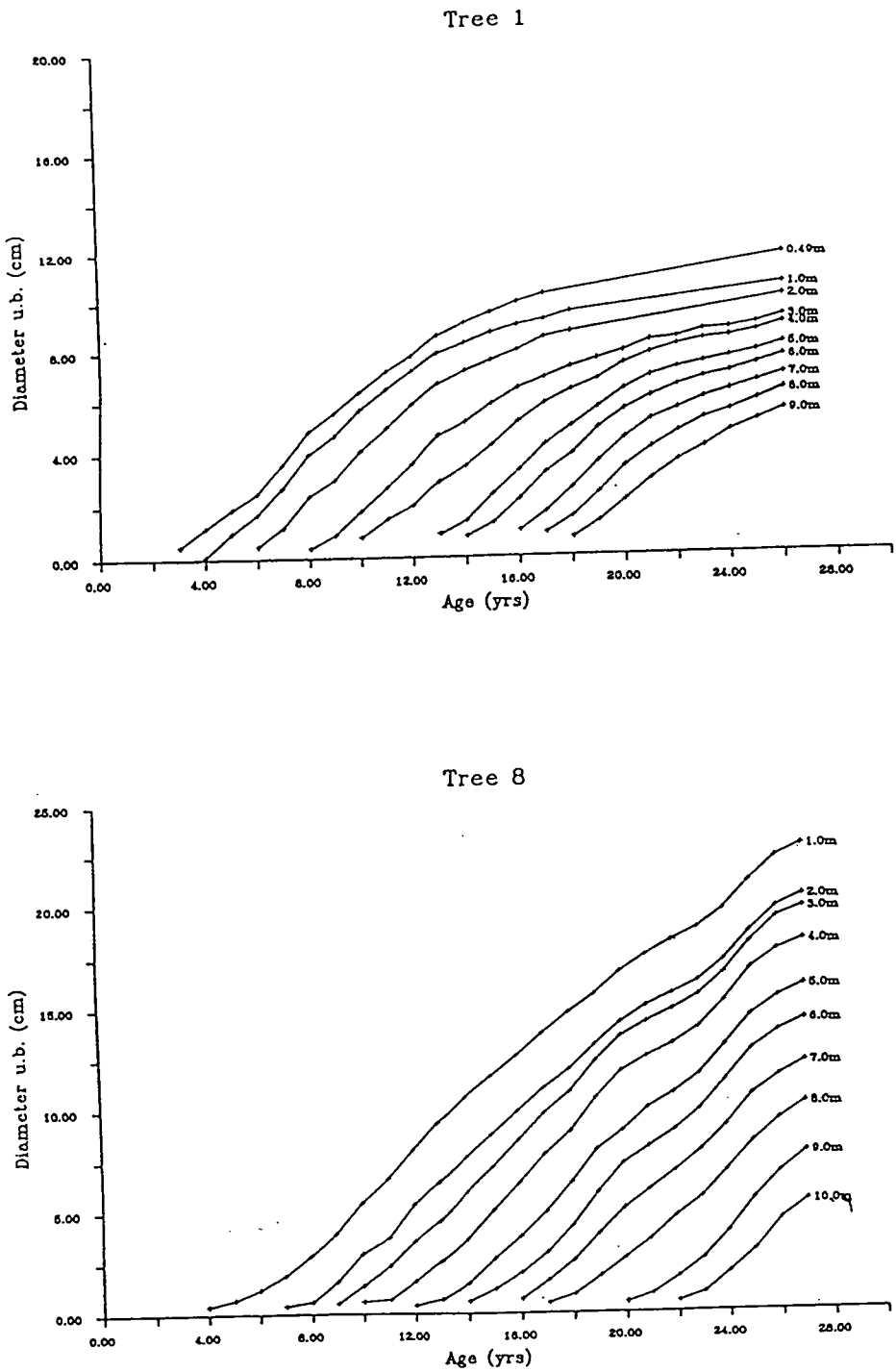

Figure 3.3 Under-bark diameter against age at various heights above the ground for Tree 1 and Tree 8

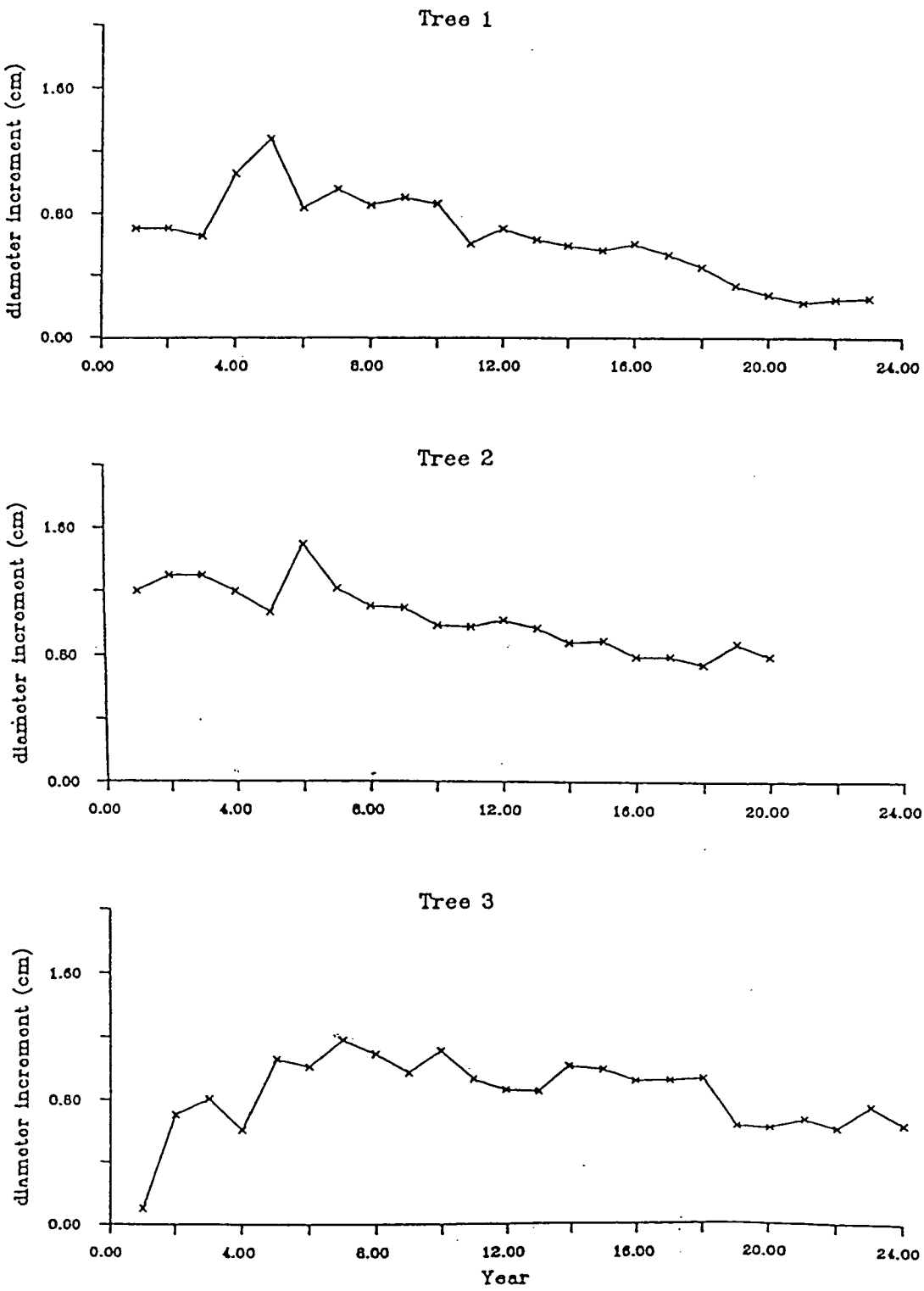

Figure 3.4 Annual under-bark diameter increment against year of growth for the eleven sample trees
(Trees 1-7 Unthinned plot; Trees 8-11 Thinned plot)

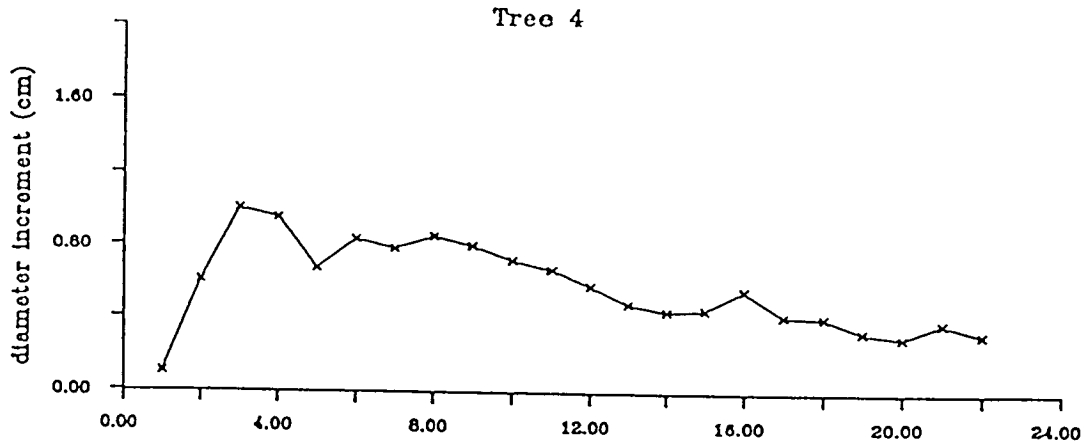
Tree 4
diameter increment (cm)
1.60
0.80
0.00
0.00
4.00
8.00
12.00
16.00
20.00
24.00

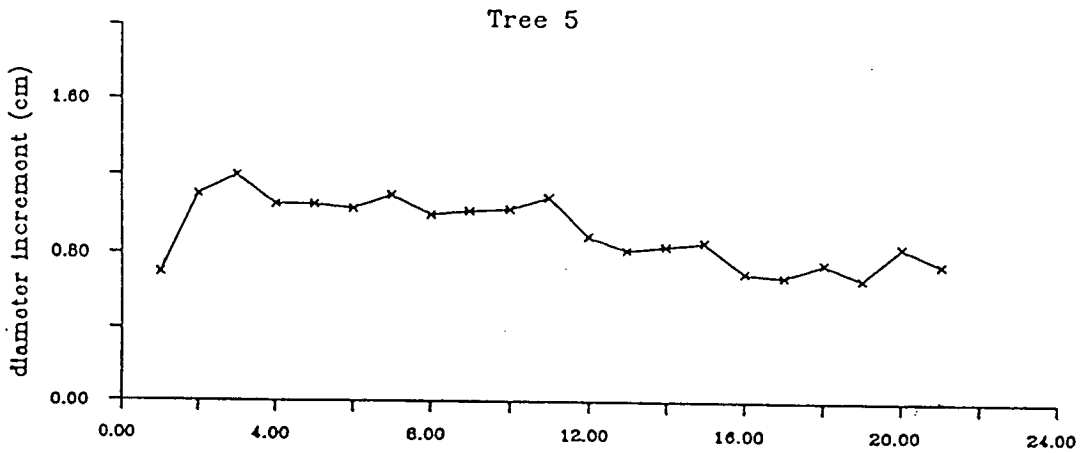
Tree 5
diameter increment (cm)
1.60
0.80
0.00
0.00
4.00
8.00
12.00
16.00
20.00
24.00

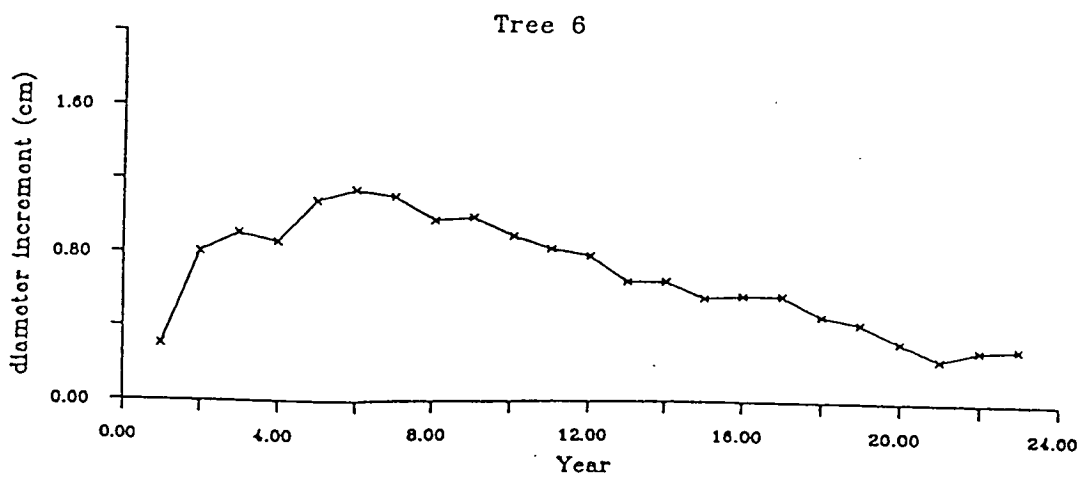
Tree 6
diameter increment (cm)
1.60
0.80
0.00
0.00
4.00
8.00
12.00
16.00
20.00
24.00
Year

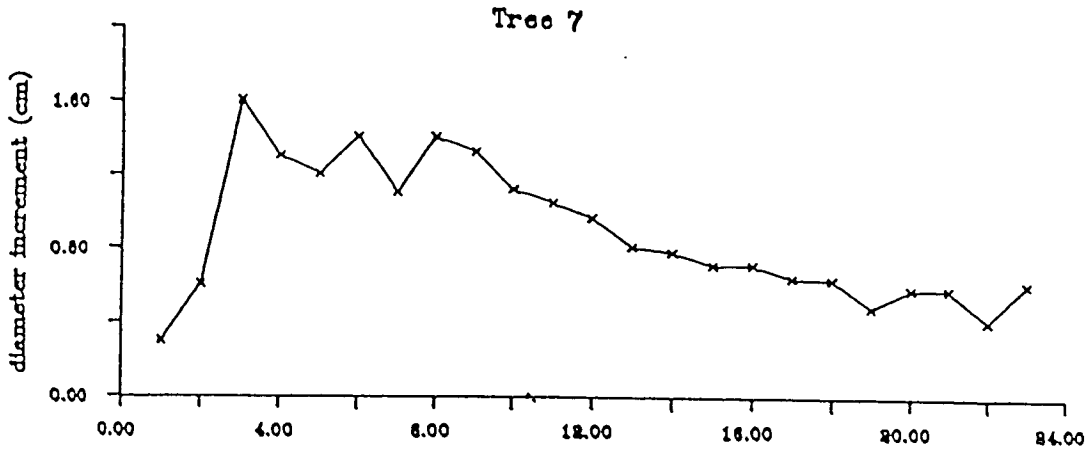
Tree 7
diameter increment (cm)
1.60
0.80
0.00
0.00
4.00
8.00
12.00
16.00
20.00
24.00


Tree 8
diameter increment (cm)
1.60
0.80
0.00
0.00
4.00
8.00
12.00
16.00
20.00
24.00

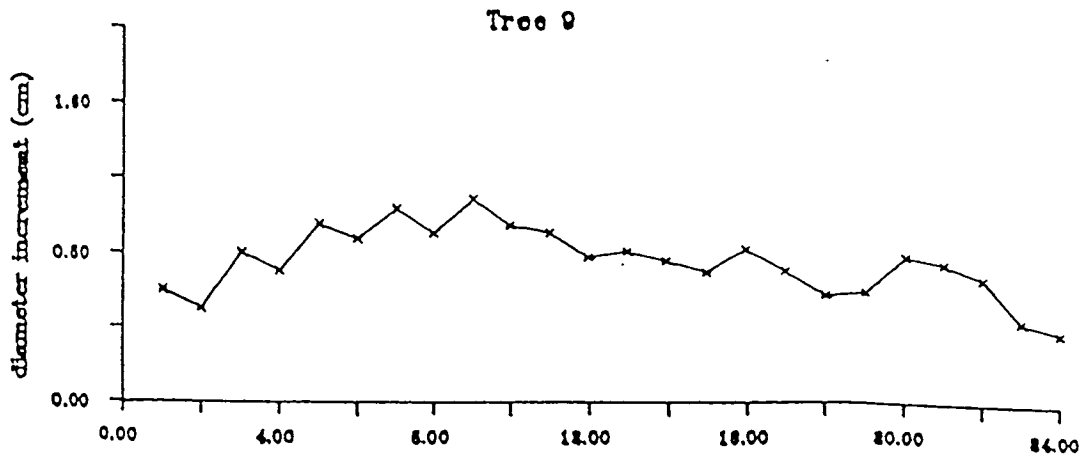
Tree 9
diameter increment (cm)
1.60
0.80
0.00
0.00
4.00
8.00
12.00
16.00
20.00
24.00

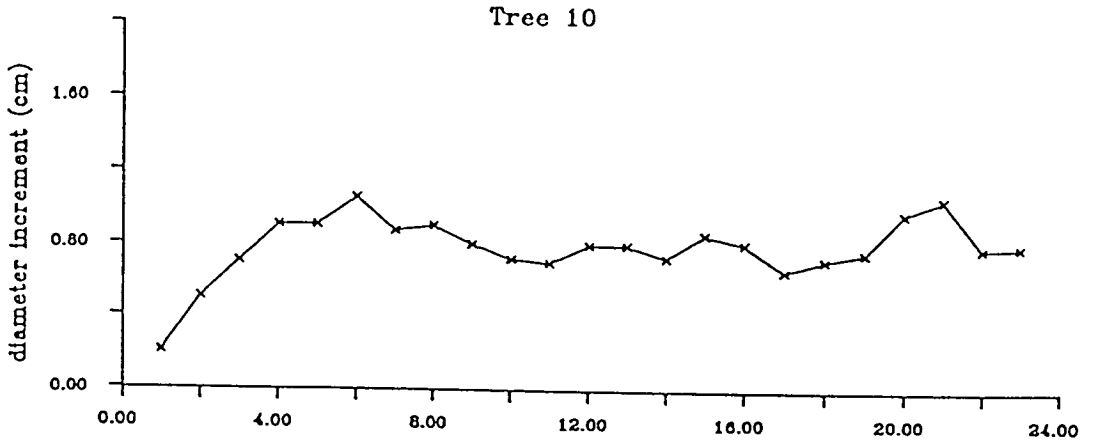

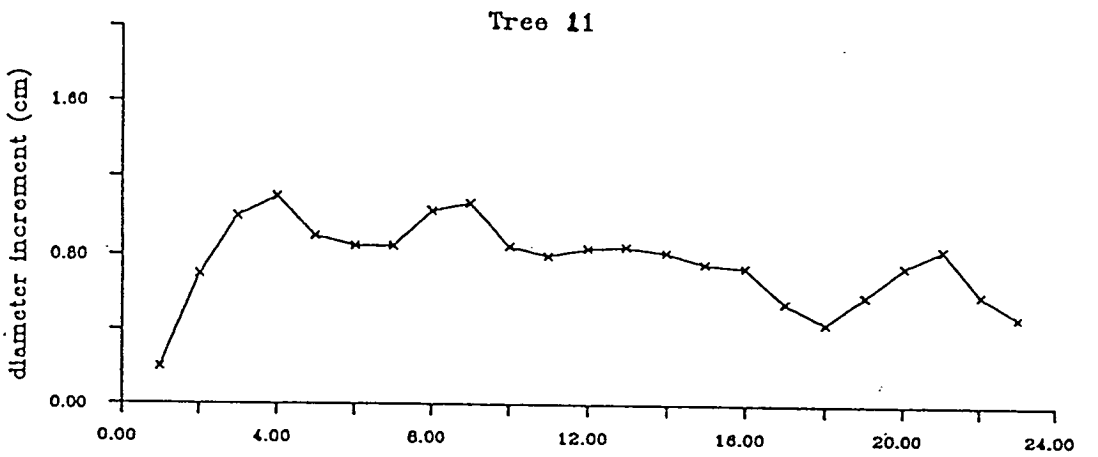

These data would appear to agree numerically with the theory that stems from a thinned plot will generally have larger diameters than those from an unthinned plot of the same age. This is due to less competition for light which results in less height growth and more radial growth. It would also appear that the rate of diameter growth is highly variable, but more so in the thinned plot, especially immediately after thinning. This may be caused by competition leading to suppression of the less well positioned stems after thinning. The sample trees used here were randomly selected with respect to their position. Therefore, it is reasonable to conclude that the stems in the unthinned plot are likely to be more uniform in their internal structure throughout the stand than those from the thinned stand. This may have repercussions later when applying engineering theories based on a uniform composition of the beam or stem.

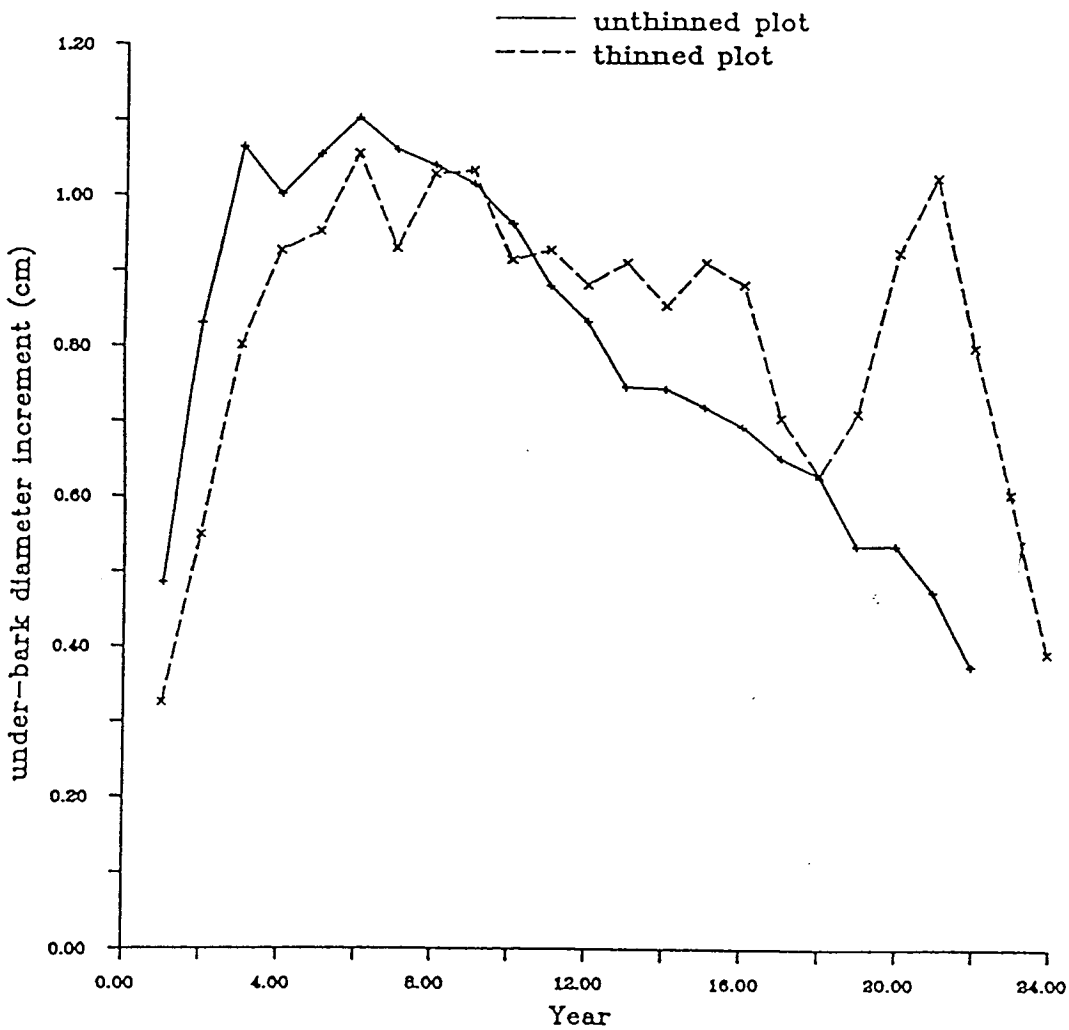

Figure 3.5 Average under-bark diameter increment against year of growth for the unthinned and thinned plots

3.4 Conclusions

A number of parameters have been derived from the sample trees and average values have been calculated in order to compare unthinned and thinned stands. A summary table is given below (Table 3.9) which shows these average values for the two plots.

Parameter	Unthinned	Thinned
Height (m)	13.87	11.55
dbh (m)	0.146	0.193
h/dbh	95.0	59.8
n	0.68	0.83
λ_t	2.57	2.77
t	1.59	3.29
λ_2	1.95	2.26
m_b (kg)	126.4	175.9
m_c (kg)	45.6	122.8
μ_1 (kg m^{-3})	1026.1	1082.1
μ_2 (kg m^{-3})	982.0	1065.1

Table 3.9 Average values for some physical parameters for the unthinned and thinned plots

From the results obtained in this part of the project it is clear that the trees in the unthinned plot are generally taller and more slender than those in the thinned plot. This leads to the unthinned plot trees having significantly higher h/dbh ratios which indicates a lower degree of stability. Brunig (1973) and Stuhr (1981) have criticised thinning on the grounds that it causes dangerously high values of h/dbh. However, in this instance the reverse would appear to be the case. As such it would appear on first sight from the results obtained here that h/dbh is not a reliable indicator of tree stability in plantations.

However, most windthrow which occurs after thinning does so soon after the thinning process has been carried out. Thus the remaining stems suddenly have much more space to sway in, and are therefore more susceptible to windthrow, until the new situation stabilises. As time proceeds though, the canopy will close again and the trees will no longer have this space to sway in and should therefore be less susceptible. Thus the h/dbh ratio is a good indicator of tree stability for open grown trees or until plantation trees are disturbed by thinning when the intrinsic stability of the tree shape is no longer the most important factor but

crown contact is.

Another conclusion which can be drawn from these results is that trees in a thinned plot are generally more heavily tapered than those from an unthinned plot. It is also clear that the power law described earlier to model stem form assuming non-linear taper (Blevins 1979) fits the trees from the unthinned plot far better than it does those from the thinned plot. The stems from the thinned plot conform better to a linear taper model. It is possible that this may be because the decrease in diameter from the base up to 9 m is very small when compared with the length of the stem, i.e. taper is negligible. This suggests that taking taper into account when estimating natural frequency of whole trees is not necessary. This suggestion forms the basis of Model 3 which assumes a columnar stem with a concentrated mass, i.e. the crown, at its free end which might be more important than the degree of taper.

Considering stem and crown mass, the heavier stems and crowns were almost always found in the thinned plot. This was as expected as these trees had far larger base diameters and broader, deeper crowns, which frequently had more and larger diameter branches. On average the crowns were more evenly distributed along the stem in the unthinned plot, and the live crown began at an average height of 6.3 m above the ground, whereas the live crown began at an average height of 3.5 m in the thinned plot and was more varied in its mass distribution along the stem. The lower starting level of the crown in the thinned plot is due to greater light penetration after thinning. The less even distribution of foliage will largely be the result of a more variable network of light patches after thinning and the crowns will develop to fill the gaps in order to take advantage of any newly available light. The size and shape of the crown will have a significant effect on the amount of energy transferred from the wind to the trees and on the extent of damping in the system.

The main parameter which was derived from the stem mass data is stem density which is also used in the determination of natural frequency using Models 1 and 2.

In general terms the stems from the unthinned plot exhibited lower densities than ones from the thinned plot but the difference was small. However, when stem density was determined up to only 9 m above the ground a larger difference was apparent. This is the result of a greater degree of variability in the density of the younger wood in the upper sections of the stem, but may also be an artifact of different weighing times. The data from the unthinned plot was obtained during autumn as opposed to summer for the thinned plot which means that the moisture content of the wood should have been greater in the thinned plot since the trees are more active at this time. Hence the density of the stems from the thinned plot should have been higher. The difference between the values of μ_1 and μ_2 within the plots is small and can be attributed to natural variation within the stems.

The final section of the chapter dealt with annual under-bark diameter increments. These results showed the expected shape of growth curve, increasing initially, levelling off and then falling as competition for light and nutrients increases. However, after thinning the growth rate increased for about 5 years. This period accounts for the larger diameters recorded in the thinned plot, but this period of improved growth can be extremely variable between trees, according to their position relative to the newly created spaces after thinning. This also suggests that the trees from the unthinned plot will have a more uniform composition and may therefore more closely approximate to the beams used in engineering theory.

The average annual under-bark increment for the unthinned plot was 0.77 cm as opposed to 0.82 cm for the thinned plot. This difference is very small but over 24 years is equivalent to an average difference of 1.2 cm. As the trees from the thinned plot were shorter and more severely tapered, the upper sections used in the above analysis tended to be smaller so this difference may be an underestimate of what actually occurs in the lower, utilisable parts of the stem.

This chapter has provided values for various physical parameters which will be used in subsequent analysis. This work has also provided an insight into some questions regarding the relative stability of the two stands and how well trees

might be modelled, as well as which processes and parameters are likely to be the most important when attempting to predict natural frequency of tree stems.

CHAPTER 4 ESTIMATION OF YOUNG'S MODULUS OF ELASTICITY

4.1 Introduction

In Chapter 3 it was explained that certain physical features of the tree stems would be used to apply engineering beam theory to predict the natural frequency or period of sway of these stems. Young's modulus of elasticity (E) is a parameter which can be derived from some of the features detailed in Chapter 3, and is a measure of the resistance to bending for any given tree. As E increases, the resistance to bending in the stem increases. Hence, this parameter is important when modelling the sway response of a tree or similar structure to any given mechanical stimulus. Equation 2.14 applies for simple structures as explained in Chapter 2 but a more complex equation is required for structures like trees.

Until recently no values of E for whole stems were available in the literature, but Cannell and Morgan (1987) have produced values based on a series of laboratory tests on green wood, they also considered treating a tapered cantilever beam as a series of untapered short sections (Morgan and Cannell 1987). Gardiner (1989) has also produced values for Sitka spruce using the bending of whole stems in the lab and swaying of trees in the forest. Milne (1989) presented figures for complete Sitka spruce using force/deflection data from trees *in situ* in a model of the stem. Gardiner (1989) derived an equation relating Young's modulus to the spring constant (i.e. force/deflection) and this equation is used in this chapter, and described in more detail in Chapter 2.

The aim of this part of the project was to estimate E for each of the stems detailed in Chapter 3, by applying a known force and measuring the deflection of the trees *in situ*. Only eleven trees were measured as a result of the time required for the complete field procedure to be carried out. However, as a result of instrument failure the complete procedure was not possible for two of the eleven trees (numbers 7 and 9). It was thought that the tabulated values of Young's modulus for structural timber (USDA 1974) and those of Cannell and Morgan (1987) might not apply to complete stems because of the presence of bark, taper, knots and

variations in the water content of the wood and over the length of the stem with season. However, the values obtained by Gardiner and Milne have been presented for comparison. Also, the estimates of natural frequency made using the engineering formulae explained in Chapter 5 require validation. If the values of E obtained here were incorrect to any great extent then the values for natural frequency obtained in the following chapter would be of little practical use.

4.2 Methods

The work carried out in this part of the study can be split into two sections. The field measurements in the unthinned plot were made in conjunction with Dr. Milne, as in Chapter 3, while those in the thinned plot were by the author alone. The methods varied slightly between the two plots as outlined below.

The estimation of Young's modulus requires a knowledge of the force required to produce a measured degree of bending in the stem at the point where the force was applied. In the thinned plot the measurements were made on the trees after the branches had been removed from the stems for the swaying measurements, while the branches were still attached when the measurements were made in the unthinned plot.

4.2.1 The unthinned plot

A cable was attached to each tree at approximately 70% of its total height (about 9 m). This height was used because 70% of the total height approximates to the centre of the live crown and equates to the point where wind loading is likely to be centred (Chapter 2). The cable was attached at the other end to a 30 kg spring balance which was in turn linked to a hand winch anchored to the ground (Figure 4.1). The spring balance was used to measure the force applied by the winch on the tree.

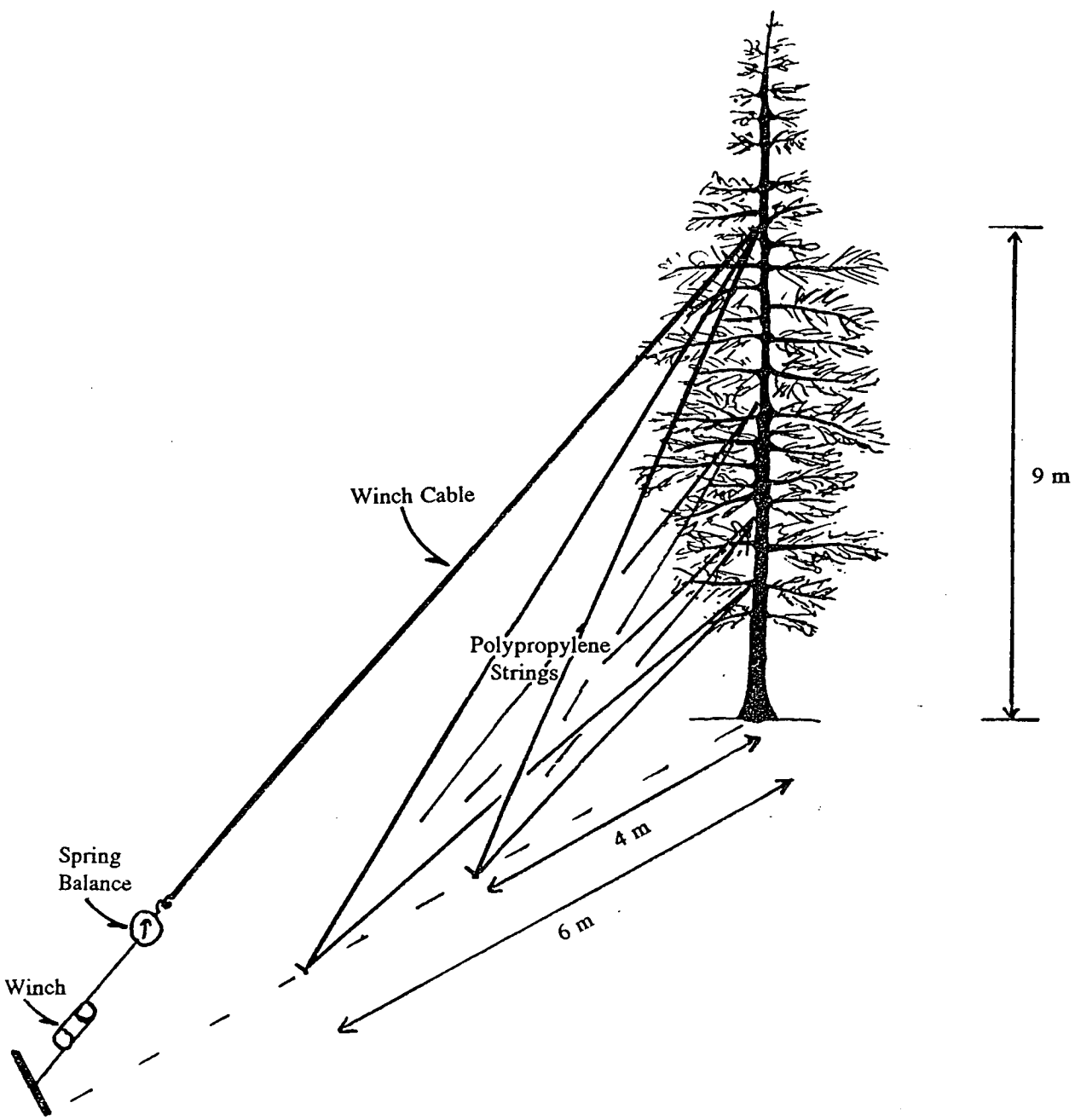

Figure 4.1 Schematic diagram illustrating the experimental set up used to estimate Spring constant (*s*) in the unthinned plot

Lengths of polypropylene string, which were to be used to measure the stem displacement, were attached to the stem at 1 m intervals from 2 m to 9 m above the ground. These strings were run down to reference points on the ground, with care being taken to ensure that none were tangled with branches. Each of these strings had previously been marked at 1 m intervals along their length using knots and tape of varying colours, to enable easy measurement of stem displacement.

To make a measurement the winch was used to take up the slack on the cable. The reading of the spring balance was taken as the zero point for measuring purposes. Each of the polypropylene strings was pulled taught and the length from the stem along each to the anchor point was recorded. This measurement was made to the nearest 1 mm. The winch was then used to apply a force on the stem until bending of the order of 1 m at the point of cable attachment was achieved. The winch was now locked while new measurements were taken from the spring balance and the polypropylene strings.

For the present analysis only the displacement at the point where the winch cable was attached was required. The remaining data on curvature are deposited with Dr. Milne for use in the verification of his iterative method of evaluating Young's modulus.

Determination of the spring constant (Figures 4.1 and 4.2)

$$s = P/y \qquad (4.1)$$

where, s = Spring constant (N m^{-1})
y = horizontal displacement at 9 m on the stem (m)
P = horizontal force applied at 9 m on the stem (N)

Force, $$P = (pg)\cos\Theta \qquad (4.2)$$

where, p = force on the spring balance (kg)
g = gravitational acceleration (9.8 m s^{-2})
Θ = angle from the horizontal to the point of attachment of the winch cable (degrees)

Displacement, $y = y_1 - y_2$

where, $y_1 = x\cos 20^\circ$
= distance from the tree to the reference point along the ground (m)

$y_2 = x\cos\Theta$

x = initial distance from reference point to point of cable attachment

This latter assumes no significant downward displacement occurs at the point of cable attachment when the stem bends. For small deflections such as those used here (0.5 m to 1.0 m) this can be accepted.

Therefore, $s = (pg)\cos\Theta/[(x_1\cos 20^\circ)-(x_2\cos\Theta)]$ (4.3)

4.2.2 The thinned plot

The basic theory behind the procedure used in the thinned plot is the same as that explained for the unthinned plot. However, for practical reasons the procedure differed slightly.

In the thinned plot the stem bending measurements were made after the branches had been removed from the stems. This was done to facilitate instrumentation of the trees and to reduce the chance of displacement lines getting snagged in the branches as the stems were bent.

The measurement of the force applied to the tree was the same as outlined earlier. The main difference between the two methods lies in the measurement of the stem displacement. In the thinned plot this was done using a single line of whipping cord running from the point of attachment of the winch cable on the tree to an LCM Position Sensing Transducer (PST 900/A, LCM Systems Ltd., Isle of Wight) attached to a wooden stake in the ground. The PST was linked to a Campbell Scientific 21x data logger (Campbell Scientific Instruments, Loughborough) programmed to read a single-ended voltage at a rate of 5 Hz. The whipping cord was used to connect the PST to the stem because of its lightweight and water resistant nature. This reduced any effect of sagging in the

line to a minimum.

Once again the initial force and stem position were recorded and then an increased force was applied using the winch with the displacement being read visually from the data logger and recorded along with the force. It was assumed once again that no vertical displacement had taken place and no reading of the angle was required as the winch cable and displacement line followed the same path (Figure 4.2). Therefore, the determination of the spring constant was as follows:

Force, $$P = pg \qquad (4.4)$$

where, p = force measured on the balance (kg)

g = gravitational acceleration (m s^{-2})

Horizontal Displacement, $$D = x_1 - x_2$$

where, x_1 = initial or static position of the stem (m)

x_2 = resultant position of the stem (m)

Thus, $$s = P/D \qquad (4.5)$$

The results from the procedures outlined above are presented in the following section. These results were analysed and used in conjunction with some of the results described in Chapter 3 to produce an estimate of Young's modulus of elasticity for nine out of the eleven sample trees. The calculation to determine Young's modulus is explained below and the computer programme used for this purpose is listed in Appendix VI.

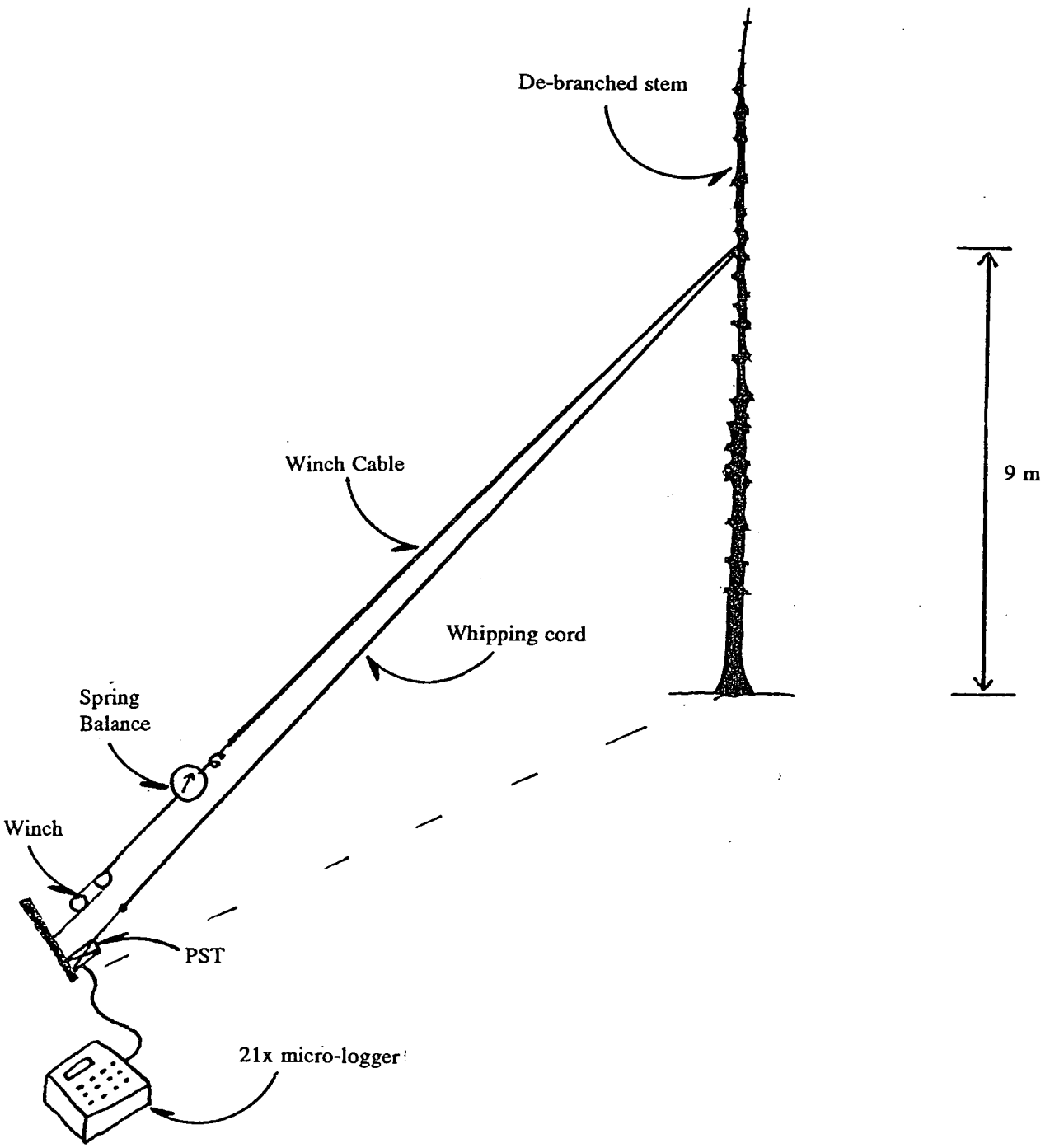

Figure 4.2 Schematic diagram illustrating experimental set up to estimate Spring constant (*s*) in the thinned plot

4.3 Results and Discussion

The results from the stem pulling experiment described above are given in Table 4.1. This table gives the force (P), the displacements (y) resulting from these forces and the resultant spring constant values.

This technique produced a wide range of values for spring constant for whole trees. The range of values is however consistent with subjective experience, for example Tree 8 was extremely difficult to bend beyond a very slight displacement which is reflected in the very high spring constant of 2009.8 N m^{-1}. Stem 4 on the other hand produced a low value of 80.1 N m^{-1}. This tree was very slender with a basal diameter of only 11.3 cm compared with the 34.1 cm for Tree 8.

Tree No.	Force (N)	Displacement (m)	Spring Constant (N m^{-1})
A 1	63.8	0.412	154.9
2	618.0	0.733	843.1
3	1010.4	0.794	1272.5
4	33.4	0.417	80.1
5	287.4	0.320	898.1
6	132.4	0.379	349.3
B 8	102.5	0.051	2009.8
10	56.5	0.072	784.7
11	56.7	0.106	534.9

Table 4.1 Spring constant values for the unthinned and thinned plots obtained by stem bending
A = Unthinned plot, B = Thinned plot.

These extreme values would appear to suggest that larger diameter stems will be harder to bend. However, the remainder of the results fail to substantiate this with values of 1272.5 N m^{-1} for a stem of only 19.5 cm basal diameter while stems of 30.6 cm and 26.1 cm have spring constants of only 784.7 N m^{-1} and 534.9 N m^{-1} respectively.

There is no clear relationship between either basal diameter or height and the spring constant where all nine trees are considered together. However, when the two plots are treated separately spring constant generally increases as both height and basal diameter of the stems increase in the thinned plot.

These results were obtained using a very basic method with a number of associated problems. First, the spring balance which was used to measure the force applied on the trees, was of a simple design with graduations of 0.2 kg. Thus it is possible that an error of the order of 0.2 - 0.4 kg could be attributed to this apparatus due to parallax. Secondly, even on the calm days selected, there was a certain amount of wind-induced motion of the stems. When this happened the stem was allowed to come to rest if possible before any readings were taken. Finally, in some cases the whole root plate moved when the stem was pulled. Clearly this would result in a different value for the spring constant as once the rootball had been disturbed it would be likely to move more easily. Hence, one might expect lower values for the spring constant. This rootball movement was more apparent in the thinned plot with the exception of Tree 8. Here the soil was wetter with surface water frequently present, which would have adversely affected root development. The area around Tree 8 had a drain running through it and this may have allowed better development of the tree's roots. If the values for spring constant for Trees 10 and 11 are low as a result of this phenomenon then variations in site conditions might explain why the relationship between basal diameter and spring constant does not apply uniformly.

This last suggestion might lead one to believe that the values of spring constant are of little use for estimating Young's modulus. However, as the rootball would probably react in a similar way when the swaying was wind-induced it is possible that these values might still be useful as a 'stem/root' elasticity and therefore were included in the following analysis.

The other parameters determined in Chapter 3 which are used along with the spring constant to calculate Young's modulus of elasticity (E) for each of the nine stems are presented in Table 4.2. The results of these calculations are also given in this table.

The trees in the unthinned plot all produce higher values of E than those from the thinned plot. However, all the values are of the same order of magnitude and in the case of the unthinned plot appear to agree reasonably with those obtained by other methods. Milne (1989) used a multi-section model of the tree stem and a matrix description of the fundamental bending laws to estimate E for Trees 1 to 6. The results of this technique are given in Table 4.3 below along with those obtained by Gardiner's method for comparison.

Other workers have also produced values for Young's modulus of Sitka spruce. Gardiner (1989) found values ranging from 3.83 to 8.43 GPa for whole Sitka spruce trees in unthinned stands. Milne and Blackburn (1989) gave values of 2.0 to 6.4 GPa for whole Sitka spruce which were bent *in situ* in a neighbouring forest block to those outlined here.

Tree	Height (m)	Basal Diameter (m)	n	Cable Height (m)	Young's Modulus (GPa)
A 1	13.0	0.133	0.71	9.0	5.18
2	14.0	0.168	0.64	9.0	9.40
3	15.5	0.197	0.72	9.0	7.47
4	13.5	0.113	0.58	9.0	4.21
5	13.5	0.197	0.63	9.0	5.41
6	13.0	0.155	0.77	9.0	6.87
Average					**6.42**
B 8	12.7	0.341	0.86	9.0	2.00
10	11.7	0.306	0.86	9.0	1.44
11	9.9	0.261	1.00	8.0	2.09
Average					**1.84**

Table 4.2 Young's modulus and the physical parameters required for its calculation for the unthinned and thinned plots
A = Unthinned plot, B = Thinned plot

Tree No.	1	2	3	4	5	6
E (GPa)	7.5	9.0	7.6	6.5	6.5	8.0 (1)
	5.2	9.4	7.5	4.2	5.4	6.9 (2)

Table 4.3 Young's modulus results according to Milne (1989) in the unthinned plot
(1 = Milne 1989; 2 = This work)

All of these values overlap well with the values obtained in the unthinned plot here. However, in the thinned plot the values are below or at the lower end of the range of the published values. It appears that thinning and the increased degree of associated taper results in lower values for Young's modulus. This may result from the slender upper stem and deep crown or juvenile core of the stem being more flexible than the stronger heartwood found below the live canopy. These low values may also be the result of the rootball movement as discussed earlier.

4.4 Conclusions

It can be concluded from this chapter that it is possible to estimate the spring constant and Young's modulus of elasticity for whole Sitka spruce trees by stem bending under a known force and measuring the displacement. The values obtained by this technique range from 4.2 to 9.4 GPa in the unthinned plot and from 1.4 to 2.1 GPa in the thinned plot. These values are consistently lower in the thinned stand which may be caused by root plate movement or less structural stiffness of the material making up the stem.

On comparison with published values these results appear satisfactory and suitable for use in the determination of natural frequency of the same stems. This will be detailed in the following chapter.

Due to the variability in the results in this chapter it might be unwise to try to use an average figure for Young's modulus for wood in whole trees, even from any given form of stand. This parameter, and its variability, is clearly dependent on a wide variety of site and tree specific features and as such needs further consideration with respect to its importance in controlling windthrow risk.

CHAPTER 5 OBSERVED AND ESTIMATED TREE SWAY

5.1 Introduction

The aim of this chapter was primarily to measure the natural frequency of the sample trees described earlier, in both the unthinned and thinned plots. Also, since engineering theory usually deals with simple beams it was considered worthwhile measuring the natural frequency of the same trees without their branches, as the bare stems would more closely approximate to engineering beams.

The other main aim of this section was to calculate the natural frequency of the stems using the three different mathematical models (Chapter 2) based on various physical features measured and estimated in the preceding chapters. It was also considered necessary to investigate the sensitivity of these models to the main parameters involved in their use.

The three models will be described as follows:

1. non-linearly tapered beam;
2. linearly tapered beam with a truncated end;
3. non-tapered beam with a concentrated mass at its free end.

Each model has its merits and the results of this study were compared with the results obtained from the field measurements and later with the results from Chapter 6.

5.2 Methods

This part of the chapter can be split into three sections. Firstly, the work carried out in the field. Secondly, the estimation of natural frequency using the various models, and finally, the sensitivity tests for each of these models to some of the parameters which are an integral part of them.

5.2.1 Fieldwork

In both the unthinned and thinned plots LCM position sensing transducers (PST 900/A, LCM Systems, Isle of Wight) linked up to a Campbell Scientific 21x data logger (Campbell Scientific Instruments, Loughborough, England) were used to measure the movement of the stems. The 21x was set to measure single-ended voltages and was connected to a tape recorder. The actual positioning and mounting of the PST's varied between plots as did the number used.

In the case of the unthinned plot four PST's were attached to each tree. These instruments were mounted on adjustable plates attached to spikes which were firmly anchored in the ground. Two of the transducers were placed at 6 m and 4 m from the base of the tree along the plough-ridge. The other two were placed at the same distances from the tree, but at 90° to the first two, i.e. across the plough-ridges (Figure 5.1). A length of whipping cord was run from each of the transducers to the tree and attached at approximately 9 m above the ground. The lengths of these lines were adjusted to ensure that each transducer was set at half extension (approximately) when the tree was static. Whipping cord was used to connect the PST's to the stems because it is lightweight and did not stretch under the force which was exerted by the spring mechanisms of the PST's. The weight of these cords was important too because heavier lines resulted in excessive sagging which reduced the accuracy of the whole system. The cord used was plastic coated 0.5 mm diameter cotton. The plastic coating prevented it from stretching or shrinking when wet.

The base plates used for the PST's were adjustable using a swivel mechanism which could be tightened to fix the position of the instrument. This enabled the PST's to be lined up correctly with the tree to reduce rubbing on the lines connected to the tree due to lateral movement.

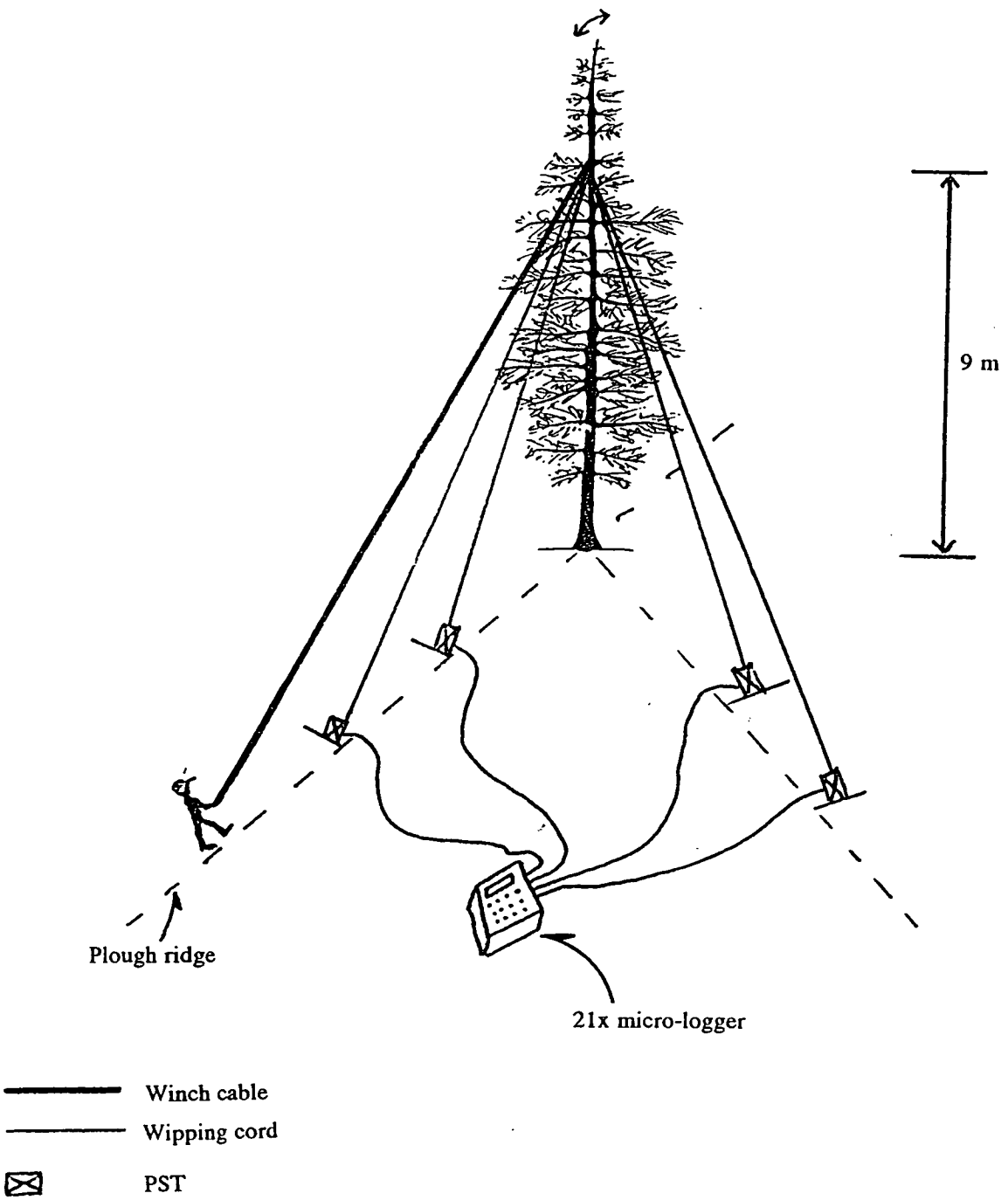

Figure 5.1 Schematic diagram illustrating the experimental set up to measure sway period of the trees in the unthinned plot

A heavier cord was attached to the tree at the same point above the ground. This cord was used as the winch cable described in Chapter 4. However, for the purposes of this experiment the cord was used to waggle the stem, which was done manually. Each stem was waggled until a significant movement was caused. The amount of movement judged to be significant varied between trees but was usually about 50 cm from the static position. The stem was then left to oscillate whilst the data logger recorded the signals from the PST's onto tape.

This waggling process was carried out four times with the pulling being directed along the plough-ridge, and four times with the pulling being directed across the ridges. The branches were then removed from the tree (as explained in Chapter 3) and the whole waggling procedure was repeated.

In the thinned plot the procedure followed was similar to that in the unthinned plot. The main differences were that only two transducers were used on each tree, and these transducers were mounted on guyed poles with the whipping cord lines being attached at 6 m above the ground (Figure 5.2).

In the unthinned plot four transducers were used as a safety measure in case any of the PST's failed to operate properly. However, this was not possible in the thinned plot due to faulty instruments. As a result some of the waggles failed to be recorded on tape in the thinned plot. However, sufficient data were obtained for analysis purposes.

The above procedure was carried out on all the trees detailed in Chapter 3 with the exception of trees 7 and 9, which were the two stems used for the wind-induced swaying measurements as described in the following chapter. The reason for these trees being omitted from the waggling procedure was that this was done at the end of the complete fieldwork procedure and too many PST's had broken, hence too few were operational for this work to be done. Fortunately, it should be possible to estimate, at least approximately, what the natural frequency should be as will be explained later.

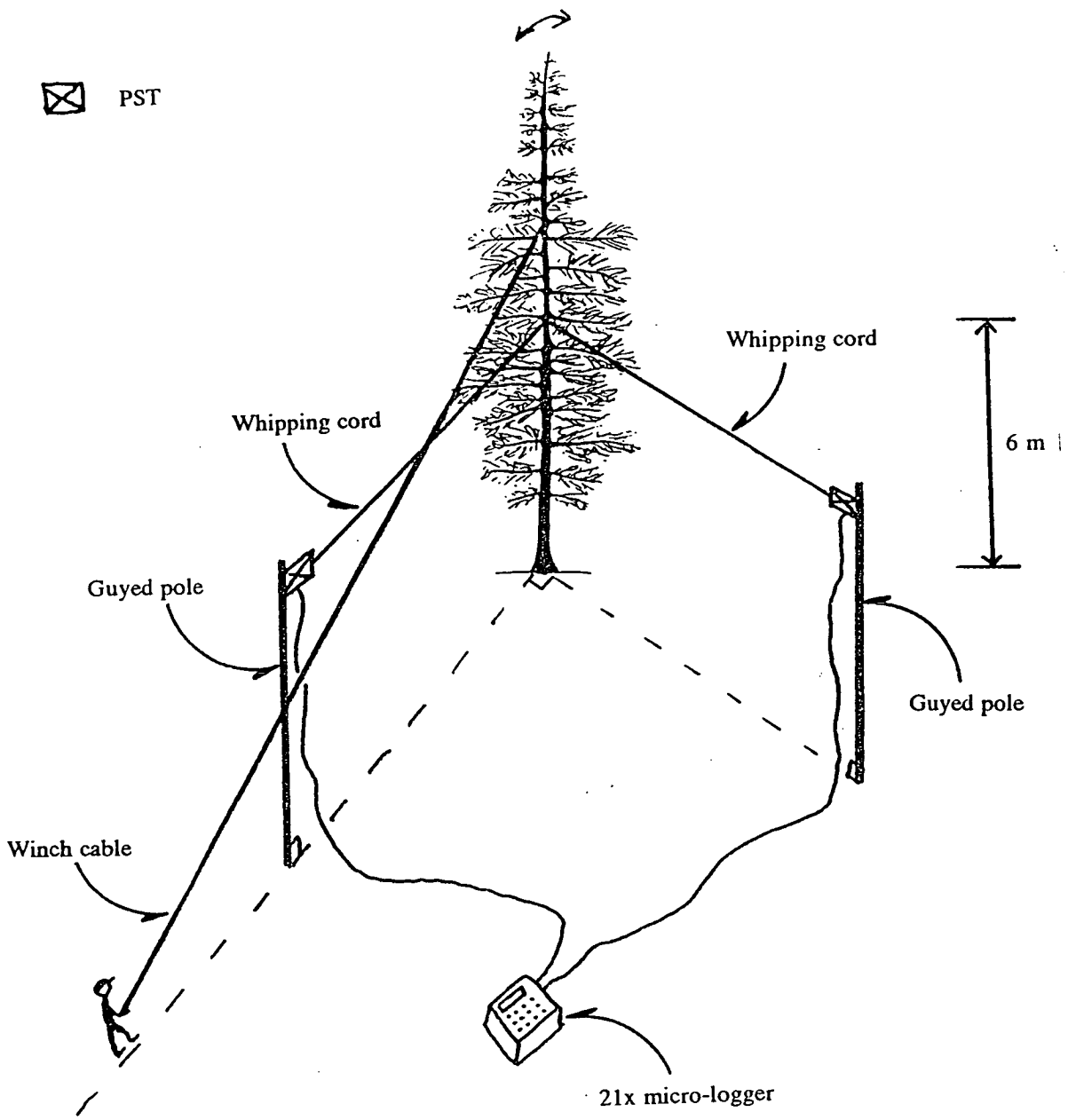

Figure 5.2 Schematic diagram illustrating the experimental set up to measure the sway period of the trees in the thinned plot

5.2.2 Estimation of natural frequency using mathematical models

The mathematical models described in Chapter 2 were used to estimate the natural frequency of the sample trees using the physical features discussed in the two preceding chapters. The three equations used to determine the natural frequency according to these models are eqs. 2.18, 2.20 and 2.21 for Models 1, 2 and 3 respectively. The computer programme used to carry out these calculations is presented at Appendix VII.

5.2.3 Sensitivity testing of the models

It was felt that testing the sensitivity of the three models outlined above to certain parameters used in them would be an essential exercise. The parameters tested were Young's modulus of elasticity (E), stem density (μ), taper parameter (λ) and stem and crown mass (m_b and m_c). These parameters were chosen largely because they themselves were the results of other models or assumptions and therefore there might be justification for some discussion as to their accuracy. Each of the models was tested for each of these parameters using the computer program presented in Appendix VII.

This sensitivity testing was a simple process of varying the parameter of concern and keeping the remaining features constant. The results of this analysis are presented in the following section along with some discussion of their importance.

5.3 Results and Discussion

The results are presented in three sections. First, the results from the field measurements of natural sway period, obtained by manually waggling whole stems, are illustrated and discussed. Secondly, the results of the calculations using the three mathematical models, detailed earlier, are presented, and finally, the sensitivity of these models to various parameters is illustrated in graphical form. Each of the above is discussed separately, and as a whole at the end of this section.

5.3.1 Stem Waggling - measured natural frequency

One set of data is presented for each of Tree 1 and Tree 8, by way of an example (Figure 5.3). These curves show how each stem was induced to sway and then allowed to come to rest from a point in time marked 'x'. Two records are given for each tree, the first shows how the stem swayed with its branches still present while subject to mechanical interference with adjacent trees, while the second gives the response after the branches had been removed. The complete set of these results is given at Appendix VIII.

The data illustrated in Figure 5.3 were used to determine the natural frequency of each stem. This was done simply by measuring the time for a given number of sways to occur (after point 'x') and dividing by that number of sways, thus the time for one sway was calculated. The inverse of this sway period is the natural frequency. This procedure was carried out for each of the sway records and an average value for natural frequency was determined for each stem with (F_m) and without branches (F_{ml}). The results of this analysis are given in Table 5.1.

Tree No.	F_m (Hz) Branches	F_{ml} (Hz) No Branches
A 1	0.30	0.49
2	0.38	0.68
3	0.37	0.63
4	0.25	0.40
5	0.40	0.65
6	0.40	0.63
8	0.55	0.56
10	0.55	0.68
11	0.59	1.45

Table 5.1 Average values for natural frequency for whole stems of Sitka spruce with and without branches
(A = Unthinned plot; B = Thinned plot)

These data show that for the complete trees with branches present the natural frequency is consistently higher in the thinned plot than in the unthinned plot, while with one exception (Tree 11) there is little difference between plots once the

branches have been removed. In the case of Tree 11, an unusually high value of 1.45 Hz was obtained. This tree was very slender and was truncated at 8 m before the second set of waggling results were obtained. This lower point of truncation was used because the stem was too thin and flexible to allow further progress up the stem while removing the branches. Thus, the total height of Tree 11 after its branches had been removed was only 8 m as compared to 12.7 m and 11.7 m for Trees 8 and 10 respectively. The loss of this height is the most likely reason for the high value of natural frequency described above.

In all cases the value of natural frequency increased after the branches had been removed, although the extent of this increase varied between trees. The increase in natural frequency can be explained in two ways. The first is the loss of momentum caused by the removal of the foliage. Secondly, a lighter object will be able to move faster for any given force.

Average values for natural frequency were measured for both plots with and without branches. In the case of the thinned plot the value for stem 11 was not included as it was considered to be unrepresentative of the main crop, due to being suppressed and poorly developed. For the unthinned plot the average natural frequency with branches and without branches were 0.35 Hz and 0.58 Hz respectively. While the estimate of average values for the thinned plot should be treated with caution, due to the lack of sample trees, these values came out as 0.55 Hz with branches and 0.62 Hz without branches.

Tree 1

With branches

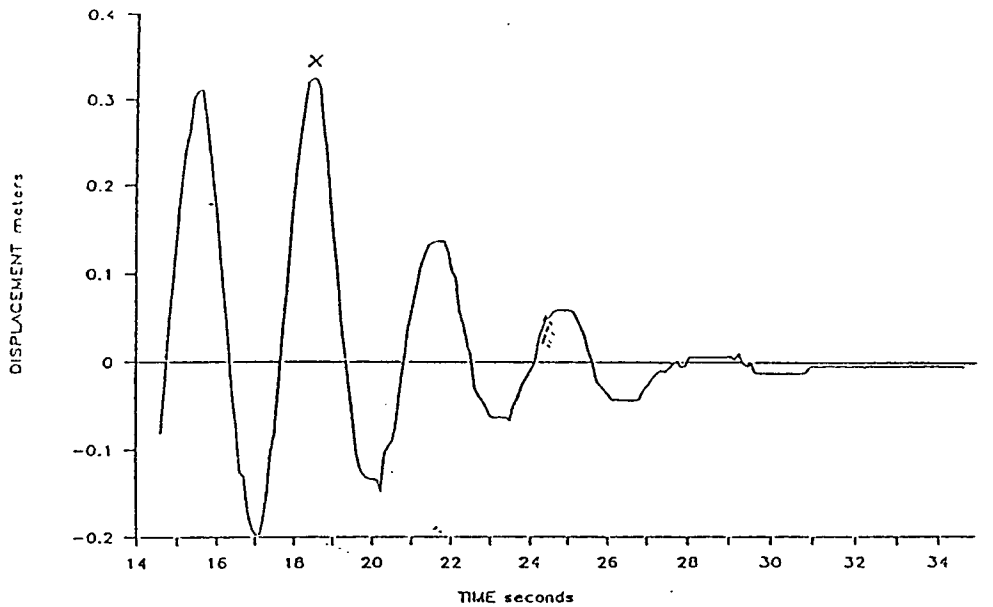

Without branches

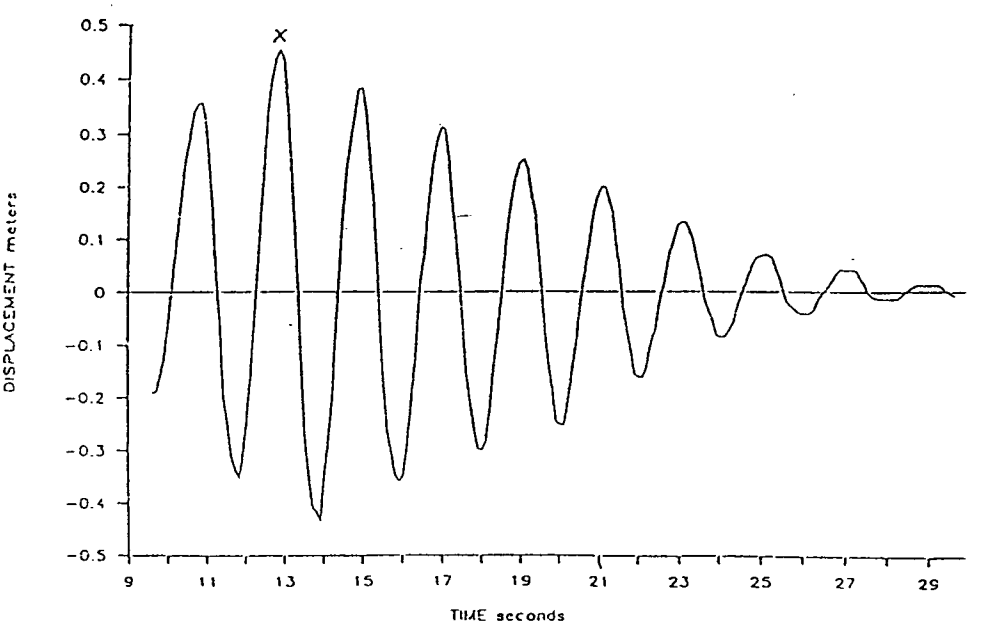

Figure 5.3 Stem displacement against time after waggling to initiate stem movement
(Tree 1 Unthinned plot; Tree 8 = Thinned plot)

Tree 8

With branches

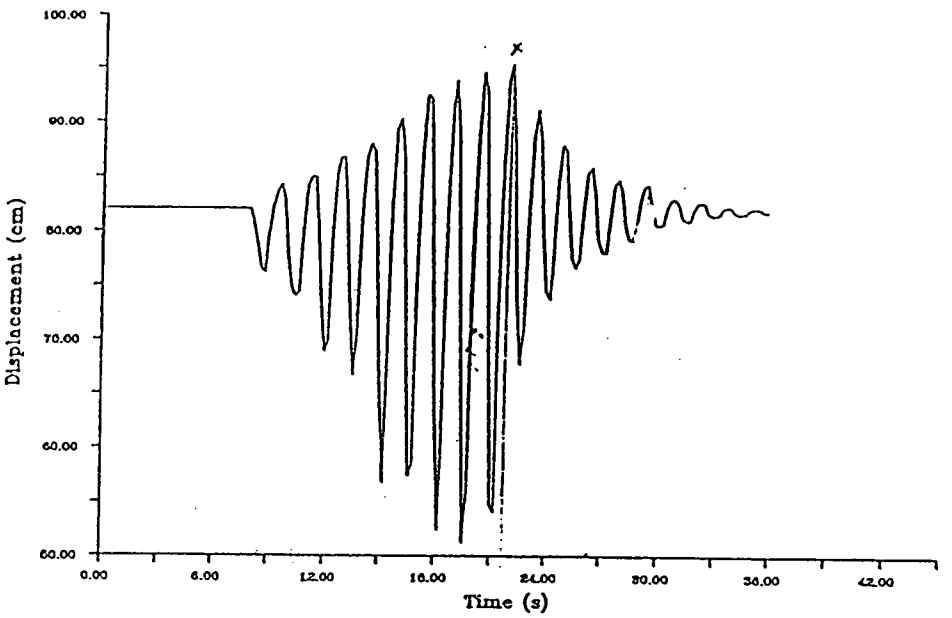

Without branches

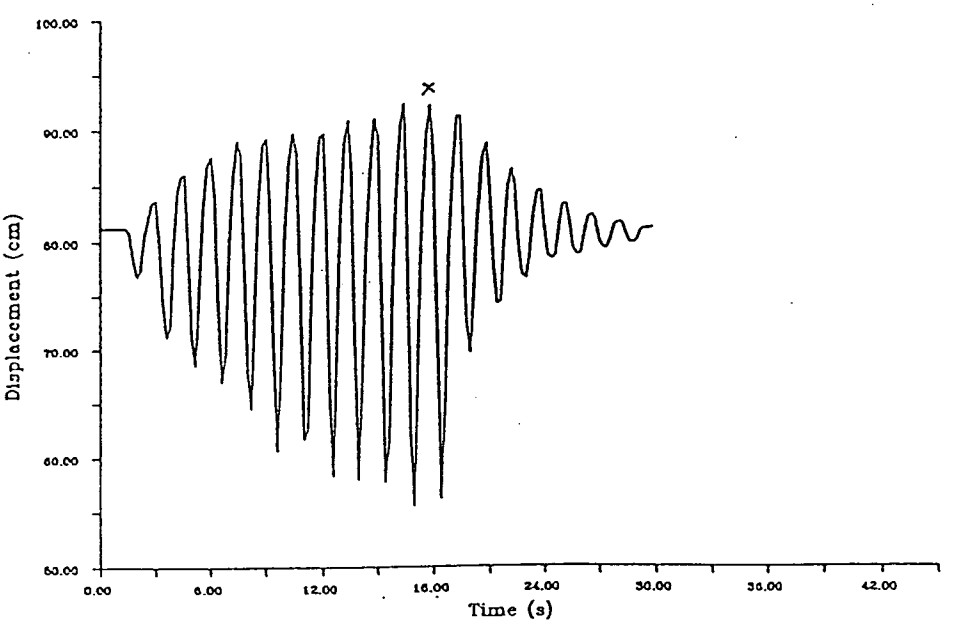

Clearly, the difference between branches being present or not is far less in the thinned plot than it is in the unthinned plot. It is possible that the reduced damping caused by removing the branches has an effect, but the interaction between damping and natural frequency is very minor and is therefore usually ignored. The more likely reason for this difference between the two plots is that the natural frequency is being effected primarily by the reduction in mass. In the unthinned plot the average foliage mass was 27.1 kg while it was 91.3 kg in the thinned plot. Thus there was a far greater reduction in mass in the thinned plot and lighter objects are able to move faster. Therefore, there should be a greater increase in natural frequency in the thinned plot than in the unthinned plot.

5.3.2 Mathematical models predicting natural frequency

The results obtained using the mathematical models detailed earlier are given in Table 5.2, along with the measured frequencies, both with and without branches, for comparison. A fourth natural frequency (F_4) is also given here. This frequency was calculated in the same manner as F_3 but the mass of all the branches was used as opposed to the mass of only the live crown in F_3. This was done to compare the two methods and to test the theory that the live crown would more closely approximate to a concentrated mass than the complete canopy would, due mainly to the former being further up the stem.

The results from the various models are as variable as the measured results, and by way of a test to check which model predicted the natural frequency most accurately, the sum of the squares of the differences between each model and the measured values was calculated. The results of this analysis are presented in Table 5.3.

Tree No.		F_m	F_{ml}	F_1	F_2	F_3	F_4
A	1	0.30	0.49	0.46	0.29	0.26	0.24
	2	0.38	0.68	0.69	0.41	0.36	0.33
	3	0.37	0.63	0.63	0.33	0.36	0.32
	4	0.25	0.40	0.31	0.20	0.22	0.19
	5	0.40	0.65	0.64	0.36	0.40	0.38
	6	0.40	0.63	0.73	0.43	0.45	0.41
	(7)	--	--	**0.53**	**0.67**	**0.24**	**0.27**
B	8	0.55	0.56	0.94	0.59	0.52	0.47
	(9)	--	--	**0.45**	**0.62**	**0.18**	**0.22**
	10	0.55	0.68	0.82	0.52	0.49	0.46
	11	0.59	1.45	1.22	0.76	0.66	0.61

Table 5.2 Natural frequency (Hz) for 9 Sitka spruce stems: measured F_m; F_{ml} and modelled, F_1-F_4
(A = Unthinned plot; B = Thinned plot)
Trees (7) and (9) were estimated using the mean value of E for each plot

The asterisked values in Table 5.3 are the best estimates. Thus, when comparing the models with the measured frequencies obtained from the whole trees, the third model is clearly the best. F_3 is the natural frequency assuming zero taper and a concentrated mass at the free end, in this case the live crown mass. The non-linear taper model (F_1) does not estimate natural frequency well for complete trees and always produces a higher value than the measured frequency, while the linearly tapered, truncated stem model (F_2) varies on either side of the measured values but is closer. The results from F_4 using the whole crown mass are consistently lower than those produced using only the mass of the live branches, but these results are still close to the measured ones. In the unthinned plot F_2 and F_3 produced virtually equally good results while all four models tended to predict natural frequency better in the unthinned plot than in the thinned one.

	Plot	F_1	F_2	F_3	F_4
F_m	Combined	0.981	0.039	0.015*	0.028
	Unthinned	0.359	0.008	0.006*	0.013
	Thinned	0.622	0.031	0.009*	0.015
F_{ml}	Combined	0.236*	0.870	1.017	1.209
	Unthinned	0.019*	0.367	0.355	0.447
	Thinned	0.217*	0.503	0.662	0.762

Table 5.3 Sums of squares of the differences between measured and modelled natural frequencies (Hz)

However, when comparing the models to the results obtained from waggling the de-branched stems the picture is quite different. In this case the non-linear taper model (F_1) is clearly the best model although it does not predict frequency as well as F_3 did for the complete stems. Here F_1 predicts the measured values very well for the unthinned plot but not quite so well for the thinned. Once again this is generally the case for all four models.

To a certain extent these results are as expected. F_1 and F_2 both take no account of the crown mass, but concentrate on modelling stem shape, while F_3 and F_4 assume no taper and concentrate on the mass of the stem and the crown. As the latter two models work for whole trees better than the former, it can be concluded that crown and stem mass are of greater importance in regulating sway period than stem shape or taper. Thus, for whole Sitka spruce trees of this size, it can be assumed that taper is not important. It can also be concluded that live crown mass more closely approximates to a concentrated mass at the end of the stem than whole crown mass does.

However, F_3 and F_4 both assume branches are present and as this is not the case for F_{m1}, it is not surprising that these models failed to produce good estimates of natural frequency. Both F_1 and F_2 produced better estimates than F_3 and F_4 in this case, but F_1 was clearly better. This suggests that bare stems more closely approximate to a non-linearly tapered beam than they do to a linearly tapering truncated one. This agrees with the visual image presented in chapter 3 (Figure 3.1).

The fact that in all cases the models predicted natural frequency more accurately for the unthinned plot than the thinned one is most likely due to the greater variation in stem form in the thinned plot, and may also be due partly to the low number of sample trees. However, it can be concluded that F_3 is the best estimate for complete stems while F_1 is better for stems with no branches.

5.3.3 Sensitivity Tests

The results of the sensitivity tests are presented in graphical form for ease of interpretation, and are averaged for the unthinned and thinned plots. Similar graphs for each individual stem are given in Appendices IX to XII.

(i) Young's modulus of elasticity (E)

The average values for natural frequency, as estimated by the three models (F_1-F_3) are given for a range of values of E (between 1 and 10 GPa) in Figure 5.4, for both the unthinned and the thinned plots. There is a non-linear relationship between frequency and Young's modulus for all three models as shown in Figure 5.4. It is also apparent that natural frequency is more sensitive to E in a thinned stand than it is in an unthinned stand. The frequency range corresponding to 1 to 10 GPa for Young's modulus is between 0.1 - 0.3 Hz and 0.4 - 0.6 Hz in the unthinned plot, while it is between 0.4 -0.6 Hz and 0.9 - 2.0 Hz in the thinned plot.

Another feature illustrated in these curves is that F_3 is less sensitive to E than F_2, which is in turn less sensitive than F_1 in the thinned plot. However, there is little difference between F_2 and F_3 in the unthinned plot, both being less sensitive than F_1. The difference in natural frequency predicted by these models also increases with Young's modulus to a greater extent in the thinned plot. Thus, it is important to use the correct value for E when calculating frequency using these models, especially in the thinned plot. The fact that F_3 is least sensitive to E may explain why it produced the best overall estimates for natural frequency for the whole stems.

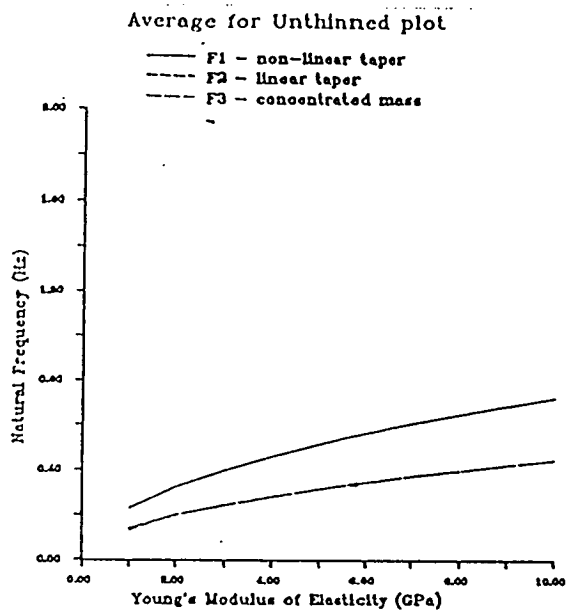

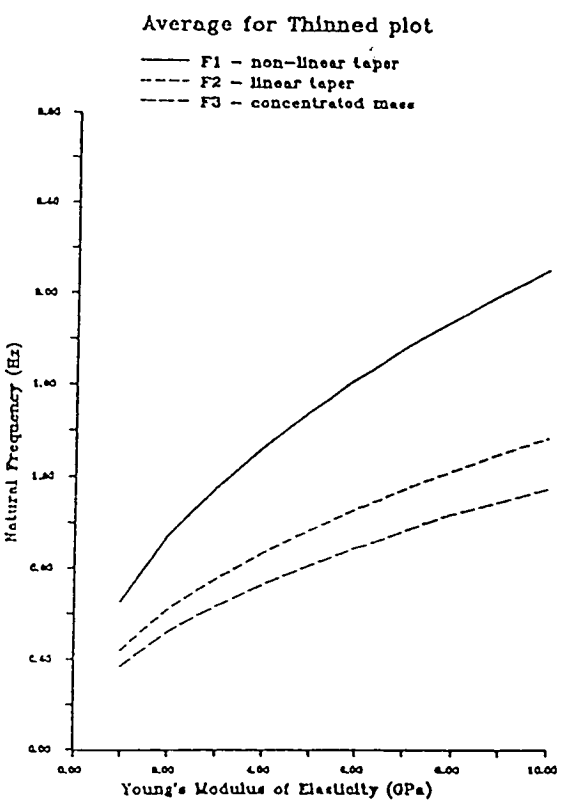

Figure 5.4 Sensitivity of natural frequency to Young's modulus of elasticity for the unthinned and thinned plots

(ii) Stem density (μ)

The linear relationship between stem density and natural frequency for the two tapered models is shown in Figure 5.5. However, in this case F_3 is independent of μ as this parameter is not included in the model. Once again F_2 is slightly less sensitive than F_1. Therefore, it is unlikely that this parameter had any great influence upon the relative merits of either of these two models for predicting natural frequency. However, as μ varied so much along the stem an average value was used for each stem, it is possible that this approximation is the source of some of the error which is not present in Model 3.

(iii) Taper parameter (λ)

Once again this parameter is not involved in Model 3, but both F_1 and F_2 show a great deal of sensitivity to it (Figure 5.6). According to work described earlier (Chapter 3), the values for λ fell between 1.8 and 2.8 for these sample trees. Therefore, this parameter must play a vital role in the effectiveness of these two models. As both models only partially describe the true shape of the stem, there is great likelihood of error arising from this part of these models. Once again, this may explain the relative accuracy of Model 3.

(iv) Stem and foliage mass (m_b, m_c)

These parameters apply only to Model 3 as they are not directly included in either Model 1 or 2, although mass is included through density and shape in these models. For both the thinned and the unthinned plots the non-linear relationships between these parameters and F_3 are shown in Figure 5.7. The natural frequency decreases as either of these parameters, m_b or m_c, increase, which supports the idea that natural frequency should increase if the branches are removed. As the sensitivity to these parameters is greatest for lower mass, then it can be assumed that any error arising from this part of the model will be less for large trees, and this would generally cover a range of frequencies of 0.25 Hz up to 0.70 Hz. This is supported by the results illustrated in Table 5.4. It is also clear from the graphs that this model is more sensitive to foliage mass than it is to stem mass, especially for lower masses.

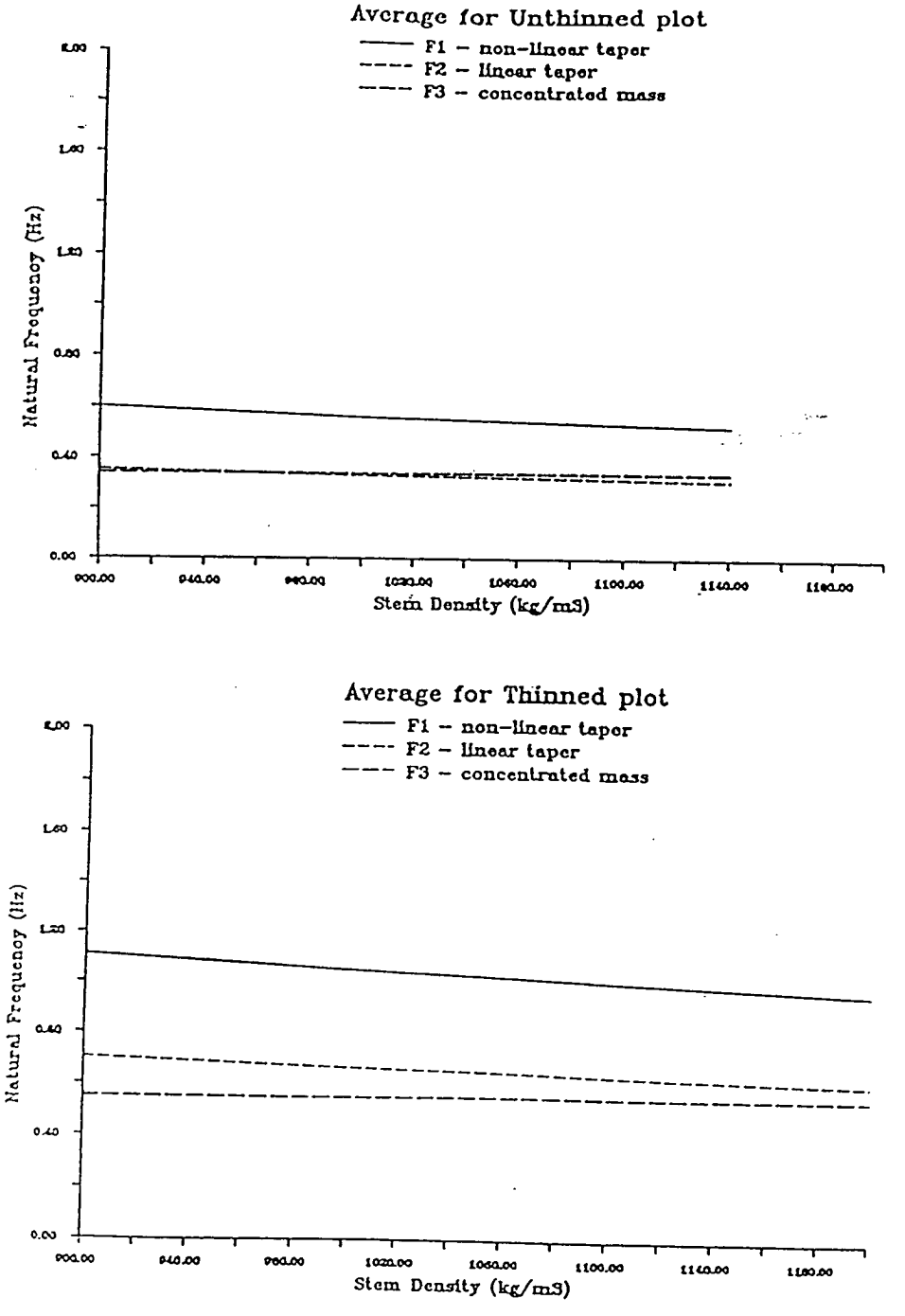

Figure 5.5 Sensitivity of natural frequency to stem density for the unthinned and thinned plots

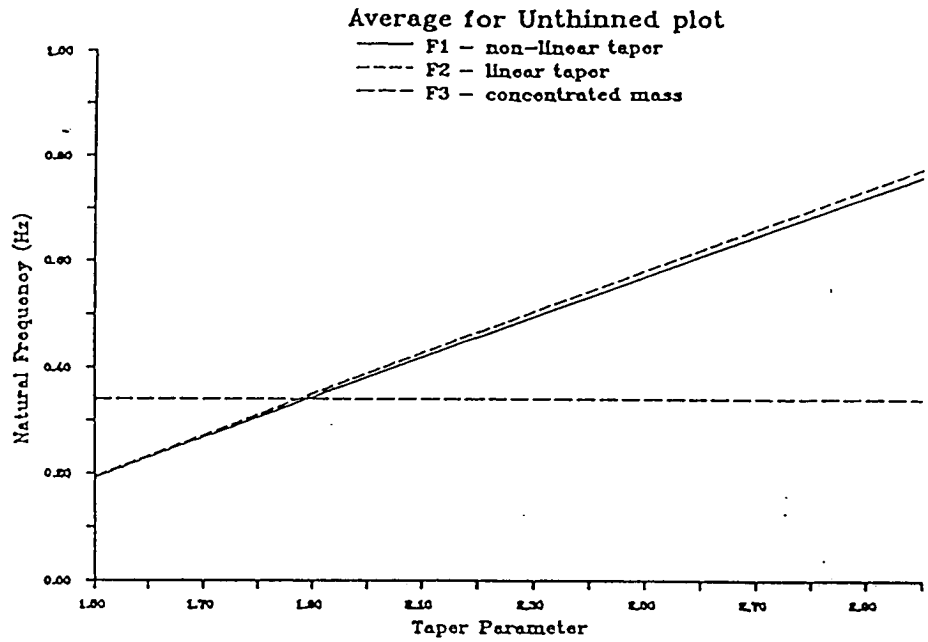

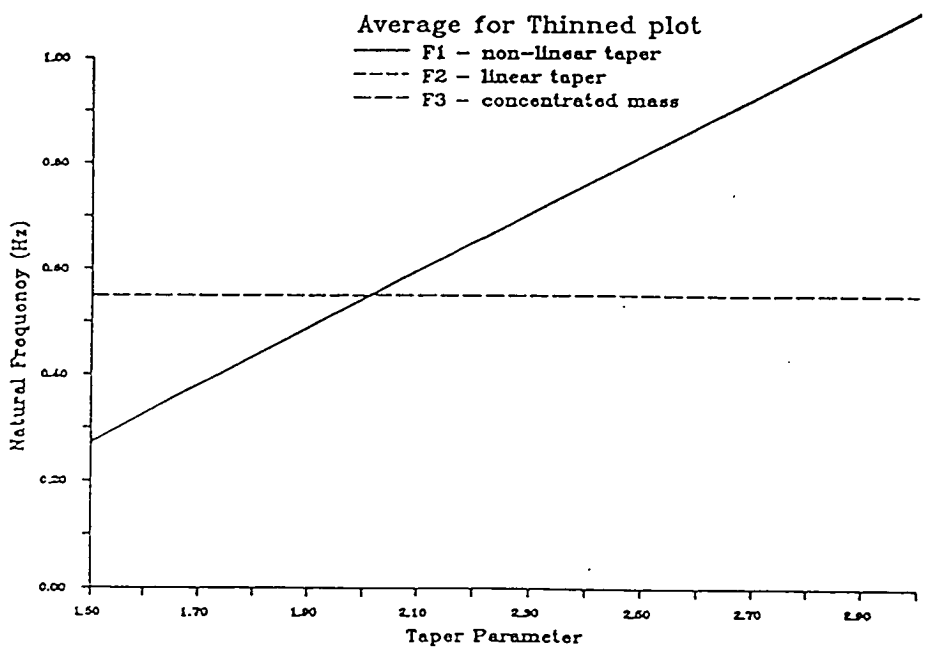

Figure 5.6 Sensitivity of natural frequency to the taper parameter for the unthinned and thinned plots

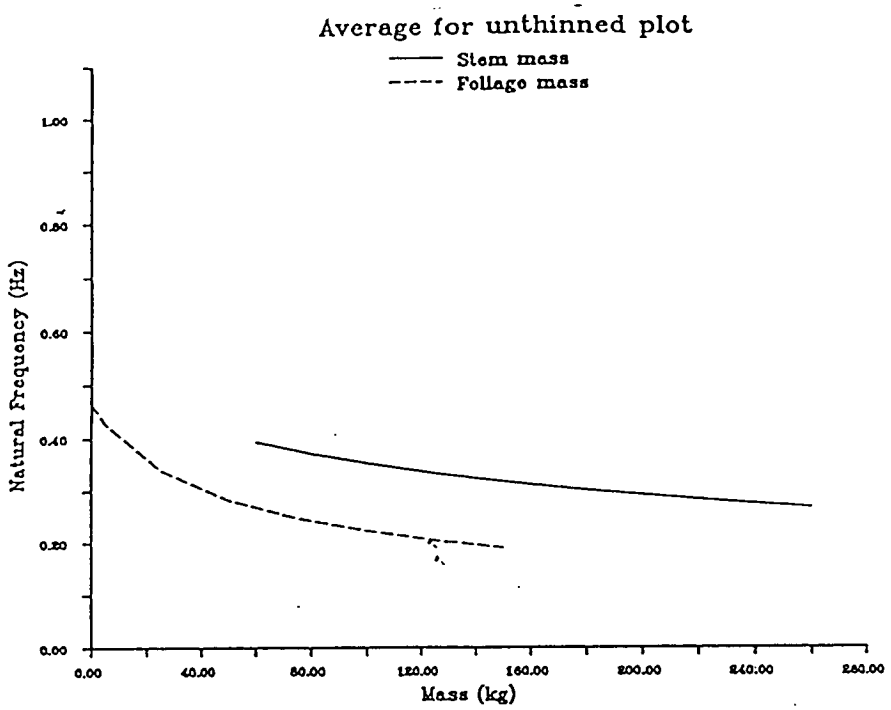

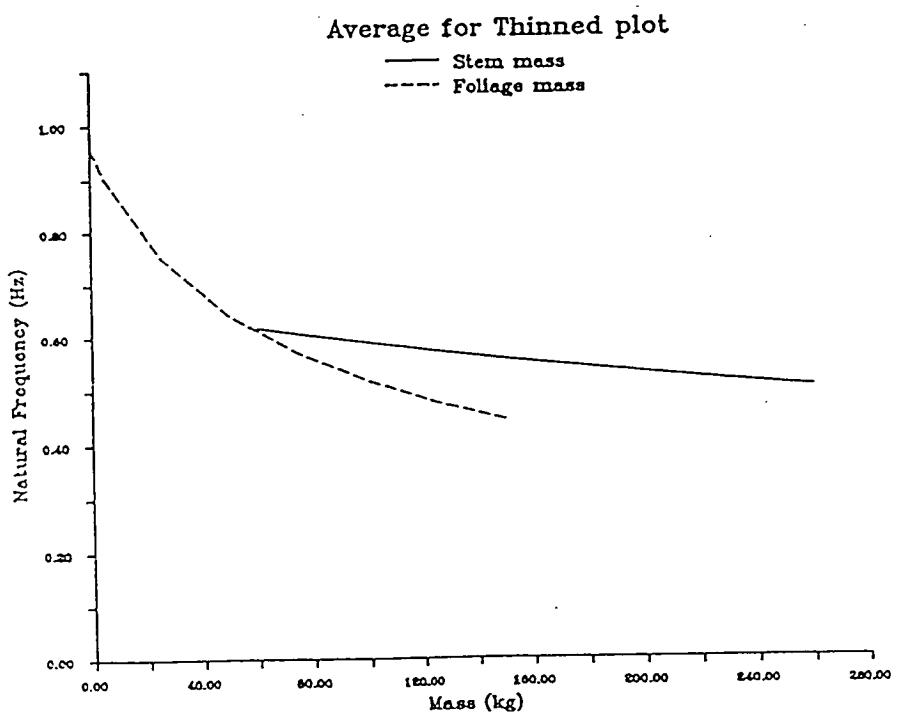

Figure 5.7 Sensitivity of natural frequency to stem and foliage mass for the unthinned and thinned plots

However, these data do not provide the answer to the question of whether this greater sensitivity to foliage mass is the result of the relative masses of the stems and foliage for the trees studied here, or more simply an artifact of the equation used where the stem mass is multiplied by 0.24 which will reduce that component's effect. This greater effect of foliage mass is likely to be caused by the position of this concentrated mass at the free end of the stem. Therefore, once the stem is displaced this mass will help further bending by the action of gravity. This effect is taken into account using the 0.24 multiplication factor for the stem mass component.

No sensitivity tests were carried out for Model 4 as the relationships would be the same as those obtained for Model 3 as the same basic equation was used for each, only the type of foliage mass was changed.

So from these four sensitivity tests some light has been thrown on the problem of why Model 3 appears to be the best estimator of natural frequency for whole stems of Sitka spruce. It can be concluded that for Models 1 and 2 the Taper parameter is most likely to cause any error, but Young's modulus and stem density will also contribute. Model 3 would appear to be more accurate for larger trees, as the model becomes less sensitive to its major components as the stem size increases.

Tree		F_m Hz	F_3	Difference	m_b Kg	m_c
A	5	0.40	0.40	0.00	160.9	37.6
	3	0.37	0.36	0.01	190.8	43.1
	2	0.38	0.36	0.02	159.7	38.9
	4	0.25	0.22	0.03	61.5	7.2
	1	0.30	0.26	0.04	78.7	23.1
	6	0.40	0.45	0.05	88.1	12.8
B	8	0.55	0.50	0.05	254.9	134.1
	10	0.55	0.49	0.06	168.6	82.5
	11	0.59	0.66	0.07	122.4	57.4

Table 5.4 Natural frequency (Hz) and Stem and Foliage mass (kg) ranked according to most accurately predicted tree first
(A = Unthinned plot; B = Thinned plot)

5.4 Conclusions

A number of conclusions can be drawn from the work described in this chapter. First, the natural frequency, or sway period, of whole Sitka spruce trees can be measured with reasonable accuracy in the field by stem waggling. Such waggling produces results which show that natural frequency increases when the branches are removed from the stem. There is an interaction between natural frequency and damping but it is very small and is therefore usually ignored. The most likely reason for this increase in natural frequency is a direct effect of reducing the mass, therefore the stem is able to move faster. By simply looking at equation 2.21 which is used in Model 3 to predict natural frequency it is easy to show the effect of removing the branches from a tree on its natural frequency. If m_c is reduced to zero then the denominator in the equation is lowered accordingly which in turn will result in a greater product of the equation, the natural frequency.

Following on from this it is possible to model the stem sway of whole Sitka spruce trees and thus predict their natural frequency from certain physical features of the stem and foliage. A model which assumes no taper of the stem and a concentrated mass, corresponding to the live crown, at its free end is the best estimator of natural frequency for whole trees. However, a model assuming non-linear taper, estimates the natural frequency of de-branched stems more accurately than the above. This is as expected as this latter model does not incorporate crown mass in its formulae. The concentrated mass model is more effective when only the live crown mass is used as opposed to the whole crown, including dead branches. This is most likely because the live crown has its centre of mass further up the stem than the whole crown and, therefore, more closely approximates to a concentrated mass at the free end of the stem.

Finally, after testing the sensitivity of the 3 models (averaged over all the sample trees) as described in the preceding sections, the first two, i.e. non-linear taper (F_1) and linear taper with a truncated end (F_2), are more sensitive to Young's modulus of elasticity (E) than the concentrated mass model (F_3), and both F_1 and F_2 are more sensitive to λ and μ, which probably explains why F_3 is a better

model to predict the natural frequency of whole stems.

CHAPTER 6 WIND TURBULENCE AND TREE SWAY

6.1 Introduction

The aim of this part of the project was to investigate the dynamics of wind-induced tree sway. Fraser (1962b, 1964) showed that the static force required to pull a tree over is far in excess of the force exerted on a tree calculated from the mean windspeed during a destructive gale. It can therefore be assumed that properties of the dynamic response to the turbulent wind come into play when trees are blown over. Several authors have considered the possibility that resonance may explain why the tree can be blown over at comparatively low mean wind speeds (Blackburn 1986, Mayer 1989).

In order to investigate the theory that some form of resonant vibration is occurring in forests it was necessary to measure both the fluctuating wind and the stem displacement caused by it. This chapter explains the methodology used to take these measurements and presents the results of the analytical methods outlined in Chapter 2 which use spectral analysis to determine a mechanical transfer function for the transfer of energy from the wind to the tree, highlighting the dynamic nature of the response.

6.2 Methods

The field measurements required for this work were made in two phases. First, the work in the unthinned plot was carried out, and second, a slightly different approach was applied to the thinned plot, although the actual measurements taken were the same. For ease of explanation a sample data set from the unthinned plot will be used as an example. The theory is explained in Chapter 2 but will be referred to frequently in this chapter using this sample data set to illustrate the concepts involved. Full results are presented later followed by a more general discussion of their significance.

6.2.1 The unthinned plot

Tree 7 was selected for these measurements because of its proximity to a Hi-way tower which had been erected at the field site some years previously. The tower was 16 m high and was used for mounting all the apparatus required to make the measurements (Figure 6.1).

Wind speed was measured using a 3 axis propellor anemometer (Model 27005 Gill UVW Anemometer, R M Young Co., Michigan, USA) mounted on a length of scaffolding tube attached to the top of the tower. The anemometer was situated 17 metres above the ground, 2.4 m above the top of Tree 7. The *u*-propellor of the anemometer was orientated north and horizontal. The Gill was connected to a 21x data logger (21x Micrologger, Campbell Scientific Instruments, Loughborough, England) which was programmed to read three single-ended voltages corresponding to the *u*, *v* and *w* components of the wind (the programme is listed at Appendix XIII).

This program determined a 10 minute running mean of the horizontal wind speed. When strong winds occurred, the secondary recording system was activated. The threshold for activation of the secondary system was set at 5 m s^{-1}. The sampling rate was set at 10 Hz because of the response time of the light-weight polystyrene propellors. The response time of the propellors depends on the wind speed, and the threshold for this model was 0.1 - 0.2 m s^{-1} with a working range of up to 22 m s^{-1}.

In this case polypropylene propellors were used to prevent them being damaged during periods of high wind speed. These propellors were 18 cm diameter x 30 cm pitch, 4 blade polypropylene (Cat No 8234) which had a higher threshold of 0.2 - 0.4 m s^{-1} and a maximum speed of 50 m s^{-1}. The 21 x was used to directly convert the voltages into wind speeds (m s^{-1}). These propellors along with the 21x programme allowed the equipment to be left running in the field until a period of windy weather occurred, after which a visit to the site would usually result in a

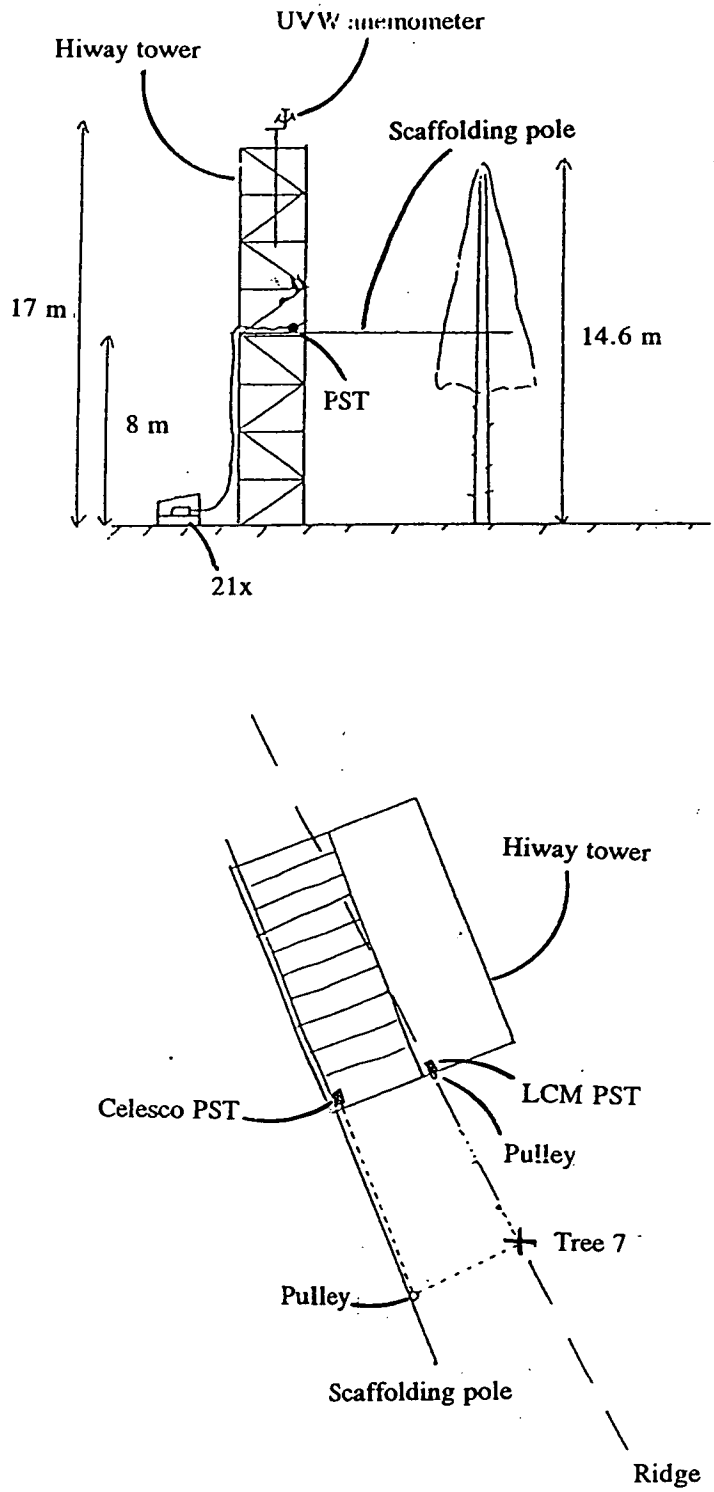

Figure 6.1 Schematic diagram of equipment layout for stem sway and wind speed measurements in the unthinned plot

tape full of data. Prior to this it had been necessary to make a 120 mile round trip to the site to switch everything on whenever windy weather was forecast. As a consequence of using the more robust polypropylene propellors the data collected would be less detailed in that the lower wind speeds would be missed. However, this was felt to be of little significance as it was the higher wind speeds and the larger gusts which were of particular interest here.

Both position-sensing transducers required a 5 V power supply which meant that after long periods of running (about 2 weeks) the battery began to lose its power and some data sets were spoiled as a result. The effect of the reduced battery power was to invalidate the calibration on the PST's as their power supply was inadequate and their output correspondingly lower. The data logger also appeared to be incapable of storing the data quickly enough, i.e. before the next sampling point 0.1 s later, when the battery voltage was low, thus some wind and displacement data appeared to get out of phase, rendering it useless. The site was therefore visited about once a week after the equipment was up and running, regardless of how windy the weather had been. At this point any data were removed and the battery taken away to be recharged.

The measurement of stem displacement used two types of position-sensing transducers, the LCM PST 900/A (LCM PST 900/A, LCM Systems, Isle of Wight) and a Celesco PT 101 (PT101 Displacement Position Transducer, Celesco Transducer Products inc., Canoga Park, California, USA). Both of these consist of a spring loaded potentiometer to which a strong cord of 1 m and 1.5 m length was attached respectively for the two models. As the cord is pulled out of the assembly the electrical resistance changes. Each transducer was calibrated in the laboratory before being used in the field. The transducer was fixed to the bench and connected to a 21x data logger programmed to read a single-ended voltage. A metre stick was fixed alongside the transducer. The voltage reading for zero extension of the cord was recorded and the cord was pulled out by 5 cm and a new voltage reading was taken. This was repeated until the cord was fully extended (900 mm for the LCM and 1500 mm for the Celesco). The calibration factor was

simply obtained by dividing the voltage by the distance extended and an average value used for the transducer. Each transducer had a different calibration so they were carefully numbered before being used in the field. The conversion of the raw voltage data into displacements was carried out in the laboratory at a later date.

Originally two Celesco transducers were used, but one was on loan from the Institute of Terrestrial Ecology and had to be returned. This Celesco was replaced by the much cheaper LCM PST 900/A which had a similar specification. However, this model experienced a series of breakdowns which resulted in the loss of a great deal of data and accounted for the major problem associated with this form of measurement.

The transducers were both mounted on the Hi-way tower, 8 m above the ground, and were connected to Tree 7 at right angles to each other using whipping cord and a pulley system (Figure 6.1). The LCM was aligned along the ridge while the Celesco was aligned across the ridge. The pulleys were used to reduce the lateral movement of the cords at the point of entry into the transducers. They also facilitated the lining up of the cords connecting the transducers to the tree. The pulleys which were used at first were too heavy and interfered with the movement of the transducers, resulting in no useful data being collected. These were later replaced by lighter plastic wheeled pulleys which worked well.

Each of the transducers was connected to the 21x logger which was programmed as explained above. The 21x provided the excitation voltage across the potentiometer and recorded the voltages produced when the position of the cord changed. Subsequently, these voltages were converted to displacements (cm), and then to x and y coordinates of displacement relative to the static position of the stem. The method of conversion is described in detail later in this chapter.

6.2.2 The thinned plot

The basic field procedure was the same as that described for the unthinned plot except for a few minor changes. First, the Gill anemometer was mounted on top of a 15 metres tall portable hydraulic mast (NK15, Hilomast Ltd, Heybridge, Essex, England) which was set on a large base plate and guyed at the top and at 3 m above the ground. The mast was erected 5 m from the base of Tree 9 which was used for this work in the thinned plot.

The two transducers were both LCM PST 900/A's which were mounted 6 m above the ground on separate guyed poles, as described earlier in Chapter 5 and illustrated in Figure 5.2. Once again the transducers were linked to the tree using whipping cord. The Gill anemometer and both PST's were connected to the 21x logger using the same program as the unthinned plot. All other aspects of the field procedure were the same for the two plots. The data from both plots were stored on tape cassette and consisted of a time series of the three components of the wind speed (m s^{-1}) along with the two displacement voltages. Each of these variables ran concurrently, separated by 0.1 seconds. The theories used in the analysis of these data were described in Chapter 2 but the chronological order followed is described briefly here using a sample data set from the unthinned plot as an example.

6.3 Analysis

The raw data were treated in a variety of ways to produce the results which are illustrated here for data set R5S3 and for all the data sets in the following section. The following forms of processing and analysis were carried out on each of the data sets, of which there were 14 from the unthinned plot and 12 from the thinned plot.

1 Correction for the non-cosine response of the Gill anemometer;
2 Coordinate rotation of the wind speed data;
3 Conversion of the displacement voltages into displacements;
4 Smoothing of the stem displacement data;
5 Calculation of stem displacement coordinates;
6 Determination of power spectra for wind speed and stem displacement data;
7 Determination of Reynold's Stress spectra;

During this procedure the mean values for the three wind speed components and the mean wind direction relative to north were determined. These values are given in the results section. Each raw data set consisted of six columns or variables and 1034 cases. The size of the data sets was determined to some extent by the spectral analysis procedure. It was necessary for the data set to consist of a number of points which was a factor of 2^n. Thus 1024 was chosen as this represented just over 100 s worth of data. The final size of 1034 data points was required to allow for smoothing of the raw data (explained later) prior to this spectral analysis which resulted in 10 points being lost. The variables will be referred to as follows:

$$time;\ u_1;\ v_1;\ w_1;\ D_{v1};\ D_{v2}$$

where, u_1 = raw data for the u component of the wind (m s^{-1})
v_1 = raw data for the v component of the wind (m s^{-1})
w_1 = raw data for the w component of the wind (m s^{-1})
D_{v1} = displacement voltage across the furrow (V)
D_{v2} = displacement voltage along the furrow (V)

and after the above mentioned analysis was complete the variables were:

$$time;\ u;\ v;\ w;\ x;\ y;\ z$$

where, u = u component of the wind (m s^{-1})
v = v component of the wind (m s^{-1})
w = w component of the wind (m s^{-1})
x = x coordinate of stem displacement (cm)
y = y coordinate of stem displacement (cm)
z = distance of the stem from its static position (cm)

6.3.1 The non-cosine response

For an anemometer to measure the resolved component of the wind speed along a particular direction, its response to off-axis components should follow a perfect cosine curve. Wind is a vector and at any instant will have a specific speed and direction in 3-dimensional space. It is convenient to describe this vector's magnitude and direction in terms of the resolved amplitude components along the

three mutually perpendicular Cartesian axes. The mathematics that does this is simply the cosine rule. Thus the anemometer should mimic this cosine 'response' to correctly measure the resolved component amplitude. The 'non-cosine response' is a statement that the propellor does not have a cosine response and correction factors compensate for this. The correction is simply carried out by use of a set of multiplication factors of between 1.0 and 2.0 depending on the direction of the wind relative to the anemometer at the instant when each case was recorded (Horst 1973).

A computer program was used to carry out this correction (Appendix XIV) but some explanation is required. The correction factors are published in the manufacturers manual and the procedure described by Horst (1973) is the basic algorithm used in the program. The raw data are used to determine the direction of the wind and the relevant vertical and horizontal correction factor (HORCOR for u_1 and v_1 and VERCOR for w_1). The direction of the wind is then determined using the new data and this is compared with the old direction. If these directions are very different, the program will iterate until the best solution, i.e. least difference between the old and new directions, is achieved. The new values for u_1, v_1 and w_1 are then stored in a new data set.

6.3.2 Coordinate rotation of windspeed data

Coordinate rotation of wind speed data is a standard procedure (Stull 1988) in treatment of meteorological data and has been explained in Chapter 2 as a prerequisite to the calculation of τ_r. This involves effectively rotating the u component of the Gill through an angle such that it faces the mean direction of the wind. The result of this process is that the mean value of v ($\overline{v}$) should be zero as the direction of the wind should vary equally on either side of the u axis. The w component was unaffected by this correction because it was orientated vertically and the rotation was purely horizontal. No vertical rotation was carried out which might result in an over or under estimation of stress. However, as this work is interested in the pattern, i.e. the peak frequency and shape of the spectra, absolute

The rotation of the data was carried out using a computer program (Appendix XV). First, the average direction of the wind for the duration of the data set (103.4 s) was determined. In the case of data set R5S3 this was 227.2° from North, or approximately South-West. This average direction, known as Θ, was entered into the program along with the complete set of non-cosine corrected data. Using a series of trigonometric equations the difference between the mean direction and the instantaneous direction of the wind was calculated. This was used to determine the new values of u and v using the following equation and a set of rules to determine the sign (positive or negative) of these components:

$$u = Y(\cos(\Theta_n))X \qquad (6.1)$$

where, u = rotated value of u component of the wind (m s^{-1})
Y = magnitude of the horizontal wind speed (m s^{-1})
$= (u^2 + v^2)^{1/2}$
Θ_n = angle between the new position (ie. after rotation through Θ degrees) of the u component of the anemometer and the instantaneous direction
X = multiplication factor of 1.0 or -1.0 depending on the angle of rotation (Θ)

A similar equation was used to determine v, but a different value of X may be used, once again depending on which quadrant the instantaneous direction falls in relative to the new position of the u component.

6.3.3 Conversion of stem displacement voltages

The calibration of the displacement transducers was carried out in the laboratory before they were used in the field (as explained in the preceding section). The conversion of the data from voltages to distances was done by multiplying the voltage by the relevant calibration coefficient.

6.3.4 Smoothing of stem displacement data

As a result of the experimental set up in the field all the displacement data showed signs of 'noise'. This random element of the data sets had to be removed before

signs of 'noise'. This random element of the data sets had to be removed before any significant analysis of the dynamics of the tree sway could be carried out. In this case appreciable 'noise' arose from small vibrations in the pulleys and cables connecting the stem to the transducers, frictional effects in the whipping cord, and some movement of the Hi-way tower during windy spells.

After visually examining the data it was felt that the amount of 'noise' was minimal but some form of smoothing was required. It was decided to use a simple running average with a 0.1 seconds step between overlapping blocks of 1 second, or 10 data points, length. This removed the majority of the extraneous peaks and produced a pattern which showed smooth sway periods of the correct order of magnitude when compared with the normal for large trees, i.e. about 1 to 3 seconds. The smoothing reduced the size of the data set from 1034 to 1024 points.

6.3.5 Calculation of stem displacement coordinates

A computer program was written to determine the x and y coordinates of the stem displacement relative to the tree's static position from the stem displacement voltages (Appendix XVI). This involved a series of trigonometric equations according to which quadrant the tree moved into. A worked example of this conversion is presented here with the help of Figure 6.2.

In Figure 6.2 the distances from the pulleys to the static tree are given as a and b, with the distance between the pulleys being c. If we take quadrant 1 as an example then the tree moves to its new position and the distances from the pulleys to the tree are d and e respectively. These form the only information which was recorded in the field. However, from these values we can calculate the angles A and B since the triangle formed by the pulleys and the tree is right-angled. Then by using the cosine rule it is possible to calculate the angles D and E as follows:

$$D = a\cos[(c^2 + e^2 - d^2)/(2ce)] \qquad (6.2)$$

$$E = a\cos[(c^2 + d^2 - e^2)/(2cd)] \qquad (6.3)$$

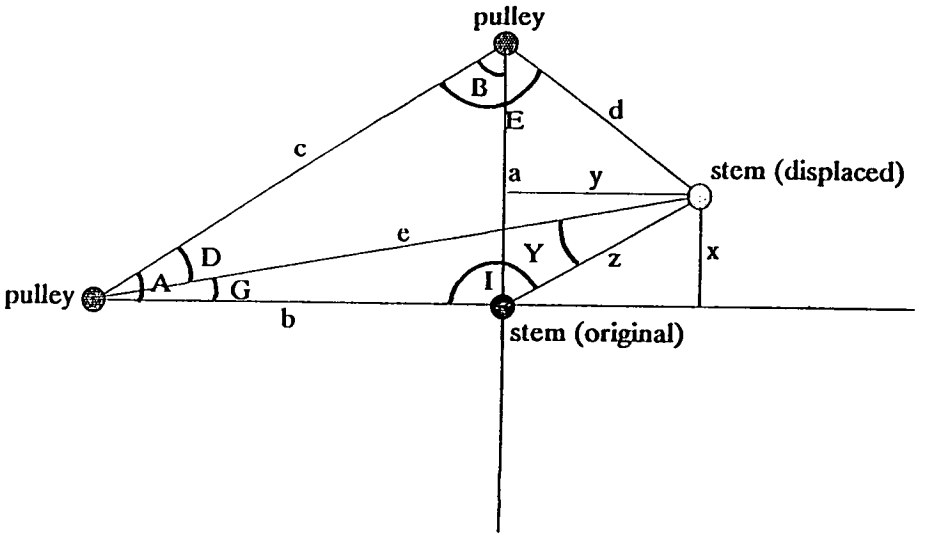

Quadrant 1

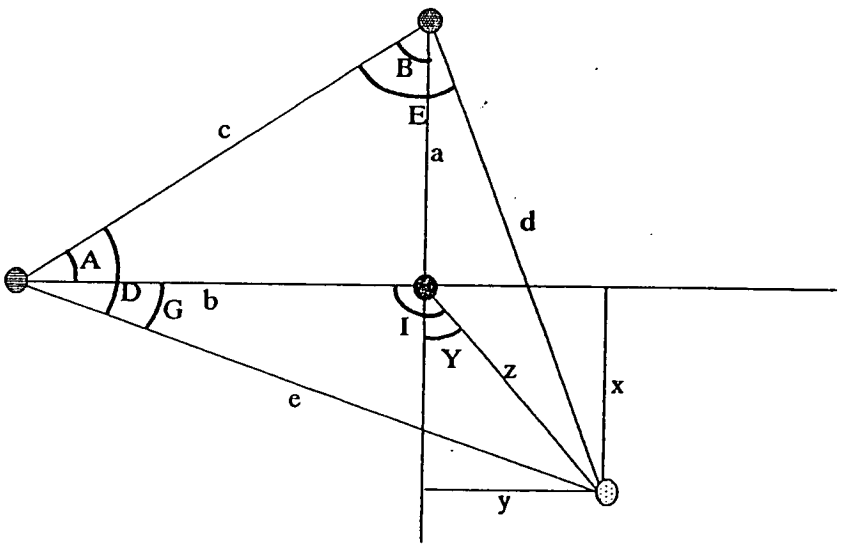

Quadrant 2

Figure 6.2 Schematic diagram illustrating the calculation of the stem displacement coordinates

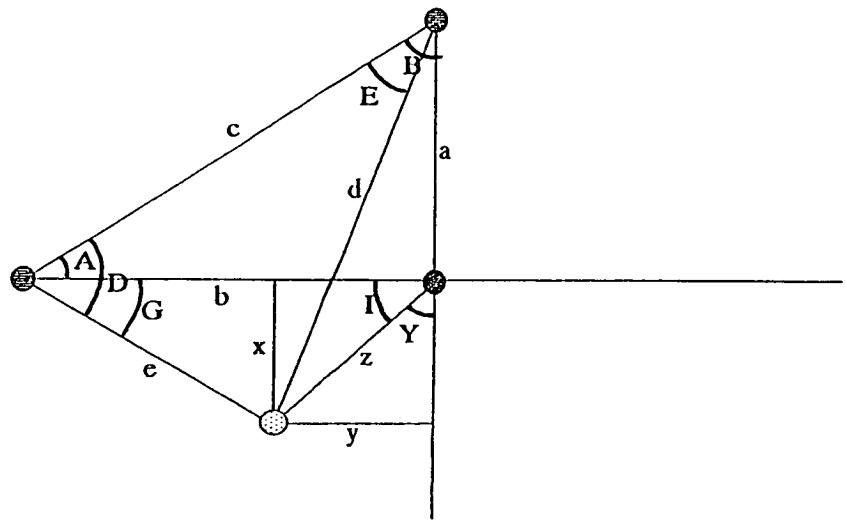

Quadrant 3

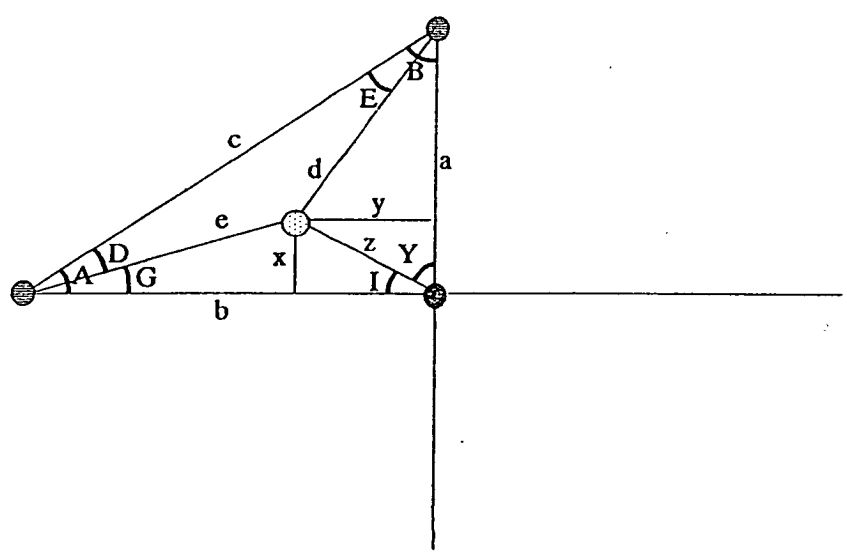

Quadrant 4

Figure 6.2 Continued Schematic diagram illustrating the calculation of the stem displacement coordinates

Depending on the relative sizes of angles A and D, and angles B and E the quadrant can be determined, then it is possible, using a combination of the cosine rule and the sine rule, to determine z and angles, G, I and Y. From these values it is then possible to determine the values of x and y. In the case of quadrant 1 the following set of equations was used:

$$G = A - D$$

$$z = [(b^2 + e^2)-(2be \cos(G))]^{1/2} \qquad (6.4)$$

$$I = a \sin(e \sin(G)/z) \qquad (6.5)$$

$$Y = I - 90^{o}$$

$$y = z \sin(Y)(-1.0) \qquad (6.6)$$

$$x = z \cos(Y) \qquad (6.7)$$

The equations 6.4 and 6.5 are the same for all four quadrants, but equations 6.6 and 6.7 change, in that the factor 1.0 or -1.0 is necessary to make the sign of the coordinate correct, as the sign of the cosine and sine vary according to which quadrant is being considered. For quadrants 1 and 4 the equations are as above, for quadrants 2 and 3 both equations are multiplied by -1.0.

Figure 6.3 shows the final product of the analysis thus far for data set R5S3. The wind speed data have been corrected for the non-cosine response and have undergone horizontal coordinate rotation, while the stem displacement data have been smoothed and converted into displacement coordinates. Similar graphs have been produced for each of the data sets and are presented in Appendix XVII for comparison, while a summary table of the average wind speed statistics is presented in the following section.

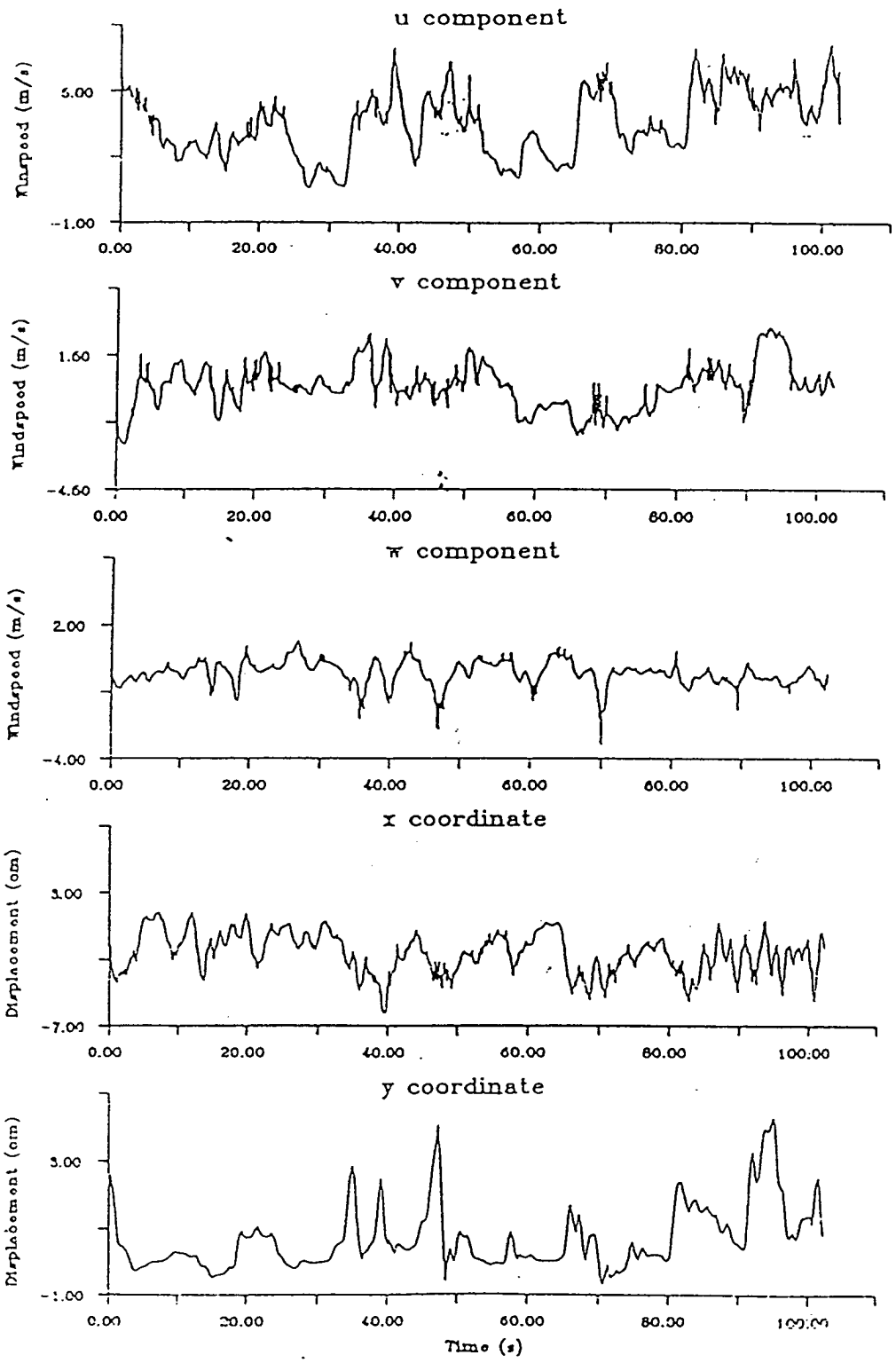

Figure 6.3 Time based plots of the wind speed components and stem displacement coordinates in the unthinned plot for data set R5S3

6.3.6 Power spectra for wind speed and stem displacement data

Spectral analysis is commonly used in meteorology to investigate time series for hidden periodicities (Chatfield 1984, Stull 1988). This use can be expanded to include any stochastic or deterministic time series although it is usual for known periodicities to be removed by smoothing first (Chatfield 1984). In this case however, no initial smoothing was carried out as any periodicities were of interest, hidden or apparent.

The theory of spectral analysis is very complex and a brief conceptual introduction is all that is required here and has been given in Chapter 2. However, some explanation of how the analysis was used follows.

The determination of the spectra for the basic wind speed and displacement coordinates time series was carried out using a NAG routine (G13CBF) written into a Fortran computer program which is listed in Appendix XVIII. The first stage was the determination of the spectral amplitudes using this program. This was done for the u and w components of the wind as these were used to determine Reynold's Stress. Both the x and y stem displacement coordinate spectra were also resolved in this way. The amplitudes were then squared to produce the power spectra shown for data set R5S3 in Figure 6.4. Thus the units for the wind speed power spectra are $m^2\ s^{-2}$, while those for the stem displacement are m^2.

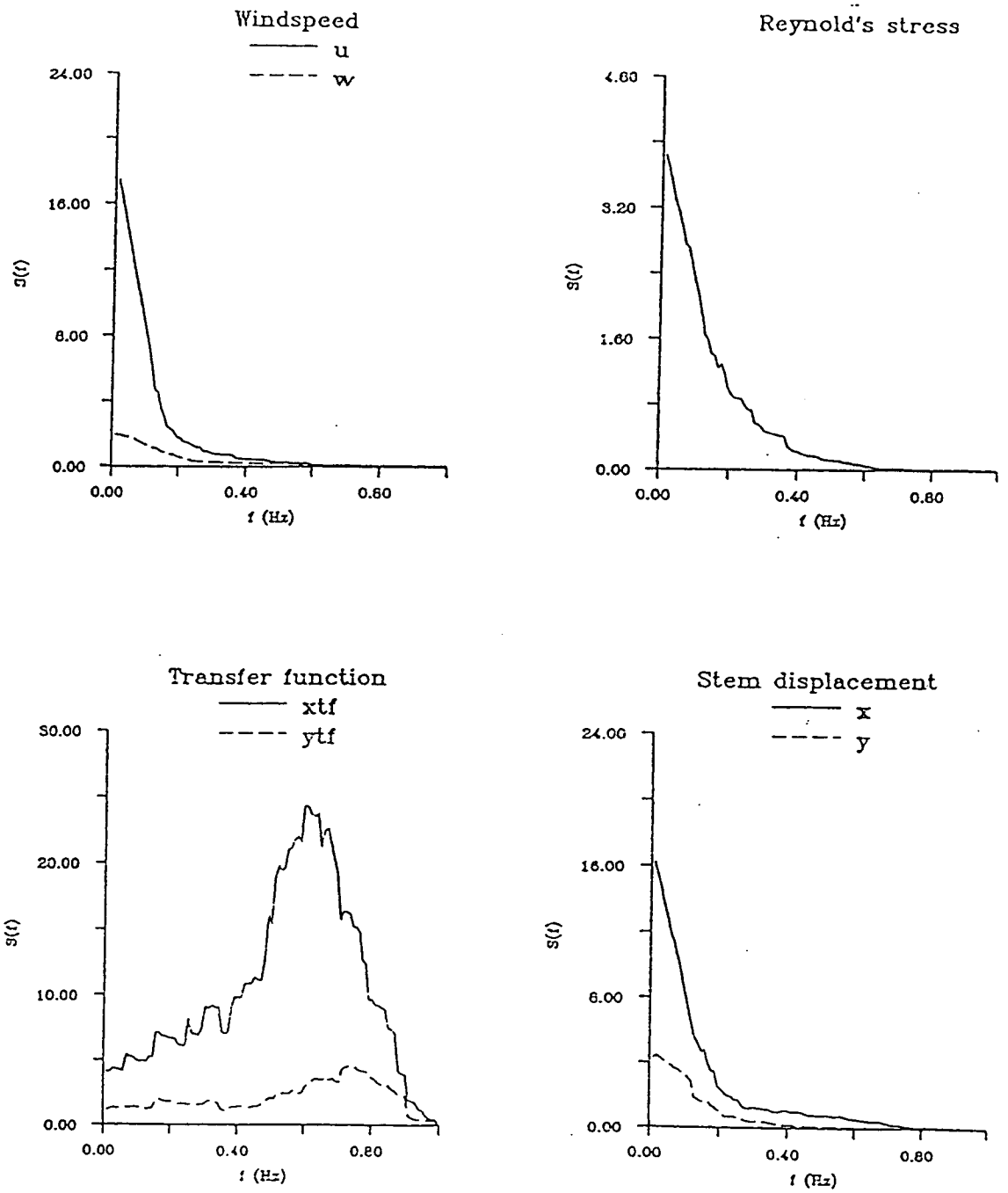

Figure 6.4 Power spectra for wind speed components *u* and *w*, Reynold's Stress and stem displacement coordinates *x* and *y* along with the mechanical transfer function
For data set R5S3 from the unthinned plot

The NAG routine G13CBF calculates a smoothed, or unsmoothed, sample spectrum of any univariate time series. This time series may be mean or trend corrected, but in this case no correction was used because it was considered that the raw data should be as unaltered as possible in order to prevent any relevant information being lost. The unsmoothed sample spectrum

$$f(\omega) = 1/2\pi\left|\sum_{t=1}^{n} x_t \exp(i\omega t)\right|^2 \qquad (6.8)$$

is then calculated for the frequency values

$$\omega_k = 2\pi k/K, \quad k = 0,1,\ldots,[K/2] \qquad (6.9)$$

where, $f(\omega)$ = amplitude for frequency ω
x_t = data point from the time series at time t
K = order of the Fast Fourier Transform, must be $>2n$ where n is the number of data points

The output from this program is a series of spectral amplitudes corresponding to frequencies ranging from zero to $K/2$. In this case only frequencies of up to 1 Hz were of interest as the trees could not possibly sway any faster than this and 1 Hz was the highest sampling rate appropriate to the response time of the Gill anemometer. These amplitudes were then squared to produce the power spectra for each of the variables as shown in Figure 6.4.

6.3.7 Determination of Reynold's Stress Spectra

The theory of Reynold's Stress has been covered in Chapter 2 but the procedure used to determine the τ_r spectra is described here.

When calculating the power spectrum for τ_r the process is somewhat different to that used for the wind speed components described earlier. In this instance the cross-spectrum between the horizontal and vertical wind variates must be determined. The cross-spectrum is produced from two, simultaneous time series, i.e. u' and w'. For the purposes of this analysis another NAG routine (G13CDF) (ERCC 1989) was used to carryout the Fourier transform.

G13CDF calculates the smoothed, or unsmoothed, cross-spectrum of any bi-variate time series. Once again the time series may be mean or trend corrected before the calculation, but this was not done here for the same reasons as before. The NAG routine was once again incorporated into a computer program to carry out the analysis required here (Appendix XIX). These spectral amplitudes were then multiplied by μ_a (air density, kg m^{-3}) to obtain the values for Reynold's Stress. The spectral amplitudes were squared to produce an energy spectrum as illustrated in Figure 6.4. For plotting purposes all four spectral plots in this figure underwent a simple smoothing process using a running average over a block of 0.06 Hz with a step of 0.003 Hz per block. This reduced the variability of the spectra while retaining the important information.

6.3.8 Calculation of the mechanical transfer function

The mechanical transfer function ($S(f)_{TF}$) between the power spectrum of the Reynold's Stress of the wind and the power spectrum of the resultant stem displacement, either $S(f)_x$ or $S(f)_y$ is of great value when looking at the dynamics of wind induced tree sway. This system of illustrating frequencies at which the tree might develop large sways was used by Mayer (1989) and is very simple to apply and to analyse. The basic theory is presented in Chapter 2. It is important to remember that this Reynold's Stress is equivalent to the drag force exerted by the wind per unit ground area passed by that parcel of air, i.e. the units of Reynold's Stress are N m^{-2}. The power spectrum obtained for Reynold's Stress as described above is the square of the amplitude spectrum, therefore the units are (N m^{-2})^2 which is equivalent to kg^2 m^{-2} s^{-4}. Therefore, the mechanical transfer function is the displacement per unit drag force and quantifies the displacement to force relationship for all turbulence regimes, i.e. the dynamic response of the tree.

The calculation of $S(f)_{TF}$ is

$$S(f)_{TF} = S(f)_x / S(f)_{rr} \qquad (6.10)$$

where, $S(f)_{TF}$ = mechanical transfer function at frequency f (m^4 s^4 kg^{-2})

$S(f)_x$ = power of the x coordinate of displacement spectrum at frequency f (m^2)

$S(f)_{rr}$ = power of the Reynold's Stress spectrum at frequency f ($kg^2\ m^{-2}\ s^{-4}$)

The Transfer function results obtained for sample data set R5S3 are given in Figure 6.4 along with the components used to determine them. The complete set of results for all the data sets is discussed in the following section.

6.4 Results and Discussion

The results from the wind-induced sway measurements are presented here for both the unthinned and thinned plots. A brief summary of the wind conditions measured in each data set is given in Table 6.1, while actual traces in the time domain for the three components of the wind as well as the x and y stem displacement coordinates (as in Figure 6.3) are given for selected data sets in Figure 6.5. A complete set of results is presented at Appendix XVII.

The results from the spectral analysis are presented in a similar form to Figure 6.4 for the same selection of data sets as above, in Figure 6.6 with a complete set of graphs being presented at Appendix XX. However, a summary, or mean spectrum was determined for each component for the unthinned plot and the thinned plot (Figures 6.7 and 6.8 respectively).

6.4.1 Mean wind statistics

Table 6.1 presents the average values from each data set for u and v prior to, and after the coordinate rotation had been carried out, along with mean values for the w component and the original wind direction. A number of important features of these results should be highlighted at this stage. The data obtained from the thinned plot were taken during substantially windier weather than those from the unthinned plot. The average wind speed (u component, after coordinate rotation) was 2.63 m s^{-1} in the unthinned plot while it was 4.33 m s^{-1} in the thinned plot.

These wind speeds might at first glance appear to be quite low, but it is important to remember that they were recorded about 1.5 m above the canopy. Therefore, they correspond to much stronger winds as measured at a meteorological station due to the drag effect of the canopy.

Data Set	Before Coordinate Rotation *u*	*v*	*w*	After Coordinate Rotation *u*	*v*	Original Direction
Unthinned plot						
R4S1	-0.28	-2.15	0.32	2.17	0.01	97.4
R4S2	-0.45	-3.09	0.31	3.13	-0.05	97.2
R5S1	-1.41	1.57	-0.04	2.10	0.13	232.0
R5S2	-1.19	1.41	0.05	1.84	-0.07	228.2
R5S3	-2.43	2.49	-0.16	3.47	0.08	227.2
R5S4	-2.90	2.18	-0.12	3.63	0.02	217.4
R6S1	-0.03	-3.02	0.28	3.03	0.01	90.7
R6S2	-0.28	-2.36	0.29	2.38	-0.03	95.9
R6S3	-0.43	-2.62	0.33	2.66	-0.03	98.6
R6S4	-0.10	-2.92	0.26	2.94	0.01	91.9
R7S1	-0.25	-2.46	0.29	2.48	-0.44	95.3
R7S2	-0.38	-2.39	0.26	2.43	-0.53	97.2
R7S3	-0.05	-2.05	0.19	2.05	-0.30	90.3
R7S4	0.02	2.49	0.25	2.49	-0.01	89.0
Average			0.20	2.63	-0.09	
Thinned plot						
R8S1	-3.32	-3.38	0.50	4.73	0.06	135.2
R8S2	-3.80	-3.52	0.21	5.17	-0.22	134.7
R8S3	-2.93	-2.80	0.14	4.06	-0.02	136.1
R8S4	-2.83	-3.15	0.34	4.24	-0.15	130.0
R8S5	-3.42	-3.24	0.36	4.72	0.30	140.0
R8S6	-2.56	-2.80	0.19	3.79	0.03	133.0
R8S7	-2.41	-2.55	0.36	3.50	-0.02	133.1
R8S8	-2.37	-2.13	0.32	3.19	-0.07	136.7
R10S1	-3.74	-4.43	0.07	5.78	-0.07	129.5
R10S2	-2.60	-3.54	0.19	4.39	-0.06	125.5
R10S3	-2.62	-3.11	0.19	4.07	-0.08	128.9
R10S4	-2.53	-3.44	0.11	4.27	0.06	127.1
Average			0.25	4.33	-0.02	

Table 6.1 Mean wind component values (m s^{-1}) and original wind direction (degrees from north) for the two sample plots

The wind data recorded in the thinned plot were also more turbulent than those from the unthinned plot, as can be seen from the spikier nature of the graphs in Figure 6.5. This greater degree of turbulence is probably the result of the higher wind speeds although the rougher canopy present after thinning might also have added to the turbulence. This thinning process has left gaps and hollows in the canopy which increases the turbulent action of the air.

As would be expected from the windier conditions, larger stem displacements were recorded in the thinned plot than in the unthinned plot. There are no mean values presented for the stem displacement coordinates because the instantaneous values should vary either side of zero as the tree swayed, resulting in an average value of zero.

6.4.2 Time domain results

By looking at the selected time domain graphs in Figure 6.5 it is clear that the stem moved further in the thinned plot data sets, as explained above. However, while the deflections in the thinned plot may have been larger they were fewer in number over a given time period. These graphs also show that the motion of the stem was more variable in the unthinned plot than it was in the thinned one. This may be due to greater inter-crown contact with neighbouring trees.

There are signs in these graphs, from both plots, that the trees became caught up with neighbours. This can be seen in data set R5S2 at about 85 to 90 seconds where the *y* coordinate of the stem is clearly displaced but not varying greatly. Again, and to a greater extent, at about 50 seconds for the *y* coordinate in R10S2 and at 75 seconds and 90 seconds in R10S3 for the *y* coordinate. This does occur in both plots but is generally more frequent in the unthinned plot, as would be expected when the tree has less space in which to sway (Appendix XVII). Alternatively, this phenomenon might arise from periods where the stem has been consistently displaced by a strong gust of lengthy duration. The stem sways are more clearly defined in the traces from the thinned plot than they are in the unthinned plot. There is obviously less interference from sources other than the wind in the thinned plot, thus the tree is more likely to sway at its natural frequency.

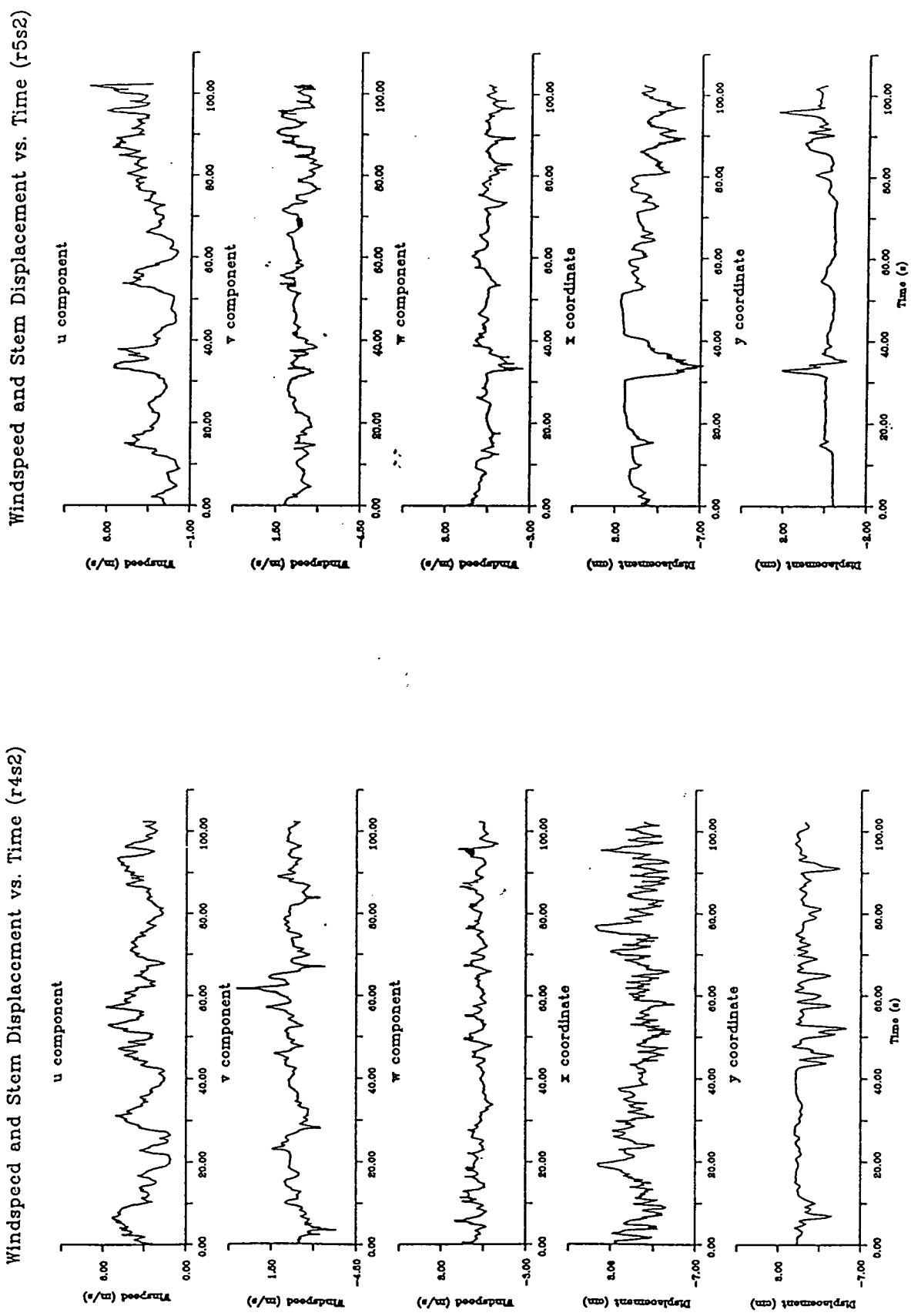

Figure 6.5 Time domain plots of the wind speed components and stem displacement coordinates from selected data sets

Windspeed and Stem Displacement vs. Time (r6s1)

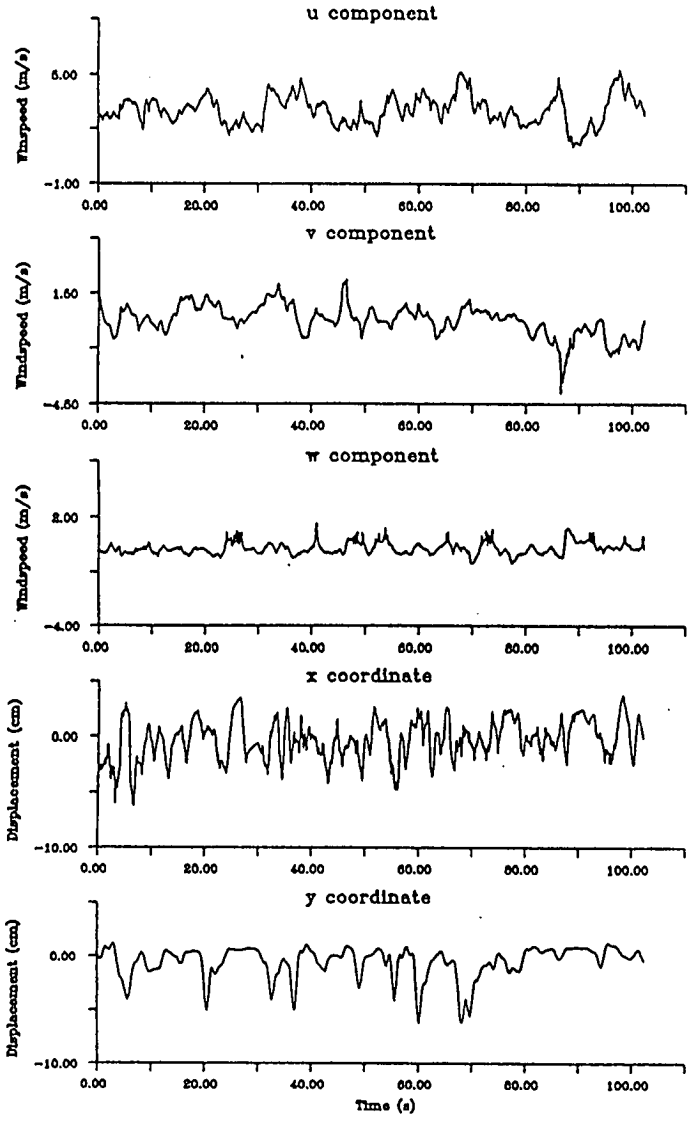

Windspeed and Stem Displacement vs. Time (r7s1)

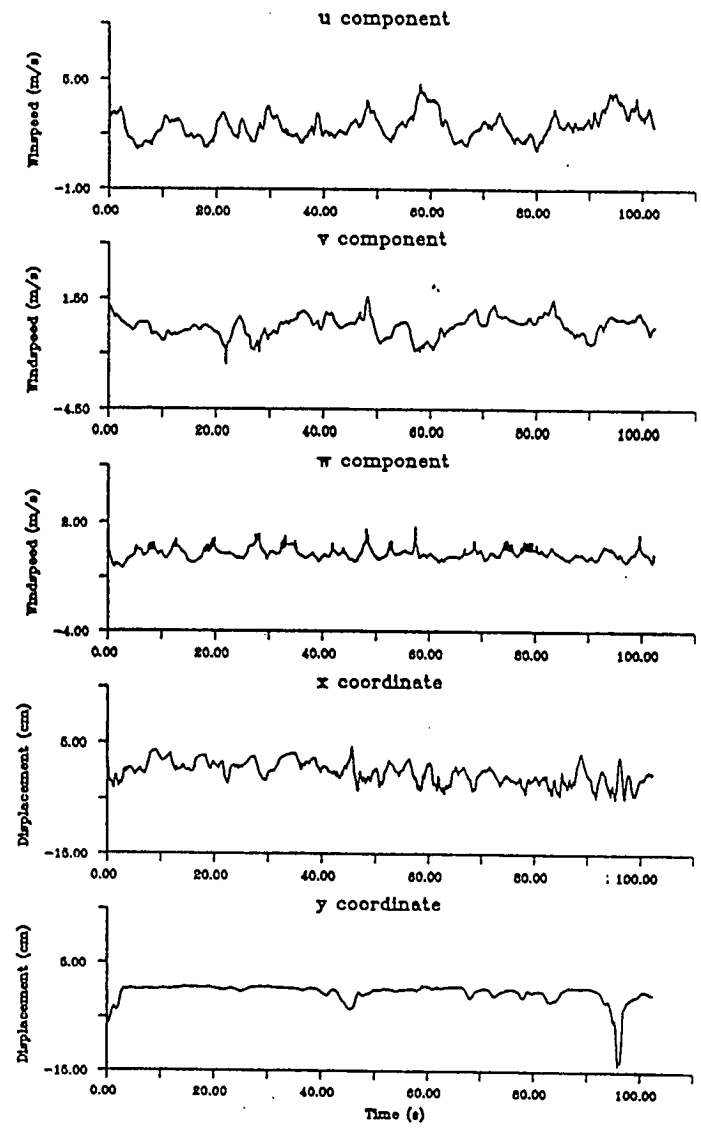

Windspeed and Stem Displacement vs. Time (r8s2)

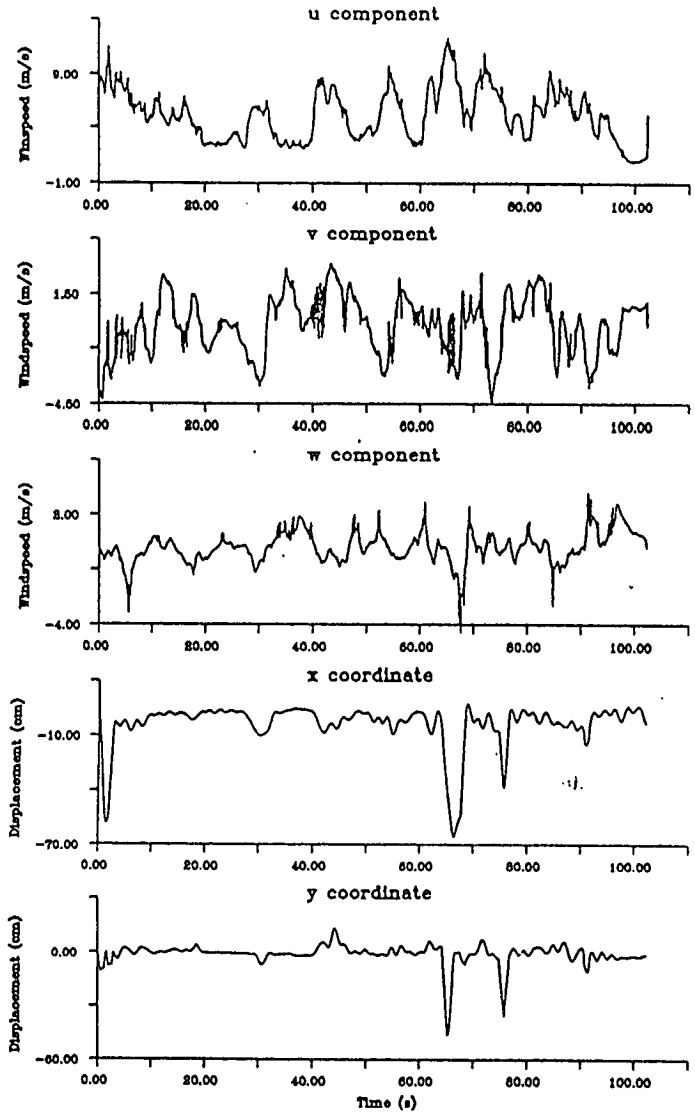

Windspeed and Stem Displacement vs. Time (r8s4)

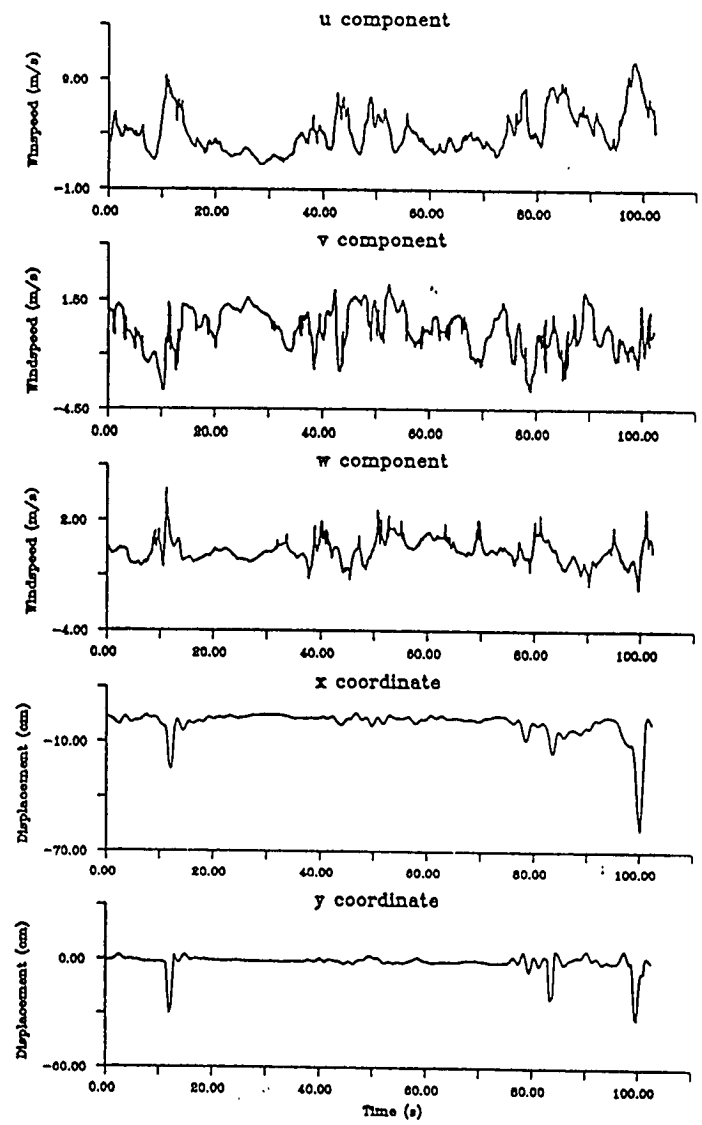

Windspeed and Stem Displacement vs. Time (r10s2)

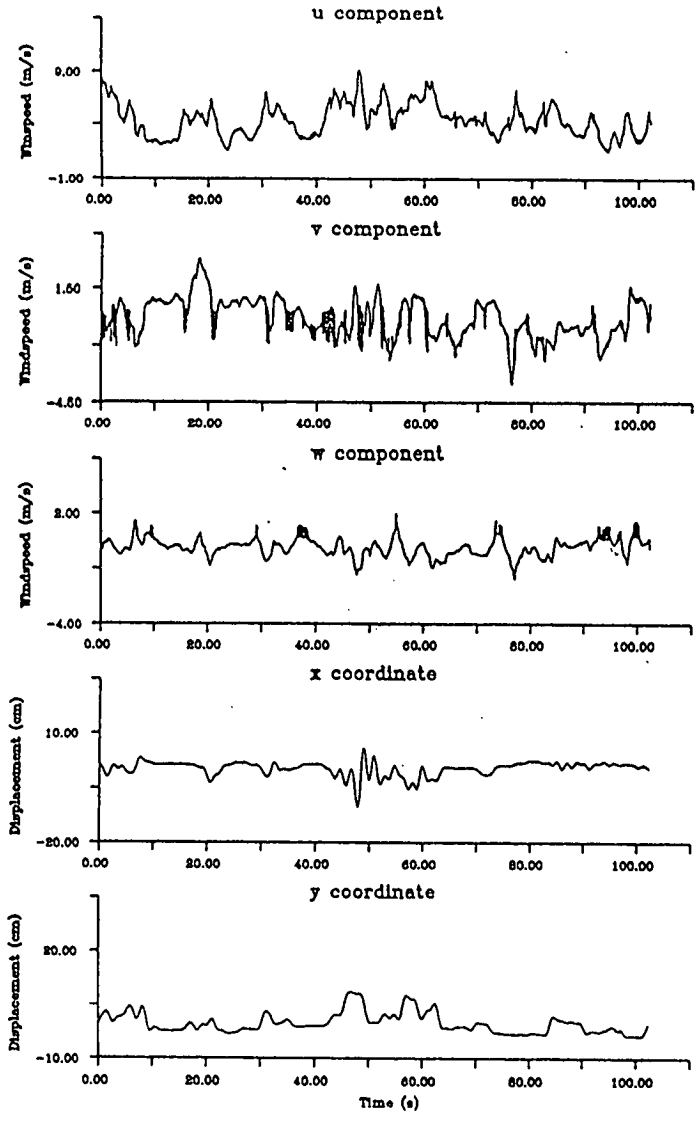

Windspeed and Stem Displacement vs. Time (r10s3)

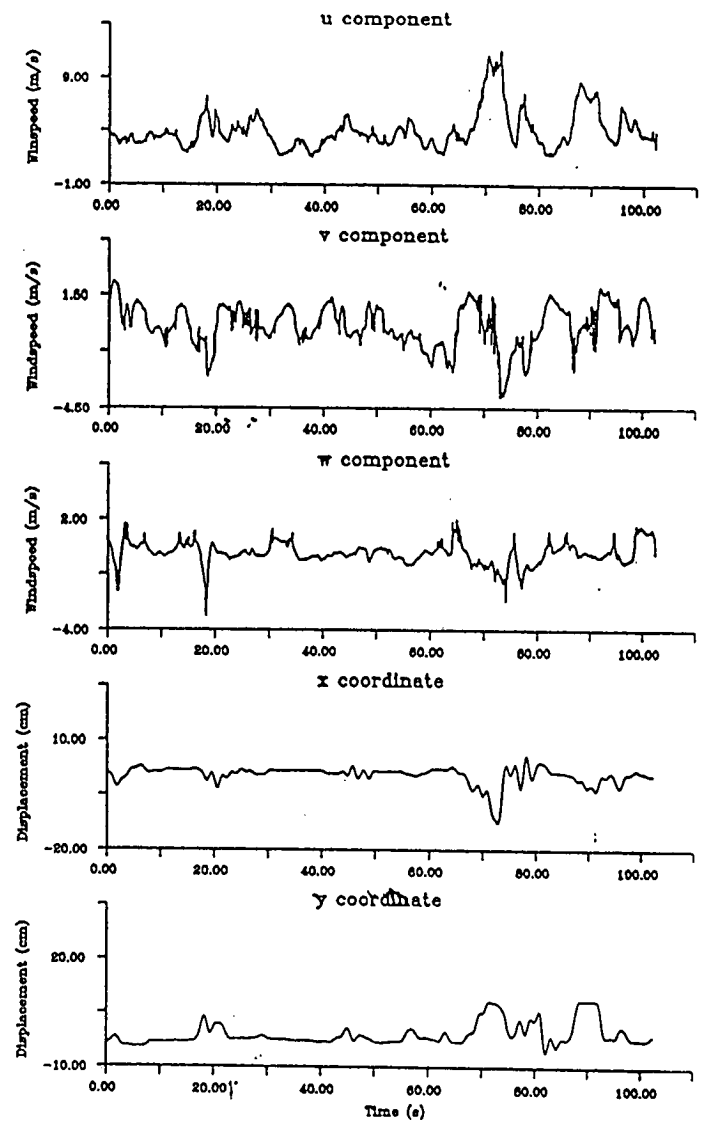

In data set R4S2 there are too many variations in the x coordinate of displacement to draw any firm conclusions, but there is some evidence that larger displacements might be developing in the y coordinate. The same applies to R5S2 but the x coordinate trace follows the w component of the wind very closely, which suggests that this might be the single most important aspect of the wind.

Data set R6S1 is a good example of why spectral analysis is useful when looking at time series data. Once again there are a great many variations in the displacement coordinates and no clear pattern is visible. However, by using spectral analysis it might be possible to pin-point any hidden periodicities.

Data set R7S1 also shows an interesting phenomenon, where there is a large displacement in the y coordinate at about 95 seconds with no obvious gust of wind to have caused it. It is possible that over perhaps two or three sways a resonant vibration has occurred here and led to a larger displacement than would normally be expected.

Moving into the thinned plot there are some signs of resonance possibly occurring, at 80 seconds in the R8S4 data set, and at about 42 seconds in R10S2, for example. However, it is impossible to firmly conclude that resonant vibration is occurring as these graphs are highly variable and the scale is too imprecise to be accurate. Therefore, it is wiser to use the spectral method of analysing these data sets for such relationships.

6.4.3 Power spectra results

Figure 6.6 presents similar figures to Figure 6.4 illustrating the power spectra for the wind speed components u and w, Reynold's stress, the mechanical transfer function and the x and y coordinates of stem displacement for the same selected data sets as shown in Figure 6.5, while a complete set of results is presented at Appendix XX.

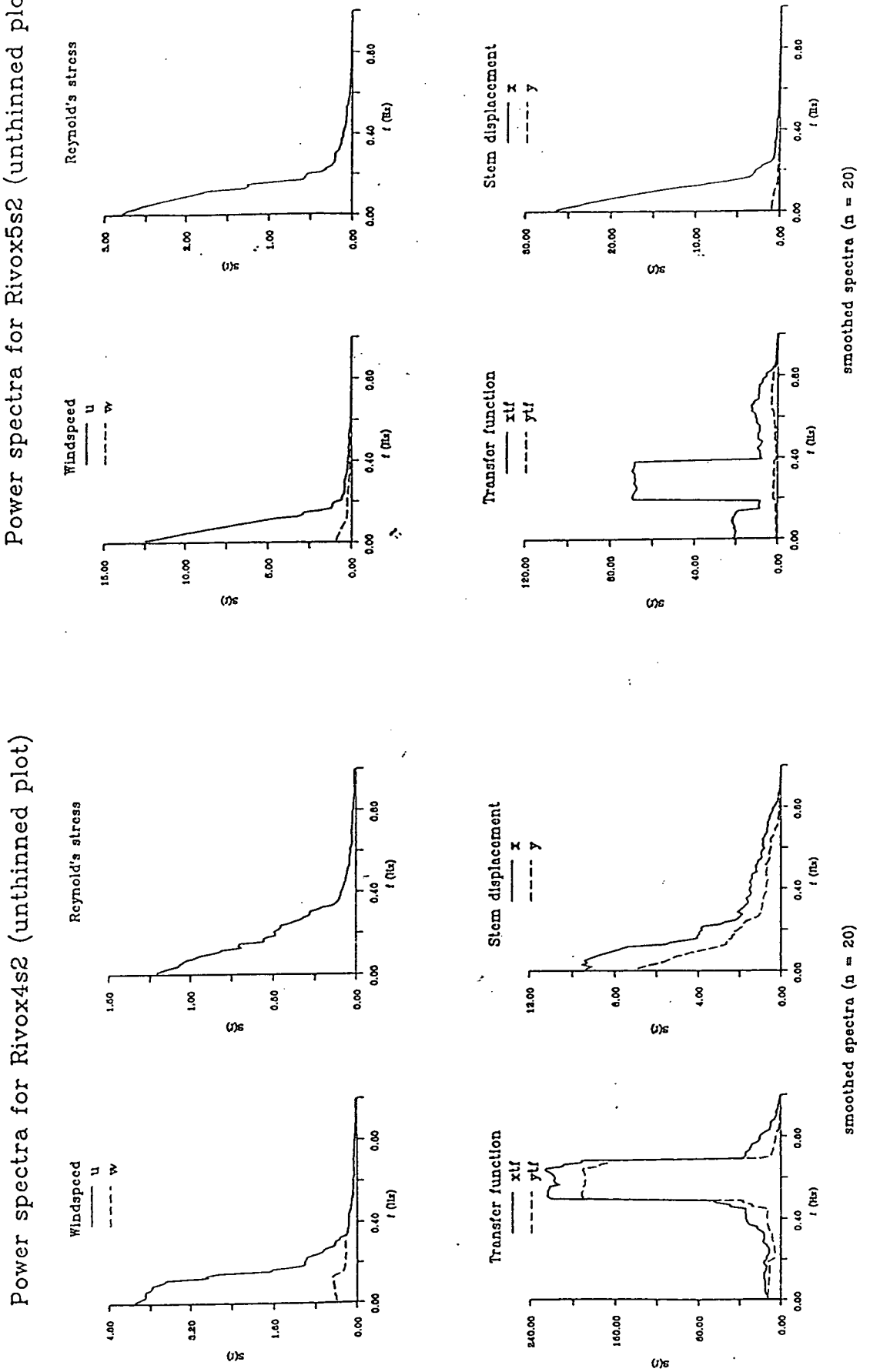

Figure 6.6 Power spectra for wind speed components u and w, Reynold's stress and stem displacement coordinates x and y, along with the mechanical transfer function for selected data sets

Power spectra for Rivox6s1 (unthinned plot)

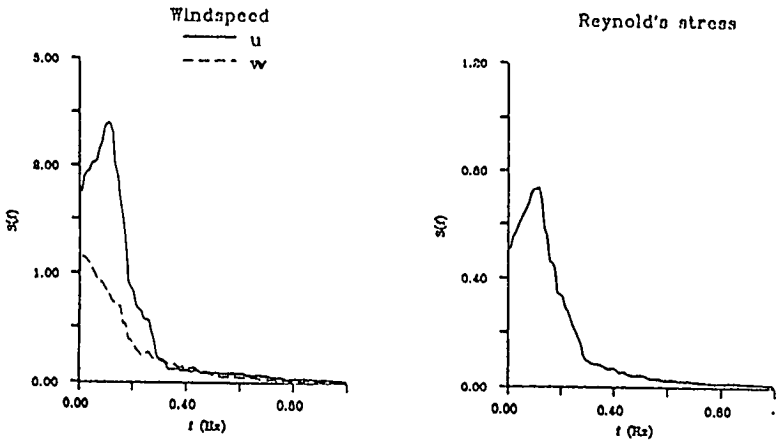

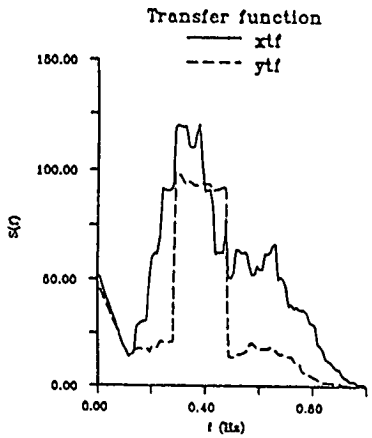

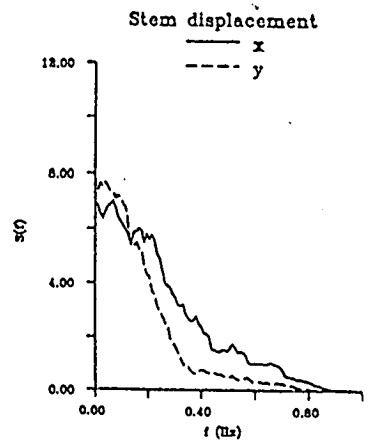

smoothed spectra (n = 20)

Power spectra for Rivox7s1 (unthinned plot)

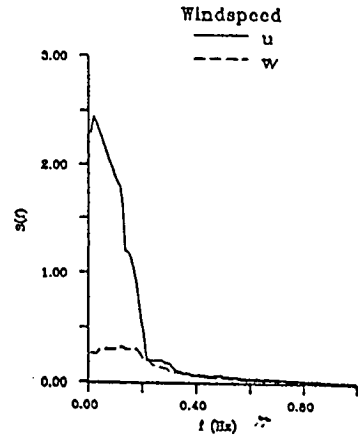

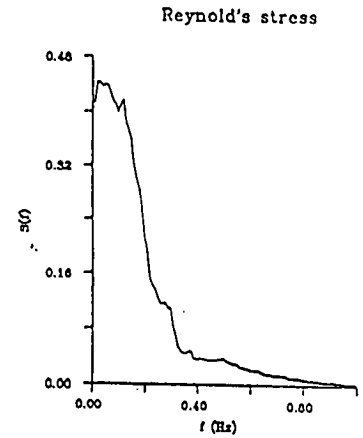

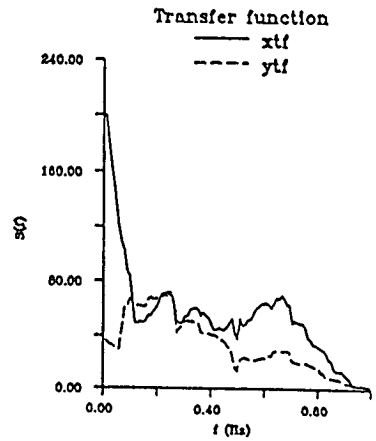

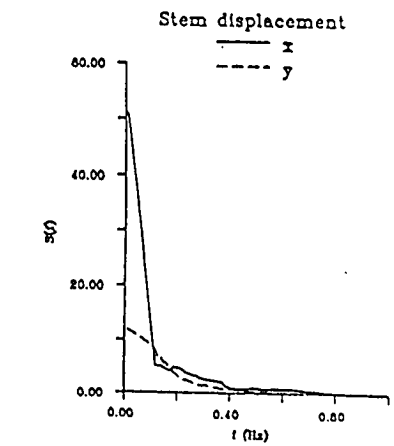

smoothed spectra (n = 20)

Power spectra for Rivox8s2 (thinned plot)

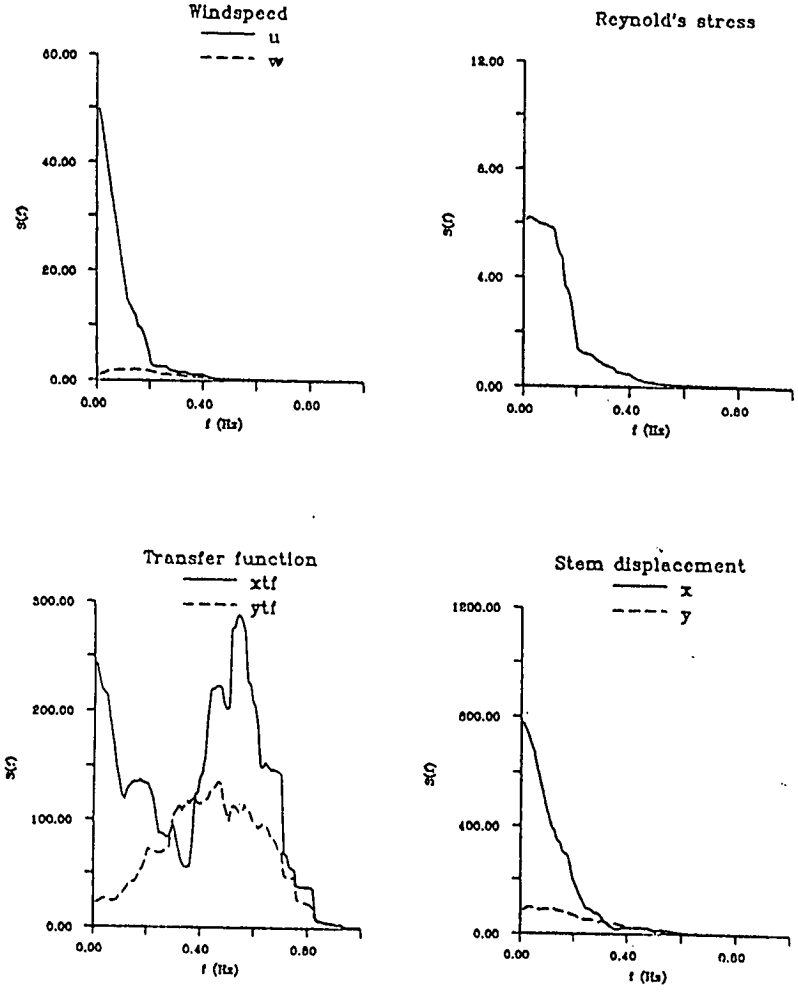

smoothed spectra (n = 20)

Power spectra for Rivox8s4 (thinned plot)

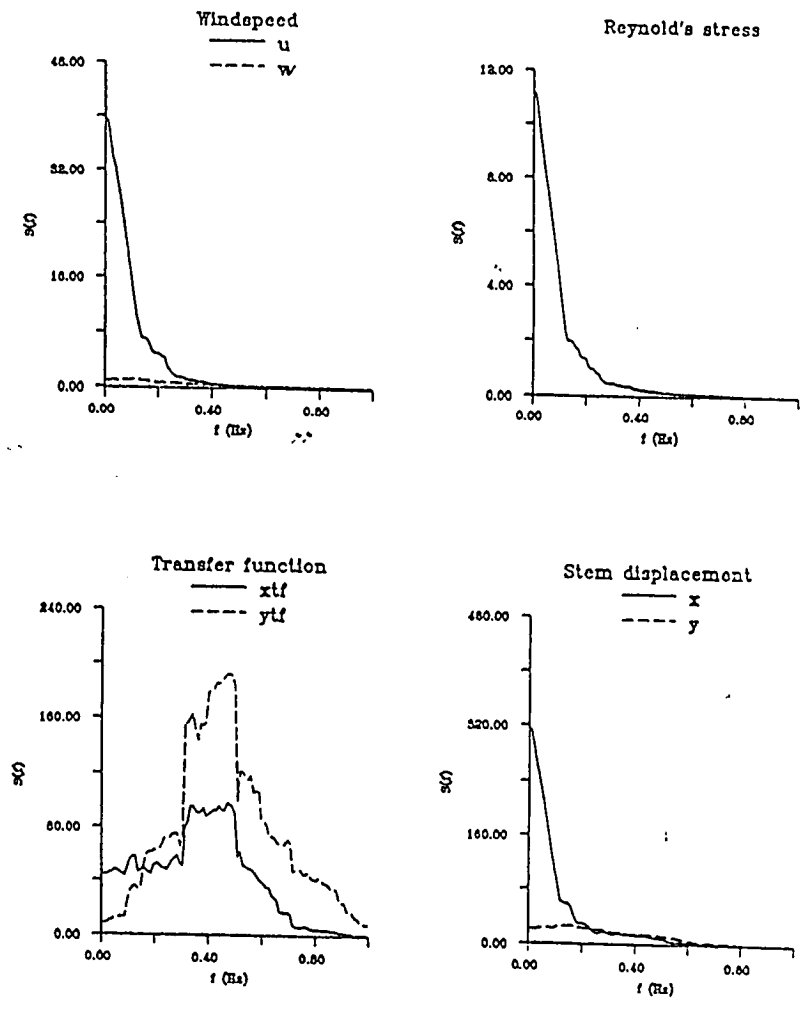

smoothed spectra (n = 20)

Power spectra for Rivox10s2 (thinned plot)

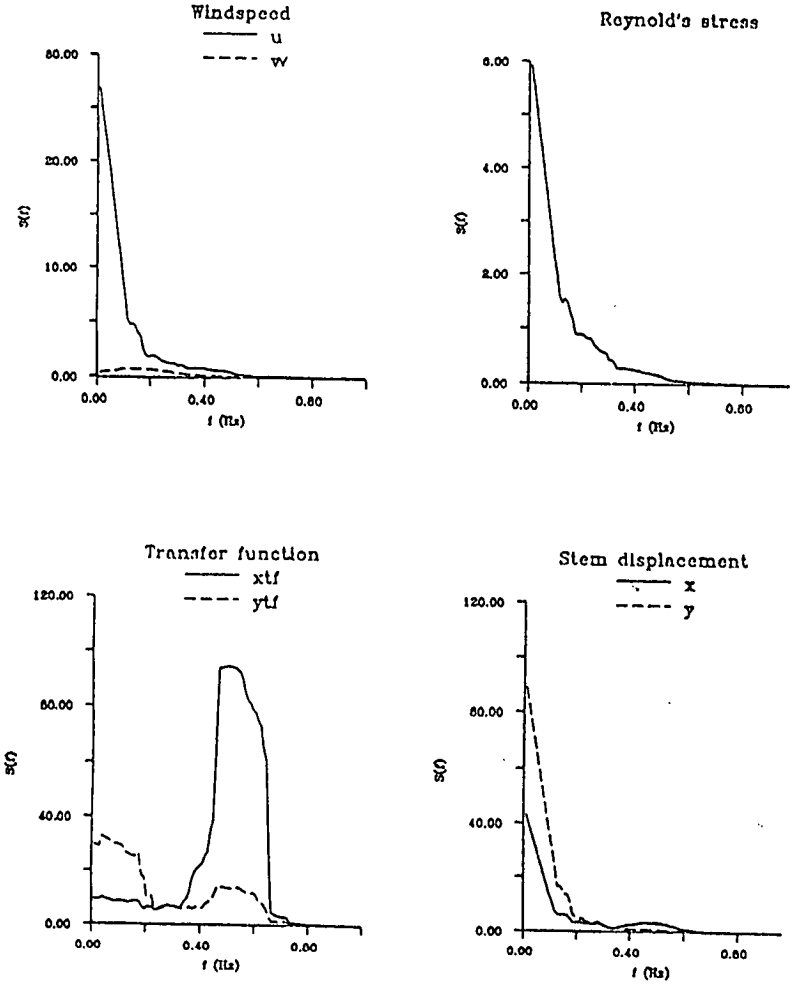

smoothed spectra (n = 20)

Power spectra for Rivox10s3 (thinned plot)

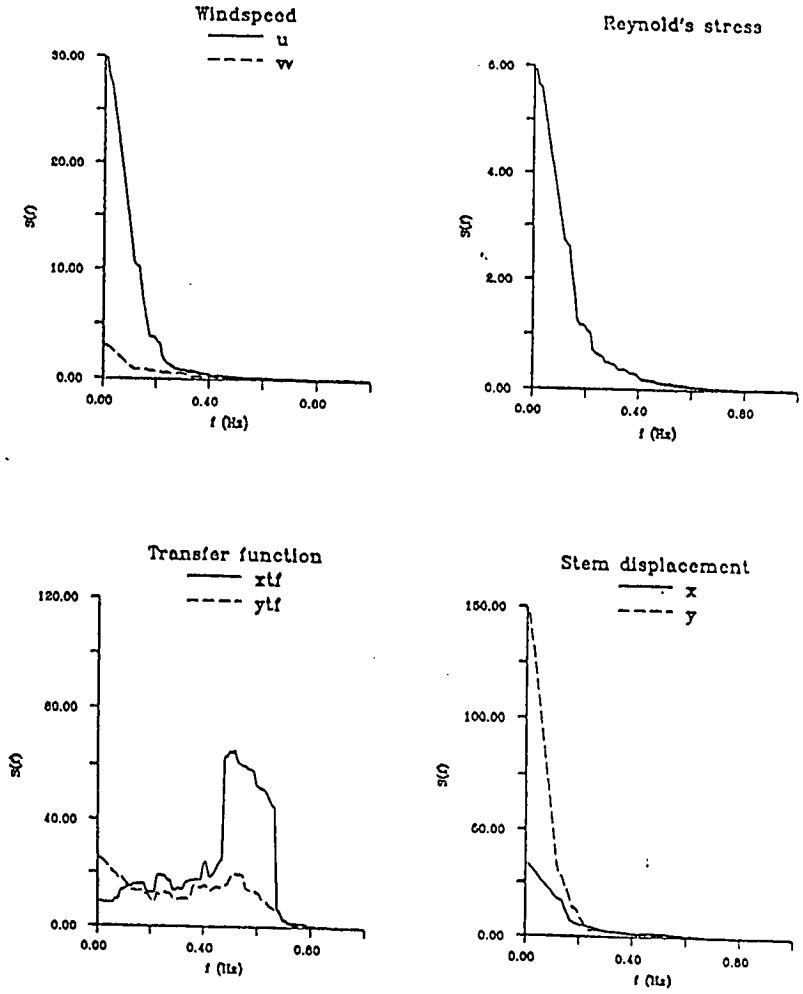

smoothed spectra (n = 20)

Average values for each of the above spectra are presented for the unthinned and thinned plots in Figures 6.7 and 6.8 respectively. There are a number of important points which can be drawn from these figures.

First, looking at the individual data sets it is obvious that there is a great deal of variation between them. The important features of these graphs are mainly related to the mechanical transfer function spectra. The main features of these spectra are the height and width of any peaks and the frequency at which they occur. However, it is also important to note the number of peaks and the area under the curve as this gives an insight into the energy of the whole system. These three main features are given for each data set, along with mean values for each plot in Table 6.2.

		x		*y*
	Peak $S(f)$ ($m^4 s^4 kg^{-2}$)	Peak Frequency Range (Hz)	Peak $S(f)$ ($m^4 s^4 kg^{-2}$)	Peak Frequency Range (Hz)
Unthinned plot				
R4S1	215	0.30-0.50	No peak	
R4S2	220	0.50-0.70	190	0.50-0.70
R5S1	60, 38	0.15-0.35, 0.40-0.65	No peak	
R5S2	70	0.20-0.39	No peak	
R5S3	24	0.47-0.79	5	0.51-0.90
R5S4	60	0.05-0.24	5	0.05-0.25
R6S1	120	0.20-0.48	100	0.28-0.50
R6S2	110, 70	0.34-0.62, 0.65-0.85	45	0.42-0.73
R6S3	42	0.33-0.79	50	0.50-0.69
R6S4	110	0.60-0.80	35	0.52-0.73
R7S1	No peak		No peak	
R7S2	65	0.25-0.80	5	0.28-0.60
R7S3	57	0.20-0.80	15	0.47-0.74
R7S4	75	0.57-0.79	No peak	
Average	24.5	0.30-0.80	8.5	0.38-0.74
Thinned plot				
R8S1	70	0.15-0.60	420	0.22-0.65
R8S2	280	0.40-0.72	130	0.20-0.71
R8S3	48	0.40-0.60	18	0.30-0.64
R8S4	100	0.20-0.57	190	0.32-0.60
R8S5	2,500	0.33-0.52	1,900	0.33-0.52
R8S6	75	0.15-0.54	125	0.18-0.73
R8S7	80	0.35-0.57	20	0.32-0.65
R8S8	30	0.25-0.62	22	0.33-0.61
R10S1	190	0.42-0.62	50	0.35-0.55
R10S2	90	0.45-0.67	15	0.45-0.64
R10S3	70	0.47-0.68	No peak	
R10S4	24	0.36-0.67	44	0.20-0.59
Average	56.0	0.34-0.67	57.5	0.23-0.65

Table 6.2 Summary results for the mechanical transfer function spectra produced by the spectral analysis procedure for the unthinned and thinned plots

To identify the frequency range of peaks in these spectra the standard approach of using the ranged frequency at the point equivalent to half the maximum amplitude was employed. In some cases no major peaks were visible, in which case no frequency range was taken. In some other cases two significant peaks were visible. In these instances the heights and frequency ranges of each peak were given. The frequency range as presented was defined as clearly as possible in each of the plots, but in some cases the rise up to the peak was quite gradual and hence the range given may have been larger.

Looking at each of the selected data sets there are some interesting points to be noted. The height of the main peak of the transfer function is generally higher in the thinned plot than in the unthinned one, although this is more apparent when averaged over all the data sets (Figures 6.7 and 6.8) where the average maximum amplitude is between 25 and 8 $m^4\ s^4\ kg^{-2}$ for the x and y components respectively in the unthinned plot while it is about 60 $m^4\ s^4\ kg^{-2}$ for both components in the thinned plot. The peaks are usually narrower in the thinned plot and more clearly defined. The wider frequency range shown in the unthinned plot indicates that there is a greater degree of damping in this plot than in the thinned one.

For data set R4S2 both the x and y coordinates have produced clear peaks of similar height which is also the case for R6S1, while R5S2 has produced a clear peak only for the x coordinate. This is most likely the result of the direction of the wind. In both R4S2 and R6S1 the direction of the wind was about 90°, where as it was about 230° for R5S2. This must have caused the tree to sway predominantly in one direction, thus producing a large displacement along the x axis, which corresponds to across the ridge. Similar trends can be seen in the thinned plot for sets R8S2, R10S2 and R10S3, but the opposite is the case for R8S4 where the y coordinate has produced the greater energy. In these cases the direction was approximately the same, hence some other form of interference must have produced this result, such as crown damping.

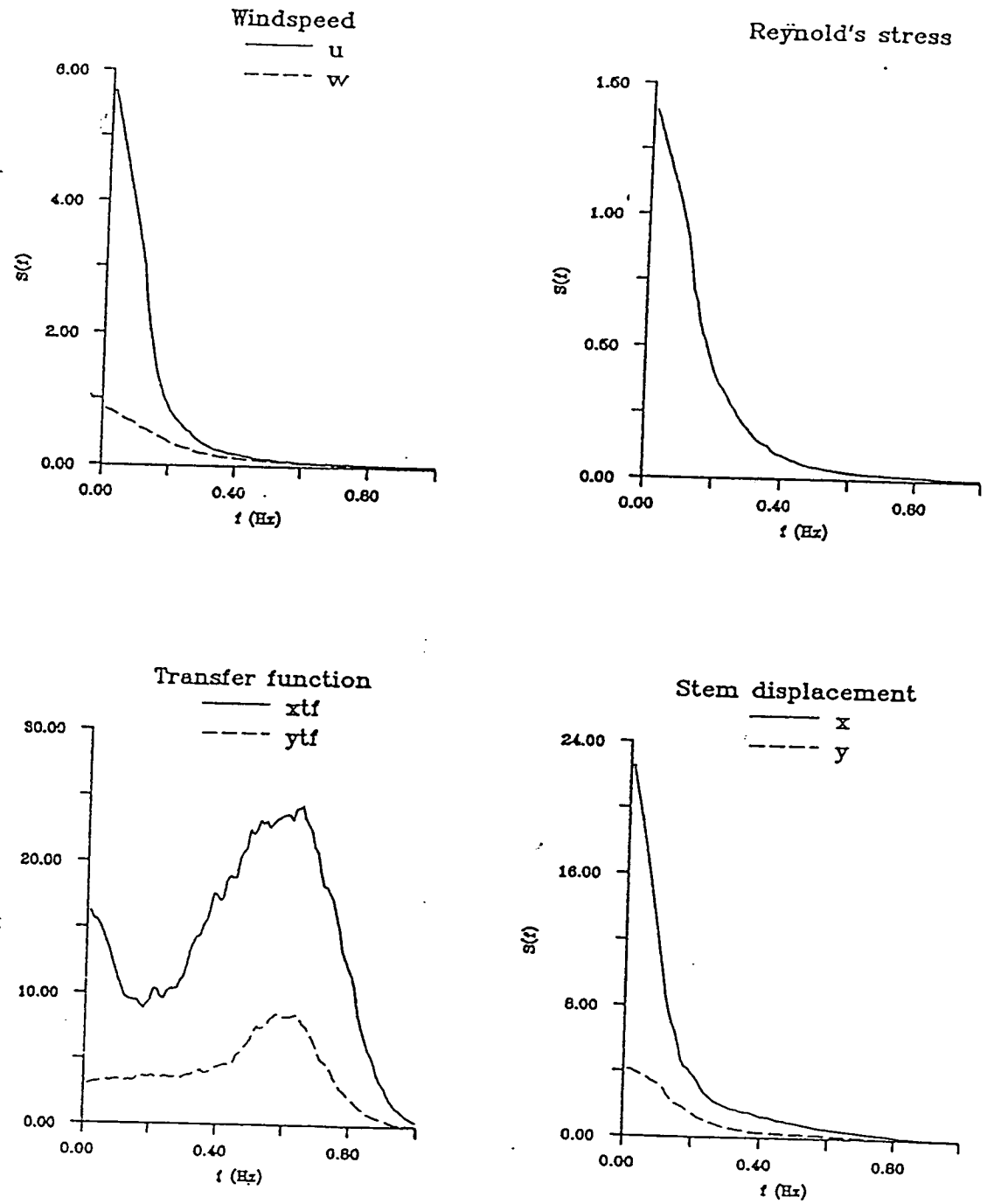

Figure 6.7 Average power spectra for the unthinned plot

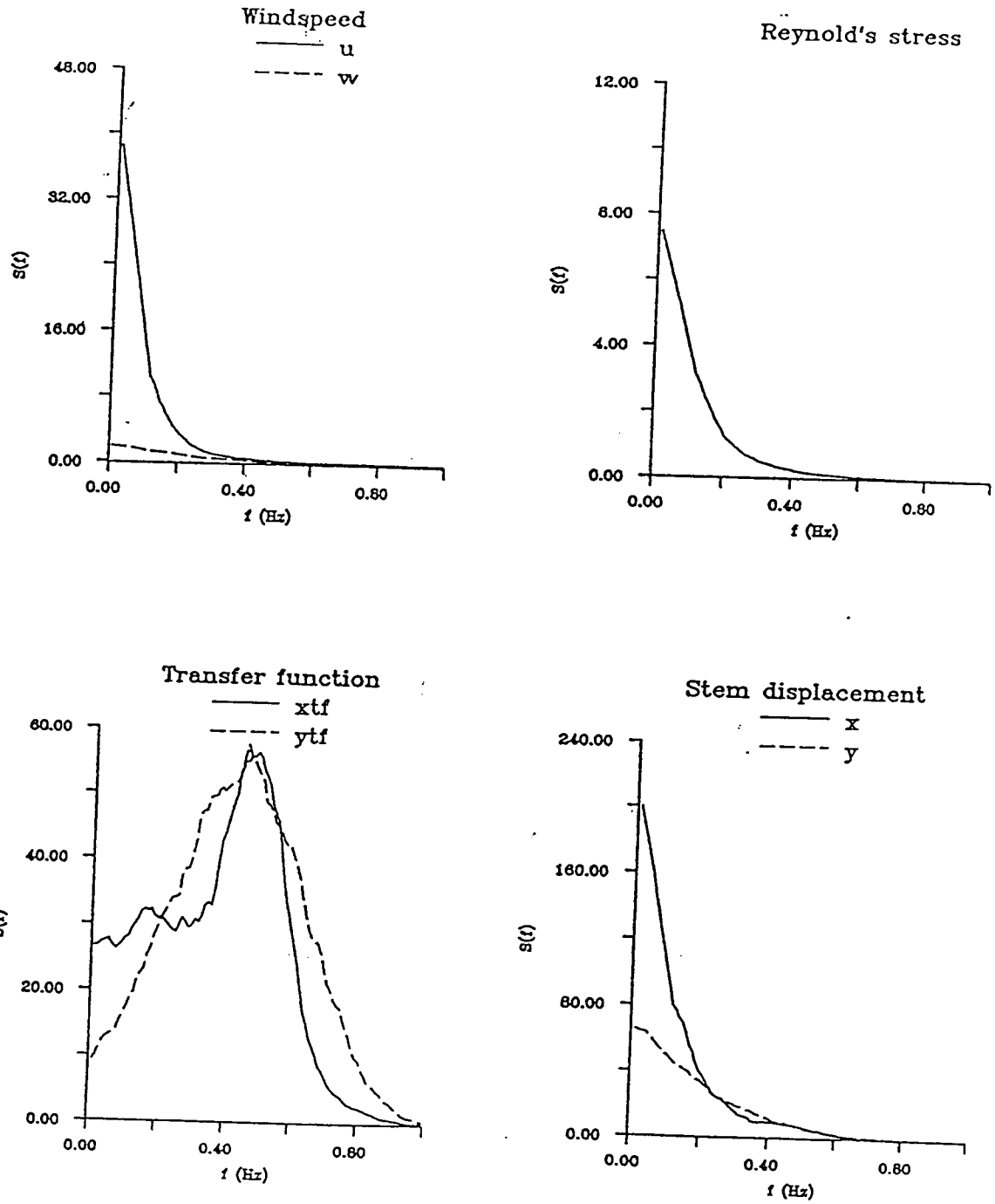

Figure 6.8 Average power spectra for the thinned plot

By averaging these results for the two plots it is possible to obtain a clearer picture of the process involved in wind-induced tree sway (Figures 6.7 and 6.8). Due simply to the higher wind speeds recorded in the thinned plot the amplitudes of the power spectra of the u and w components of the wind were far greater in the thinned plot. The u component was about seven times greater while the w component was about twice as large at their maximum amplitudes. In both plots these graphs illustrate the standard shape expected from a random signal, or stochastic data set. The values for the Reynold's stress spectra are also higher in the thinned plot, once again following the typical pattern of decay. These larger values are simply a product of the greater wind speed and turbulence measured in the thinned plot. This implies that more force is being exerted on the trees in the windier conditions measured in the thinned plot than when the unthinned plot was measured.

Looking at the spectra for the x and y coordinates of the stem displacement, the thinned plot once again produces higher values, by a factor of about seven, but it is the shape of these curves which is of interest here. In both cases the curves drop very sharply to begin with but show a slight levelling off at about 0.1-0.2 Hz. This is followed by another drop and another more level period between 0.3 and 0.5 Hz. Finally the curves gently decline towards zero at the higher frequencies. In the unthinned plot the first kink in the curve occurs at 0.2 Hz while it is at 0.1 Hz in the thinned plot. The second, and possibly more significant, period is less obvious in the unthinned plot but occurs between 0.25 and 0.5 Hz in the thinned plot. These features in the curves are caused by periodic swaying of the stems at these frequencies. If resonant vibration was to occur in its true form then these frequencies would have to correspond with the natural frequency of the stems. Thus although periodic swaying may occur it contains little energy compared to the low frequency movement.

To look more closely at these slight deviations from the usual decay curve it is useful to apply the mechanical transfer function analysis as described in Chapter 2. This function simply divides the displacement spectrum by the force, or Reynold's

stress spectrum, which caused it. Thus, as the Reynold's stress spectrum drops away as frequency increases, then these slightly raised displacement amplitudes are being caused by lower forces than would be expected, leading to higher energy levels in the transfer function. Thus, it is possible that some form of resonant vibration might be occurring.

The mechanical transfer function spectra for both plots show clear peaks. In the unthinned plot the *x* component transfer function peak reaches 25 m^4 s^4 kg^{-2} and covers the frequency band from 0.30-0.80 Hz, while the *y* component peak reaches only 15 m^4 s^4 kg^{-2} and covers the range of frequencies from 0.40-0.74 Hz. In the thinned plot, the *x* component peak reaches a height of 56 m^4 s^4 kg^{-2} and covers a frequency band of 0.24-0.60 Hz, and the *y* component reaches 57.5 m^4 s^4 kg^{-2} and covers a wider band of frequencies from 0.20-0.63 Hz. These results show that larger sways are developing in the thinned plot for a given input of energy than in the unthinned plot. The power of the transfer function in the thinned plot is at least twice that of the unthinned plot.

The frequency bands are also important in that the wider the range of the peak the greater the damping, thus large sways are less likely to develop. In this case the combined components of deflection cover a range of approximately 0.20-0.65 Hz in the thinned plot with the actual peak being centred at approximately 0.43 Hz, while the range is 0.30-0.80 Hz in the unthinned plot with the main peak corresponding to 0.54 Hz. There is therefore a slight difference in these ranges which signifies a greater level of damping in the unthinned plot as would be expected due to greater inter-crown contact between neighbouring trees. However, if these frequencies are compared with the typical values for natural frequency of the trees in the two plots (Chapter 5) then the importance of the difference between the spectra for the two plots can be seen.

In the unthinned plot the average measured natural frequency was calculated as 0.35 Hz as opposed to 0.55 Hz in the thinned plot. Unfortunately no actual values for natural frequency are available for the two sample trees due to instrument

failure as explained earlier. However, by substituting the average values for E into the three models and using the other physical parameters of Trees 7 and 9 it is possible to estimate their natural frequencies. This analysis produced natural frequency values of 0.53 Hz, 0.67 Hz and 0.24 Hz for Tree 7 using the three models respectively, and 0.45 Hz, 0.62 Hz and 0.18 Hz for Tree 9. In both cases Model 3 has produced very low values for natural frequency, probably due to a poor estimate of E and also both trees were heavily buttressed so the value for I_o might have been inappropriate. However, if the mid-value for natural frequency is used (that from Model 1) then a comparison between these values and the spectral peaks can be made. The peak for the unthinned plot is at approximately 0.54 Hz and for the thinned plot it is at 0.42 Hz. These estimates of natural frequency using Model 1 are clearly very close to the peak frequencies taken from the average spectra.

This small difference between the modelled frequencies and the spectral peaks can possibly be attributed to damping but it is not possible to be certain since the difference is very small and the models can not be guaranteed to be this accurate.

However, it is possible that damping will be affected by the way the trees are swaying in that if neighbouring trees are swaying in phase with each other there will be less inter crown contact which will mean less damping. This idea is an interesting one. In both plots the time domain graphs showed some evidence of large sways developing. These sways might correspond to neighbouring trees swaying in phase with each other for a short period of time. The fact that they will all have different natural sway periods would soon cause them to become out of phase, thus reducing the scale of the displacements.

Due to the smaller amount of damping experienced in the thinned plot it is more likely that a tree might sway undisturbed by its neighbours, thus resonant vibration might be more likely to occur assuming the wind gusts were in phase with the stem's natural frequency for any period of time. However, in the unthinned plot another condition would require to be met before resonant vibration, in any sense

of the term, could possibly occur to any great extent. That is, the neighbouring trees would have to be swaying in phase with the sample tree as well as the gusts of wind being of the same frequency as the natural frequency of the tree. Hence, any form of resonant vibration which does develop in the unthinned plot is likely to be of shorter duration than it might be in the thinned plot. This suggests that trees in the unthinned plot should be at less risk from endemic windthrow than those in the thinned plot, a theory which is borne out to some extent by the fact that windthrow has already occurred in both plots at Rivox, but to a greater extent in the thinned one.

6.5 Conclusions

A method of measuring wind speed above the canopy and stem displacement of the trees in a Sitka spruce plantation has been developed using a 3-dimensional anemometer and position-sensing transducers. This system could, however, be improved upon in a number of ways. The LCM PST900/A transducers could be replaced by an alternative, and preferably linear transducer model which has fewer working parts which might be susceptible to damage when in constant use. The Celesco PT101 transducers were better in this respect, but a simpler system for mounting and attachment to the tree stem would be useful.

By simply looking at the results in the time domain it is possible to state that the wind speeds and stem displacements recorded were higher in the thinned plot than in the unthinned plot. The larger displacements were an obvious result of the higher wind speeds, although it is possible that these higher wind speeds are an artifact of the lower zero-plane displacement in the thinned plot, which in measurement terms would mean that in effect the anemometer was higher above the canopy in the thinned plot. The data from the thinned plot were also more variable as a result of the rougher nature of the canopy and this higher wind speed. This was also reflected in the stem displacements. Apart from these simple observations very little can be firmly concluded from the time domain results alone. Therefore, it was necessary to use spectral analysis to investigate any underlying patterns in the data.

It has been shown here that it is possible to use spectrum analysis to show periodic swaying is stands of trees, and to compare different stands. The method used to compare the two plots studied here was that of determining a mechanical transfer function between the Reynold's stress and the stem displacement (Mayer 1989). This analysis showed that on average the energy of the transfer function spectrum in the thinned plot was higher than that of the unthinned plot. This suggests that more energy is being transferred to the trees from the wind for any given wind speed in the thinned plot at the peak frequencies. In addition to this the peak frequency of these transfer functions also differed between the two plots, as did the frequency bands covered by these peaks. The range is slightly wider in the unthinned plot suggesting a greater degree of damping, while the peak frequency was 0.75 Hz in the unthinned plot and 0.45 Hz in the thinned plot.

The measured natural frequency (see Chapter 5) of the stems most similar to Tree 7 (unthinned plot) agree less well with the peak of the transfer function spectrum obtained for the unthinned plot than the measured value for natural frequency of the tree most similar to Tree 9 (thinned plot) compared to the transfer function spectrum peak from the thinned plot. This is probably due to the greater level of damping in the unthinned plot which means that trees in the unthinned plot would collide more frequently with their neighbours in the unthinned plot than in the thinned one. Thus, the situation in the thinned plot would better approximate to that which existed when the stems were waggled for the measurement of natural frequency (Chapter 5).

This leads to the idea that not only is resonant vibration dependent on the wind gusting in phase with the natural sway period of the tree, but also that neighbouring trees must be swaying in phase with each other to avoid this contact which dampens down any large deflections. Hence, as the trees are closer together and more severely damped in the unthinned plot this effect will reduce the chance of large sways developing through some form of resonant vibration more than it will in the thinned plot. Also, not only will this effect reduce the chance of

any form of resonant vibration occurring, but should such a phenomenon develop, it is unlikely that neighbouring trees will remain swaying in phase for long due to their different natural frequencies, thus it is likely to have a shorter duration in the unthinned plot than in the thinned one. Therefore, it can be concluded that trees in the thinned plot are more susceptible to resonant vibration, and hence the risk of windthrow occurring is greater. This last conclusion is supported by the fact that windthrow is already more prevalent in the thinned plot than in the unthinned one, and that this is generally the case in forests, i.e. the onset of wind damage often follows thinning.

So to sum up, the spectral analysis technique used here, based on the estimation of a mechanical transfer function appears to provide some quantifiable evidence which supports the generally accepted view that thinned stands are more at risk from windthrow than unthinned ones. Therefore, although only two different silvicultural systems were investigated here, this technique could provide a valuable tool for investigating other silvicultural regimes and methods of establishment, which in turn might shed some light on the best way to minimise the damage which occurs to Britain's forests every year from endemic windthrow.

CHAPTER 7 GENERAL DISCUSSION AND CONCLUSIONS

7.1 Introduction

This project set out to investigate the influence which silvicultural practices have on the way trees respond to the wind and the dynamic nature of wind-induced tree sway. It was intended that this work should focus on the forestry aspects of the windthrow problem and avoid taking too theoretical an approach. However, by the very nature of the inter-relationships between the trees in a forest and the wind it was necessary to include a certain amount of engineering principles to provide ideas as to how trees respond to their wind environment. Nonetheless it is important that these engineering concepts are used with a great degree of care since they always relate to ideal circumstances and standard conditions which all too frequently are not matched in the forest. It is also important to remember that although many mechanical aspects of the trees and their response to the wind have been looked at here there are also many others which have not. With this in mind there is, however, much that can be concluded from the work described in the preceding chapters.

A number of physical features of 11 sample trees were collected, primarily to be used to determine their natural frequency, but also to look at the growth characteristics of the stems and foliage. From this information estimates have been made of the structural elasticities, i.e. Young's Modulus (E). This in turn was used to estimate the natural frequency of the stems using a variety of models which have been used in engineering theory for standard beams of various forms. These estimated natural frequencies were then compared with measured values taken in the field to determine which, if any, was the best estimator for whole Sitka spruce trees. These data formed the first part of the project while the second concentrated on measuring the stem displacement which resulted from the wind above the canopy. Using spectral analysis, simultaneous wind speed and stem displacement data were analysed by producing a mechanical transfer function between the two, which produced peaks of varying widths, heights and frequency range. These spectra provide an interesting insight into the dynamic processes

involved in wind induced tree sway.

This chapter draws together the most important points from each of the preceding chapters and puts the results into the forest context. As stated above, it is very easy to become too deeply immersed in the physics and engineering behind the concepts which have been used here and in the process to overlook the objective of the work, which was to investigate tree swaying particularly in relation to forestry practices as these are under the direct control of forest managers. Therefore, some of the engineering theory used in this work has only been briefly described, with the understanding that the concepts involved appeared to be broadly appropriate to the forest situation and that the theory had already been accepted as proven in engineering systems such a beams.

7.2 Discussion

Stem height (h) and diameter at breast height (dbh) were measured in both the unthinned and thinned plots, and showed a wide range of values. The trees from the unthinned plot were generally taller and more slender. This difference in stem form is presumed to be the result of the greater level of competition for light in the unthinned plot, but it could be the result of less swaying due to greater crown contact with neighbouring trees. The h/dbh ratio was determined for each of the eleven sample trees used. This parameter has frequently been used as an indicator of stability for trees, a high value indicating an unstable tree. The values obtained for h/dbh were lower in the thinned plot which contained shorter stems with larger diameters. The average value was 97.3 in the unthinned plot and 60.5 in the thinned plot. These values compared with 64 to 104 in unthinned Sitka spruce at various planting spacings according to Savill (1983), with a value of 96 for approximately the same stocking density as was used at Rivox. Only two trees in the unthinned plot appeared to have dangerously high values. The value of this ratio could change with age as well as with spacing and the extent of the root-plate must be important too with regard to stability. The extent of the root-plate may be determined to some extent by spacing but there are a number of

other factors, such as soil conditions and cultivation techniques, which can influence this too. All the trees in the thinned plot produced substantially lower values and would therefore appear to be very stable.

This result was slightly unexpected as, in general terms, more trees tend to be blown down after thinning and the amount of damage from windthrow was already greater in the thinned stand at Rivox. Thus it is suggested that this loss of stability associated with the thinning process may be more as a result of the altered crown damping characteristics and below ground processes than the intrinsic stability of the stem shape, therefore *h*/dbh may not be a very good indicator of stability for plantation trees. The most likely reasons for this loss of intrinsic stability after thinning are the reduction in inter-crown contact between neighbouring trees, and perhaps less obviously, the raising of the water-table after thinning due to the reduced requirement for water from the lower number of trees on any given area of ground. This rise in the moisture content of the soil will often result in die-back of tree roots with the obvious effect of reducing the tree's stability. This result also illustrates the importance of a dynamic approach to investigating the windthrow problem as a simplistic approach, such as the *h*/dbh ratio, fails to take into account all the variable factors involved.

Stem shape was measured, both over-bark and under-bark, as this information was required firstly to describe the shape of the stem to decide which engineering model was most likely to be appropriate, secondly to illustrate the variable nature of the wood within the stem in terms of its uniformity of construction and to investigate the changes in growth after thinning. Two models were fitted to the over-bark observations of stem shape. These models were chosen from a range of empirical formulae (Blevins 1979) because they apply to beams which are the most similar to the normal shape of a tree stem.

The first model assumed non-linear taper and uses a power '*n*' to describe the degree of taper. The second model assumed linear taper to a height of truncation which was 9.0 m in the case of the sample trees. Both models were used to

estimate the natural frequency of the stems.

The shapes of stems in the unthinned plot were more accurately described by the non-linear taper while those in the thinned plot more closely fitted the linear taper. Buttressing of roots presents a potential problem when looking at tree stems in terms of simple engineering beams. This was not dealt with in this work, except for using the diameter at 0.5 m above the ground as the value for basal diameter in the above models, but might be worth some attention in future work as buttresses could have a significant impact on the stability of stems, particularly on steep slopes where buttresses are more noticeable. This might be investigated by segmenting the stem and using a combination of the above techniques.

The under-bark diameter measurements, which were made using ring analysis, show a very similar pattern of growth in the two plots until the thinning was carried out after which the rate of diameter increment in the thinned plot undertakes a noticeable rise for about five years. In both plots the average annual diameter increment increased for the first 2 or 3 years and then levelled off until about year 5 to 8 when it began to drop. This drop in production may be caused by competition for light being very intense once canopy closure is achieved (about 5 to 8 years) but it could also be the result of competition for nutrients or water. In the thinned plot the increment rose from year 18 for 3 years and then dropped again until it met the unthinned production 5 to 6 years after thinning. This increased rate of growth was most likely caused by the thinning which would reduce the level of competition for light in the thinned stand.

With regard to modelling trees using beam theory, it is important to remember that because of these growth rate changes, in both plots, the internal structure of the trees is not uniform. This non-uniform internal structure is often exaggerated by eccentric development where trees grow on slopes or tend to sway predominantly in one direction. As most forests are planted on slopes and experience prevailing winds from a particular direction this could be a significant problem. Therefore it is probable that engineering formulae which are based on

beams of uniform construction of circular cross-section will fail to model tree stems to the same level of accuracy as they would standard engineering beams.

Stem mass and crown mass were also investigated by measuring each in 1 m sections of the stem which produced a picture of the mass distribution along the length of the stem. Both the stems and the crowns were heavier in the thinned plot where crown distribution was also more variable. The average mass for the stem was 126.4 kg in the unthinned plot and 175.9 kg in the thinned plot. The average crown mass was 45.6 kg and 122.8 kg respectively. The live crown began at a lower height above the ground in the thinned plot, presumably as a result of more light penetrating the canopy and therefore the branches remaining alive longer. The data for stem and foliage mass was used to estimate the natural frequency of the stems using a third engineering model based on a linear cantilever beam with a concentrated mass at its free end.

Stem density was calculated using the stem mass measurements. This was calculated for the whole stems (μ_1) and for the stems up to the height of truncation (μ_2) (in the linear taper model). The mean values for stem density were 1026 and 1082 kg m^{-3} for μ_1 in the unthinned and thinned plots respectively, and 982 and 1065 kg m^{-3} for μ_2. The higher value for μ_2 in the thinned plot compared to the unthinned plot is most likely due to higher growth rates after thinning resulting in less dense wood, most of which occurs in the top part of the stem within the crown. Therefore, the truncation of the stem used for the linear taper model means that the situation in the real world is not being reproduced which would suggest that errors might arise from this procedure. Added to this possibility is the fact that the weights were measured at different times of the year which would result in different moisture content of the wood.

Young's modulus of elasticity (E) for each tree was calculated from the spring constant (s) and the shape and size of the stem. The spring constant is a measure of the resistance of the wood to elastic bending and was determined by measuring the stem displacement produced by a measured force. There were few published

values of E for complete stems until recently, and as this parameter was required for the estimation of natural frequency of the stems it was necessary for it to be measured.

The values for E fell between 4.2 and 9.4 GPa in the unthinned plot and between 1.4 and 2.1 GPa in the thinned plot. Milne (1989) produced figures for E for the same unthinned plot of trees, using a segmental method of calculation, ranging from 6.5 to 9.0 GPa. Cannell and Morgan (1987) also produced figures for E by bending stem sections and branch sections of 35 years old Sitka spruce ranging from 3.9 to 6.7 GPa where the bark was included and ranging from 5.7 to 10.0 GPa where the bark was ignored. The values obtained here for the unthinned plot agree well with the figures presented for Sitka spruce by these authors, but the values in the thinned plot are at the low end of the range. These low values are most likely due to a combination of the rootball movement and more flexible juvenile wood being present in the live canopy portion of the stem which is greater in the thinned plot.

It is possible that these low values for E in the thinned plot may have resulted from rootball movement. When the trees were pulled by the winch the rootball tended to move slightly, especially in the thinned plot where the soil was wetter. This effect would reduce the force required to displace the stem by a given distance and hence reduce the spring constant. The thinned plot was a more level site and there was water lying in some of the furrows which suggests that the trees might have been suffering from waterlogging and subsequent root die-back. The rootball movement might be thought of as rendering the values of s less useful for determining E but as the rootball movement will occur when the tree sways naturally the value obtained for E will be representative of a "whole tree's elasticity".

The parameters which have been described above were all used to estimate the natural swaying frequency of the sample trees using the three models described. The only other parameters required were determined using the parameters n and t

described above and a series of solutions of elastic equations for different shapes and sizes of beams described by Blevins (1979). The result was two taper parameters, λ_1 and λ_2. These taper parameters were then used with the physical data described earlier to estimate the natural frequency of the stems using the first two models but not the third.

The measurement of natural frequency for the sample trees was carried out in the field on nine of the eleven sample trees. This was done with branches intact (F_m) and with the branches removed (F_{m1}). The latter experiment was carried out to illustrate the effect of the canopy on the natural frequency of the trees. In the unthinned plot the average value for F_m was 0.35 Hz and for F_{m1} it was 0.58 Hz. In the thinned plot the average values were 0.56 Hz and 0.90 Hz respectively. The higher average natural frequency value obtained for whole trees in the thinned plot compared with the unthinned plot are due to the trees in the thinned plot being shorter and therefore vibrating more rapidly. There is an increase in the natural frequency of the trees in both plots when the branches are removed but this is greater in the thinned plot. The increase in natural frequency is caused by the loss of mass which allows the stem to sway faster, although the decrease in damping might have a very small effect, and since the foliage mass was greater in the thinned plot there was a greater reduction in mass which resulted in a greater increase in the natural frequency.

Three models were used to estimate the natural frequency of the trees and the results were compared to those measured in the field. The average values for natural frequency using these models for the two stands were 0.58 Hz, 0.34 Hz and 0.34 Hz for the three models respectively in the unthinned plot, and 0.99 Hz, 0.62 Hz and 0.56 Hz for the three models in the thinned plot.

The results for the nine sample trees are given in Chapter 5 in Table 5.2. Model 3 gives the best estimate of natural frequency for whole trees while Model 1 is better for bare stems. This result is no surprise in that Model 1 takes no account of the canopy foliage but concentrates on modelling the shape of the stem, while

Model 2 does neither of the above very well. Model 3 simplifies the stem shape but concentrates on the mass and length of the stem and its foliage. This suggests that stem and foliage mass along with the length of the stem are the main factors in determining the natural frequency of the stem, and that perhaps expending a great deal of effort developing complex engineering formulae to accurately describe the shape and mechanical characteristics of a tree stem (with the exception of E which is still required) is unnecessary in order to obtain a useful estimate of the natural frequency. Once again this might be the result of the difference between trees and standard engineering beams, and the fact that there are so many sources of error in the forest situation that a simple estimate is as likely to be as useful as a complex one.

A series of sensitivity tests were carried out on the models looking at the effect of varying the input values of Young's modulus (E), stem density (μ), taper parameter (λ), and stem and foliage mass (m_b and m_c) on the estimate of natural frequency to highlight the likely main sources of error in the models. These sensitivity tests also had another function in relation to silviculture, to show which parameters are the most important ones to manipulate if one is trying to alter the natural frequency of the trees in a stand. It was found that the models were most sensitive to the taper parameter, but Young's modulus and stem density were also important. Since Model 3 produced the best estimate and the stem waggling results showed that removing the branches from a tree altered its natural frequency and that shorter stems swayed faster, it can be concluded that the natural frequency can best be controlled by silvicultural techniques which alter the stem and foliage mass and the height of the stem, which might be expected as the period of a pendulum is largely dependent on its length and its mass.

This might offer some way forward in the effort to reduce windthrow in plantations. If silvicultural techniques can be used which will produce stems with natural frequencies which differ from their neighbours they would be unlikely to sway in phase with each other. Therefore, there should be greater crown damping due to a higher number of collisions between them, thus damping such motion

and reducing the risk of large sways and windthrow.

When looking for ways to alter the natural frequency of trees to reduce the risk of windthrow, as hypothesised above, this mass effect might offer some possibilities. By randomly pruning trees to variable heights, i.e. removing varying amounts of foliage, it should be possible to ensure that the trees have different natural frequencies and hence are unlikely to sway in phase. This might lead to a reduction in the number of large sways and thus the risk of windthrow might be reduced. However, such a silvicultural regime would be very intensive in labour terms and might therefore not prove to be practicable, but other methods of altering the foliage mass, such as selective thinning, might also prove to be worth considering.

Information regarding the risk of windthrow on various trees and their silvicultural regimes can be gathered from experimental measurements in the forest. However, it is necessary to look at the dynamic response of the tree to wind to get a better picture of the processes involved. Therefore, a measurement programme of the wind speed and the stem movement caused by it was set up in both the unthinned and thinned plots. Very little could be concluded from the time domain results (Figure 6.5) as there were no clear patterns or relationships between the wind components and the stem displacement. However, the wind speed and stem displacement values obtained in the thinned plot were generally greater than those obtained from the unthinned plot. The average horizontal windspeed in the unthinned plot was 2.63 m s^{-1} while it was 4.33 m s^{-1} in the thinned plot, both at 1.5 m above the top of the canopy. However, this may be the result of different zero-plane displacements in the two plots which would mean that in effect the windspeed was measured higher above the canopy in the thinned plot than in the unthinned one, which should lead to higher windspeeds. The wind was also more turbulent over the thinned plot which was probably caused by the higher wind speeds and the rougher nature of the canopy due to the thinning process. The *w* (vertical) component appears to be of some importance as there is some evidence that stem displacement follows a downthrust of air towards the

canopy. Large downward movements of air will increase momentum transfer to the canopy.

Due to the lack of information which can be gathered from the time-based results, spectral analysis was employed to investigate the dynamics of the relationship. The main result from the spectral analysis was the mechanical transfer function. This is a function which results from the power spectra of the displacement being divided by the power spectra of the Reynold's stress causing that displacement, therefore the transfer function is frequency-based. The amplitude of the transfer function provides information about the displacement per unit force at different frequencies.

$$S(f)_{TF} = S(f)_x / S(f)_{rr} \qquad (7.1)$$

where, $S(f)_{TF}$ is the mechanical transfer function for frequency f; $S(f)_x$ is the power spectrum amplitude for the stem displacement at frequency f and $S(f)_{rr}$ is the corresponding power spectrum amplitude for the Reynold's stress, which is a measure of the force being exerted on the canopy from the wind. The mechanical transfer function can yield a great deal of information regarding the processes involved in tree sway. The position of any peaks illustrates the frequencies at which the largest sways occur and the width of these peaks provides some information regarding the level of damping going on in the plantation, and the likelihood of resonant vibration occurring. Average spectra were calculated for both plots to give a clear view of the differences between the two plots (Figures 6.7 and 6.8).

The peak amplitude of the mean transfer function in the thinned plot was about twice that of the unthinned plot, which means that a larger stem displacement was arising from a given drag force at the peak frequencies. The position of the peak and its width is also of some importance here. In the unthinned plot the peaks

covered the band from 0.30 to 0.80 Hz while they covered the band from 0.25 to 0.60 Hz in the thinned plot. Therefore the frequency range covered by the peak in the unthinned plot was 0.50 Hz as opposed to 0.35 Hz in the thinned plot. The slightly narrower peak in the thinned plot signifies that less damping was occurring in this plot, which is as expected due to the wider spacing of the remaining trees and the larger gaps in the canopy. The greater degree of damping in the unthinned plot means that there is less chance of large sways developing, even at the peak frequencies, therefore, the risk of windthrow should be less in the unthinned plot. This suggestion is supported by the fact that there was less evidence of the onset of windthrow in the unthinned plot than in the thinned one.

Due to instrument failure, no measurements were made of the actual natural frequency of the two stems used for transfer function estimation. However, by using the average values for E for the two plots and applying the other physical parameters obtained from Chapter 3 to the natural frequency models described in Chapter 5, it is possible to make approximate estimates of natural frequency for these trees. This was done producing values of 0.53 Hz using models 1 for Tree 7 from the unthinned plot, and 0.45 Hz for Tree 9 from the thinned plot. Model 1 was used to estimate the natural frequency for these trees because the values obtained using Model 3 were very low, and unlikely to have been accurate. This result is most likely due to a poor estimate of E being used. However, the values obtained using Model 1 were more realistic and corresponded very well with the peaks on the average transfer function spectra. In the unthinned plot the spectrum peak was at 0.54 Hz and in the thinned plot it was 0.42 Hz. These peaks should agree with the measured natural frequencies as they represent the resonant frequency of the stems.

Therefore, it can be concluded that resonant vibration of trees is possible if the input of energy from the wind is in phase with the natural frequency of the stems, however, due to the variable nature of the wind it is very unlikely that this situation will prevail for any significant amount of time which means that the energy input frequency will often fall outwith the peak range, resulting in smaller

deflections. Also if neighbouring trees collide then their motion will be disturbed and large sways will be damped, which will result in a broader, and flatter peak on the transfer function. This means that there will be even less chance of the very large sways required to cause windthrow.

If neighbouring trees began to sway in phase with each other then the chance of this resonant vibration would be greater, however, this is also unlikely to happen for any prolonged period of time. By managing the forest to ensure that the natural frequencies of the trees are highly variable it would be possible to reduce the risk of in-phase swaying.

These results therefore suggest that since the peak is broader on the transfer function in the unthinned plot than it is in the thinned plot, the risk of windthrow from resonant vibration, or large sways developing through a process similar to resonant vibration, is less likely in the unthinned plot due to a greater amount of damping. The most likely source of this damping is inter-crown contact between neighbouring trees since the trees in the unthinned plot had much less space in which to sway. Damping has no significant effect on the natural frequency of the tree so if neighbouring trees were to have similar natural frequencies it is possible that they could sway in phase with each other, and resonant vibration could then occur if the meteorological conditions were suitable. However, since the trees in the thinned plot are subjected to less damping there is a greater chance of pure resonant vibration, and the associated large sways, occurring. Hence, trees in the thinned plot should be at greater risk from windthrow.

7.3 Conclusions

Generally, this work has clarified certain aspects of the windthrow process and it has certainly provided the basis for future developments in research into the dynamic relationship between the wind and the resultant stem displacement in forest plantations. There are a number of points which should be highlighted as forming the base for further work in this area which might provide useful insights

into how forest managers can reduce the amount of damage caused by wind to forests in Britain.

This work has employed a variety of techniques to investigate the processes involved in windthrow of trees, ranging from simple static bending and analysis of physical characteristics, through various models for estimating the natural frequency of stems, to more complex dynamic analysis producing a mechanical transfer function between the windload and the stem movement. Each technique has thrown valuable light on the problems and processes involved. By simply using information on the physical shape, size and composition of the trees it is possible to draw some conclusions about their intrinsic stability. The established method of doing so is to look at the *h*/dbh ratio, but this work has illustrated that although this appears to make sense for individual trees, it does not work for plantation trees where a more complex process of interactions between the form of the individual tree and its neighbours occurs.

Moving one stage further it has been possible to use simple physical data to estimate the natural frequency of a tree using engineering formulae. The results, perhaps a little surprisingly, showed that the simplest of the three models produced the best results compared with measured natural frequencies obtained from field experiments. This model was largely based upon the length of the stem and its mass and the mass of its branches, there was no consideration as to the stem's shape. The more complex models which incorporated terms describing the shape and scale of the stem, but took no account of foliage mass, were poorer indicators of natural frequency. Thus it can be concluded that the most important features of a tree with regard to determining its natural frequency are its overall length, or height, and the mass of its stem and branches.

This highlights the fact that it is easy to be over elaborate when attempting to model a dynamic system like a swaying tree. Since forests are usually managed by non-engineers it is important that any attempts to discover the processes involved in windthrow use theories which are relatively simple to understand

whenever possible.

The most important aspect of the work carried out here looks at the relationship between the windload on the trees and the resultant displacement of the stems. The concept of a mechanical transfer function has previously been used for trees with good results. In this case the analysis was used to compare two different plots, which had undergone different silvicultural management, to see if there was any difference in the spectra produced. Both transfer functions had peaks which matched the estimated natural frequencies of the trees concerned, but the peak was broader in the plot which had not been thinned. This means that there was more damping of sways in the unthinned plot than in the thinned one. The presence of a natural frequency peak does show that there is some risk of resonance, however, illustrated by the broad nature of the peaks, damping will reduce this effect. So in practice there will be small chance of resonant vibration directly causing windthrow.

It may be possible that over a period of years, with large sways occasionally developing as a result of the semi-resonant vibration substantial damage may occur to the roots of the trees. Therefore, during slightly higher wind speeds the situation might arise where the tree finally falls over, although no large sways may have developed.

The results have clearly shown the importance of the dynamic response of trees to their environment and also the importance of the natural frequency of the trees in determining the stability of a stand. If a group of neighbouring trees is swaying there will normally be a large number of collisions amongst them. This effectively reduces the chance of dangerous large sways developing. However, if the trees start swaying in phase, which would be more likely to happen if they all had the same natural frequency, then the number of collisions would be less, and hence larger sways might occur. This means that for trees to be more stable they should ideally be surrounded by other trees with different periodicities, since there would then be less chance of them swaying in phase, especially over a significant

period of time. Therefore, it is suggested that forest managers might look at silvicultural techniques which produce trees of varying form, which will have different natural frequencies, if the aim is to reduce the risk of wind damage.

Added to the above ground processes are those occurring below ground. This study did not directly address this aspect of the system but they are obviously of great importance, and it is recommended that further work should involve root systems in some way. Displacement transducers could be attached to large stakes in the ground and connected to the roots to measure the extent of their movement while the stem is swaying.

This work has only looked at two different forms of silvicultural management, thus the results have a limited direct value in management terms. However, it has been shown that the techniques employed can illustrate the processes occurring in the forest and explain why one stand is more likely to blow over compared to another. There is, therefore, scope for further research using these techniques to compare other management regimes by varying the thinning intensity, the method of establishment, tree spacing, pruning, species choice, the effect of intricate mixtures, and the difference between planted and naturally regenerated woodland. By looking at these aspects it should be possible to obtain more information about the processes involved in windthrow and determine the best way to combat it.

At the same time, it is also important to remember the economic aspect of forest management. It is stated above that foresters should seek to grow a crop of diverse structure with the purpose of having trees with different natural frequencies, thus reducing the risk of in phase swaying, but this takes no account of the cost of doing so. Forestry is a long term industry and the economics are often marginal, so it is important to produce a product which is readily managed and harvested. By attempting to diversify the structure of forest blocks the costs of management will undoubtedly rise. Therefore, it is important that work in this area also looks at the practical aspects of forest management, not just the theory which in many cases will not be applicable due to financial constraints. Any

solution must be viable in management terms as well as theoretically appropriate.

BIBLIOGRAPHY

Armstrong, W.; Booth, T.C.; Priestly, P. and Read, D.J. (1976)
The relationship between soil aeration, stability and growth of Sitka spruce on upland peaty gleys.
Journal of Applied Ecology 13 : 585-591.

Bisshopp, K.E. and Drucker, D.C. (1945)
Large deflections of cantilever beams.
Quarterly of Applied Mathematics III.

Blackburn, P. (1986)
Factors affecting wind damage to Sitka spruce trees.
PhD Thesis, University of Aberdeen.

Blackburn, P.; Petty, J.A. and Miller, K.F. (1988)
An assessment of the static and dynamic factors involved in windthrow.
Forestry 61: 29-44.

Blackwell, P.G.; Rennolls, K. and Coutts, M.P. (1990)
A root anchorage model for shallowly rooted Sitka spruce.
Forestry 63(1): 73-91.

Blevins, R.D. (1979)
Formulas for Natural Frequency and Mode Shape.
Van Nostrand Reinhold, London.

Booth, T.C. (1977)
Windthrow Hazard Classification.
Forestry Commission Research Information Note 22/77/SILN,
Forestry Commission, Edinburgh.

Bouchon, J. (1986)
Susceptibility of different conifer species to blow down.
In *Minimising wind damage to conifer stands.*
pp. 33-34.

Boyd, D.M. and Webb, T.H. (1981)
The influence of the soil factor on tree stability in Balmoral forest, Canterbury, during the gale of August 1975.
New Zealand Journal of Forestry 26(1): 96-102.

Campbell, G.S. (1977)
An introduction to Environmental Biophysics - Chapter 4: Wind,
pp. 32-45. Springer Verlag, New York.

Cannell, M.G.R. and Morgan, J. (1987)
Young's modulus of sections of living branches and tree trunks.
Tree Physiology 3: 355-364.

Chatfield, C. (1984)
The analysis of time series, 3rd edition.
Chapman and Hall, London.

Cionco, R.M. (1972)
Intensity of turbulence within canopies with simple and complex roughness elements.
Boundary-layer Meteorology 2: 456-465.

Coutts, M.P. (1983)
Root architecture and tree stability.
Plant and Soil 71: 171-188.

Coutts, M.P. (1986)
Components of tree stability in Sitka spruce on peaty gley soil.
Forestry 59(2): 173 197.

Cremer, K.W.; Borough, C.J.; McKinnell, F.H. and Carter, P.R. (1982)
Effects of stocking and thinning on wind damage in plantations.
New Zealand Journal of Forestry Science 12(2): 244-268.

Curtis, J.D. (1943)
Some observations on wind damage.
Journal of Forestry 41: 877-882.

Day, W.R. (1950)
Soil conditions which determine windthrow in forests.
Forestry 23(1): 90-95.

Deans, J.D. (1983)
Distribution of thick roots in a Sitka spruce plantation 16 years after planting.
Scottish Forestry 37(1): 17-31.

Finnigan, J.J. (1979)
Turbulence in waving wheat. I. Mean statistics and Honami.
Boundary-layer Meteorology 16: 213-236.

Fraser, A.I. (1962a)
The soil and roots as factors in tree stability.
Forestry 35(2): 117-127.

Fraser, A.I. (1962b)
Wind tunnel studies of the forces acting on the crowns of small trees.
Forestry Commission Report on Forest Research: 178-183, H.M.S.O., London.

Fraser, A.I. (1964)
Wind tunnel and other related studies on coniferous trees and tree crops.
Scottish Forestry 18(2): 84-92.

Fraser, A.I. (1965)
The uncertainties of wind-damage in forest management.
Irish Forestry 22(1): 23-30.

Galinski, W. (1989)
A windthrow-risk estimation for coniferous stems.
Forestry 62(2): 139-146.

Gardiner, B.A. (1989)
Mechanical properties of Sitka spruce.
Unpublished report to Forestry Commission, Roslin, Midlothian.

Gardiner, B.A. (1990)
Mechanical characteristics of Sitka spruce.
Forestry Commission Occasional Paper 24, HMSO, London.

Goss, D.W. (1960)
Windthrow in young plantations on ploughed heathland.
Sylva 41: 18.

Grace, J. (1983)
Plant-atmosphere relationships.
Chapman and Hall, London and New York.

Grayson, A.J. (Ed.) (1989)
The 1987 storm impacts and responses.
Forestry Commission Bulletin 87, H.M.S.O., London.

Hendrick, E. (1986)
Appropriate cultivation and drainage techniques for sites liable to windthrow.
In *Proc. Danish Forest Expt. Station and C.E.C, Denmark*
Minimising wind damage to conifer stands.
pp. 30 - 32.

Holbo, H.R.; Corbett, T.C. and Horton, P.J. (1980)
Aeromechanical behaviour of selected Douglas-fir.
Agricultural meteorology 21: 81-91.

Holland, M.R.; Grace, J. and Hedley, C.L. (1991)
Momentum absorption by dried-pea crops. I. Field measurements over and within varieties of differing leaf structure.
Agricultural and Forest Meteorology 54: 67-79.

Holland, M.R.; Grace, J. and Hedley, C.L. (1991b)
Momentum absorption by dried-pea crops. II. Wind tunnel measurements of drag on isolated leaves and pods.
Agricultural and Forest Meteorology 54: 81-93.

Holtham, B.W. (Ed.) (1971)
Windblow of Scottish forests in January 1968.
Forestry Commission Bulletin No. 45
HMSO, London, 53 pp.

Horst, T.W. (1973)
Correction for response errors in a three-component propellor anemometer.
Journal of Applied Meteorology 12: 716-725.

Jacobs, M.R. (1954)
The effect of wind sway on the form and development of *Pinus radiata.*
Australian Journal of Botany 2: 35-51.

Kilpatrick, D.J.; Sanderson, J.M. and Savill, P.S. (1981)
Treatments on the growth of Sitka spruce.
Forestry 54(1): .

King, D. (1986)
Tree form, height growth and susceptibility to wind damage in *Acer saccharum.*
Ecology 67: 980-990.

King, D. and Loucks, O.L. (1978)
The theory of tree bole and branch form.
Rad. Environ. Biophys. 15: 141-165.

Kuiper, L.C. (1986)
Tree pulling experiments with Douglas fir in the Netherlands.
In *Proc. Danish Forest Expt. Station and CEC, Denmark*
Minimising wind damage to conifer stands.
pp. 17-20.

Landsberg, L.C. and James, G.B. (1971)
Wind profiles in plant canopies: studies on an analytical model.
Journal of Applied Ecology 8: 729-741.

Landsberg, L.C. and Jarvis, P.G. (1973)
A mechanical investigation of the momentum balance of a spruce forest.
Journal of Applied Ecology 10: 645-655.

Landsberg, L.C. and Thom, A.S. (1971)
Aerodynamic properties of a plant of complex structure.
Quarterly Journal of the Royal Meteorological Society 97: 565-570.

Larson, P.R. (1965)
Stem form of young *Larix* as influenced by wind and pruning.
Forest Science 11(4): 412-424.

Legg, B.J., Long, I.F. and Zemroch, P.J. (1981)
Aerodynamic properties of field beans and potato crops.
Agricultural Meteorology 23: 21-43.

Leiser, A.T. and Kemper, J.D. (1973)
Analysis of stress distribution in the sapling tree trunk.
Journal of the American Society of Horticultural Science 98: 164-170.

MacDonald, A.J. and Morgan, J. (Unpubl.)
A method for calculating the vibration amplitudes of slender structures in turbulent winds.

MacMahon, T.A. and Kronauer, R.E. (1976)
Tree structures: deducing the principles of mechanical design.
Journal of Theoretical Biology 59: 443-466.

Mayer, H. (1987)
Wind-induced tree sways.
Trees 1: 195-206.

Mayer, H. (1989)
Windthrow.
Phil. Trans. R. Soc. Lond. B 324: 267-281.

Mayhead, G.J. (1973)
Sway periods for forest trees.
Scottish Forestry 27(1): 19-23.

Mayhead, G.J; Gardiner, G.B.H. and Durrant, D.W. (1975)
A Report on the physical properties of conifers in relation to plantation stability.
Forestry Commission Research and Development Paper, HMSO, London.

Mergen, F. (1954)
Mechanical aspects of wind-breakage and windfirmness.
Journal of Forestry 52: 119-125.

Miller, K. (1985)
Windthrow Hazard Classification.
Forestry Commission Leaflet 85, HMSO, London.

Miller, K. (1986)
Recent aeromechanical research in forest plantations.
In *Proc. Danish Forest Expt. Station and CEC, Denmark*
Minimising wind damage to conifer stands. p 7-11.

Milne, R. (1986)
Methods of modelling tree stem bending under wind loading.
In *Proc. Danish Forest Expt. Station and CEC, Denmark*
Minimising wind damage to conifer stands. p 12-16.

Milne, R. (1990)
Dynamics of swaying *Picea sitchensis*.
Unpublished report to ITE, Penicuik, Edinburgh.

Milne, R. (1991)
Dynamics of swaying of *Picea sitchensis*.
Tree Physiology 9: 383-399.

Milne, R. (1992)
Extreme wind speeds over a Sitka spruce plantation in Scotland.
Agricultural and Forest Meteorology 61: 39-53.

Milne, R. and Blackburn, P. (1989)
The elasticity and vertical distribution of stress within stems of *Picea sitchensis*.
Tree Physiology 5: 195-205.

Montieth, J.L. and Unsworth, M.H. (1990)
Principles of Environmental Physics.
Edward Arnold, London.

Moore, D.G. (1976)
Oceanic Forestry.
Irish Forestry 33: 4-15.

Morgan, J. and Cannell, M.G.R. (1987)
Structural analysis of tree trunks and branches: tapered cantilever beams subject to large deflections under complex loading.
Tree Physiology 3: 365-374.

Neckelmann, J. (1986)
Choice of species, topping and high pruning as means to prevent windthrow in permanent or recent stand edges.
In *Proc. Danish Forest Expt. Station and CEC, Denmark*
Minimising wind damage to conifer stands. p 42-45.

Oliver, H.R. and Mayhead, G.J. (1974)
Wind measurements in alpine forest during a destructive gale.
Forestry 47(2): 185-194.

Papesch, A.J.G. (1974)
A simplified theoretical analysis of the factors that influence windthrow of trees.
In *5th Australian Conference on Hydraulics and Fluid Dynamics, University of Canterbury, New Zealand.*

Papesch, A.J.G. (1983)
Wind and its effects on (Canterbury) forests.
PhD. Thesis, University of Canterbury, New Zealand.

Petty, J.A. and Swain, C. (1985)
Factors influencing stem breakage of conifers in high winds.
Forestry 58(1): 75-84.

Petty, J.A. and Worrell, R. (1981)
Stability of conifer stems in relation to damage by snow.
Forestry 54(2): 115-128.

Priest, G.I.; Quine, C.P. and Cameron, A.D. (1991)
Windthrow of five year old Sitka spruce on an upland restocking site.
Scottish Forestry 45(2): 120-128.

Prior, K.W. (1959)
Wind damage to exotic forests in Canterbury.
New Zealand Journal of Forestry 8(1): 57-68.

Putz, F.E., Parker, G.G. and Archibald, R.M. (1983)
Mechanical abrasion and intercrown spacing.
American Midland Naturalist 112: 24-28.

Pyatt, D.G. (1970)
Soil groups of upland forests.
Forestry Commission Forest Record No. 71, HMSO, London.

Savill, P.S. (1976)
The effects of drainage and ploughing of surface water gleys on rooting and windthrow of Sitka spruce in Northern Ireland.
Forestry 49(2): 133-141.

Savill, P.S. (1983)
Silviculture in windy climates.
Forestry Abstracts 44(8): 473-488.

Shaw, R.H., den Hartog, G., King, K.M. and Thurtell, G.W. (1974)
Measurements of mean wind flow and three-dimensional turbulence within a mature corn crop.
Agricultural Meteorology 13: 419-425.

Simiu, E. and Scanlan, R.H (1986)
Wind effects on structures.
2nd Ed, Wiley, New York.

Stuhr, G. (1981)
Growth and thinning of Norway spruce in *Schleswig-Holstein.*
Allegemeine Forst-und Jagdzeitung 152(1): 15-20.

Stull, R.B. (1988)
An Introduction to Boundary Layer Meteorology.
Kluwer, London.

Takahashi, K. and Wakabayashi, R. (1981)
Stem sway and tree form of Akamatsu, Japanese red pine.
Journal of Japanese Forestry Society 63(4): 133-136.

Thom, A.S. (1975)
Momentum, mass and heat exchange of plant communities.
In *Vegetation and the Atmosphere (J.L. Montieth, ed.), Vol 1: 57-105*
Academic Press, London.

Thomson, W.T. (1988)
Theory of Vibration with Appliances.
Allen & Unwin, London.

Thompson, D.A. (1979)
Forest drainage schemes.
Forestry Commission Leaflet 72, HMSO, London.

Thompson, D.A. (1984)
Ploughing of forest soils.
Forestry Commission Leaflet 61, HMSO, London.

Timoshenko, S.P. and Gere, J.M. (1961)
Theory of elastic stability.
McGraw Hill, New York.

USDA (1974)
Wood Handbook: wood as an engineering material.
United States Department of Agriculture Handbook 72,
Madison, Wisconsin.

Van Gardingen, P. and Grace, J. (1991)
Plants and wind.
Advances in Botanical Research 18: 189-246.

White, R.G.; White, M.F. and Mayhead, G.J. (1976).
Measurement of the motion of trees in two dimensions.
University of Southampton, Institute of Sound and Vibration Research, Technical Report No. 86, p 16.

Appendix I Location maps of the eleven sample trees with respect to their neighbours

Key to symbols: nos. = d.b.h. values of tree stems (cm)
+ = position of tree stem
. = position of sample tree
f = forked stem (diameter of largest stem given)
..... = displacement transducer lines
_ _ _ = line of the ridge
____ = line of a ditch

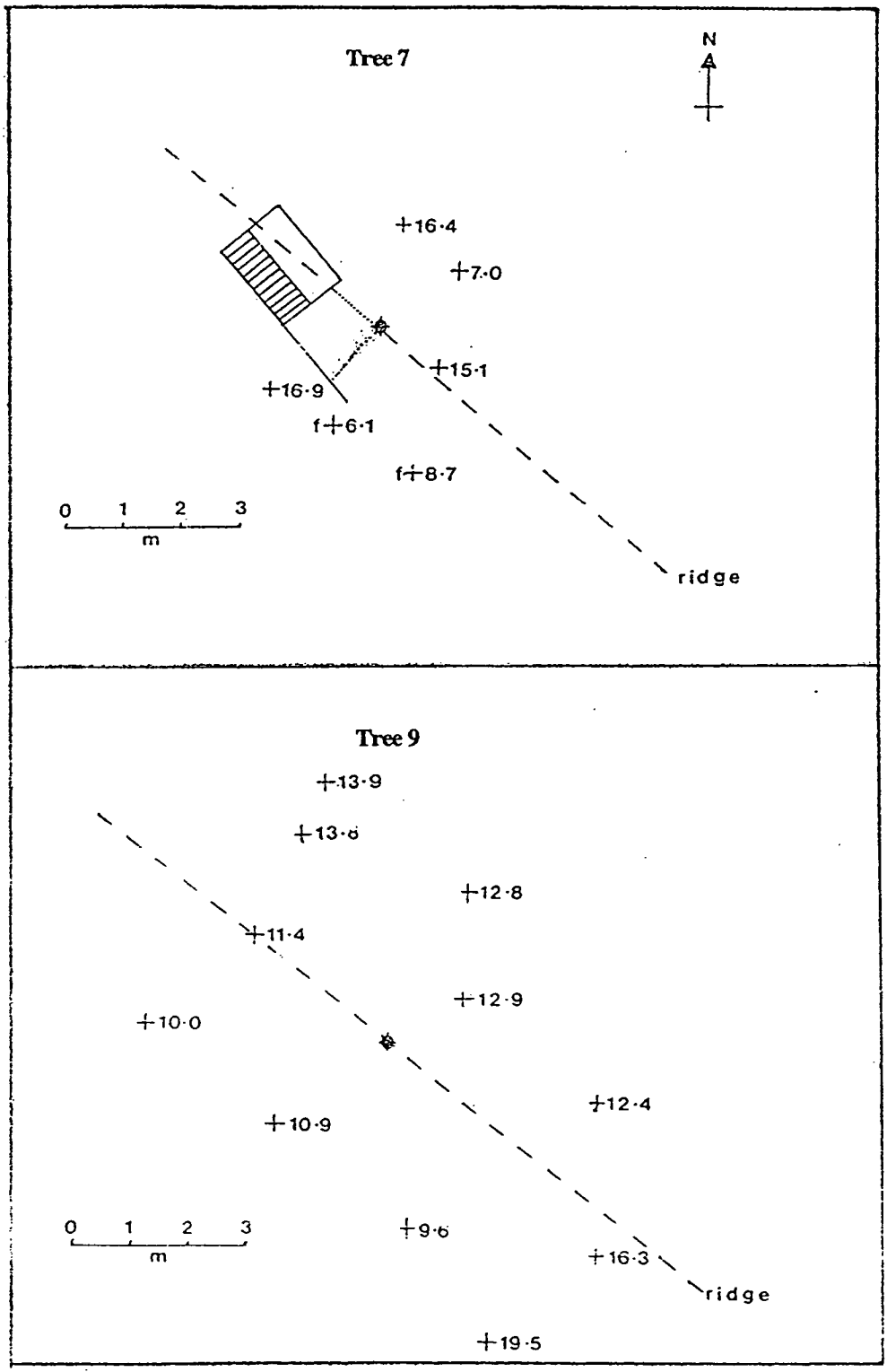

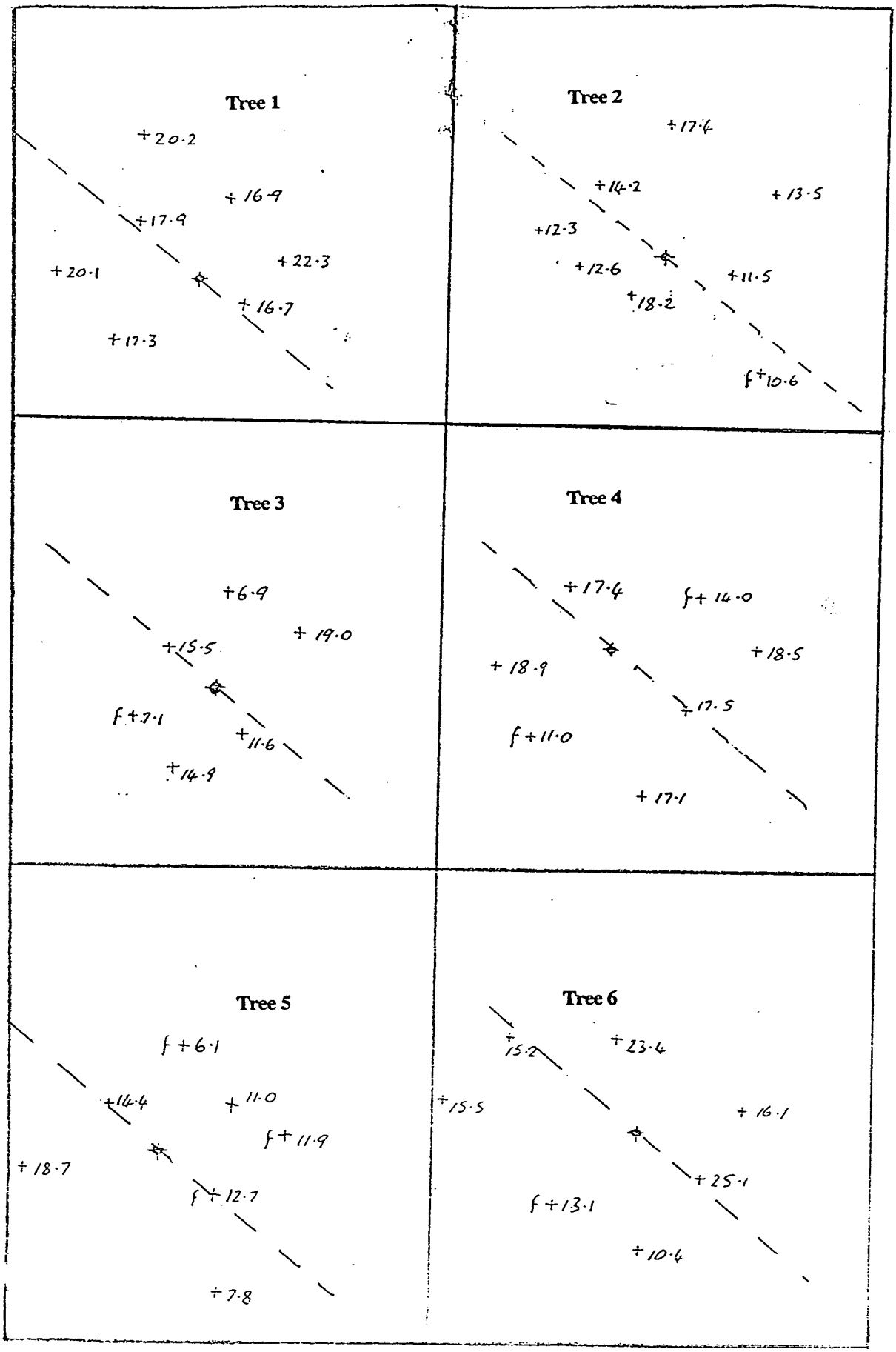
Tree 1
+20·2
+16·9
+17·9
+22·3
+20·1
+16·7
+17·3
Tree 2
+17·4
+14·2
+13·5
+12·3
+12·6
+11·5
+18·2
f+10·6
Tree 3
+6·9
+19·0
+15·5
f+7·1
+11·6
+14·9
Tree 4
+17·4
f+14·0
+18·5
+18·9
+17·5
f+11·0
+17·1
Tree 5
f+6·1
+14·4
+11·0
f+11·9
+18·7
f+12·7
+7·8
Tree 6
+15·2
+23·4
+15·5
+16·1
+25·1
f+13·1
+10·4

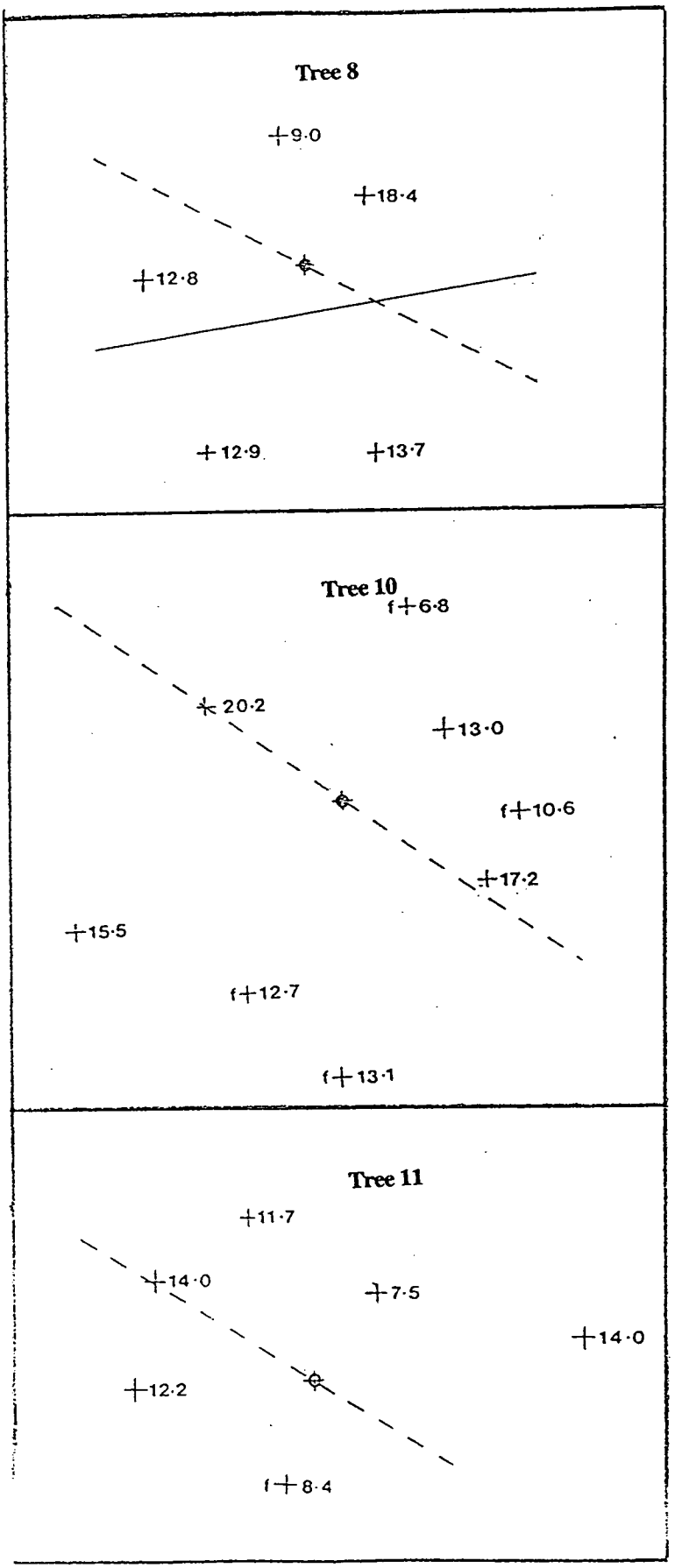
Tree 8
9·0
18·4
12·8
12·9
13·7
Tree 10
f 6·8
20·2
13·0
f 10·6
17·2
15·5
f 12·7
f 13·1
Tree 11
11·7
14·0
7·5
14·0
12·2
f 8·4

Appendix II Diameter vs. Height graphs for the eleven sample trees
(Trees 1-7 Unthinned plot, Trees 8-11 Thinned plot)

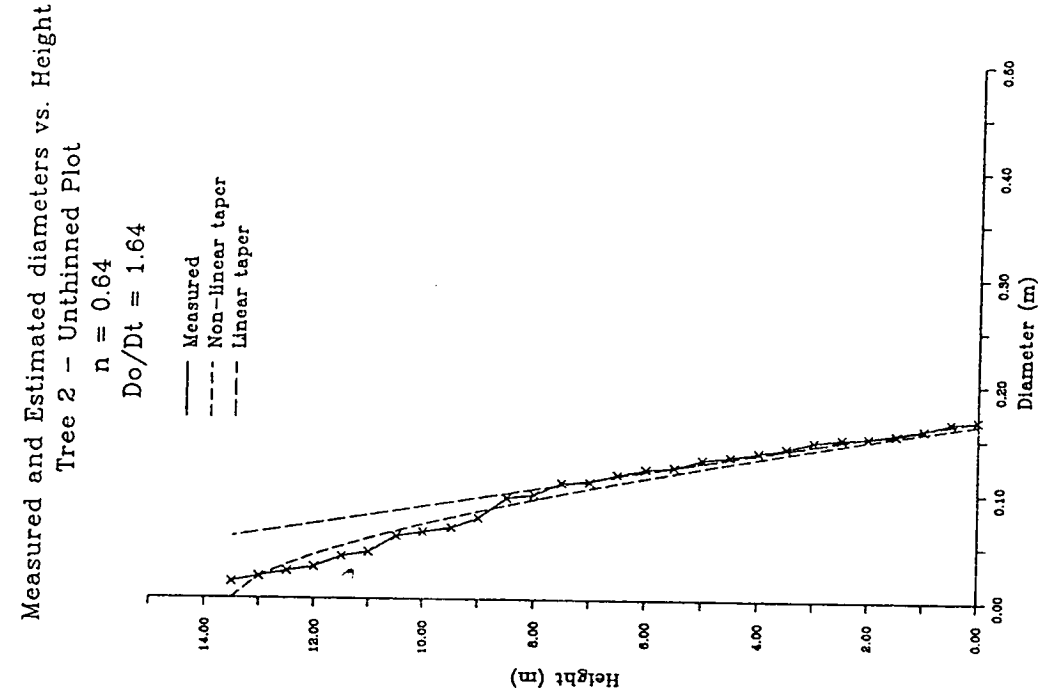

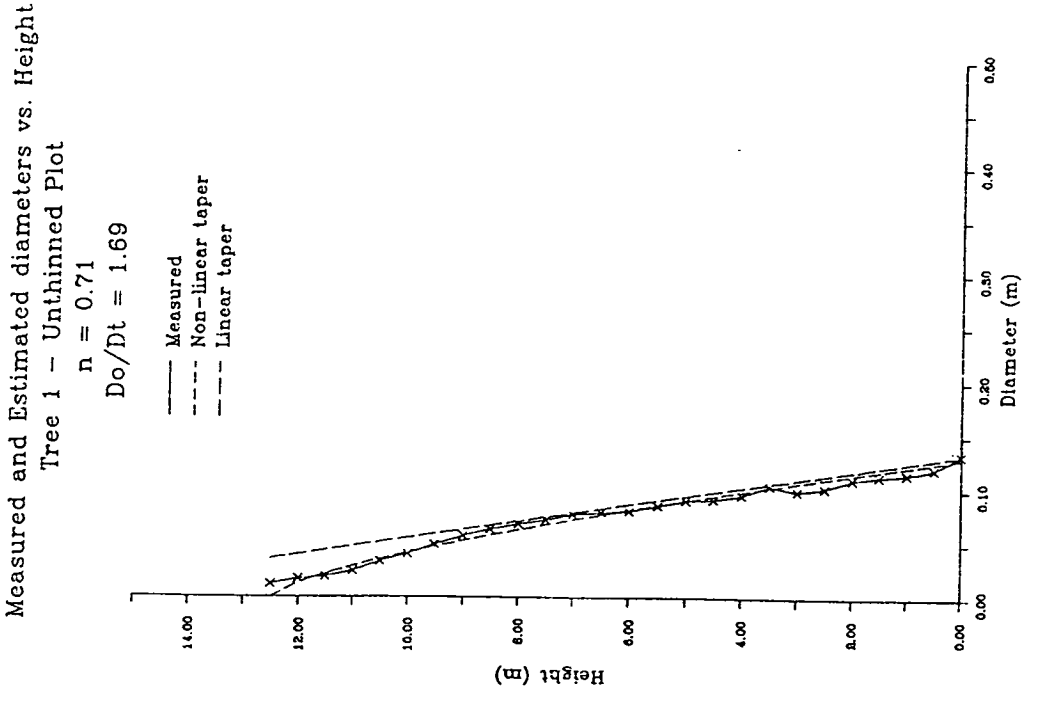

Measured and Estimated diameters vs. Height
Tree 3 – Unthinned Plot
n = 0.72
Do/Dt = 1.52

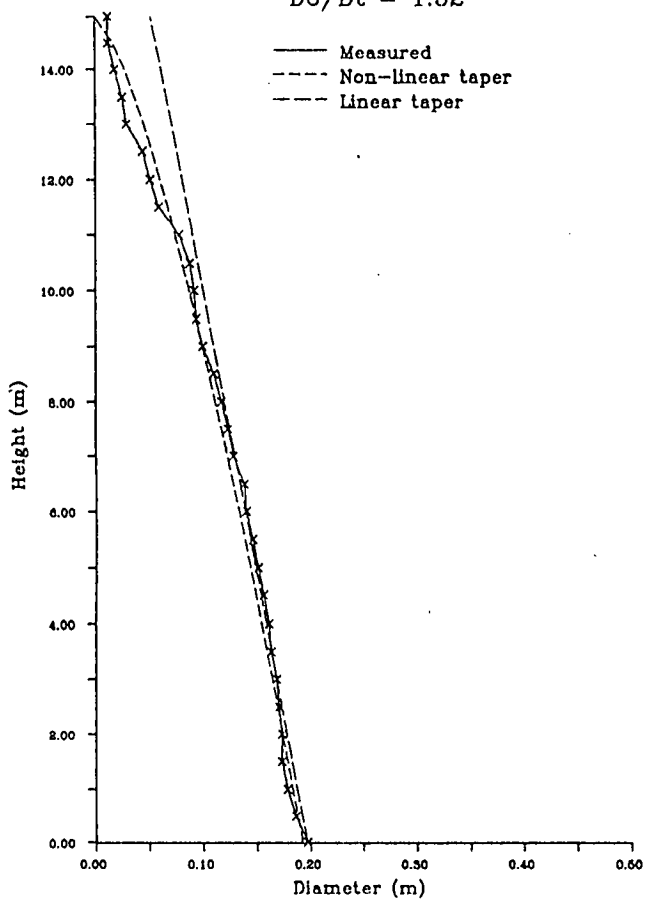

Measured and Estimated diameters vs. Height
Tree 4 – Unthinned Plot
n = 0.58
Do/Dt = 1.60

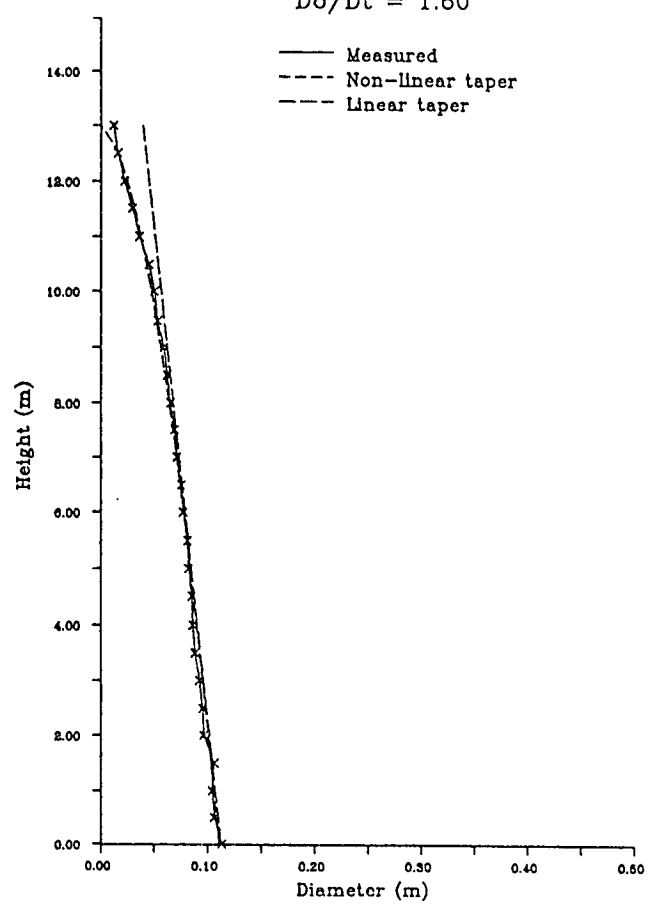

Measured and Estimated diameters vs. Height
Tree 5 – Unthinned Plot
n = 0.63
Do/Dt = 1.48

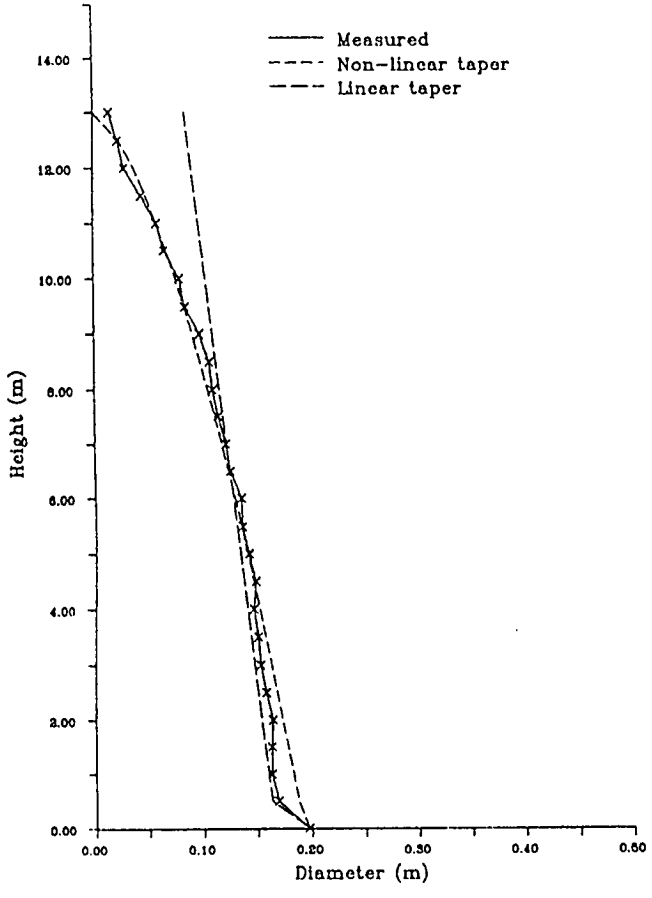

Measured and Estimated diameters vs. Height
Tree 6 – Unthinned Plot
n = 0.77
Do/Dt = 1.78

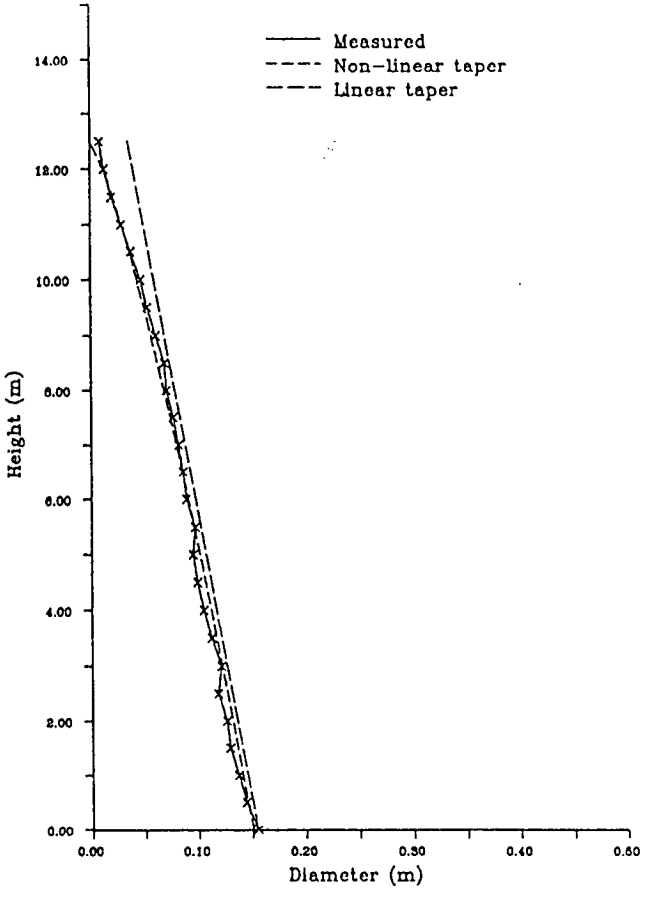

Measured and Estimated diameters vs. Height
Tree 7 – Unthinned Plot
n = 0.69
Do/Dt = 1.41

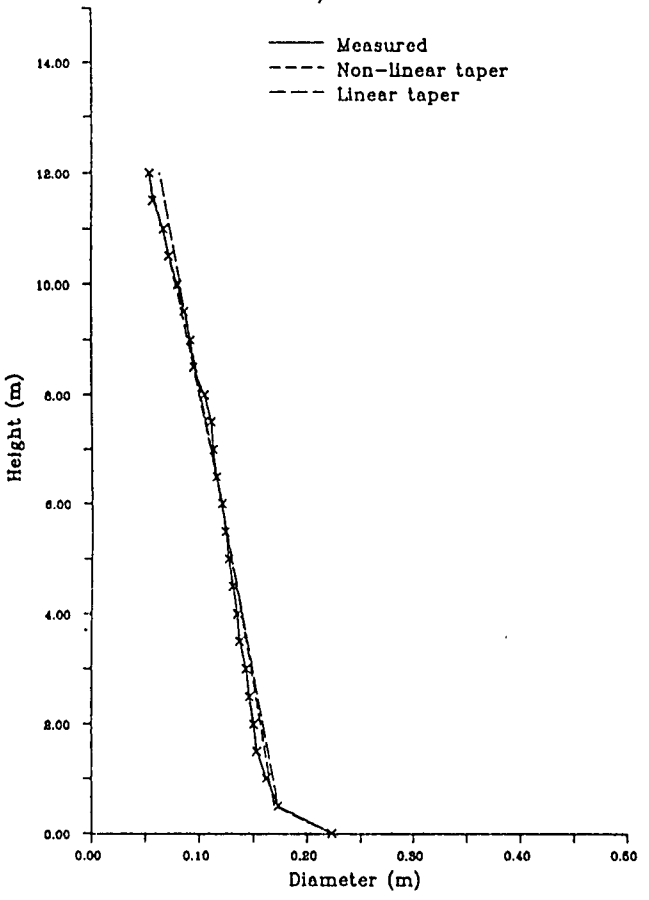

Measured and Estimated diameters vs. Height
Tree 8 – Thinned Plot
n = 0.86
Do/Dt = 3.13

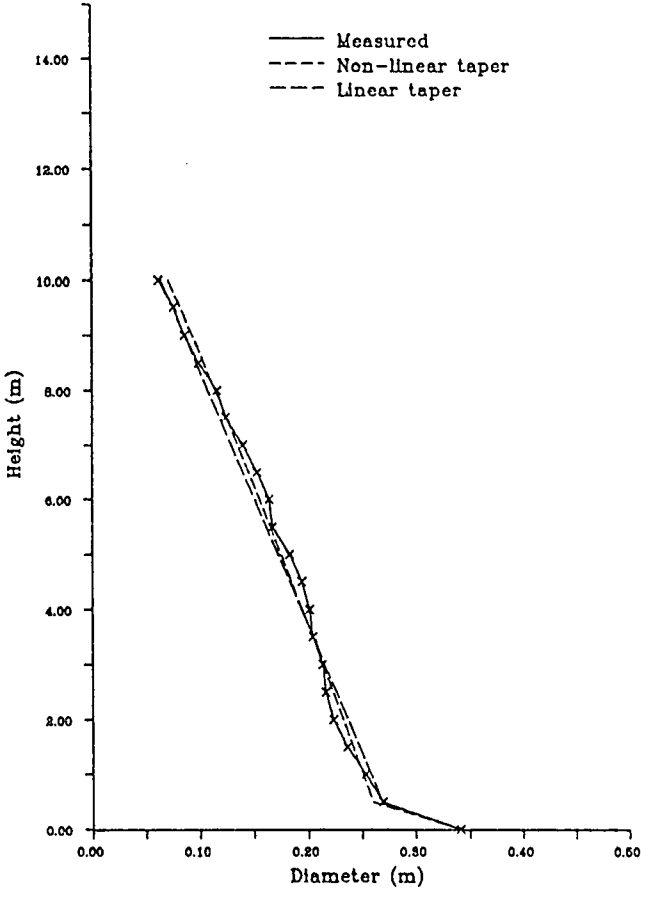

Measured and Estimated diameters vs. Height
Tree 9 – Thinned Plot
n = 0.61
Do/Dt = 2.42

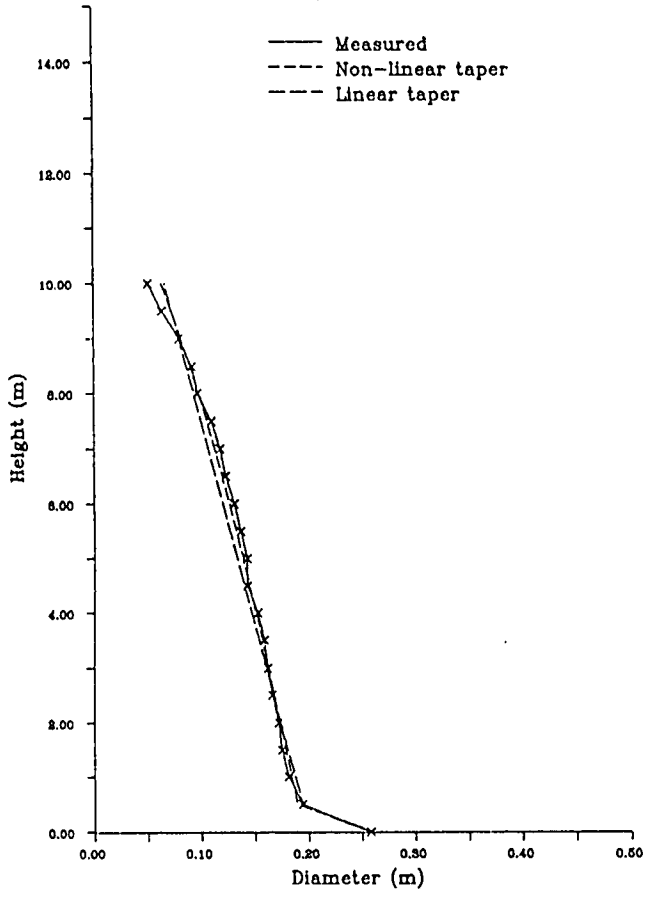

Measured and Estimated diameters vs. Height
Tree 10 – Thinned Plot
n = 0.86
Do/Dt = 3.52

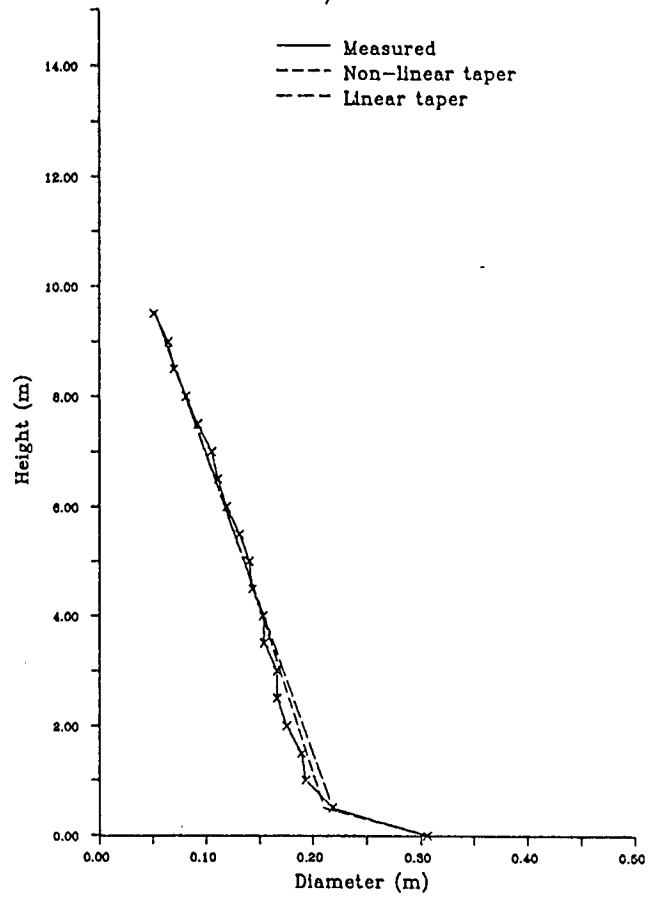

Measured and Estimated diameters vs. Height
Tree 11 – Thinned Plot
n = 1.00
Do/Dt = 4.08

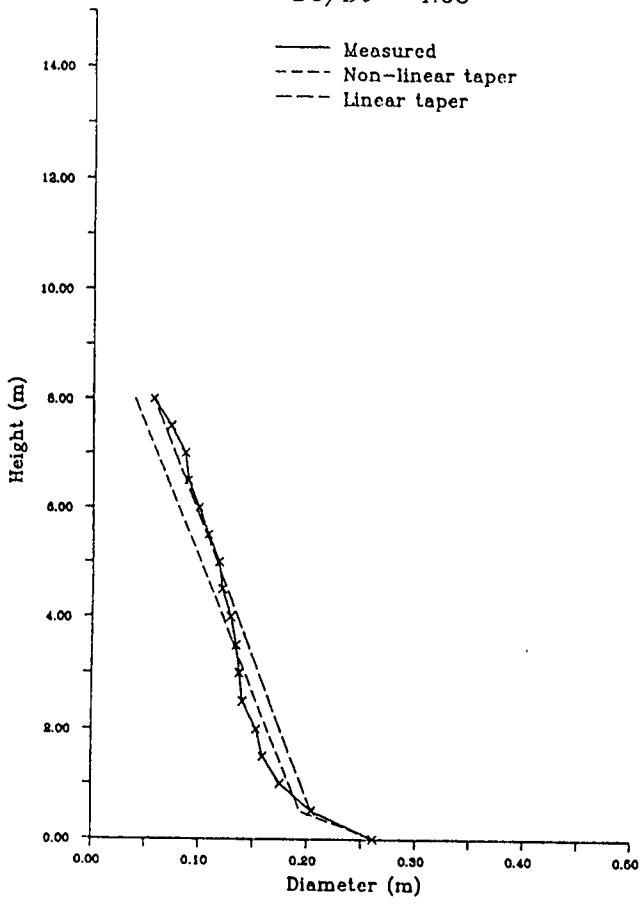

Appendix III Computer program to determine *n* to describe the stem taper assuming non-linear taper

Filename: NDET

Language: Fortran

```
C     ------------------------------------------------------------
C     Program to determine "n"
C     ------------------------------------------------------------

C     Input parameters from the screen
10    Call emas3prompt ('Enter basal diameter (cm): ')
      Read *, Do
      Call emas3prompt ('Enter stem height (m): ')
      Read *, RL
      Call emas3prompt ('Enter a value for n (between 0.0 and 1.0): ')
      Read *, Rn

20    H = 0.0
      SUMSQ = 0.0

C     Input real stem diameter data (m)
30    Read (7,*) DIAM

C     Determine modelled value for diameter at height x
40    x = RL - H
      y = (((Do/2)*((x/RL)**Rn))*2)

C     Calculate ths sum of the squares of the difference between
C     the modelled value "y" and DIAM
50    DIAM = DIAM/100
      DIFF = DIAM - y
      SUMSQ = SUMSQ + (DIFF**2)

C     Write results into an output file
60    WRITE (8,*) H, y, DIAM, SUMSQ
      IF (DIAM.EQ.99) GOTO 70

C     Increase height unit by 0.5 m and loop to calculate next value for y
      H = H + 0.5
      GOTO 30

70    STOP
      END
```

Appendix IV Mass of the stem and branches vs Height for the eleven sample trees
(Trees 1-7 Unthinned plot, Trees 8-11 Thinned plot)

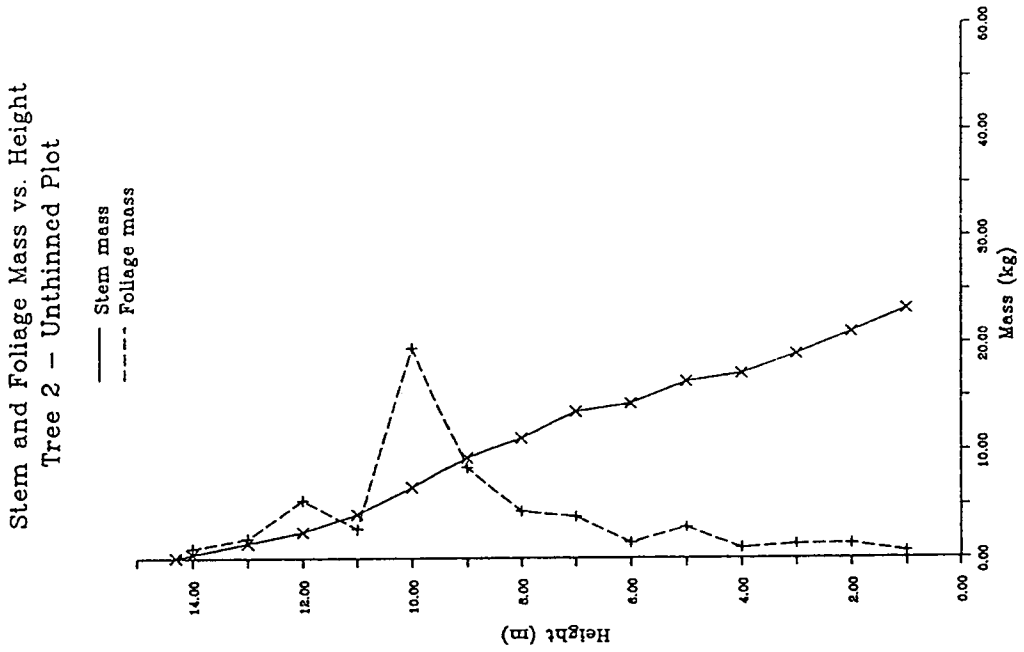

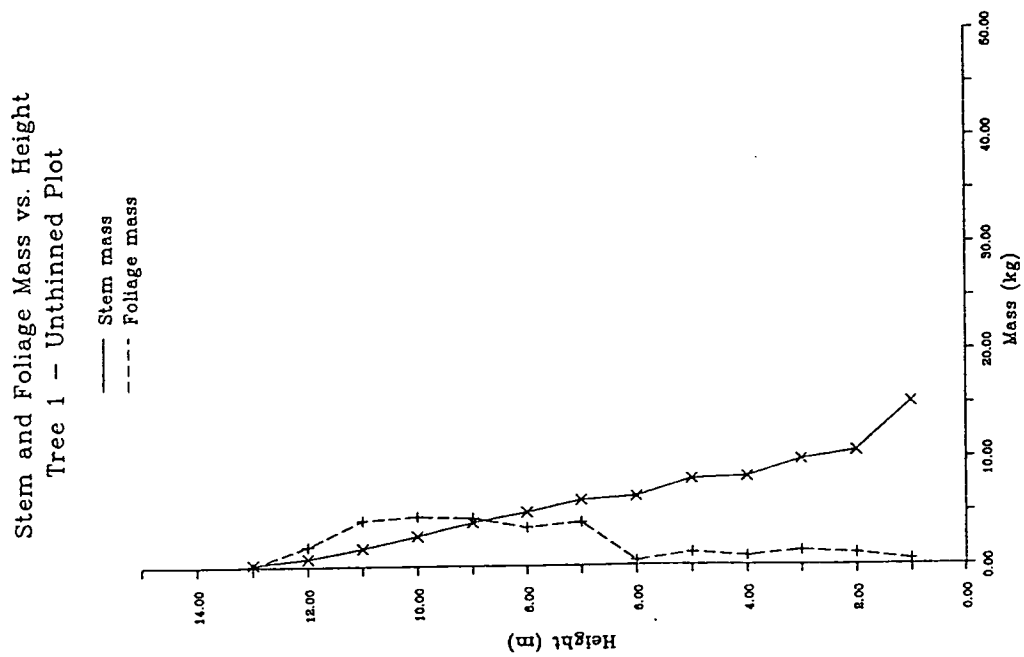

Stem and Foliage Mass vs. Height
Tree 3 – Unthinned Plot

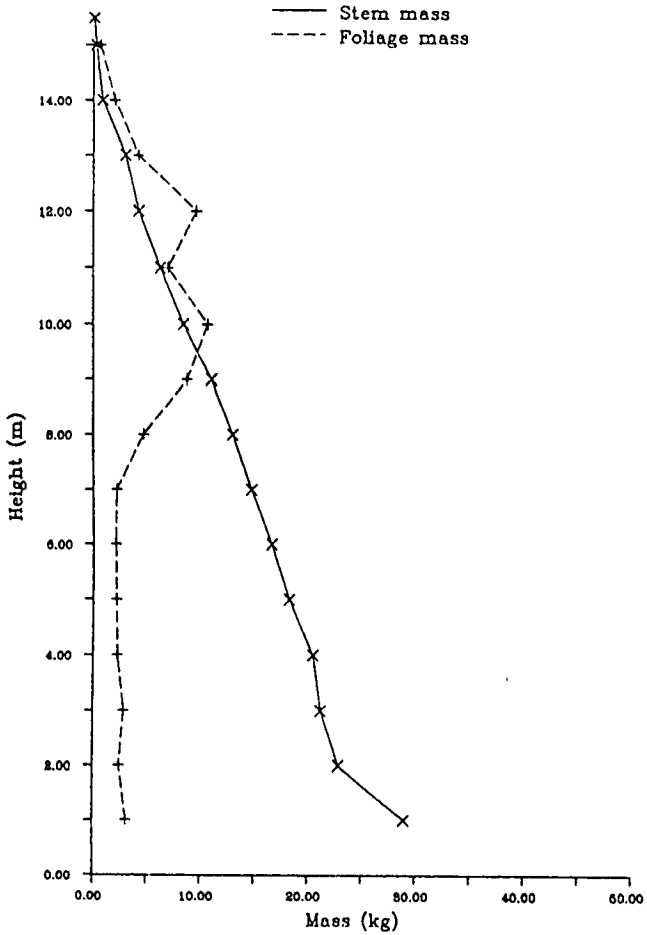

Stem and Foliage Mass vs. Height
Tree 4 – Unthinned Plot

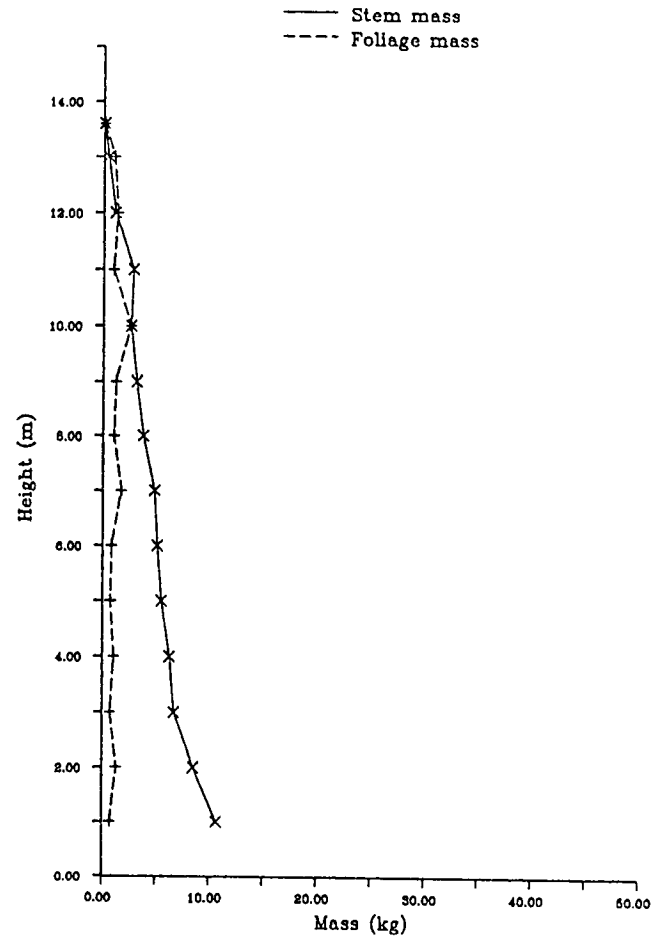

Stem and Foliage Mass vs. Height
Tree 5 – Unthinned Plot

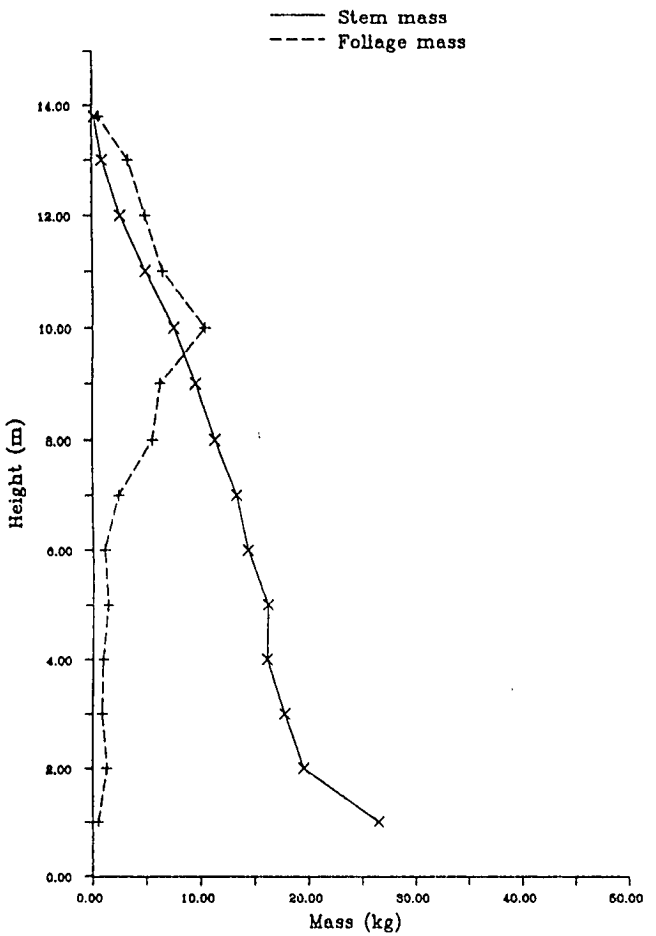

Stem and Foliage Mass vs. Height
Tree 6 – Unthinned Plot

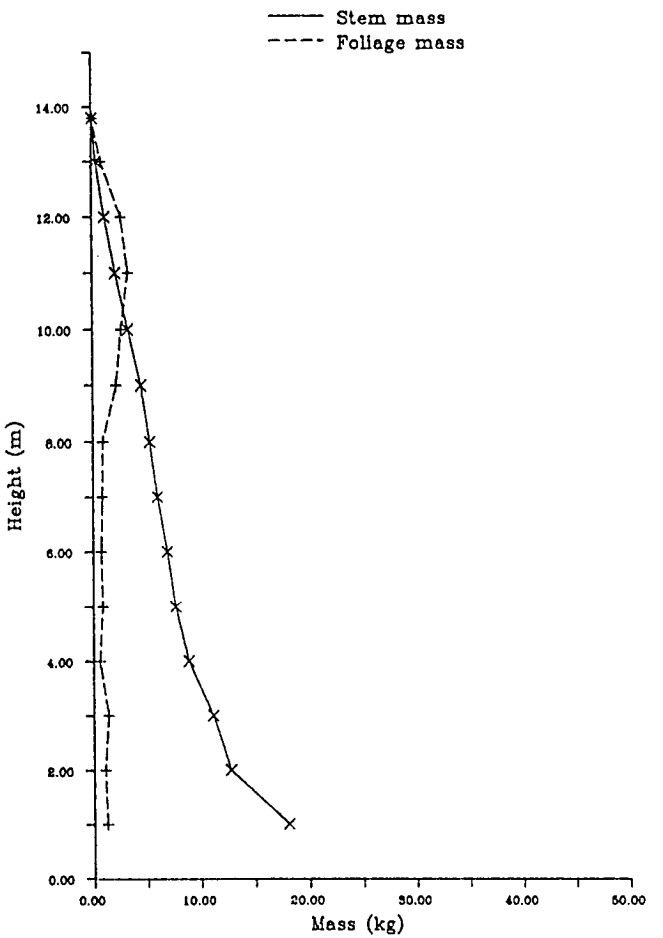

Stem and Foliage Mass vs. Height
Tree 7 – Unthinned Plot

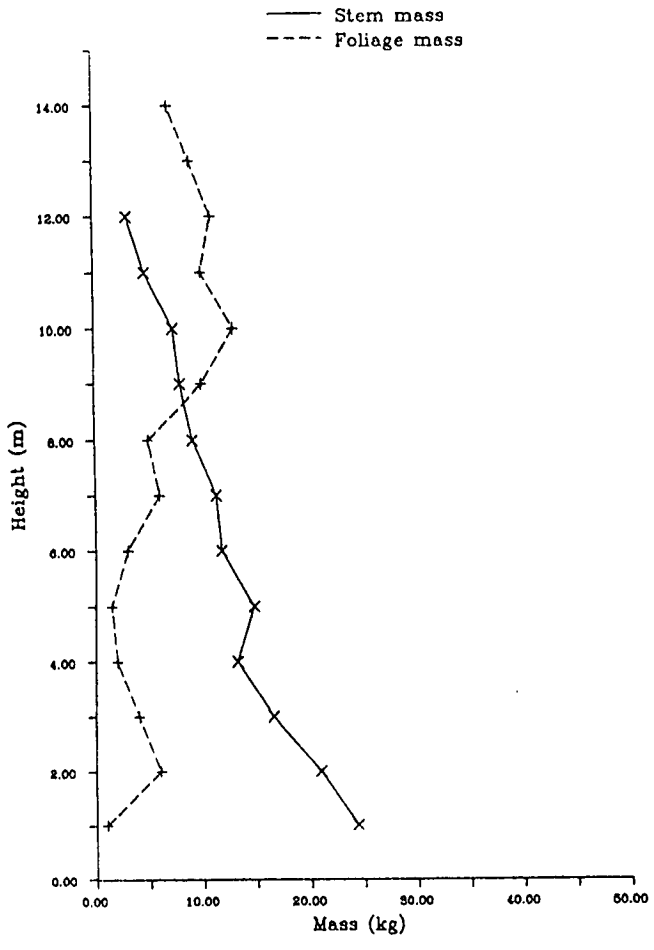

Stem and Foliage Mass vs. Height
Tree 8 – Thinned Plot

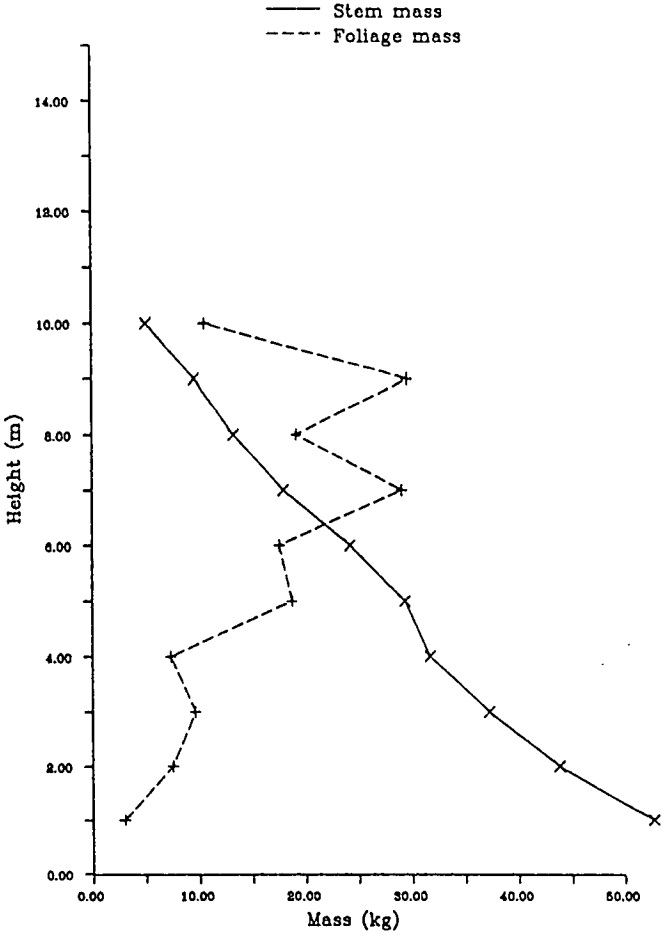

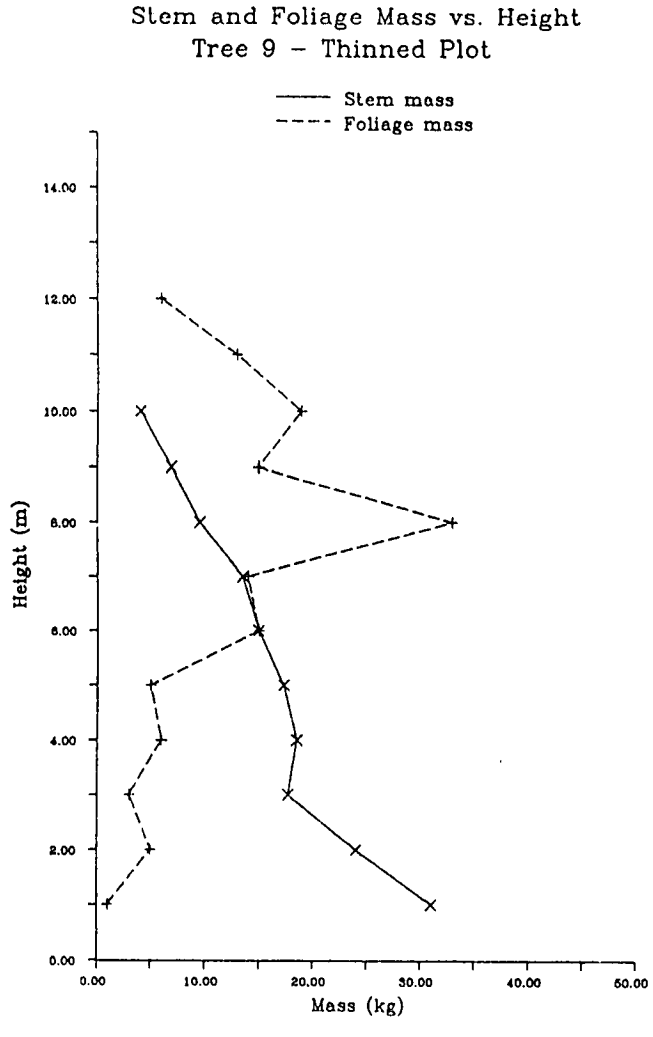
Stem and Foliage Mass vs. Height
Tree 9 – Thinned Plot
Stem mass
Foliage mass
Height (m)
Mass (kg)
0.00
2.00
4.00
6.00
8.00
10.00
12.00
14.00
0.00
10.00
20.00
30.00
40.00
50.00

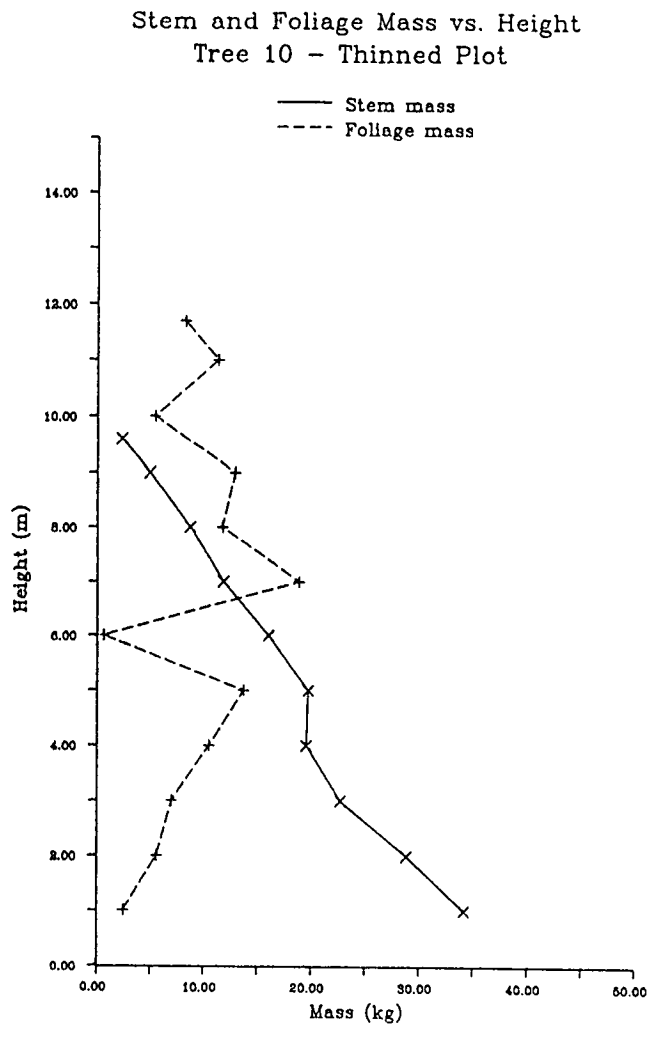
Stem and Foliage Mass vs. Height
Tree 10 – Thinned Plot
Stem mass
Foliage mass
Height (m)
Mass (kg)
0.00
2.00
4.00
6.00
8.00
10.00
12.00
14.00
0.00
10.00
20.00
30.00
40.00
50.00

Stem and Foliage Mass vs. Height
Tree 11 – Thinned Plot

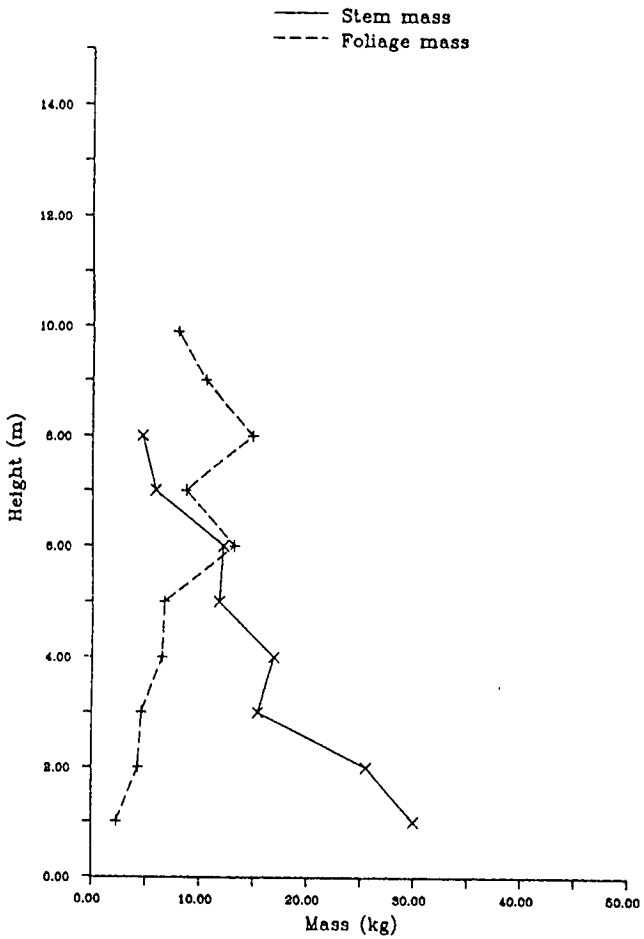

Appendix V Under-bark Diameter vs. Age and Height for the eleven sample trees
(Trees 1-7 Unthinned plot, Trees 8-11 Thinned plot)

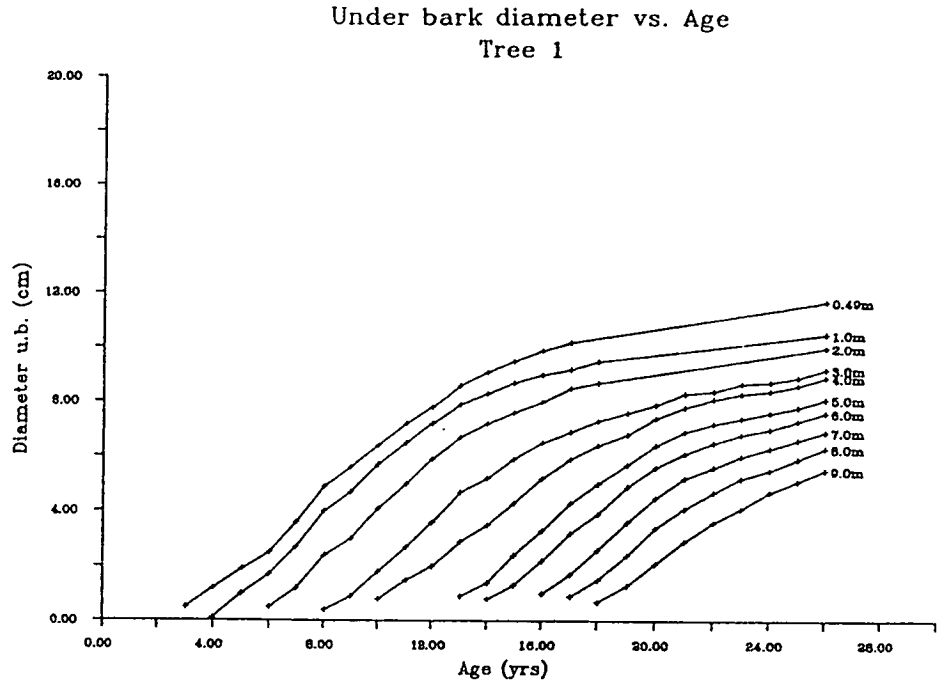

Under bark diameter vs. Age
Tree 3

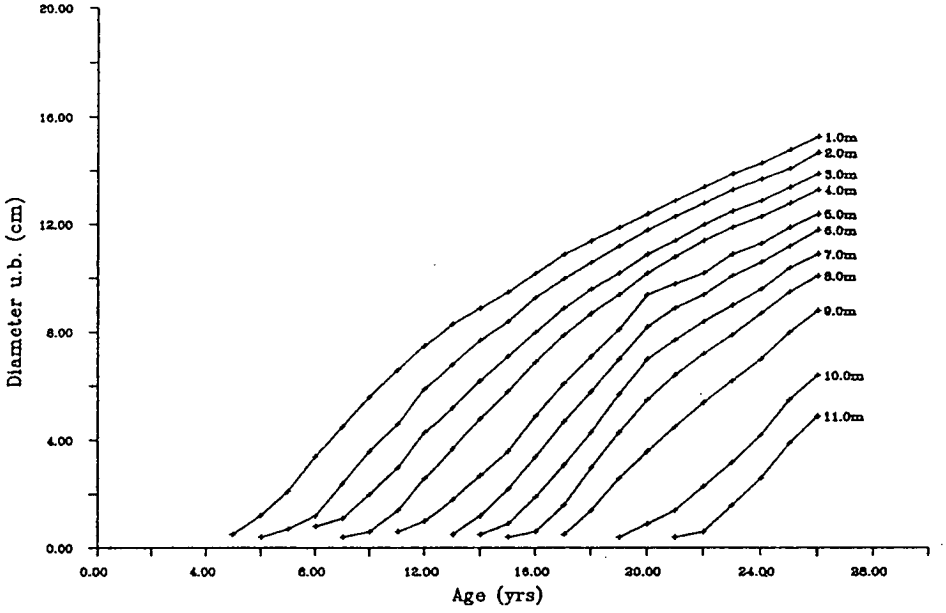

Tree 4

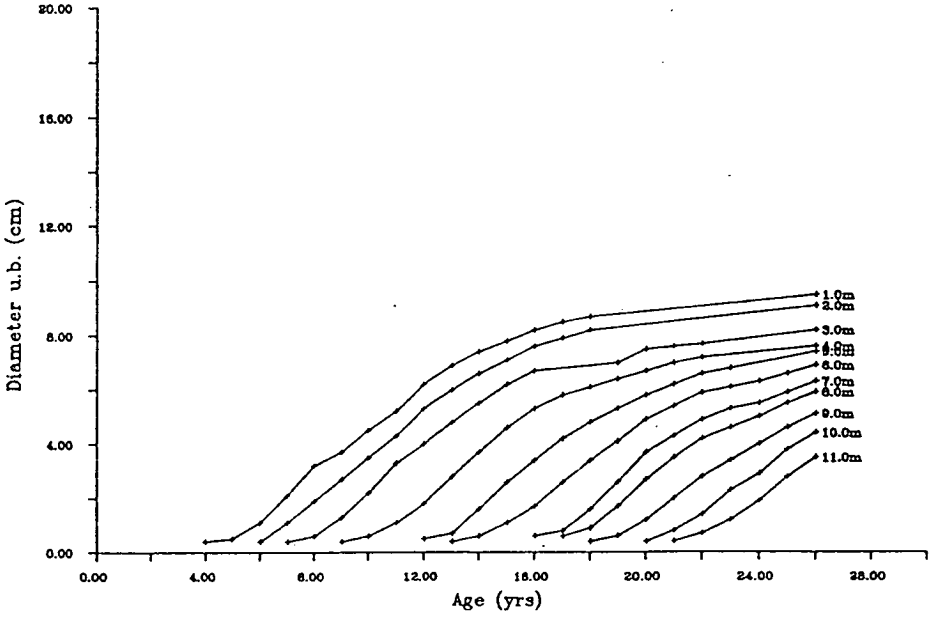

Under bark diameter vs. Age
Tree 5

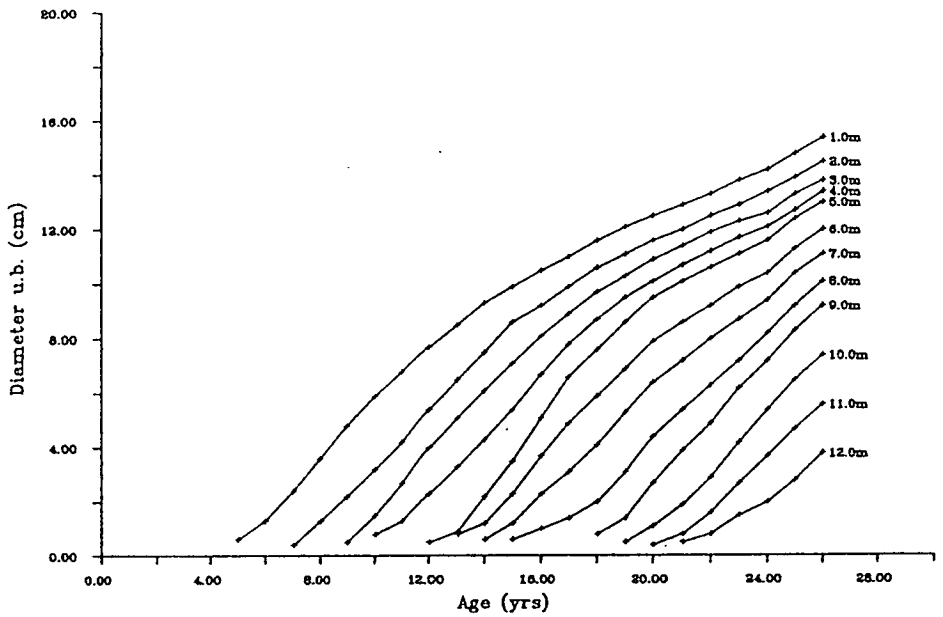

Tree 6

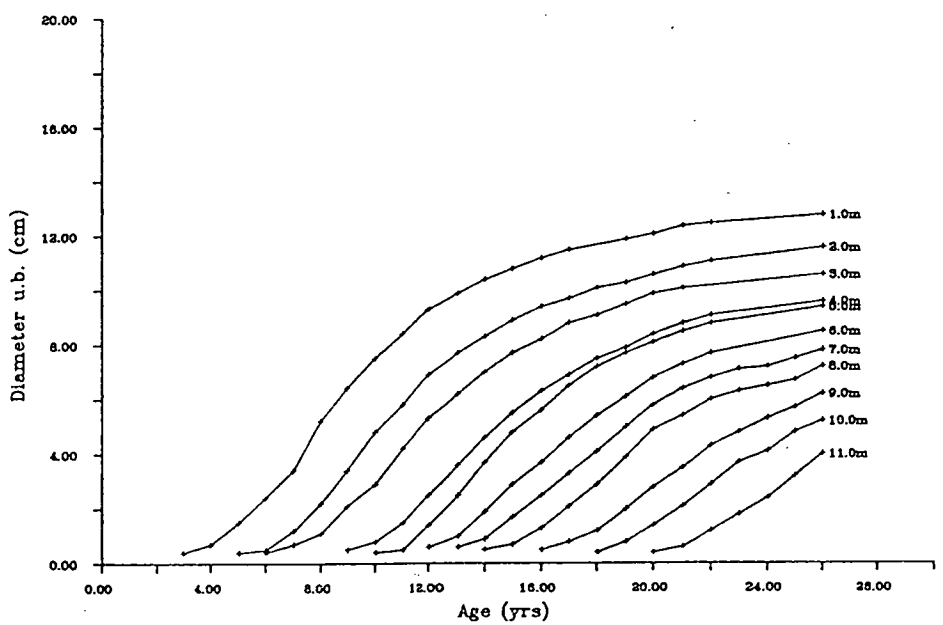

Under bark diameter vs. Age
Tree 7

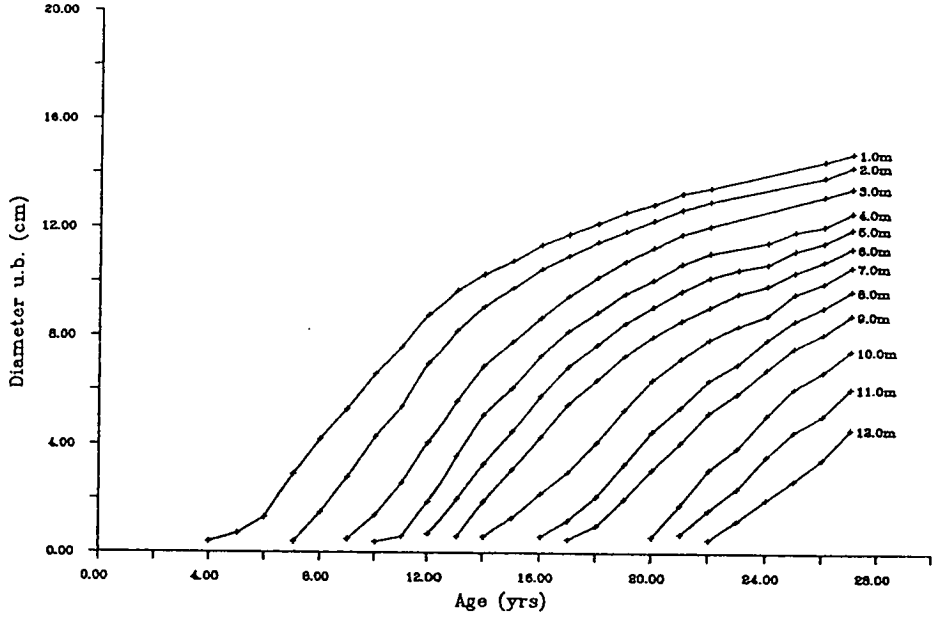

Tree 8

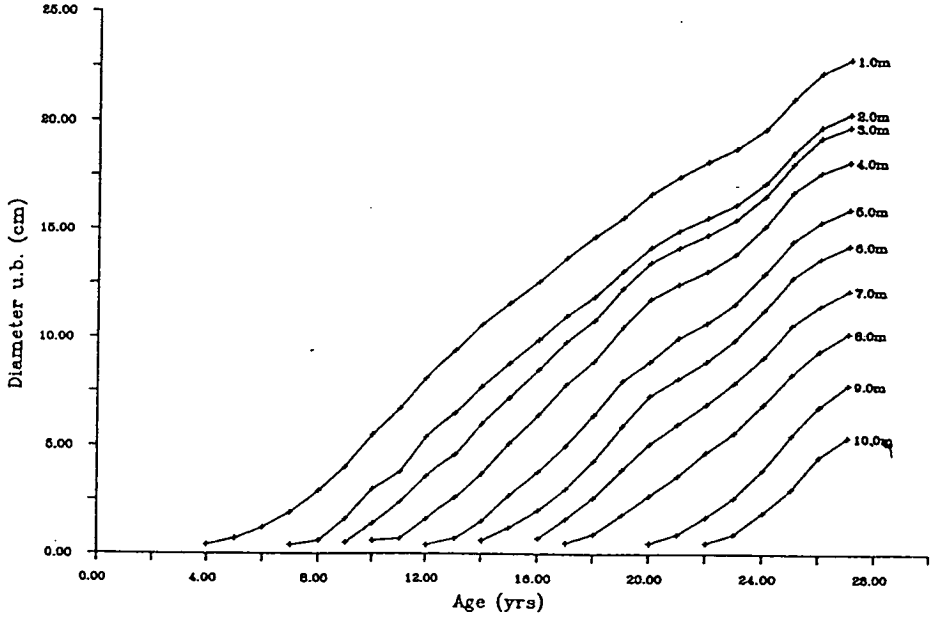

Under bark diameter vs. Age
Tree 9

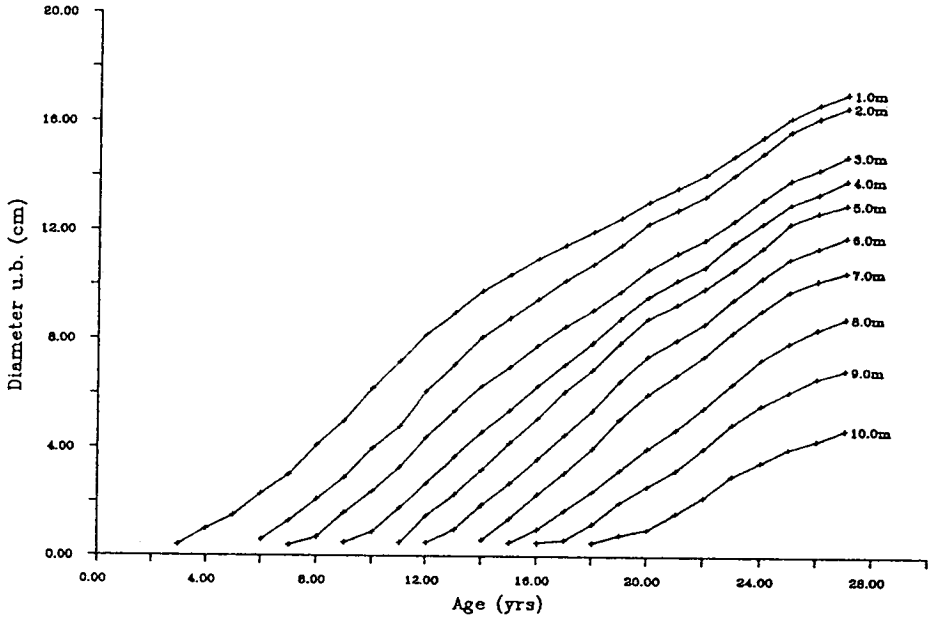

Tree 10

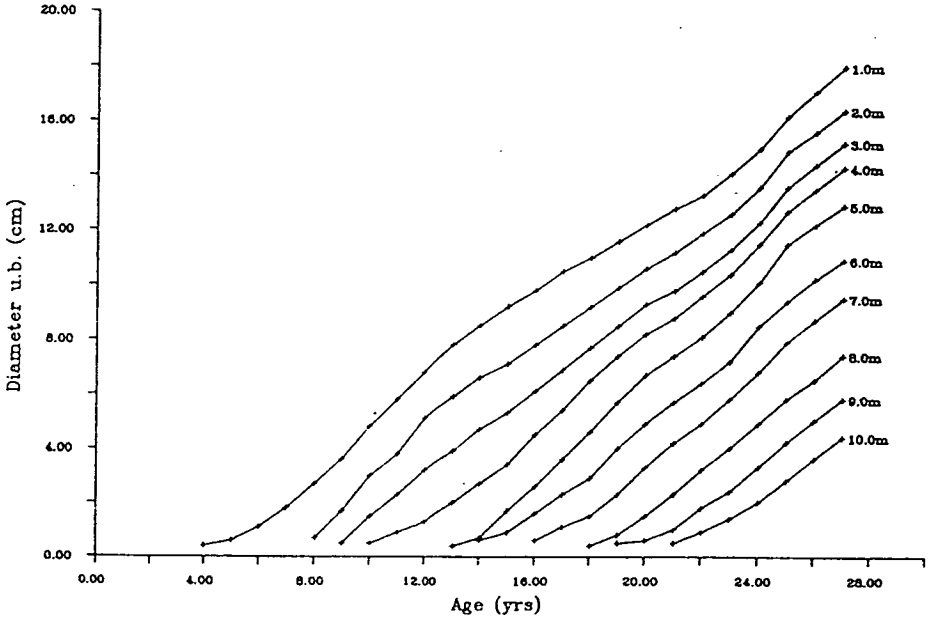

Under bark diameter vs. Age
Tree 11

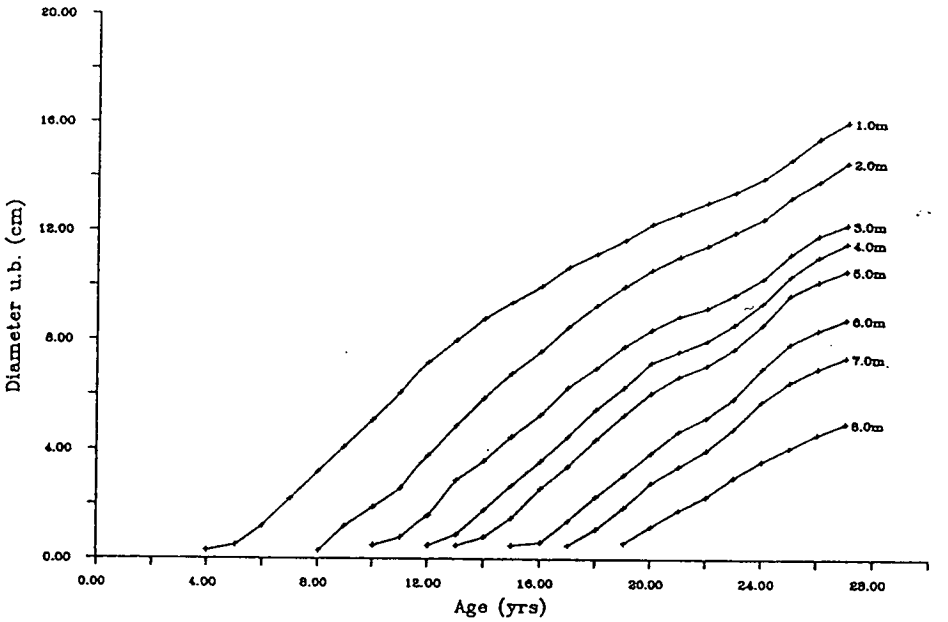

Appendix VI Computer program to determine Young's modulus of elasticity (E)

Filename: EDET

Language: Fortran

```
C       ------------------------------------------
C       Program to determine "E"
C       ------------------------------------------
C       Input physical parameters
10      Call emas3prompt ('Enter force exerted (N): ')  read *,P
20      Call emas3prompt ('Enter tree height  (m): ')  read *,RL
30      Call emas3prompt ('Enter stem deflection (m):')  read *,y
40      Call emas3prompt ('Enter basal diameter (m): ')  read *,Do
        RI = 0.25(3.14159*((D/2)**4))
50      Call emas3prompt ('Enter power law, n: ')  read *,RN
        H = (1-(4*RN))*(2-(4*RN))*(3-(4*RN))
60      Call emas3prompt ('Enter height of cable (m):')  read *,C
        x = RL - C  R = x/RL
70      B1 = ((1-(4*RN))*((x/RL)**(3-(4*RN))))
        B2 = (R*(3-(4*RN))*((x/RL)**(2-(4*RN))))
        B3 = (R*(2-(4*RN))*(3-(4*RN)*(x/RL))
        B4 = (1-(4*RN))*(3-(4*RN))*(x/RL)
        B5 = R*(1-(4*RN))*(30(4*RN))
80      E = ((P*RL**3))/(y*RI*H))*(B1-B2+B-B4+B5-B6)
        E = E*1.0E-09
90      Write (6,*) 'Young's modulus (GPa) =',E
100     Stop
110     End
```

Appendix VII Computer program to calculate natural frequency estimates using engineering fomulae

Filename: FREQDET

Language: Fortran

```
C     ------------------------------------------------------------------------------
C     Program to determine natural frequencies of tree stems
C     according to Blevins (1979)
C     ------------------------------------------------------------------------------

10    Call emas3prompt ('Enter Tree Height (m): ')
      READ *, H
      Call emas3prompt ('Enter Basal Diameter (m): ')
      READ *, D
      Call emas3prompt ('Enter Stem Density (kg/m3): ')
      READ *, DENSITY
      Call emas3prompt ('Enter Taper parameter, T1: ')
      READ *, T1
      Call emas3prompt ('Enter Taper parameter, T2: ')
      READ *, T2
      Call emas3prompt ('Enter Youngs modulus of elasticity (GPa): ')
      READ *, E
      Call emas3prompt ('Enter Stem Mass (kg): ')
      READ *, RMb
      Call emas3prompt ('Enter Crown Mass (kg): ')
      READ *, RMc

C     Determine natural frequencies according to the three models
      E = E*1e+09
      AI = (3.14159*(D/2)**4)/4
      A = 3.14159*((D/2)**2)
      F1 = ((T1**2)/(2*3.14159*H**2))*((E*AI)/(DENSITY*A))**0.5
      F2 = ((T2**2)/(2*3.14159*H**2))*((E*AI)/(DENSITY*A))**0.5
      F3 = (1/(2*3.14159))*((E*AI)/(((H**3)*(RMc+(0.24*RMb))))**0.5
      E = E*1e-09

C     Print results onto the screen
      WRITE (6,*) 'F1 (non-linear taper) = ', F1
      WRITE (6,*) 'F2 (truncated, linear taper) = ', F2
      WRITE (6,*) 'F3 (concentrated mass, no taper) =', F3

      STOP
      END
```

Appendix VIII Table showing the sway periods measured for the nine sample trees (Trees 1-6 Unthinned plot, Trees 8,10 and 11 Thinned plot)

Stems 1 to 6 were measured by Dr. R. Milne and only the average results are given here.

Tree No.	Natural Frequency (Hz)	
	With branches	No Branches
1	0.30	0.49
2	0.38	0.68
3	0.37	0.63
4	0.25	0.40
5	0.40	0.65
6	0.40	0.63

For the thinned plot all useable results are presented here.

Tree	Sway	Frequency (Hz)	Branches Present	Average
8	(i)	0.54	yes	
	(ii)	0.54	yes	
	(iv)	0.56	yes	
	(v)	0.55	yes	
	(vii)	0.55	yes	
	(viii)	0.56	yes	0.55
	(ix)	0.56	no	
	(x)	0.57	no	
	(xii)	0.55	no	
	(xiii)	0.57	no	0.56
10	(i)	0.55	yes	
	(ii)	0.54	yes	
	(iii)	0.56	yes	
	(viii)	0.56	yes	0.55
	(ix)	0.65	no	
	(x)	0.70	no	
	(xi)	0.69	no	
	(xii)	0.64	no	
	(xiii)	0.70	no	0.68
11	(i)	0.58	yes	
	(viii)	0.60	yes	0.59
	(ix)	1.44	no	
	(x)	1.45	no	
	(xi)	1.50	no	
	(xii)	1.44	no	
	(xiii)	1.41	no	
	(xiv)	1.43	no	
	(xv)	1.49	no	
	(xvi)	1.41	no	1.45

Appendix IX Graphs showing the sensitivity of the natural frequency models to Young's Modulus of Elasticity
(Trees 1-7 Unthinned plot, Trees 8-11 Thinned plot)

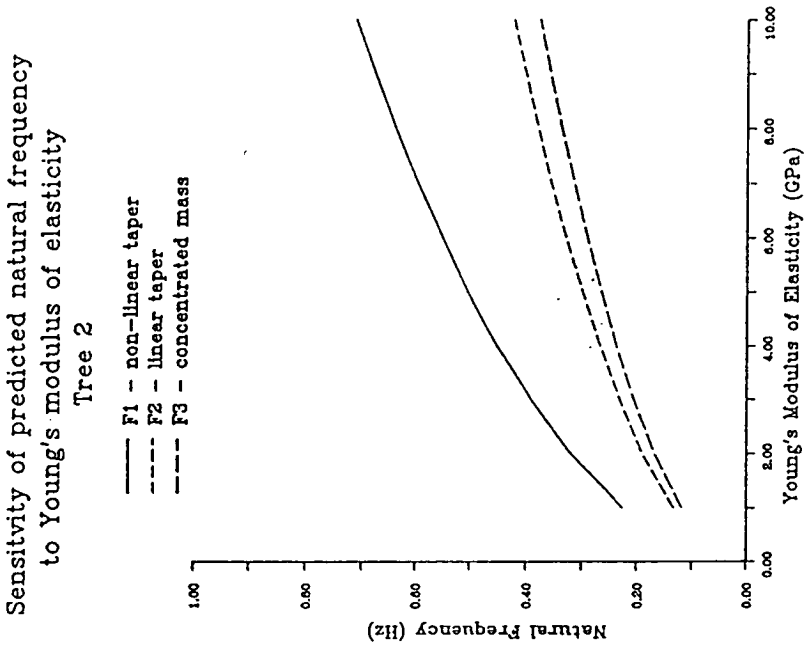

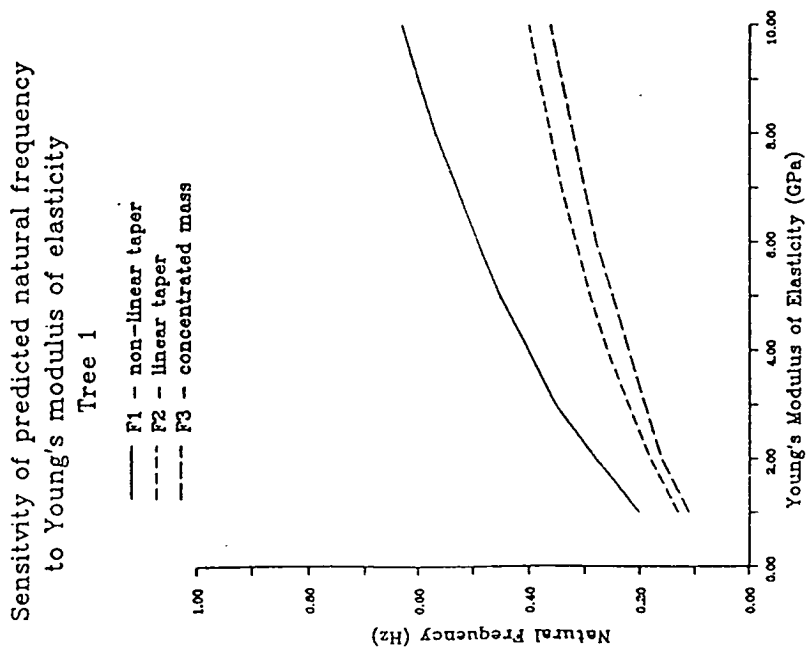

Sensitvity of predicted natural frequency
to Young's modulus of elasticity
Tree 3

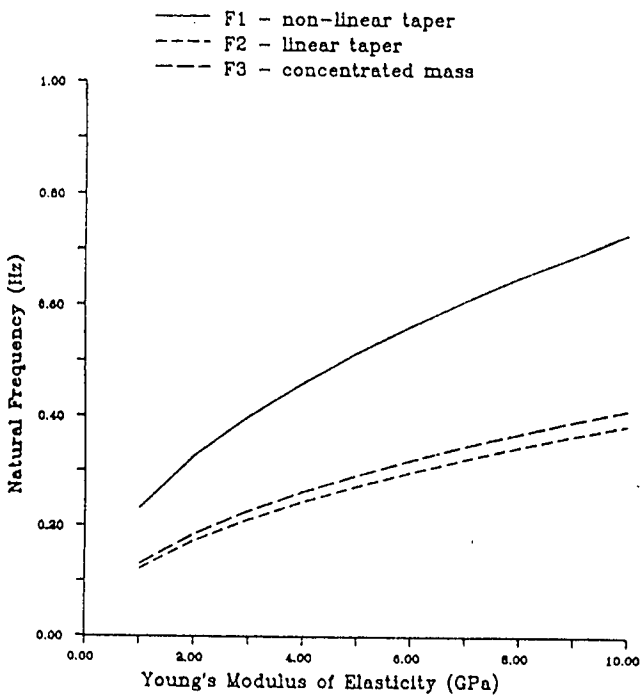

Sensitvity of predicted natural frequency
to Young's modulus of elasticity
Tree 4

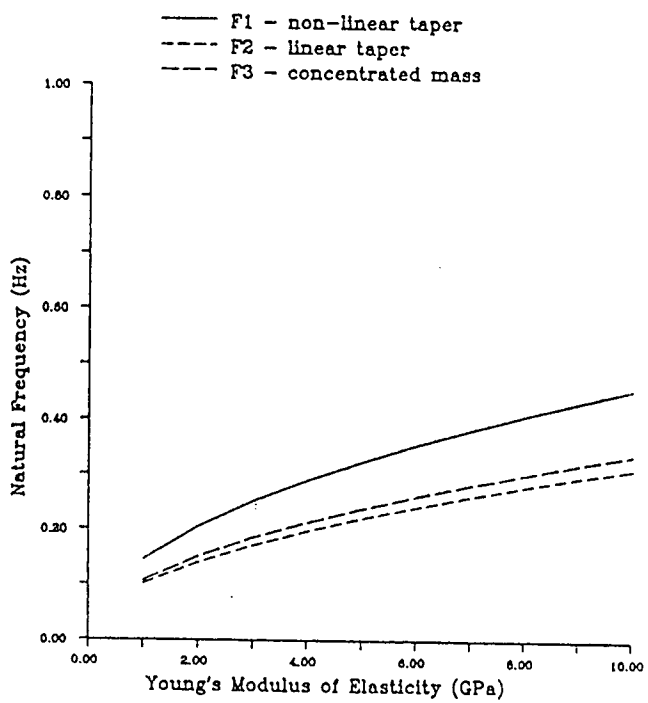

Sensitvity of predicted natural frequency
to Young's modulus of elasticity
Tree 3

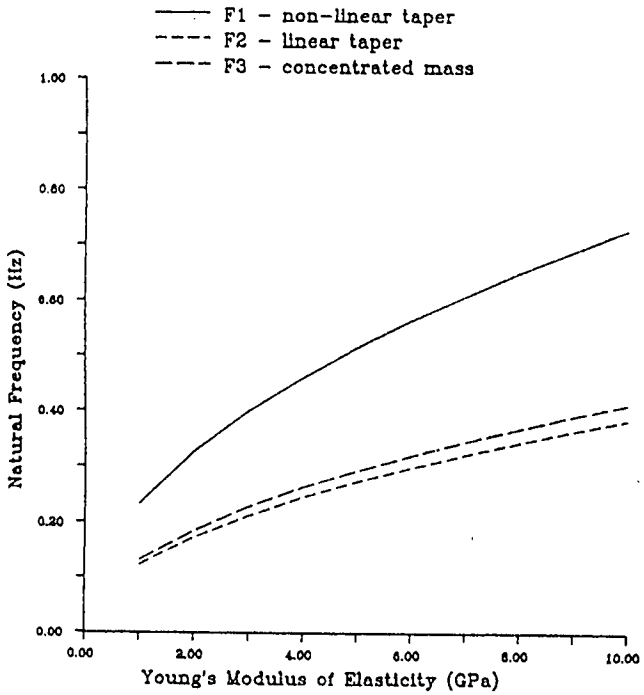

Sensitvity of predicted natural frequency
to Young's modulus of elasticity
Tree 4

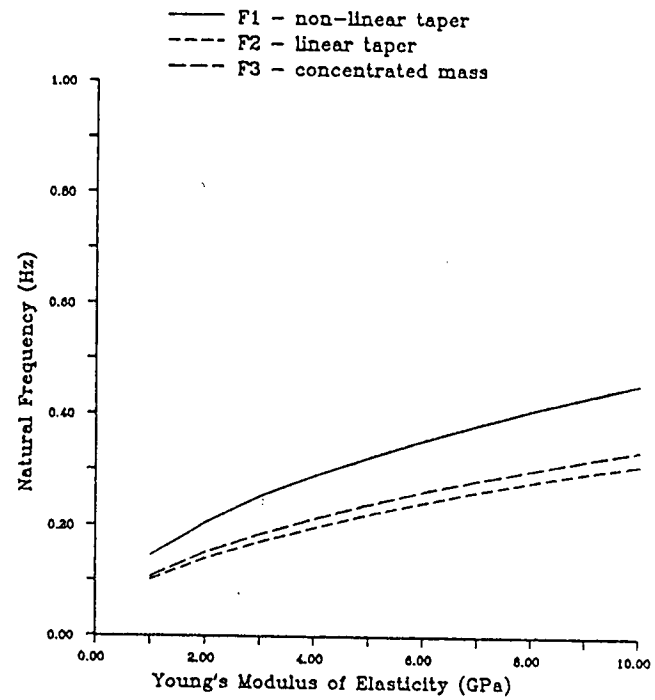

Sensitvity of predicted natural frequency
to Young's modulus of elasticity
Tree 5

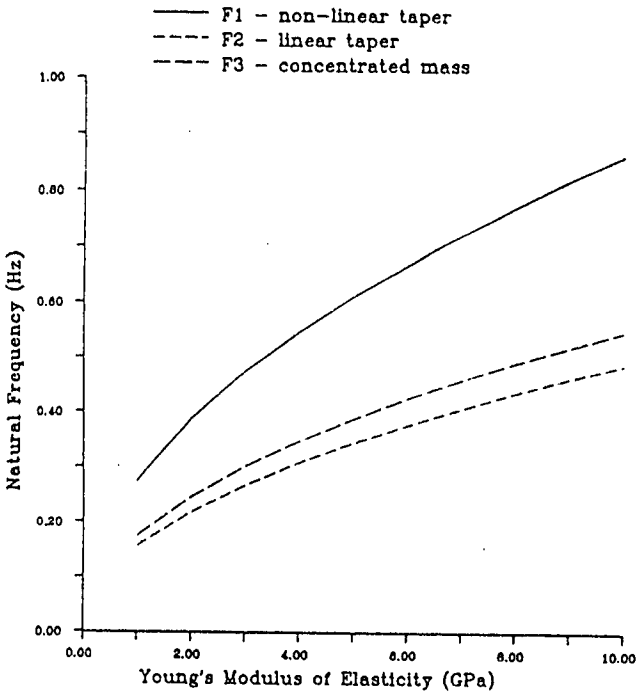

Sensitvity of predicted natural frequency
to Young's modulus of elasticity
Tree 6

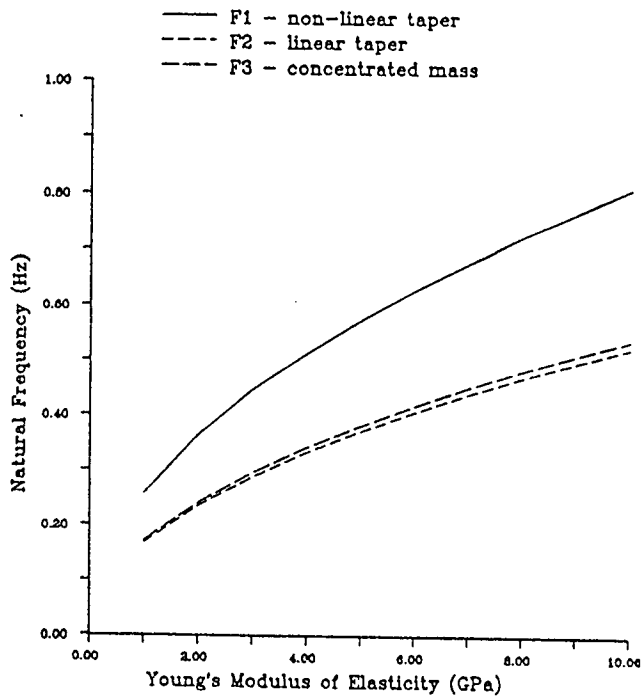

Sensitvity of predicted natural frequency
to Young's modulus of elasticity
Tree 7

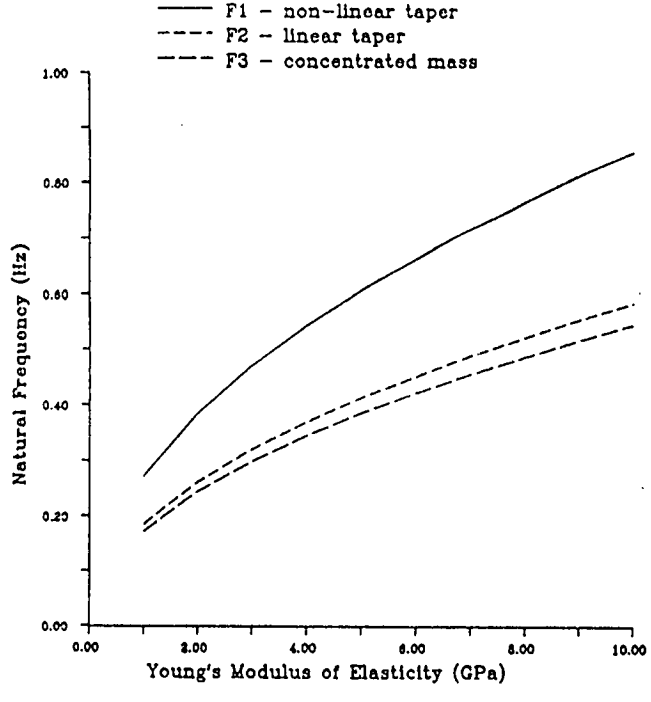

Sensitvity of predicted natural frequency
to Young's modulus of elasticity
Tree 8

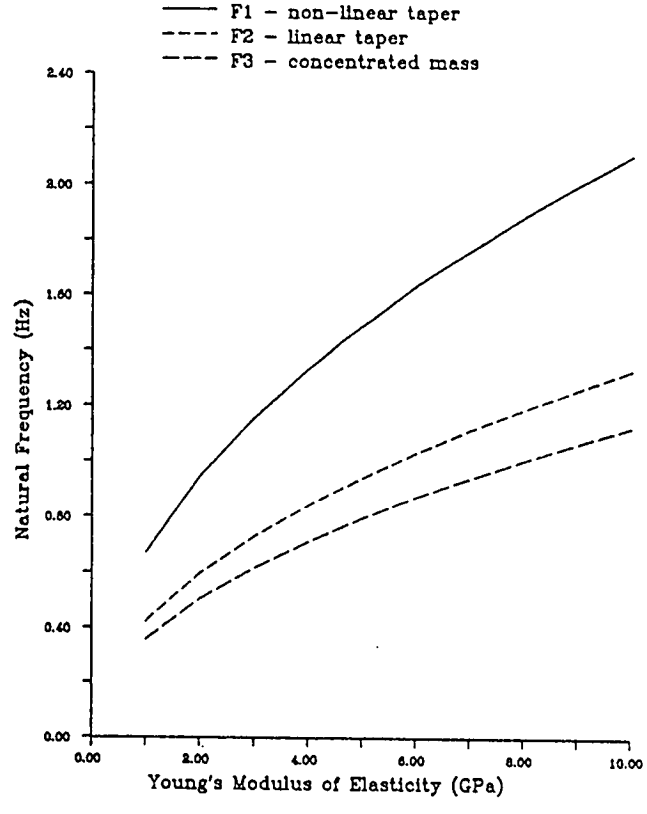

Sensitvity of predicted natural frequency
to Young's modulus of elasticity
Tree 9

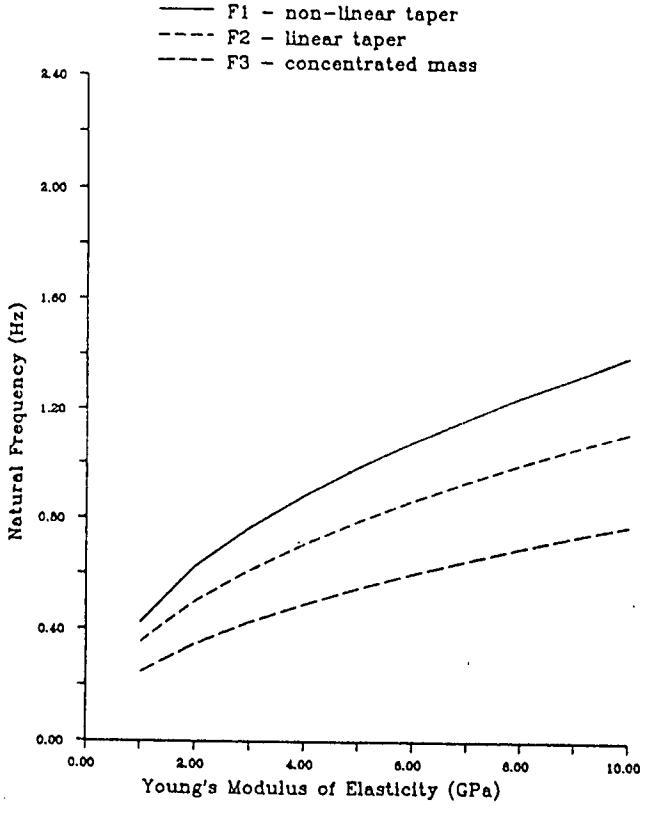

Sensitvity of predicted natural frequency
to Young's modulus of elasticity
Tree 10

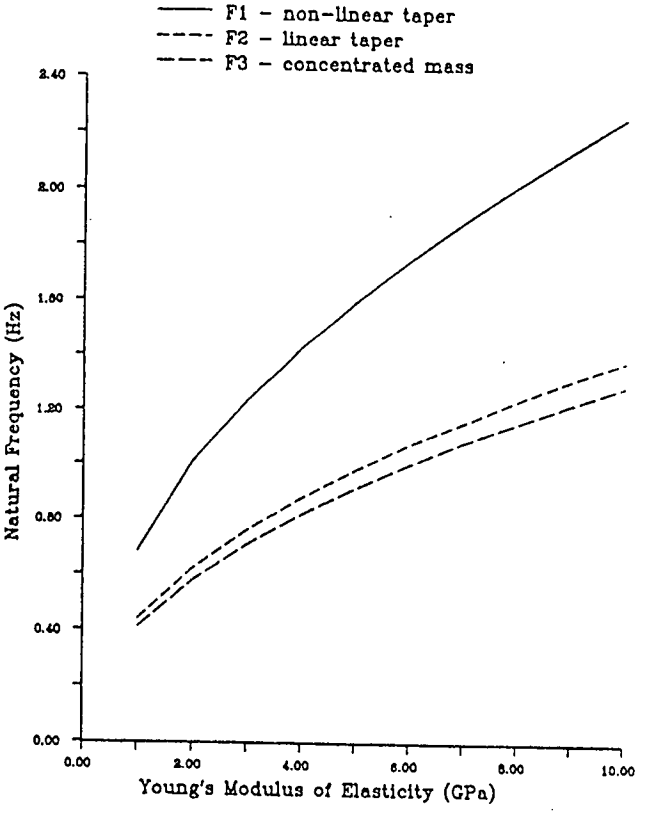

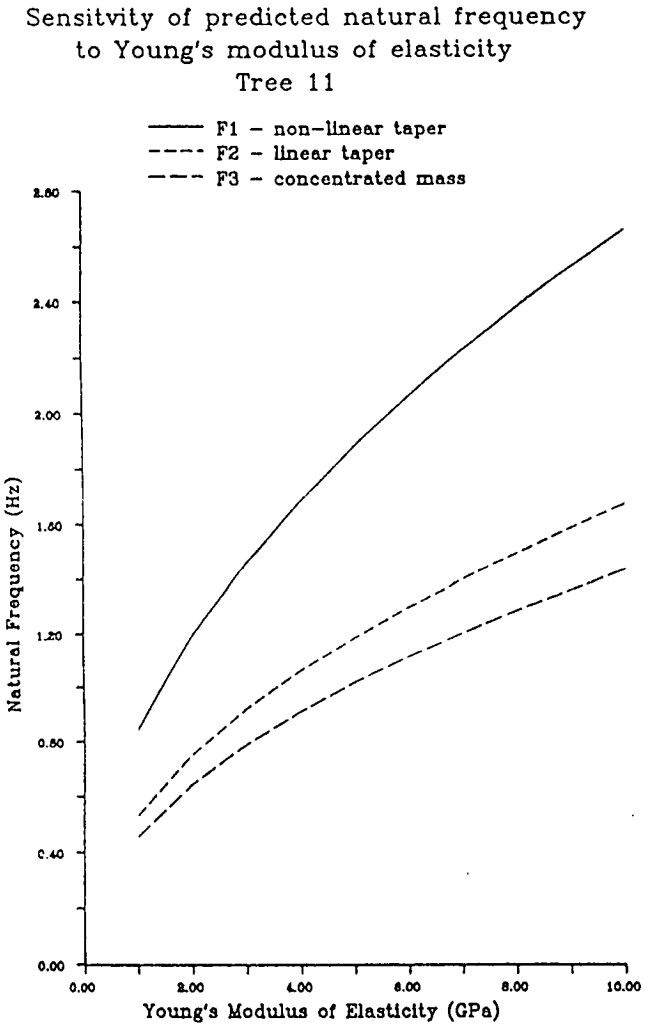
Sensitvity of predicted natural frequency
to Young's modulus of elasticity
Tree 11
F1 - non-linear taper
F2 - linear taper
F3 - concentrated mass
Natural Frequency (Hz)
2.80
2.40
2.00
1.60
1.20
0.80
0.40
0.00
0.00
2.00
4.00
6.00
8.00
10.00
Young's Modulus of Elasticity (GPa)

xxx(a)

Appendix X Graphs showing the sensitivity of the natural frequency models to stem density (Trees 1-6 Unthinned plot, Trees 8, 10, and 11 Thinned plot)

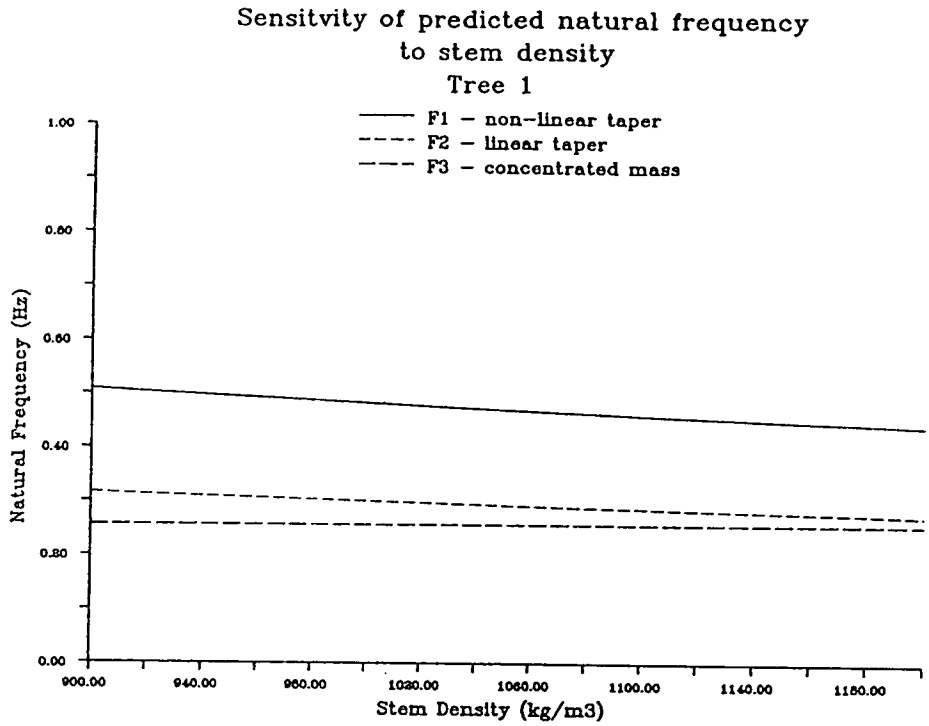

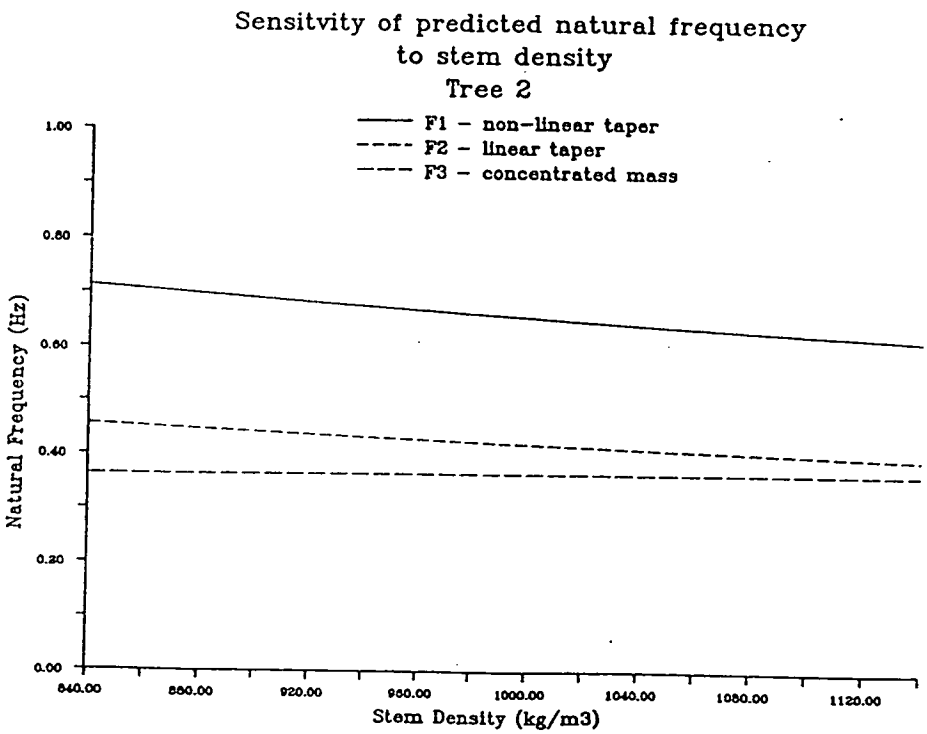

Sensitvity of predicted natural frequency
to stem density
Tree 3

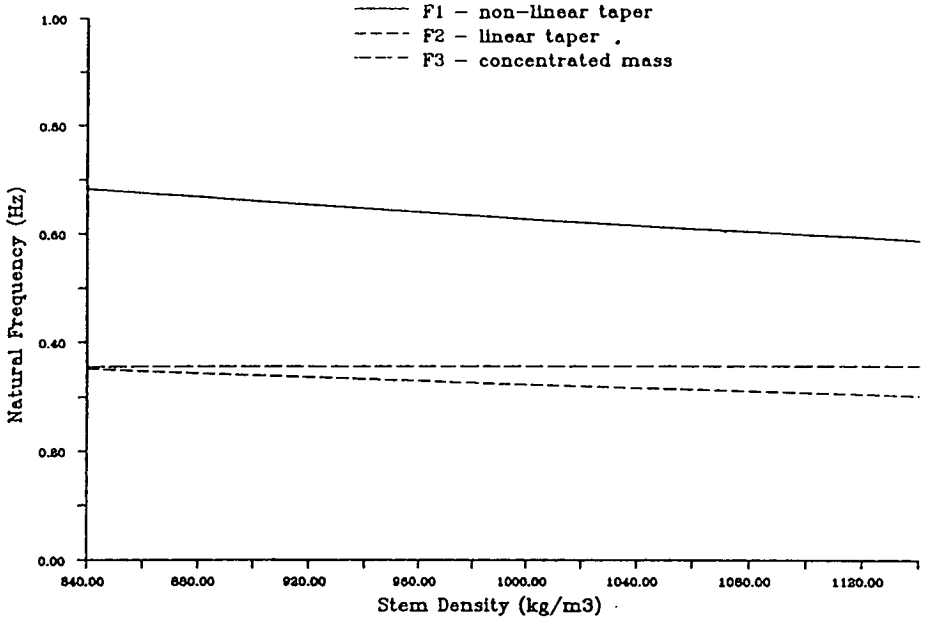

Sensitvity of predicted natural frequency
to stem density
Tree 4

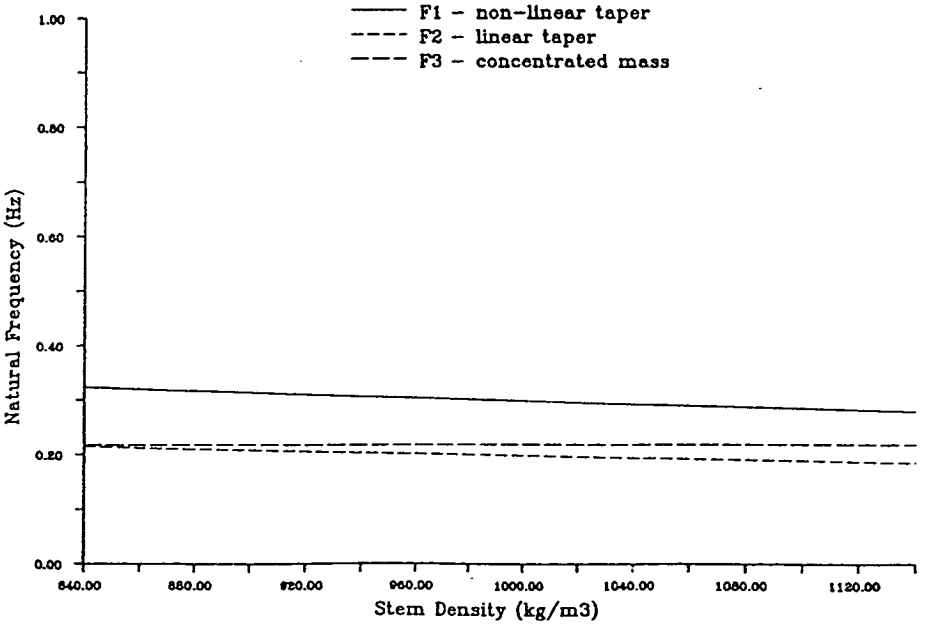

Sensitvity of predicted natural frequency
to stem density
Tree 5

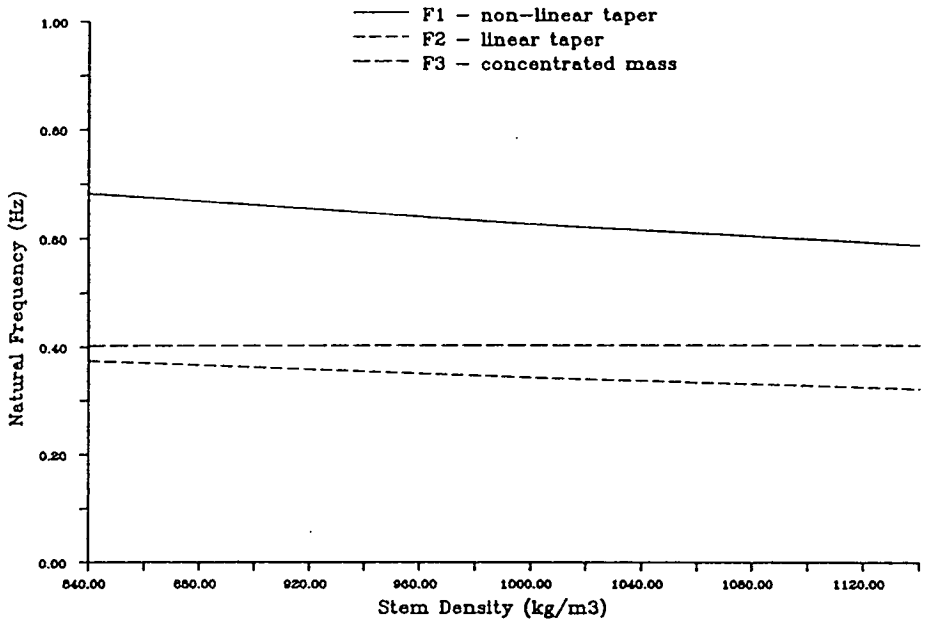

Sensitvity of predicted natural frequency
to stem density
Tree 6

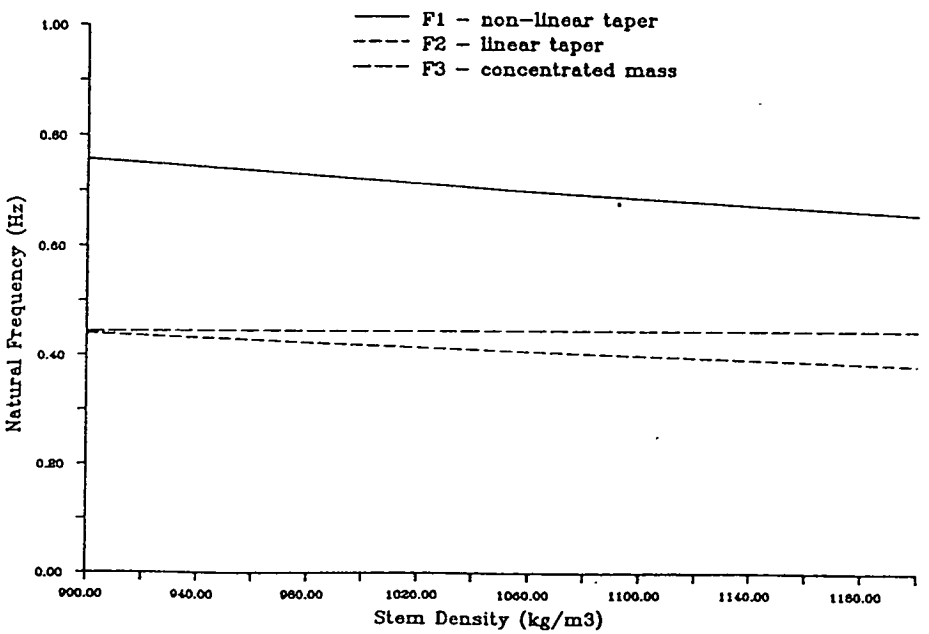

Sensitvity of predicted natural frequency
to stem density
Tree 8

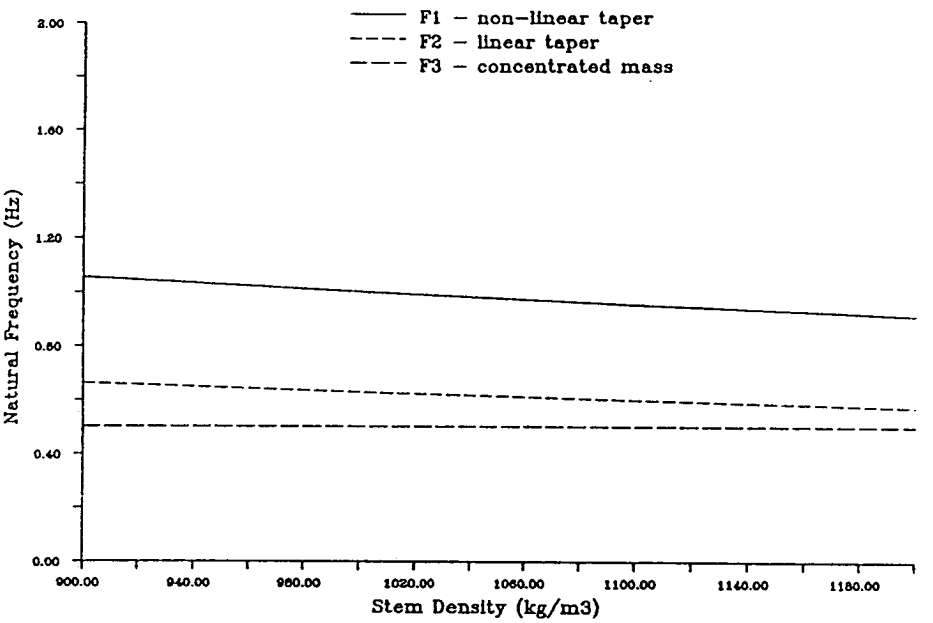

Sensitvity of predicted natural frequency
to stem density
Tree 10

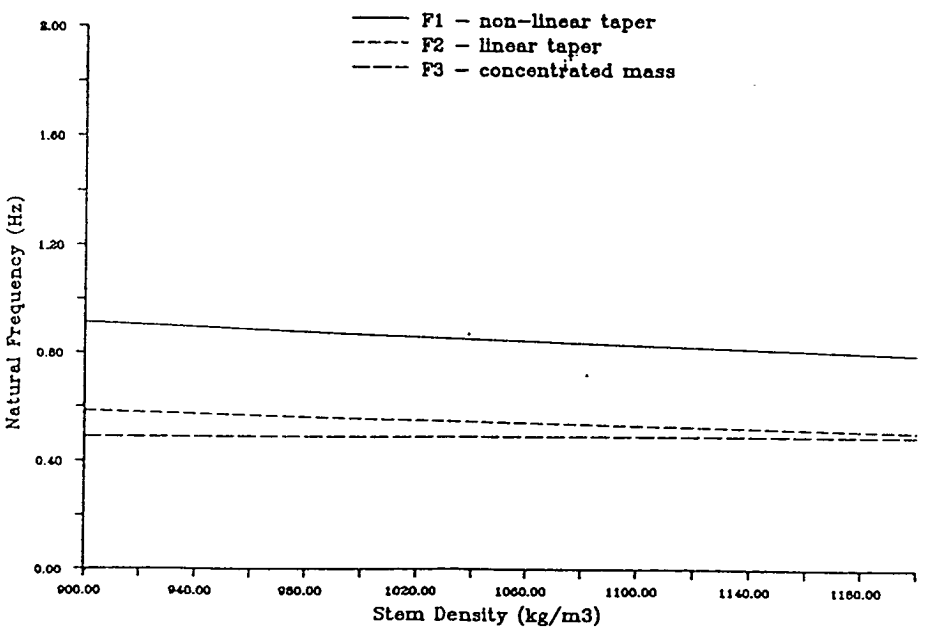

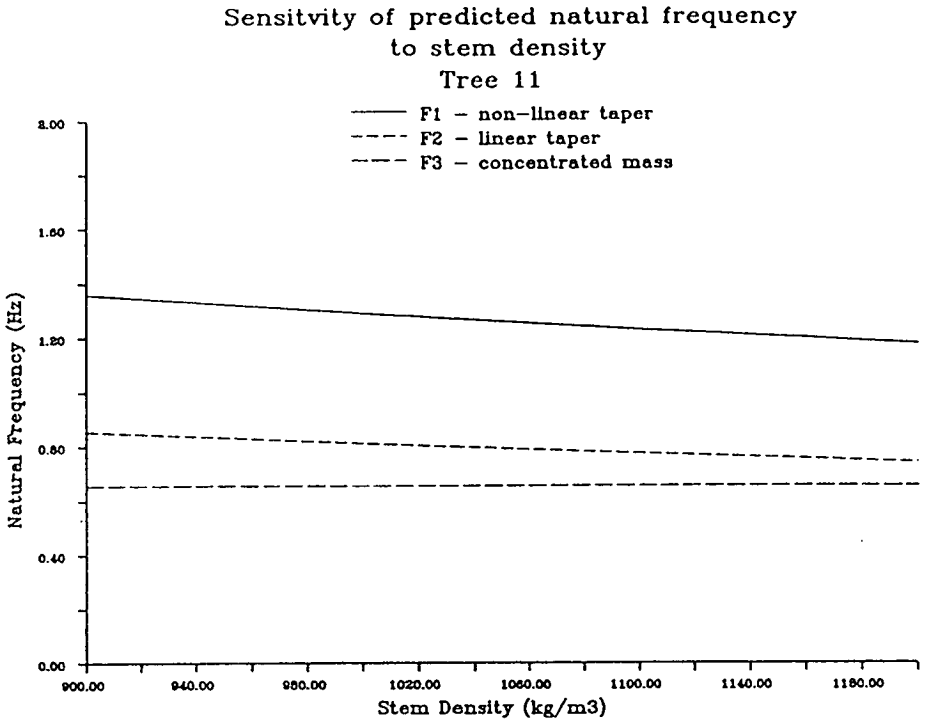
Sensitvity of predicted natural frequency
to stem density
Tree 11
F1 – non-linear taper
F2 – linear taper
F3 – concentrated mass
Natural Frequency (Hz)
2.00
1.60
1.20
0.80
0.40
0.00
900.00
940.00
980.00
1020.00
1060.00
1100.00
1140.00
1180.00
Stem Density (kg/m3)

Appendix XI Graphs showing the sensitivity of the natural frequency models to the taper parameter
(Trees 1-6 Unthinned plot, Tress 8, 10 and 11 Thinned plot)

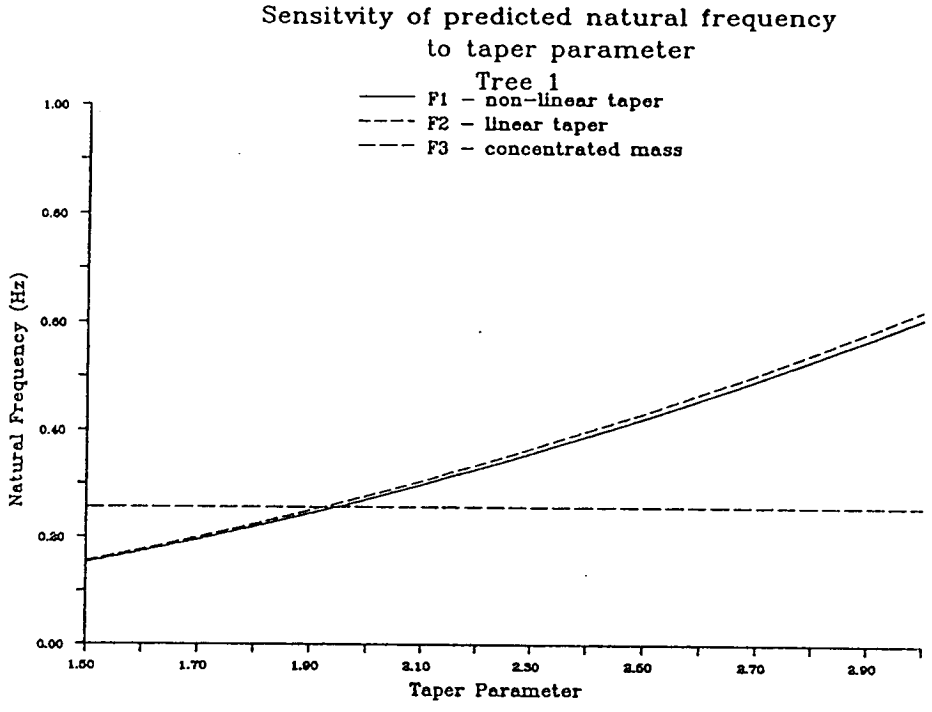

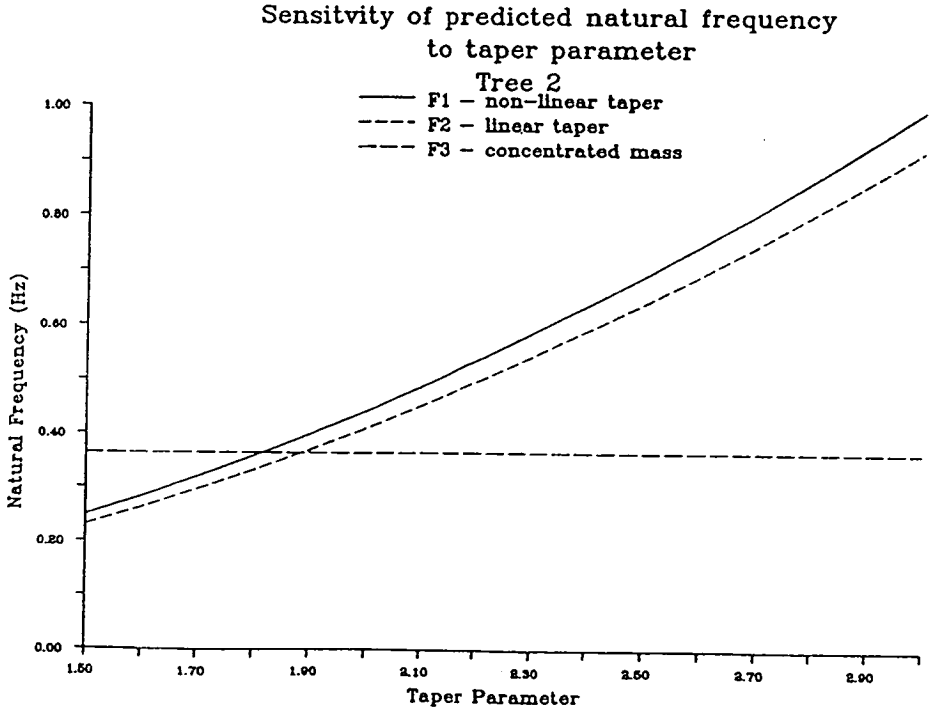

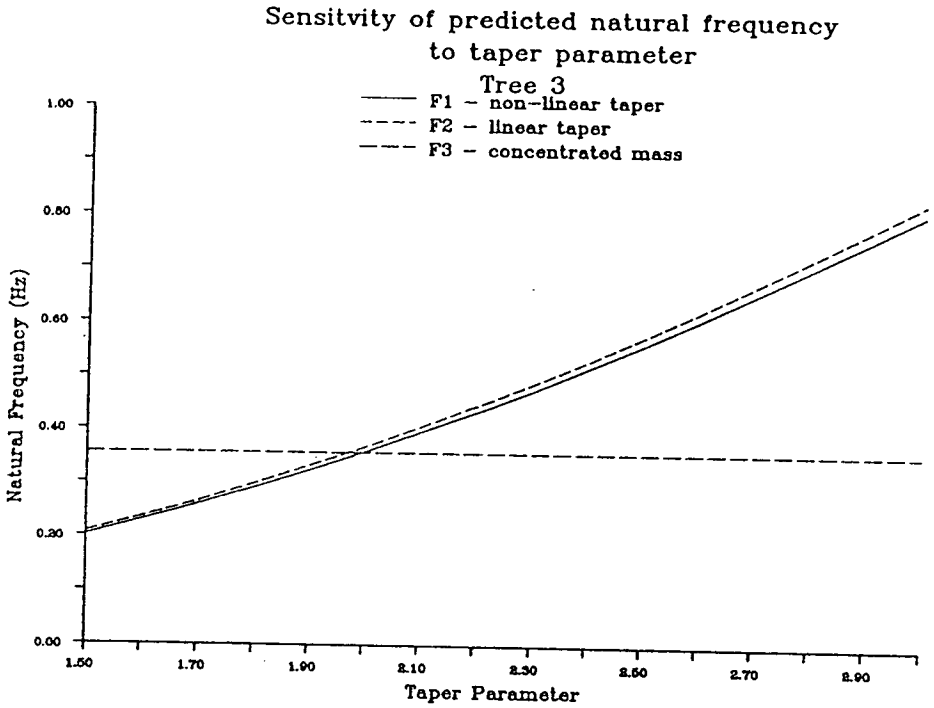
Sensitvity of predicted natural frequency
to taper parameter
Tree 3
F1 – non–linear taper
F2 – linear taper
F3 – concentrated mass
Natural Frequency (Hz)
1.00
0.80
0.60
0.40
0.20
0.00
1.50
1.70
1.90
2.10
2.30
2.50
2.70
2.90
Taper Parameter

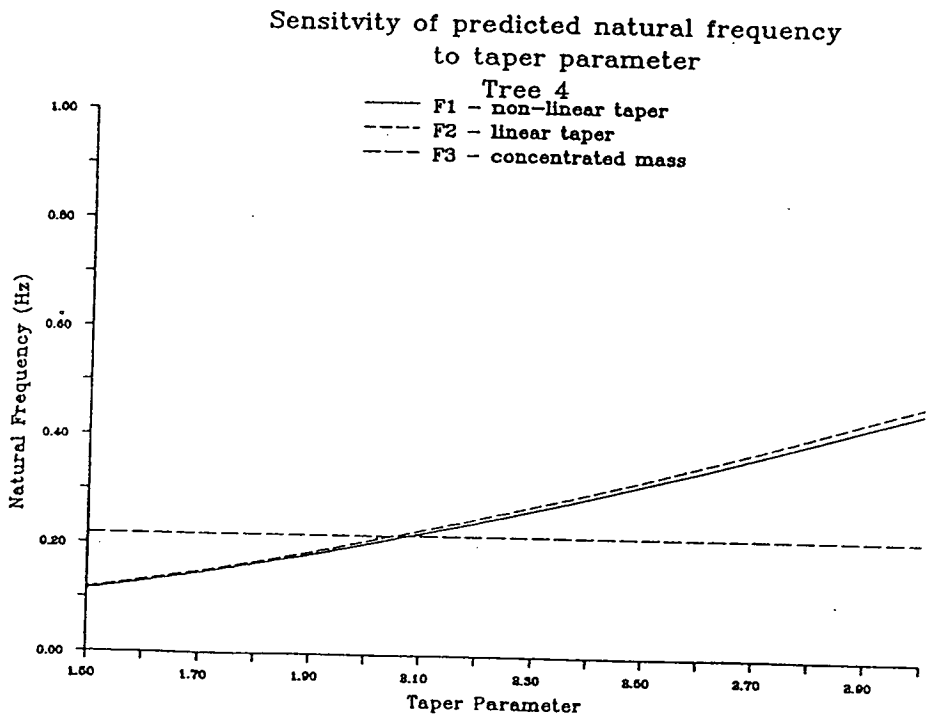
Sensitvity of predicted natural frequency
to taper parameter
Tree 4
F1 – non–linear taper
F2 – linear taper
F3 – concentrated mass
Natural Frequency (Hz)
1.00
0.80
0.60
0.40
0.20
0.00
1.50
1.70
1.90
2.10
2.30
2.50
2.70
2.90
Taper Parameter

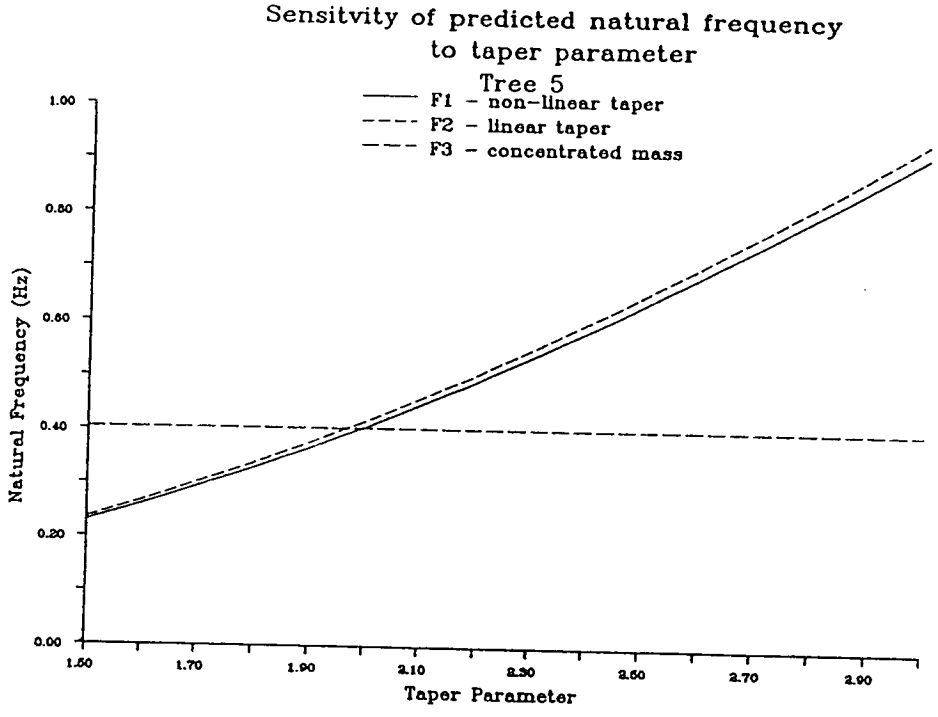
Sensitvity of predicted natural frequency
to taper parameter
Tree 5
F1 – non-linear taper
F2 – linear taper
F3 – concentrated mass
Natural Frequency (Hz)
1.00
0.80
0.60
0.40
0.20
0.00
1.50
1.70
1.90
2.10
2.30
2.50
2.70
2.90
Taper Parameter

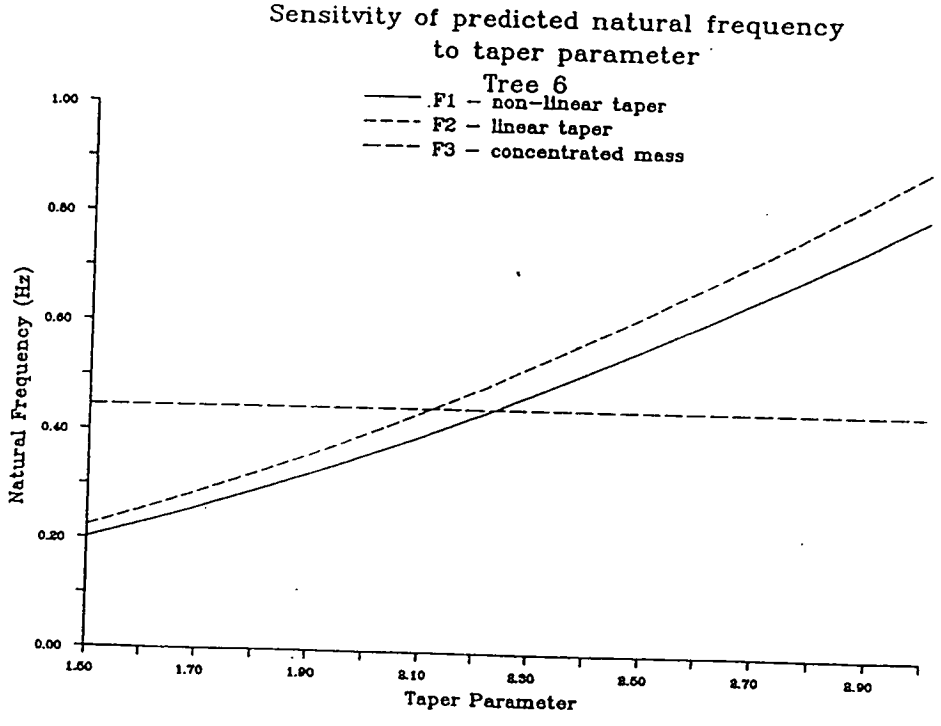
Sensitvity of predicted natural frequency
to taper parameter
Tree 6
F1 – non-linear taper
F2 – linear taper
F3 – concentrated mass
Natural Frequency (Hz)
1.00
0.80
0.60
0.40
0.20
0.00
1.50
1.70
1.90
2.10
2.30
2.50
2.70
2.90
Taper Parameter

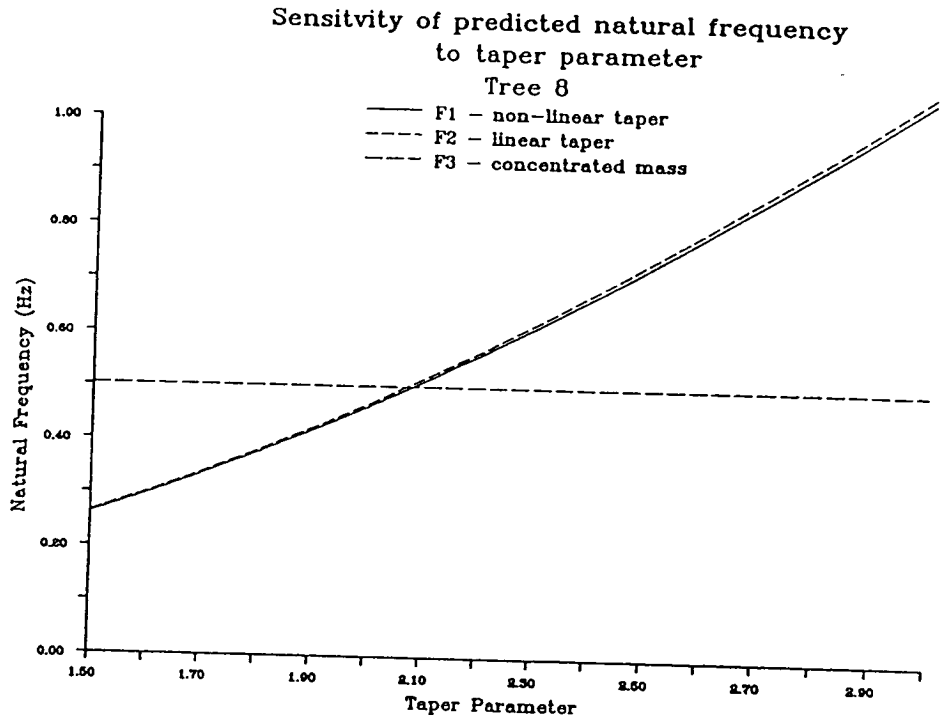
Sensitvity of predicted natural frequency
to taper parameter
Tree 8
F1 – non-linear taper
F2 – linear taper
F3 – concentrated mass
Natural Frequency (Hz)
1.00
0.80
0.60
0.40
0.20
0.00
1.50
1.70
1.90
2.10
2.30
2.50
2.70
2.90
Taper Parameter

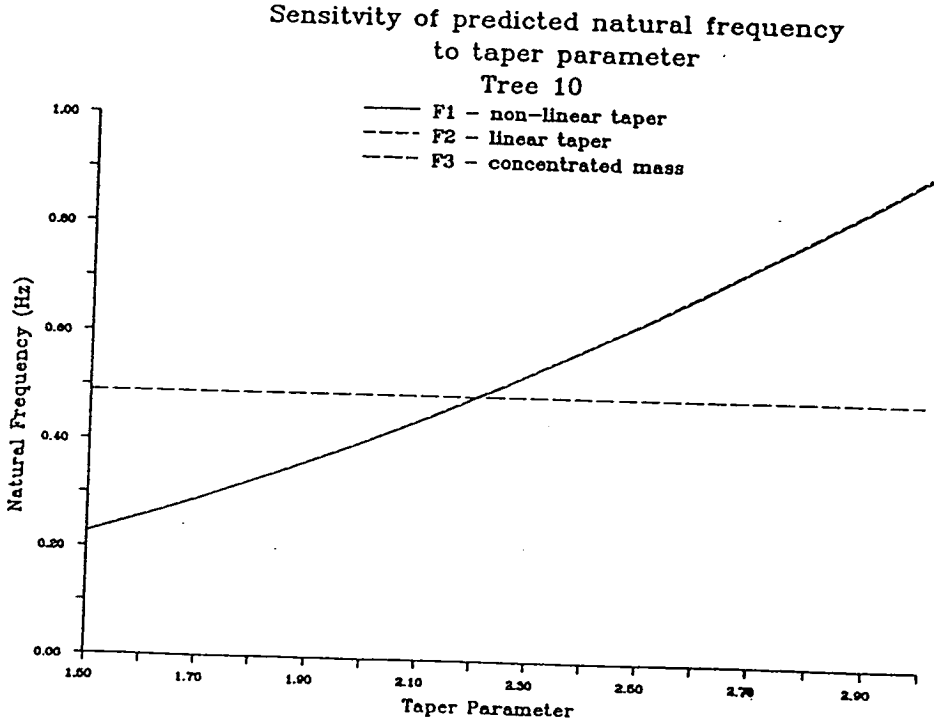
Sensitvity of predicted natural frequency
to taper parameter
Tree 10
F1 – non-linear taper
F2 – linear taper
F3 – concentrated mass
Natural Frequency (Hz)
1.00
0.80
0.60
0.40
0.20
0.00
1.50
1.70
1.90
2.10
2.30
2.50
2.70
2.90
Taper Parameter

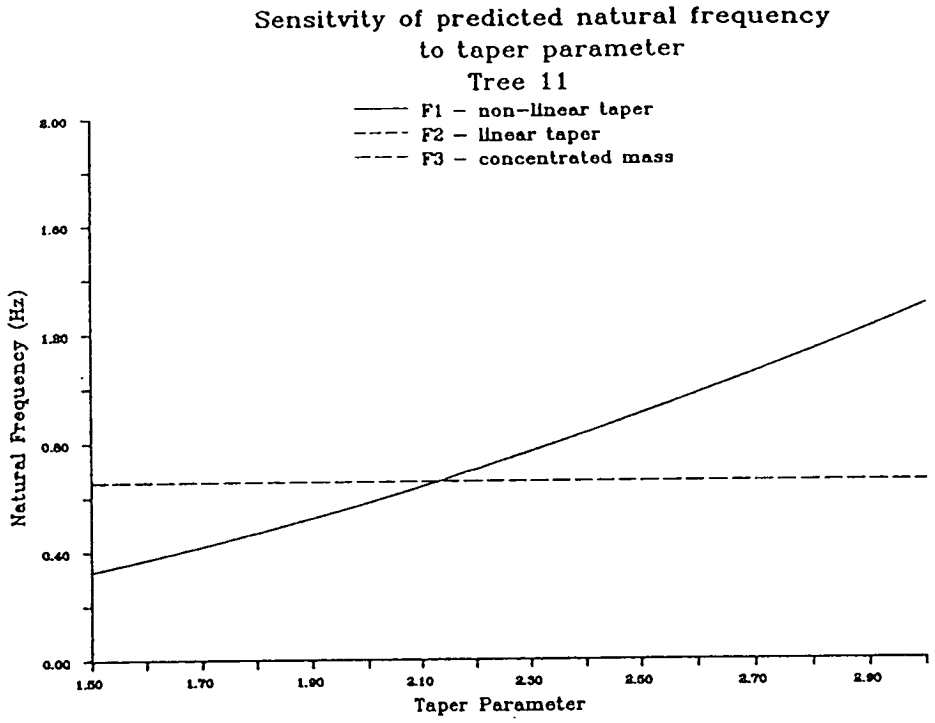
Sensitvity of predicted natural frequency
to taper parameter
Tree 11
F1 – non-linear taper
F2 – linear taper
F3 – concentrated mass
Natural Frequency (Hz)
2.00
1.60
1.20
0.80
0.40
0.00
1.50
1.70
1.90
2.10
2.30
2.50
2.70
2.90
Taper Parameter

Appendix XII Graphs showing the sensitivity of the natural frequency models to stem and branch mass
(Tress 1-6 Unthinned plot, Trees 8, 10 and 11 Thinned plot)

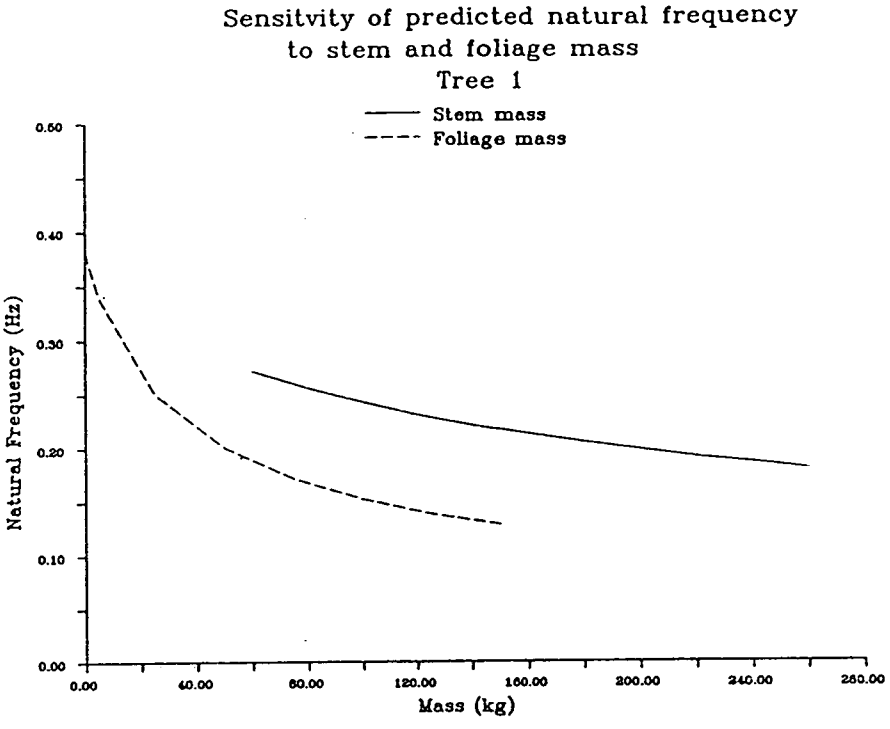

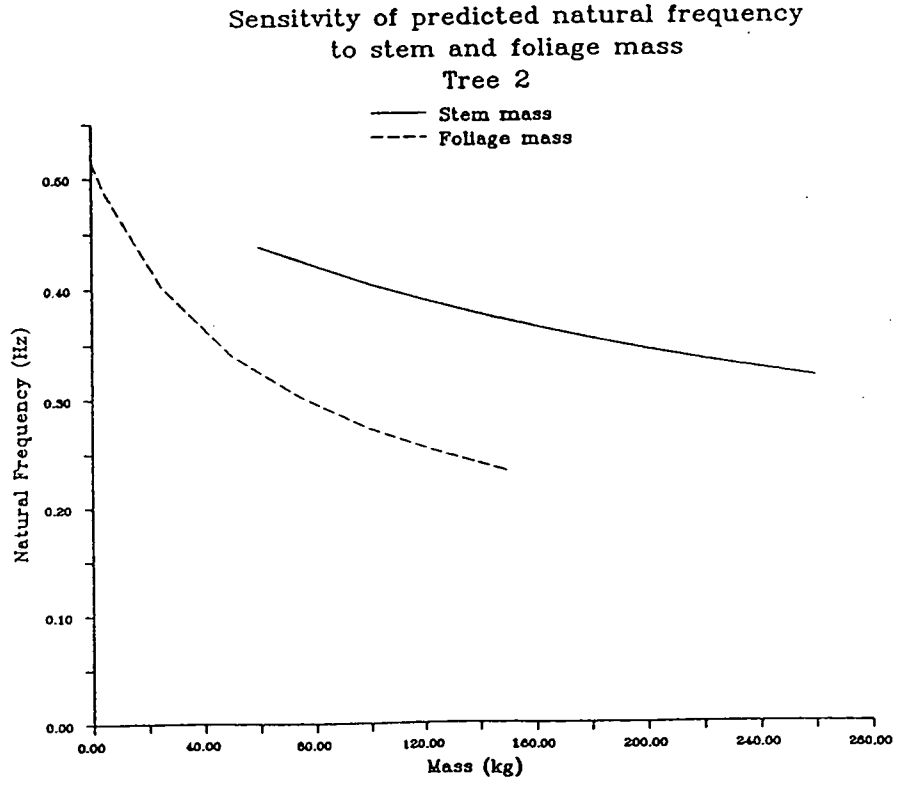

Sensitvity of predicted natural frequency
to stem and foliage mass
Tree 3

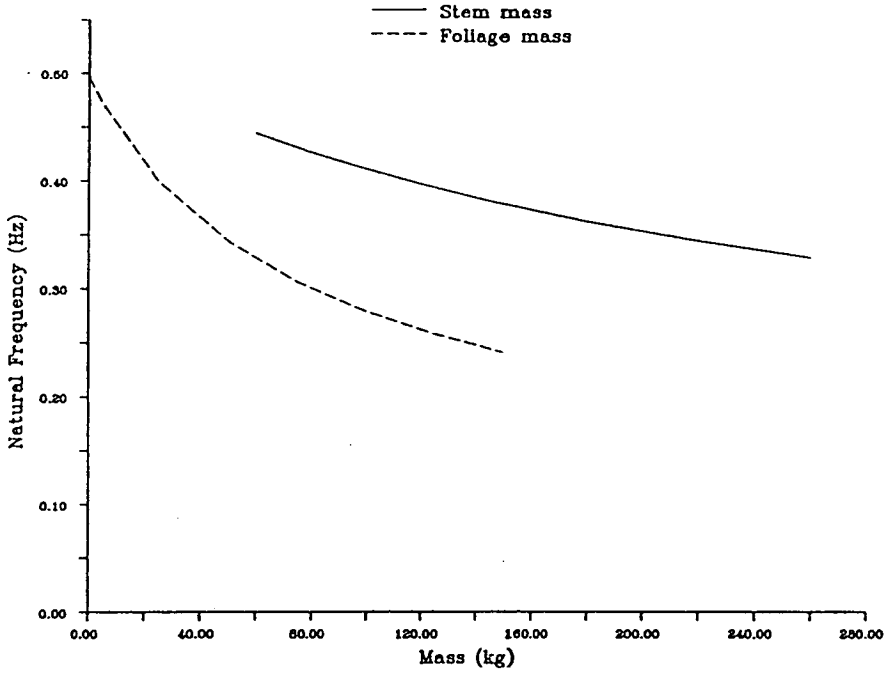

Sensitvity of predicted natural frequency
to stem and foliage mass
Tree 4

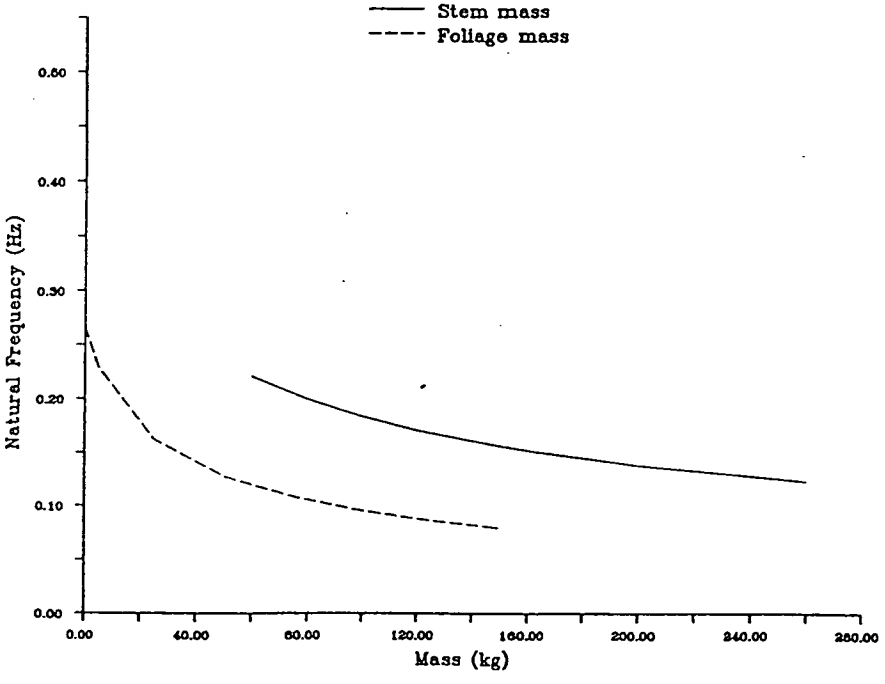

Sensitvity of predicted natural frequency
to stem and foliage mass
Tree 5

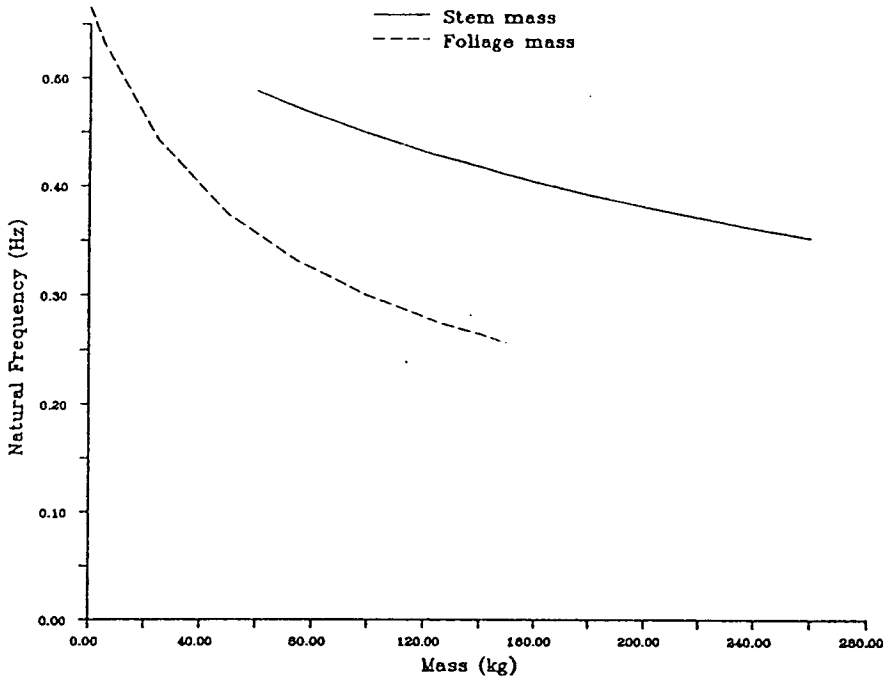

Sensitvity of predicted natural frequency
to stem and foliage mass
Tree 6

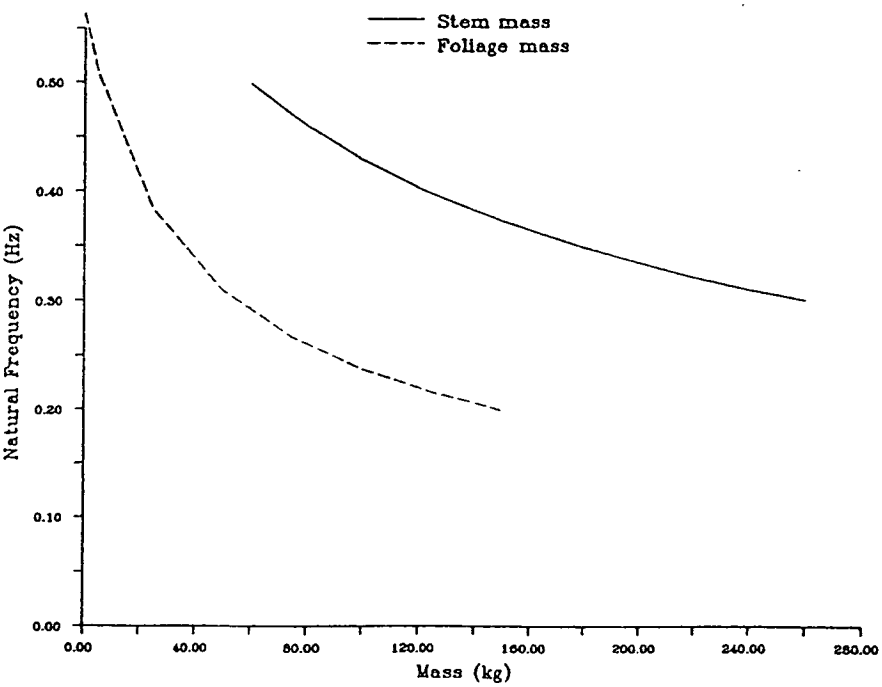

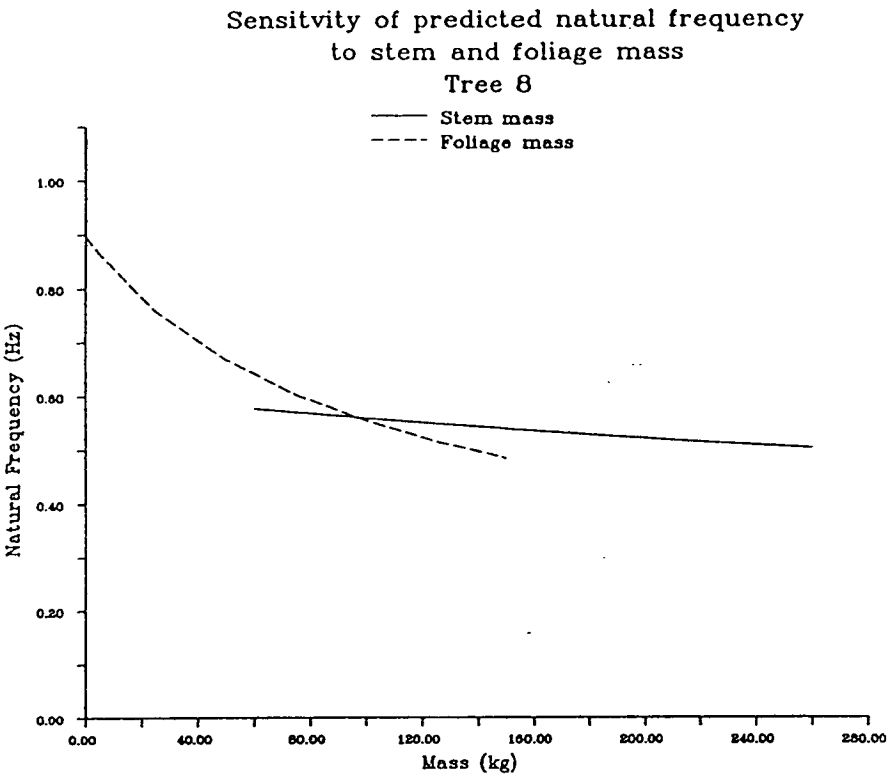
Sensitvity of predicted natural frequency
to stem and foliage mass
Tree 8
Stem mass
Foliage mass
Natural Frequency (Hz)
1.00
0.80
0.60
0.40
0.20
0.00
0.00
40.00
80.00
120.00
160.00
200.00
240.00
280.00
Mass (kg)

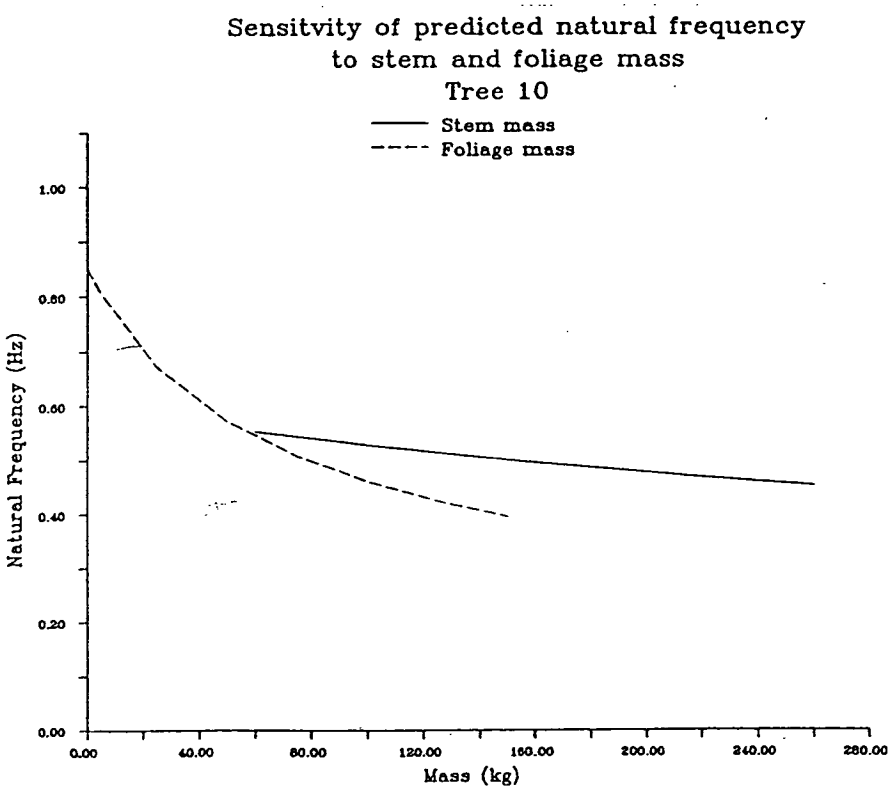
Sensitvity of predicted natural frequency
to stem and foliage mass
Tree 10
Stem mass
Foliage mass
Natural Frequency (Hz)
1.00
0.80
0.60
0.40
0.20
0.00
0.00
40.00
80.00
120.00
160.00
200.00
240.00
280.00
Mass (kg)

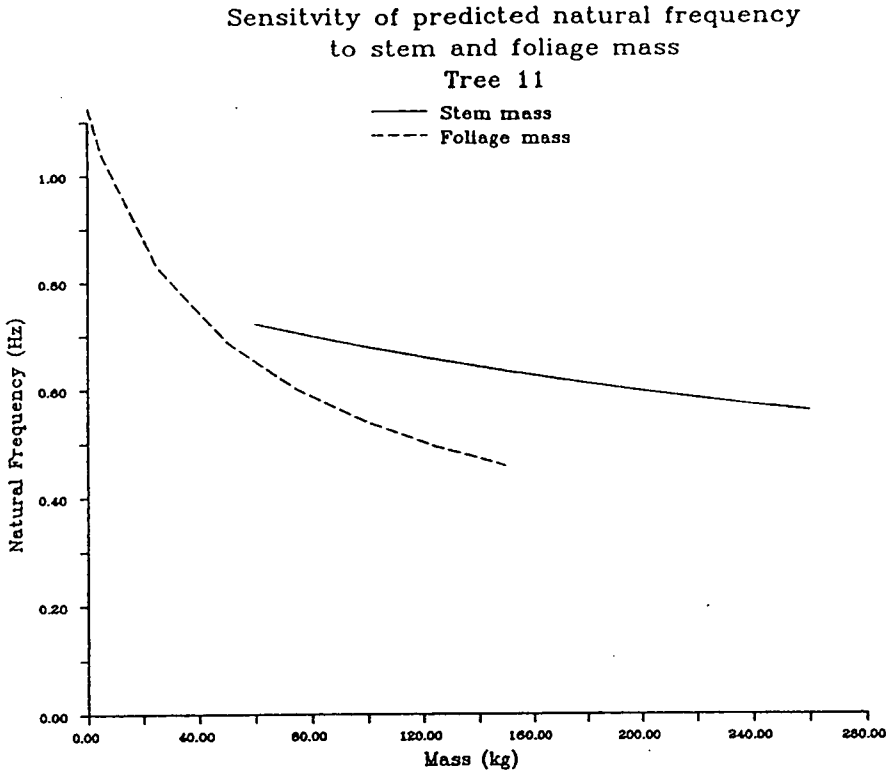
Sensitvity of predicted natural frequency
to stem and foliage mass
Tree 11
Stem mass
Foliage mass
Natural Frequency (Hz)
1.00
0.80
0.60
0.40
0.20
0.00
0.00
40.00
80.00
120.00
160.00
200.00
240.00
280.00
Mass (kg)

Appendix XIII CR 21x Micro-logger program to monitor average wind speed and initiate recording of windspeed and stem displacement data when a threshold of 5 ms^{-1} was reached

CR 21x DATA LOGGER PROGRAMME

```
*      1                Table 1 programs
01:    0.1              Execution Interval (seconds)

01:    P18              Time
       01:  2           Hours into current year  (max. 8784)
       02:  0000        Mod/by
       03:  13          Location  [current time]
Load current time into Loc. 13 for the test below

02:    P91              If Flag
       01:  12          2 is set
       02:  30          Then Do
If we are waiting for n hours to pass by THEN

03:    P88              If X<=>Y
       01:  13          X Location of Current Time
       02:  4           <
       03:  14          Y Location of Next Time
       04:  00          Go to end of Program Table
If the Current Time has not got to the next start time then jump to the end of
the program table to save power,  i.e.  do not log anu I/Ps

Otherwise,

04:    P86              Do
       01:  22          Reset Flag 2
Reset Flag 2 as end of wait period

05:  P95                End.
```

Then measure the analogue inputs

```
06:    P1               Voltage  (single ended)
       01:  3           Repetitions
       02:  5           5000 mV slow range
       03:  4           Input Channel
       04:  1           Location  [U Gill]
       05:  0.0108      Multiplier
       06:  0000        Offset

07:    P36              Z=X*Y
       01:  1           X Location U Gill
       02:  1           Y Location U Gill
       03:  4           Z Location [ U**2]

08:    P36              Z=X*Y
       01:  2           X Location V Gill
       02:  2           Y Location V Gill
       03:  5           Z Location [V**2]
```

```
09:   P33              Z=X+Y
      01:  4           X Location U**2
      02:  5           Y Location V**2
      03:  6           Z Location [U**2+V**2]

10:   P39              Z=SQRT(X)
      01:  6           X Location  U**2+V**2
      02:  7           Z Location  [Horizontal Windspeed]
```
Calculate the horizontal windspeed

```
11:   P58              Low Pass Filter
      01:  1           Repetition
      02:  7           Sample Location Horizontal Windspeed
      03:  8           Location  [Filter Windspeed]
      04:  0.00105     Weighting Factor
```
This gives a 600 second time constant with a logging frequency of 10 Hz.

```
12:   P91              If Flag
      01:  21          1 is reset
      02:  30          Then Do
```
If not logging already AND

```
13:   P89              If X<=>F
      01:  8           X Location Filter Windspeed
      02:  3           >=
      03:  5           F
      04:  30          Then Do
```
If the Windspeed > 5 m/s SET FLAG 1 to start storing data and reset the timer, also store the start time.

```
14:   P86              Do
      01:  11          Set Flag 1

15:   P26              Timer
      01:  0000        Set Timer to zero

16:   P86              Do
      01:  10          Set Flag 0  (output)

17:   P77              Real Time
      01:  110         Day,  Hour - Minute
```
Also outputs the day, hour and minute when a run of data starts, in a separate data array.

```
18:   P86              Do
      01:  20          Reset Flag 0  (output)
```
To finnish the data array

```
19:   P95              End.

20:   P95              End.
```

Now log the data if FLAG 1 is set, i.e. the Windspeed was greater than the 5 m/s threshold.

```
21:   P91          If FLAG
      01:  11      1 is set
      02:  30      Then Do

22:   P86          Do
      01:  10      Set FLAG 0  (output)

23:   P26          Timer
      01:  12      Location of timer

24:   P70          Sample
      01:  3       Repetitions
      02:  1       Location U Gill
```

Stores the three I/Ps previously measured above.

```
25:   P4           Excite - Delay - Measure (S.E. Voltage)
      01:  1       Repetition
      02:  1       Range  5000 mV slow
      03:  3       Input Channel
      04:  1       Excitation Channel
      05:  0       Delay (seconds)
      06:  5       Excitation Voltage
      07:  10      Location  Celesco transducer
      08:  25.4    Multiplier
      09:  0000    Offset

26:   P2           Differential Voltage
      01:  1       Repetition
      02:  5       Range  5000 mV slow
      03:  1       Input Channel
      04:  9       Location  LCM transducer
      05:  0.019   Multiplier  (for No. 3 transducer)
      06:  0000    Offset

27:   P86          Do
      01:  10      Set FLAG 0  (output)

28:   P70          Sample
      01:  2       Repetitions
      02:  9       Location  LCM transducer
```

Stores the 2 I/Ps measured above.

```
29:   P89          If X<=>F
      01:  12      X Location  (Timer)
      02:  3       >=
      03:  18000   F  (30 minutes = 18000*0.1s,  can be changed)
      04:  30      Then Do
```

If have been logging for greater than 30 minutes THEN

```
30:   P86          Do
      01:  21      Reset FLAG 1
```

Reset FLAG 1 to stop data being stored.

```
31:   P18          Time
      01:  2       Hours into current year  (max. 8784)
      02:  0000    Mod/by
      03:  13      Location  [ Current Time]
```
Load the current time into Location 13.

```
32:   P34          Z=X+F
      01:  13      X Location Current Time
      02:  24      F n hours wait period,  can be changed if necessary
      03:  14      Z Location  [ Next Time]
```
Calculate the next time to test the windspeed, i.e. now + n hours, this constant can be changed if necessary.
N.B. Logging will start at midnight on 31st December as the number of hours into the year is reset to zero.

```
33:   P86          Do
      01:  12      Reset FLAG 2
```
To indicate that we must wait for a fixed period before testing the windspeed again.

```
34:   P30          Z=F
      01:  0       F
      02:  8       Z Location  [Filter windspeed]
```
By setting the filtered windspeed to zero, when the windspeed is next logged, after n hours, the windspeed must average > 5 m/s for at least 10 minutes before the threshold is crossed.

```
35:   P95          End

36:   P95          End.

37:   P            End Table 1

*     4            Mode 4 Output Options
01:   10           (Tape On)  (Printer Off)
02:   02           Baud Rate 9600
```
Tape set ON.

Appendix XIV Computer program to carryout the non-cosine response correction for data obtained using the Gill UVW Anemometer

Filename: NONCOS

Language: Fortran

```
C     ------------------------------------------------------------------
C     Non-cosine response correction
C     ------------------------------------------------------------------
      Dimension horcor(101), vercor(101)
      DATA (horcor(i), i = 1,101)/ 100, 101, 101, 102, 102,
     * 103, 104, 105, 106, 106, 107, 108, 110, 111, 113,
     * 113, 116, 118, 120, 121, 122, 122, 122, 123, 124,
     * 123, 123, 123, 122, 121, 121, 121, 121, 120, 119,
     * 119, 118, 118, 117, 116, 115, 114, 114, 117, 120,
     * 125, 133, 150, 200, 200, 200, 200, 200, 180, 173,
     * 167, 160, 156, 153, 150, 148, 147, 145, 144, 144,
     * 128, 127, 126, 124, 123, 122, 121, 120, 119, 117,
     * 116, 114, 112, 111, 110, 109, 108, 106, 105, 104,
     * 103, 102, 102, 101, 100, 100/

      DATA (vercor(i), i = 1,101)/ 104, 104, 104, 104, 105,
     * 105, 105, 105, 106, 106, 106, 105, 104, 104, 105,
     * 106, 107, 110, 113, 118, 125, 133, 150, 200, 200,
     * 200, 200, 200, 150, 133, 128, 122, 121, 119, 117,
     * 114, 113, 112, 111, 111, 111, 110, 109, 107, 106,
     * 105, 105, 104, 103, 102, 100, 100, 100, 100, 100,
     * 100, 100, 100, 100, 100, 100, 100, 100, 100, 100,
     * 100, 100, 100, 100, 100, 100, 100, 100, 100, 100,
     * 100, 100, 100, 100, 100, 100, 100, 100, 100, 100,
     * 100, 100, 100, 100, 100, 100/

      i = 0
      isave = 50
      jsave = 50
      ksave = 50

    1 READ (7,*) gU, gV, gW, x, y
C     Initialise direction cosines
      IF (isave.lt.0.00) GOTO 2
      GOTO 6

    2 isave = isave*(-1.00)
      IF (jsave.lt.0.00) GOTO 3
      GOTO 6

    3 jsave = jsave*(-1.00)
      IF (ksave.lt.0.00) GOTO 4
      GOTO 6
```

```
    4   ksave = ksave*(-1.00)

    6   n = 0
        i = isave
        j = jsave
        k = ksave

C       Correct data for non-cosine response,
C       using current direction cosines

   40   u = gU*horcor(i)/100
        v = gV*horcor(j)/100
        w = gW*vercor(k)/100

C       Calculate new direction cosines,
C       and convert to subscripts

   50   fuz = u**2
        fvz = v**2
        fwz = z**2
        s = SQRT(fuz + fvz + fwz)*0.5
        ii = (u*1000/s + 10)/20.51
        jj = (v*1000/s + 10)/20.51
        kk = w*1000/s + 10)/20.51

C       Compare new cosine with old,
C       iterate if too different

        IF (iabs(ii-i)-1) 10,10,20

   10   IF (iabs(jj-j)-1) 15,15,20

   15   IF (iabs(kk-k)-1) 30,30,20

C       Check number of iterations,
C       stop if too large

   20   n = n + 1
        IF (6 - n) 30,30,80

C       Reiterate with new direction cosines

   80   IF (ii.lt.0.00) ii = ii*(-1.00)
        IF (jj.lt.0.00) jj = jj*(-1.00)
        IF (kk.lt.0.00) kk = kk*(-1.00)
        i = ii
        j = jj
        k = kk
```

```
      IF (i.eq.0.00) i = 1
      IF (j.eq.0.00) j = 1
      IF (k.eq.0.0) k = 1
      GOTO 40

C     Replace raw data with corrected data

 30   gU = u
      gV = v
      gW = w

C     Save current cosines to initialise
C     correction of next data sample

      isave = i
      jsave = j
      ksave = k
      WRITE (8,*) gU,  gV, gW, x, y
      l = l + 1
      IF (l.eq.1024) GOTO 100
      GOTO 1

100   STOP
      END
```

Appendix XV Program for coordinate rotation of windspeed data

Filename: ROTATE

Language: Fortran

```
C     ------------------------------------------------------------------------------
C     Windspeed coordinate rotation to mean windspeed direction
C     ------------------------------------------------------------------------------


      i = 0
      Call Emas3Prompt ('Enter mean wind direction in degrees from North: ')
10    Read *,TBAR
      TBAR = (TBAR/180)*3.142


C     Read in raw windspeed data
20    Read (7,*) Time,U,V,W,V1,V2
      i = i + 1
      r = SQRT((U**2)+(V**2))
      IF (U.EQ.0.00E+00) GOTO 30
      GOTO 35
30    U = U + 1.00E-02
35    IF (V.EQ.0.00E+00) GOTO 40
      GOTO 45
40    V = V + 1.00E-02


C     Determine which quadrant the wind direction lies in
45    IF (U.GE.0.and.V.LT.0) GOTO 50
      IF (U.LT.0.and.V.LT.0) GOTO 52
      IF (U.LT.0.and.V.GE.0) GOTO 54
      IF (U.GE.0.and.V.GE.0) GOTO 56


C     Determine angle of instantaneous wind record
50    t = ATAN(V/U)*(-1.0)
      GOTO 60
52    t = (3.142/2)+ATAN(U/V)
      GOTO 60
54    t = 3.142 + ATAN(V/U)*(-1.0)
      GOTO 60
56    t = (1.5*3.142) + ATAN(U/V)


C     Determine angle of instantaneous wind record after rotation of Gill axis
60    IF (t.GE.TBAR) GOTO 64
      IF (t.LT.TBAR) GOTO 66
64    TNEW = t - TBAR
      GOTO 70
66    TNEW = TBAR - t


C     Determine new quadrant of wind direction
70    IF (TNEW.GE.0.and.TNEW.LT.(3.142/2)) GOTO 80
      IF (TNEW.GE.(3.142/2).and.TNEW.LT.3.142) GOTO 82
```

```
      IF (TNEW.GE.3.142.and.TNEW.LT(1.5*3.142) GOTO 84
      IF (TNEW.GE.(1.5*3.142).and.TNEW.LT.(2*3.142) GOTO 86

C     Determine new values for U and V
80    UNEW = r*COS(TNEW)
      VNEW = r*SIN(TNEW)*(-1.0)
      GOTO 90
82    UNEW = r*SIN(TNEW-(3.142/2))*(-1.0)
      VNEW = r*COS(TNEW-(3.142/2))
      GOTO 90
84    UNEW = r*COS(TNEW-3.142)
      VNEW = r*SIN(TNEW-3.142)*(-1.0)
      GOTO 90
86    UNEW = r*SIN(TNEW-(1.5*3.142))*(-1.0)
      VNEW = r*COS(TNEW-(1.5*3.142))

C     Write new data into data output file
90    Write (8,*) Time,UNEW,VNEW,W,V1,V2
      IF (i.GE.1034) GOTO 100
      GOTO 10
100   STOP
      END
```

Appendix XVI Computer program to calculate stem displacement coordinates

Filename: COORDS

Language: Fortran

```
C     ------------------------------------------------------------------------------
C     Program to calculate stem displacement coordinates
C     ------------------------------------------------------------------------------

C     Input distances of stem from the pulleys
10    Call Emas3Prompt ('Enter distances dx and dy (cm): ')
      READ *,a,b
      c = SQRT(a**2+b**2)

C     Read in raw data
20    READ (7,*) T,U,V,W,d,e

C     Determine angles A,B,D and E
30    ANGLEA = ASIN(a/c)
      ANGLEB = ASIN(b/c)
      ANGLED = ACOS(((c**2)+(e**2)-(d**2))/(2*c*e))
      ANGLEE = ACOS(((c**2)+(d**2)-(e**2))/(2*c*d))

C     Determine which quadrant the tree has moved to
40    IF (ANGLEA.GE.ANGLED.and.ANGLEB.LE.ANGLEE) GOTO 50
      IF (ANGLEA.LE.ANGLED.and.ANGLEB.LE.ANGLEE) GOTO 60
      IF (ANGLEA.LE.ANGLED.and.ANGLEB.GE.ANGLEE) GOTO 70
      IF (ANGLEA.GE.ANGLED.and.ANGLEB.GE.ANGLEE) GOTO 80

C     Calculate new coordinates of the stem
C     Quadrant 1
50    ANGLEG = ANGLEA - ANGLED
      z = SQRT((b**2)+(e**2)-(2*b*e*COS(ANGLEG)))
      ANGLEI = ASIN((e*SIN(ANGLEG))/z)
      ANGLEY = ANGLEI - ASIN(1.0)
      y = z*SIN(ANGLEY)*(-1.0)
      x = z*COS(ANGLEY)
      GOTO 90

C     Quadrant 2
60    ANGLEG = ANGLED - ANGLEA
      z = SQRT((b**2)+(e**2)-(2*b*e*COS(ANGLEG)))
      ANGLEI = ASIN((e*SIN(ANGLEG))/z)
      ANGLEY = ANGLEI - ASIN(1.0)
      y = z*SIN(ANGLEY)*(-1.0)
      x = z*COS(ANGLEY)*(-1.0)
      GOTO 90

C     Quadrant 3
70    ANGLEG = ANGLED - ANGLEA
      z = SQRT((b**2)+(e**2)-(2*b*e*COS(ANGLEG)))
      ANGLEI = ASIN((e*SIN(ANGLEG))/z)
      ANGLEY = ASIN(1.0) - ANGLEI
      y = z*SIN(ANGLEY)*(-1.0)
```

```
      x = z*COS(ANGLEY)*(-1.0)
      GOTO 90

C     Quadrant 4
80    ANGLEG = ANGLEA - ANGLED
      z = SQRT((b**2) + (e**2)-(2*b*e*COS(ANGLEG)))
      ANGLEI = ASIN((e*SIN(ANGLEG))/z)
      ANGLEY = ASIN(1.0) - ANGLEI
      y = z*SIN(ANGLEY)*(-1.0)
      x = z*COS(ANGLEY)

C     Round off new values to 2 decimal places
90    YNEW = y*100
      IYNEW = YNEW
      y = IYNEW/100
      XNEW = x*100
      IXNEW = XNEW
      x = IXNEW/100
      ZNEW = z*100
      IZNEW = ZNEW
      z = IZNEW/100

C     Write new data into new data file
100   WRITE (8,*) T,U,V,W,x,y,z
      IF (T.LT.1034) GOTO 20
      Call Emas3Prompt (End of raw data set.')
      STOP
      END
```

Appendix XVII Time base graphs illustrating the wind and stem displacement time series obtained from the two plots
(Rivox 4-7 Unthinned plot, Rivox 8 and 10 Thinned plot)

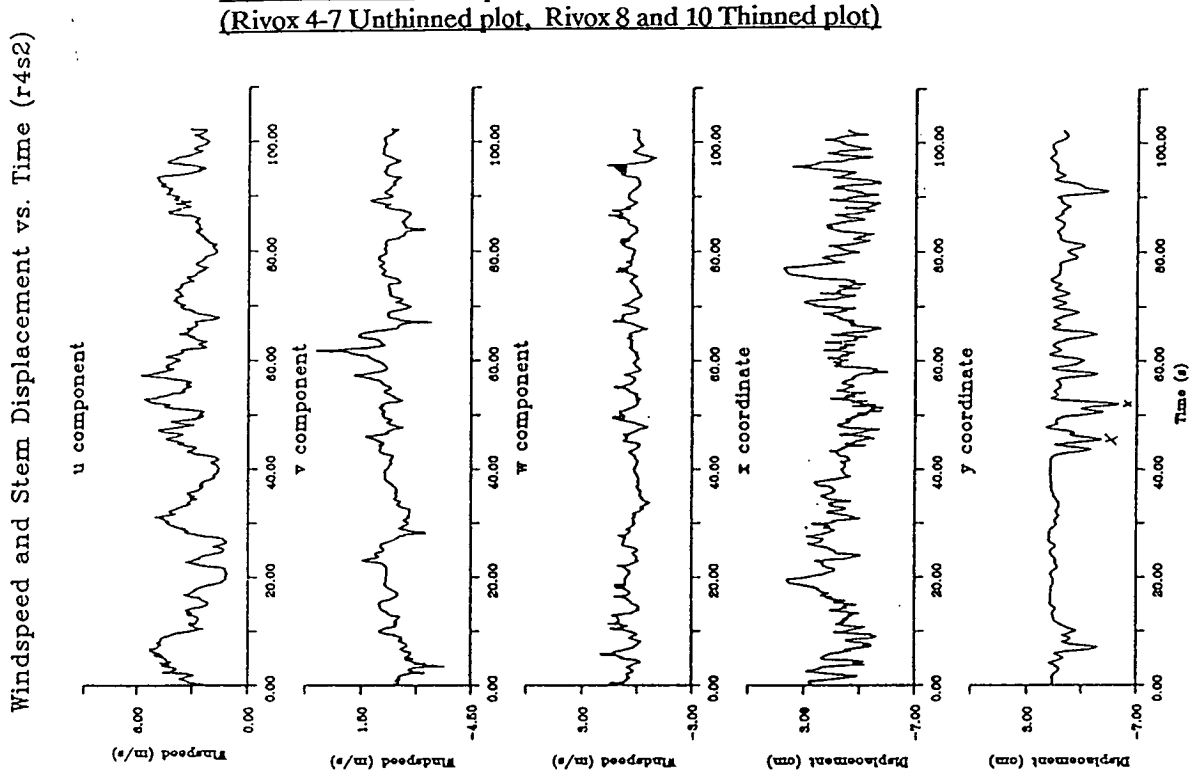

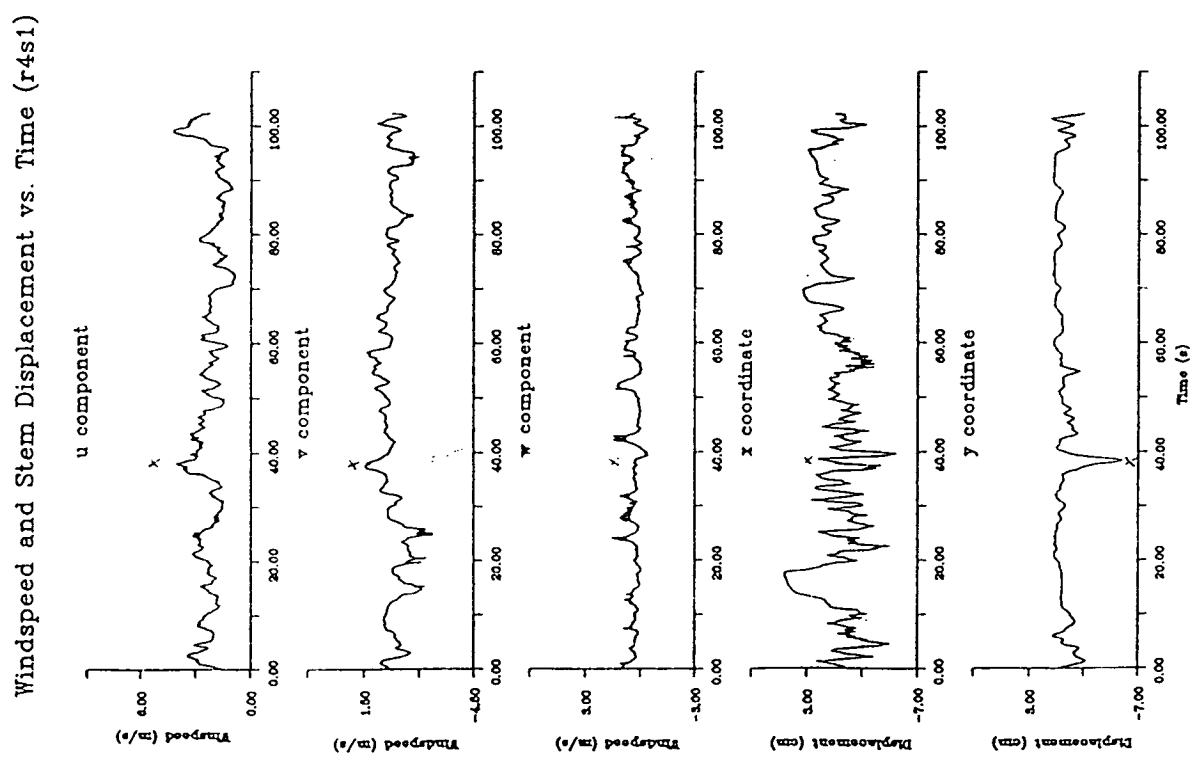

Windspeed and Stem Displacement vs. Time (r5s1)

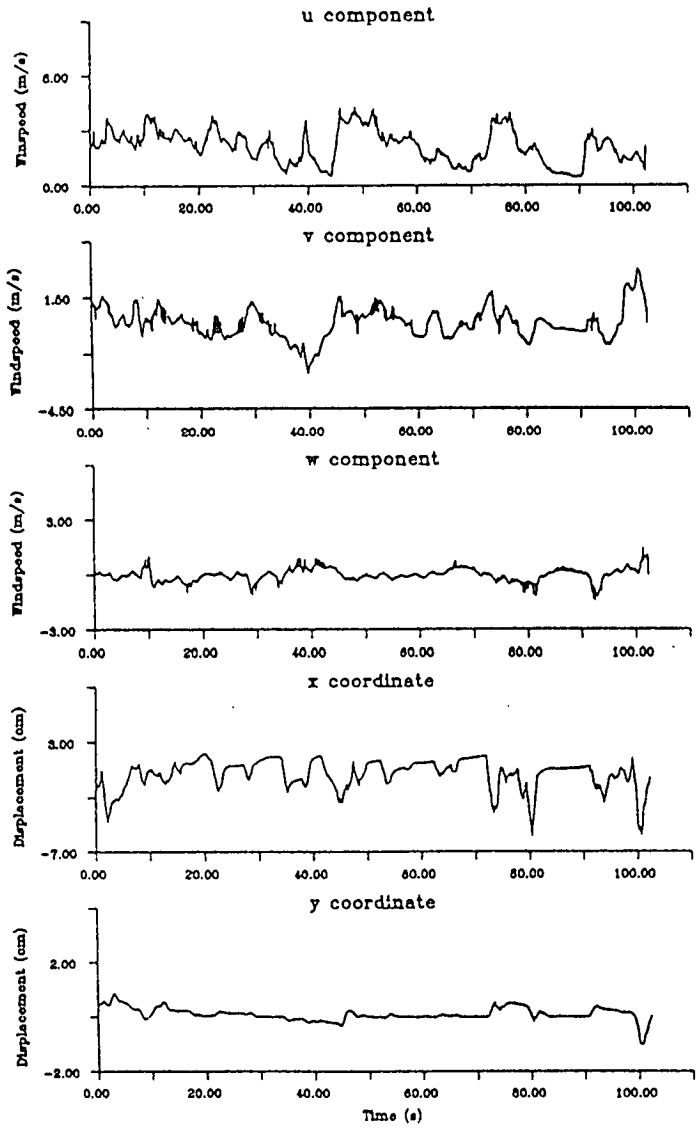

Windspeed and Stem Displacement vs. Time (r5s2)

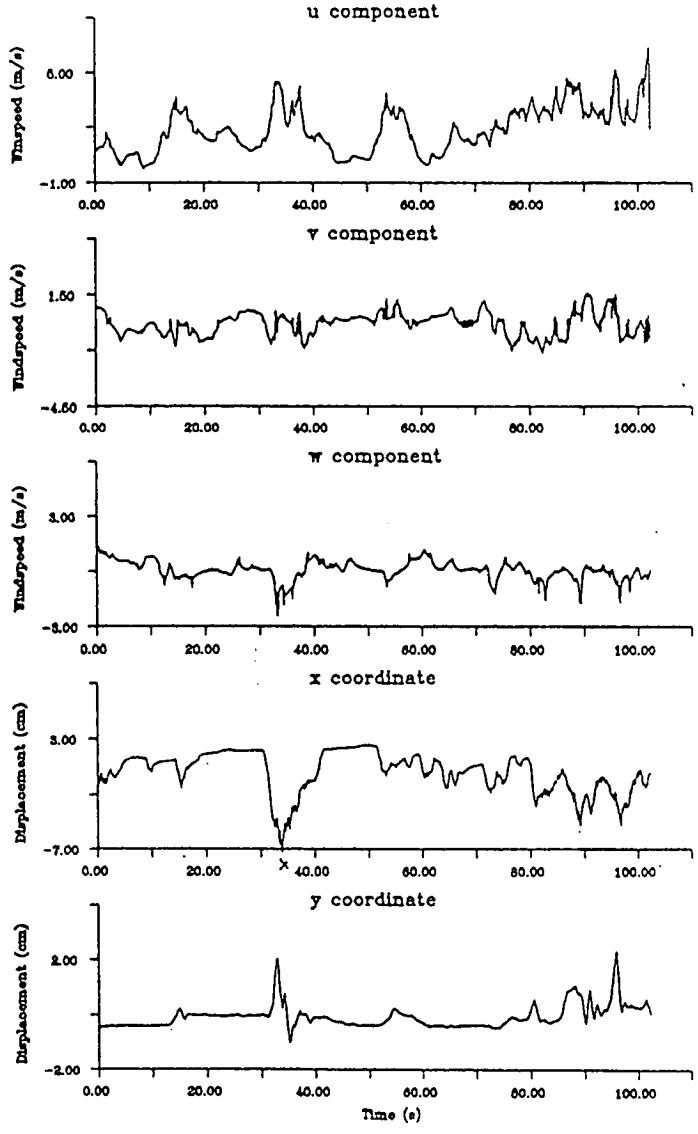

Windspeed and Stem Displacement vs. Time (r5s3)

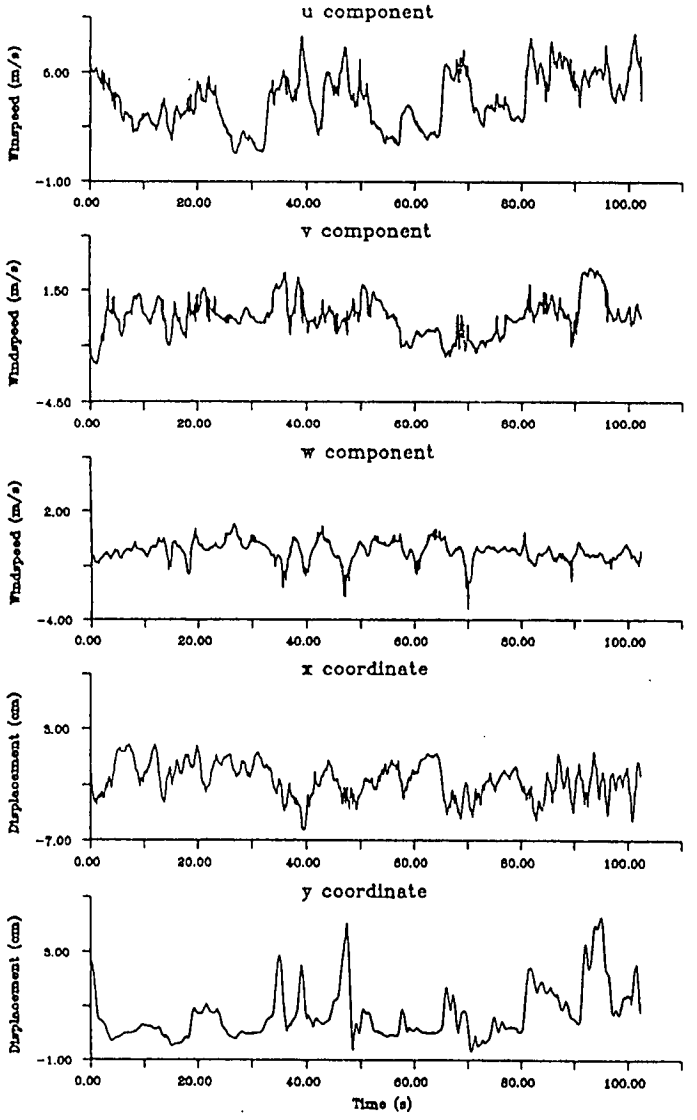

Windspeed and Stem Displacement vs. Time (r5s4)

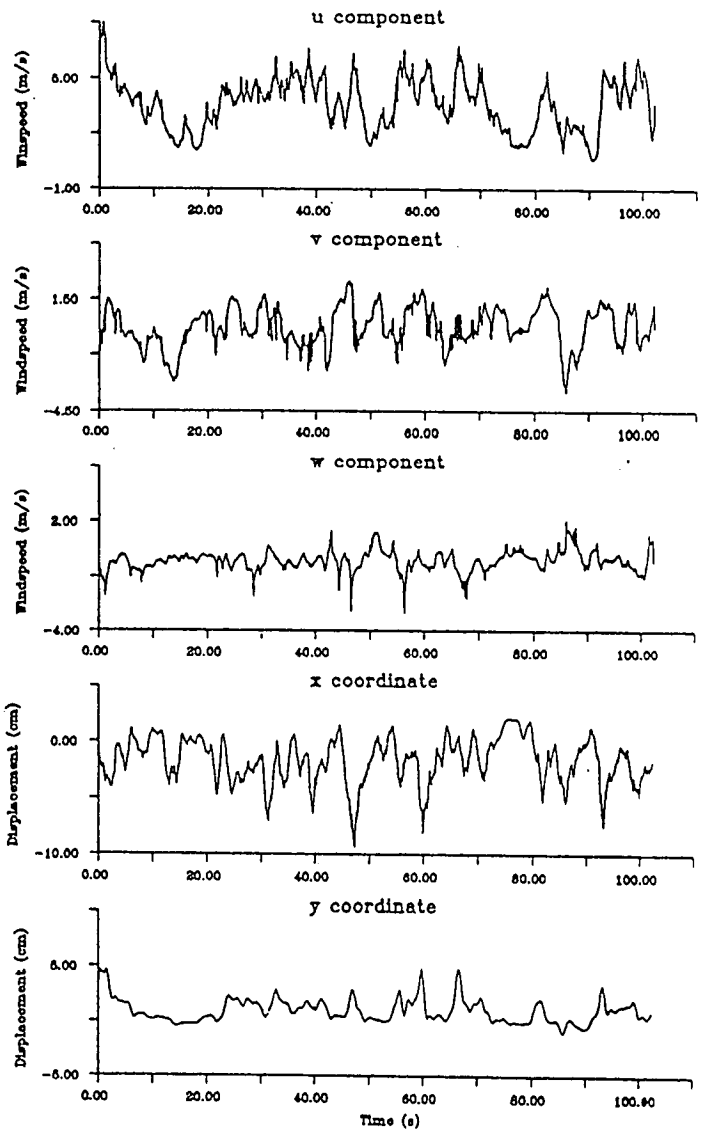

Windspeed and Stem Displacement vs. Time (r6s1)

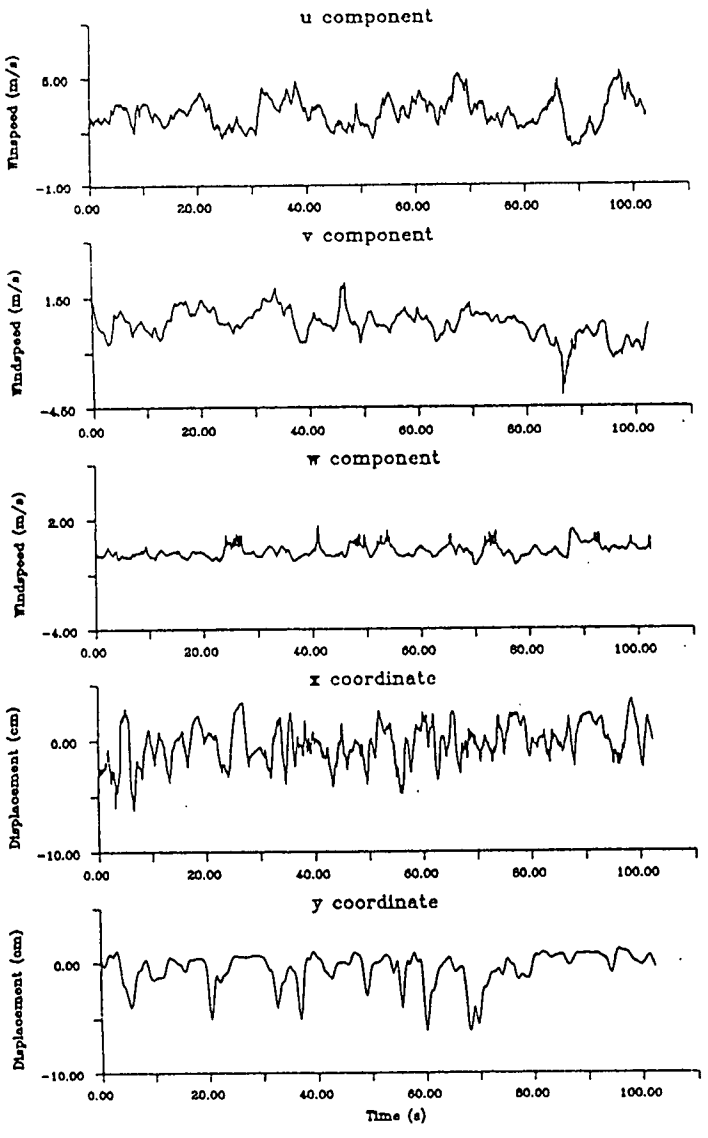

Windspeed and Stem Displacement vs. Time (r6s2)

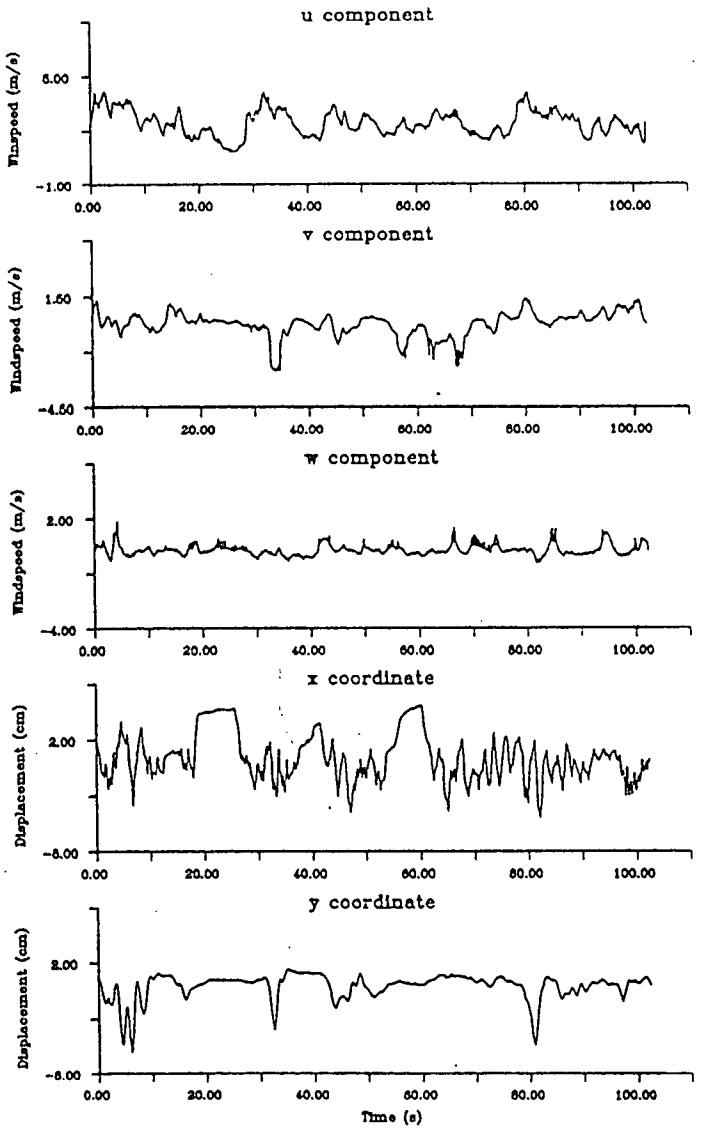

Windspeed and Stem Displacement vs. Time (r6s3)

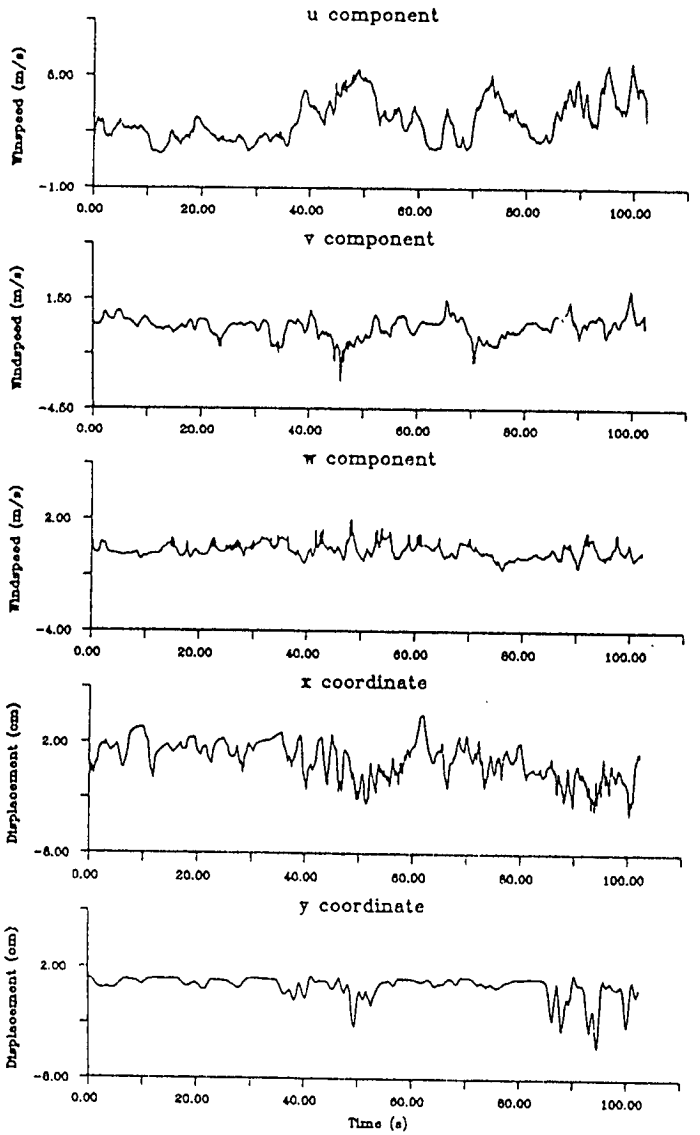

Windspeed and Stem Displacement vs. Time (r6s4)

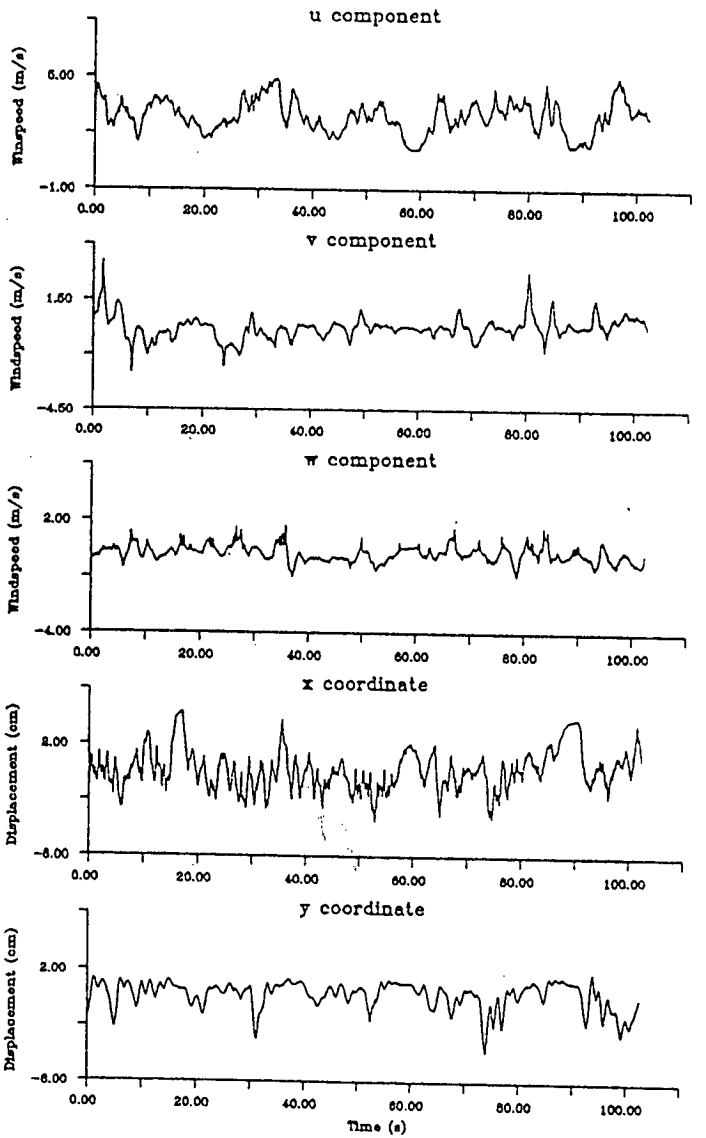

Windspeed and Stem Displacement vs. Time (r7s1)

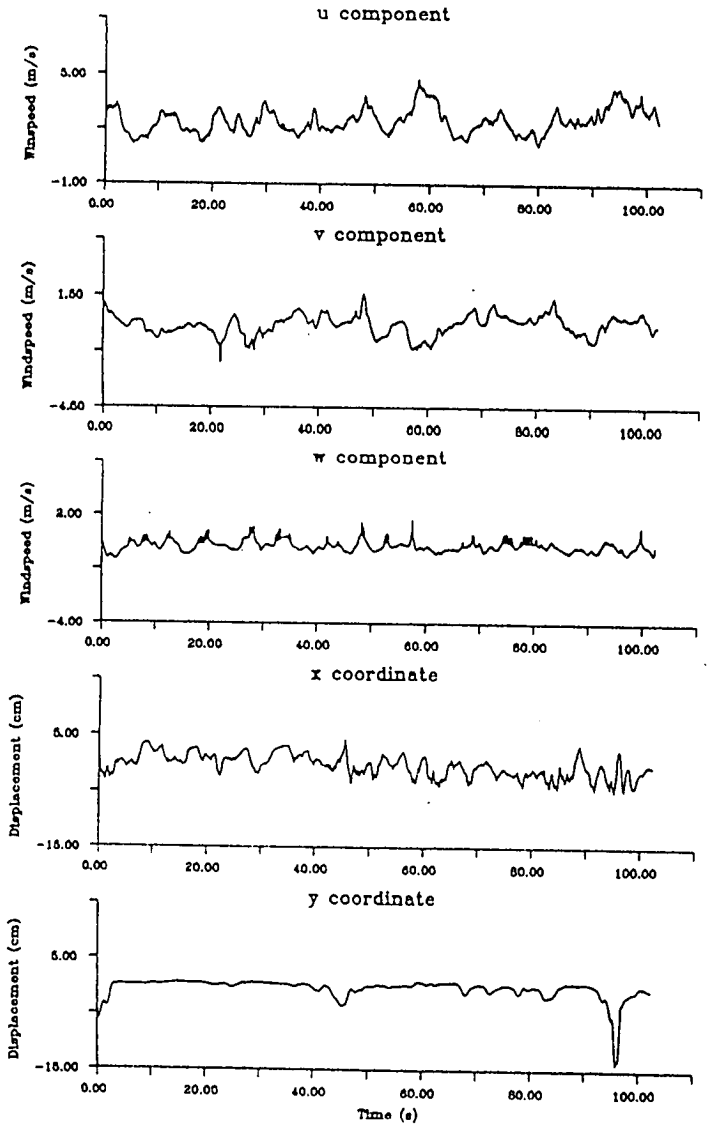

Windspeed and Stem Displacement vs. Time (r7s2)

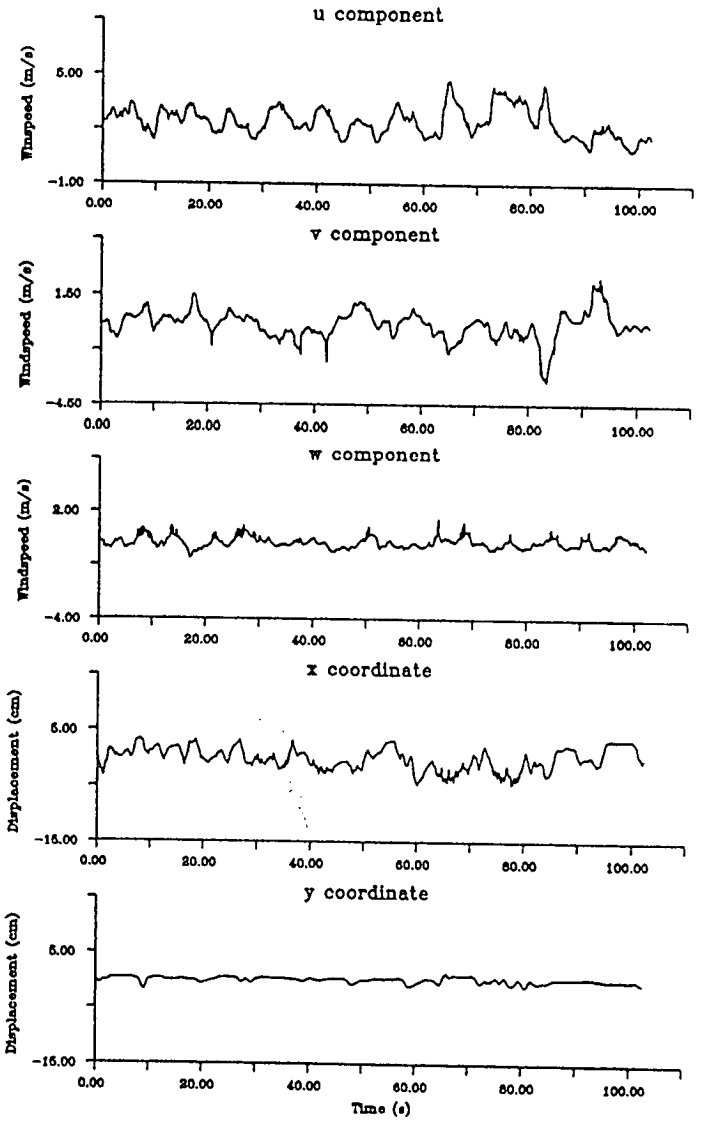

Windspeed and Stem Displacement vs. Time (r7s3)

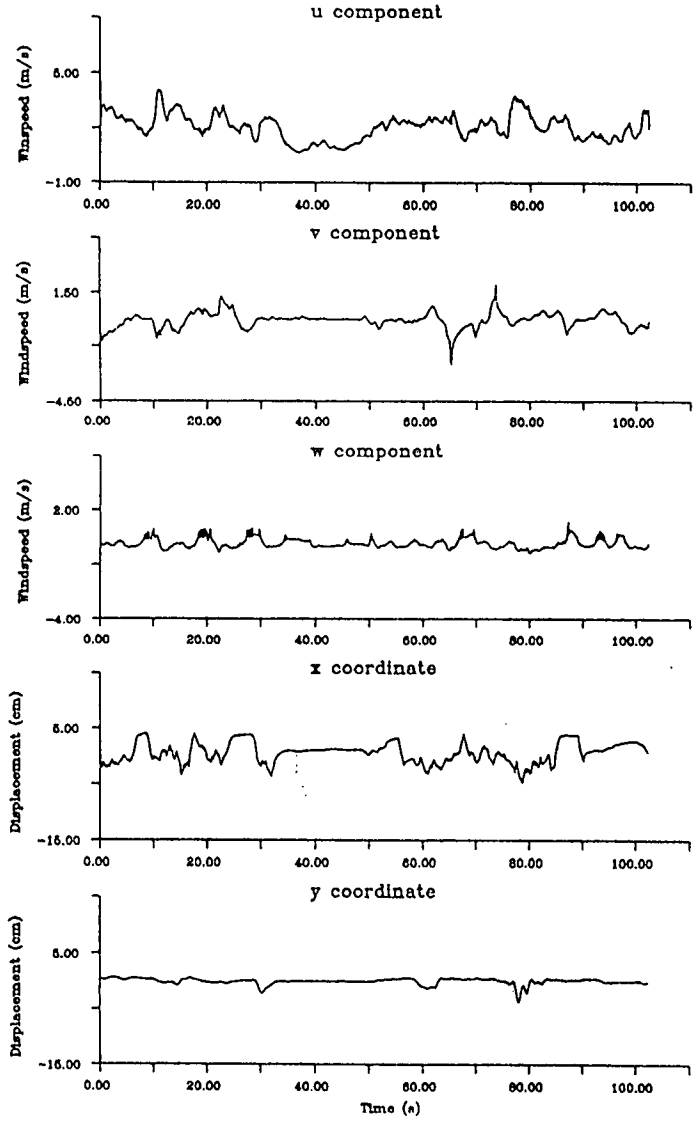

Windspeed and Stem Displacement vs. Time (r7s4)

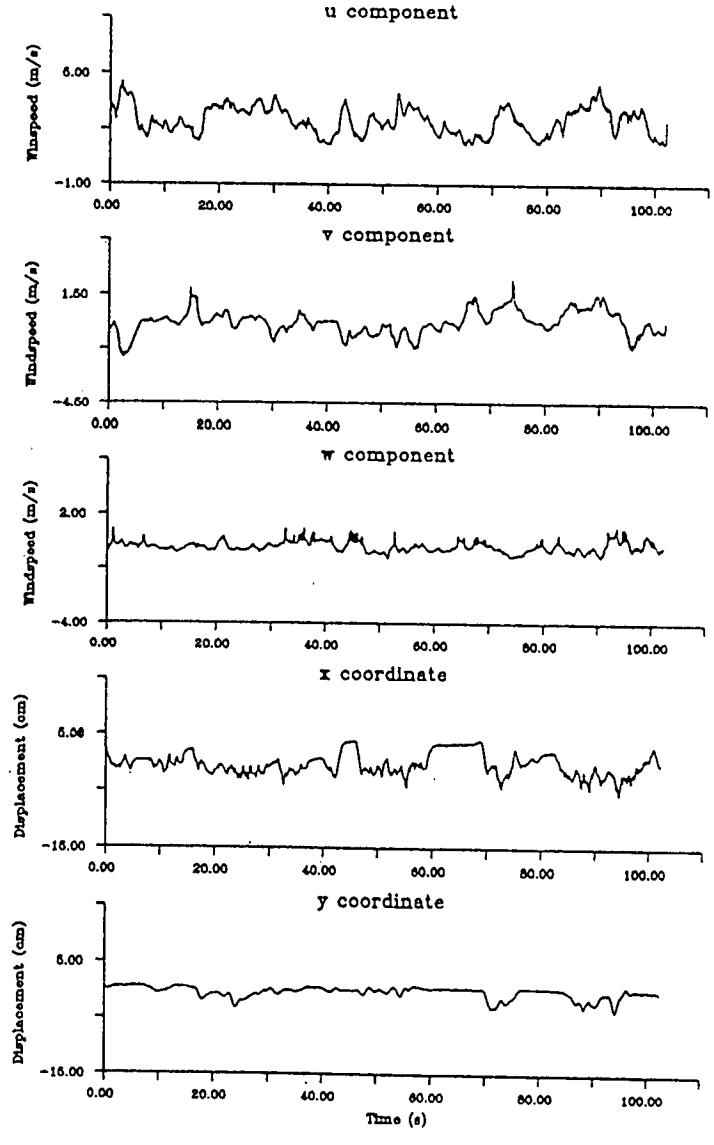

Windspeed and Stem Displacement vs. Time (r8s1)

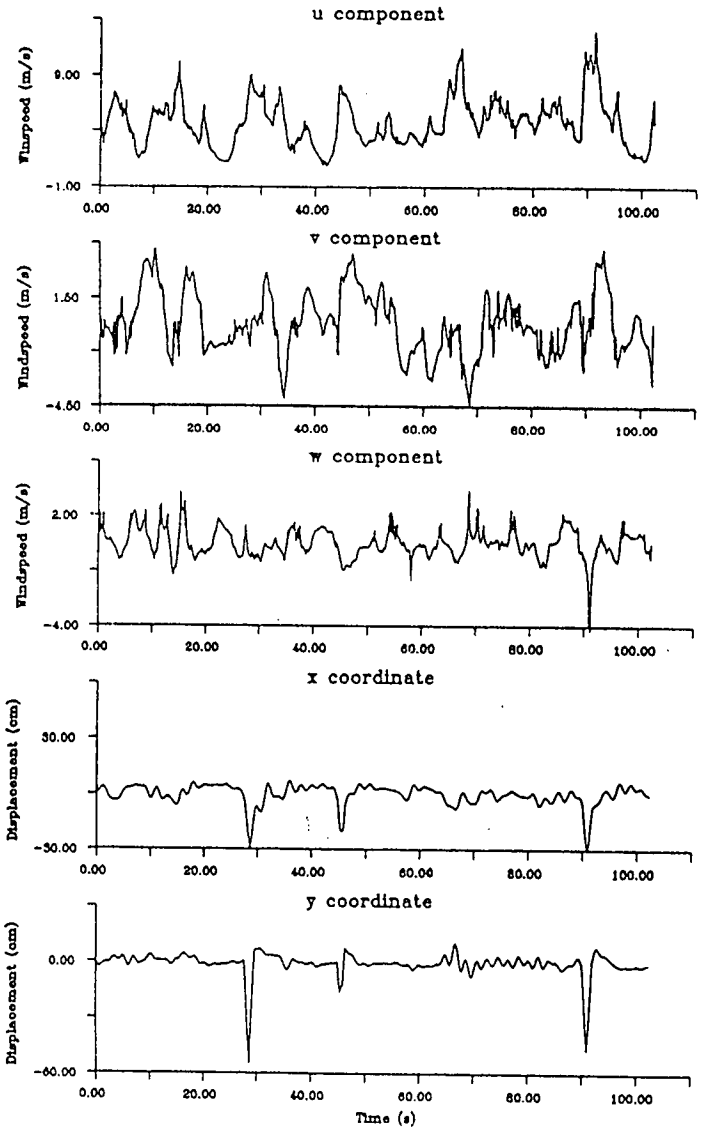

Windspeed and Stem Displacement vs. Time (r8s2)

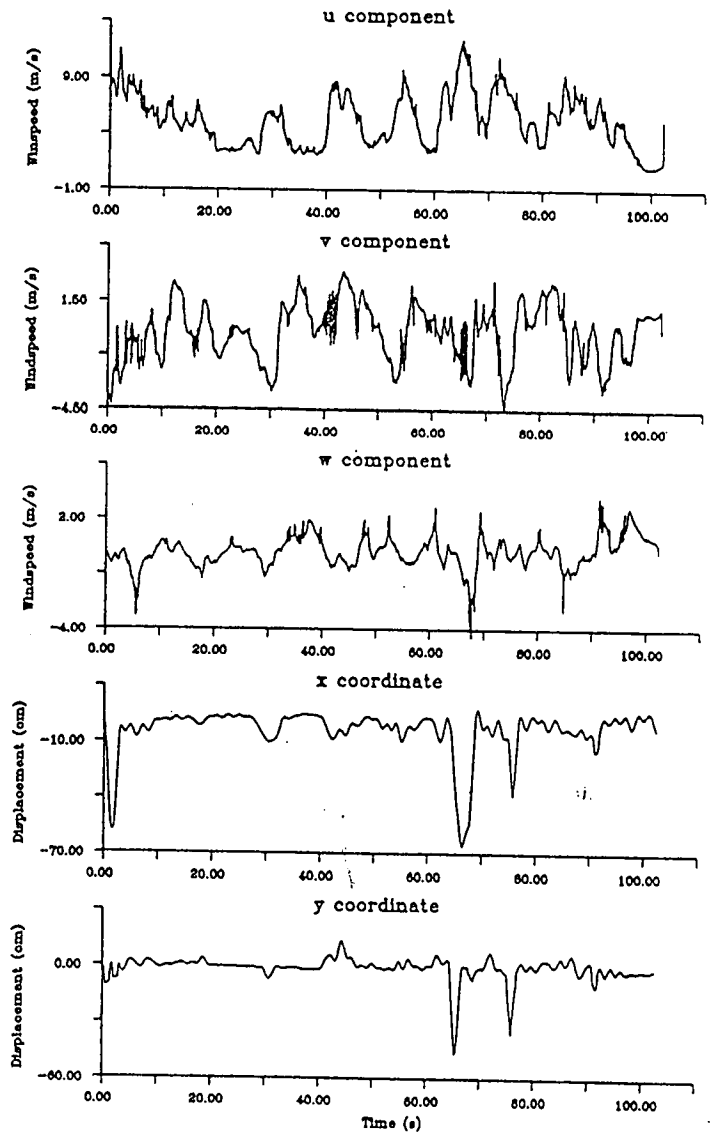

Windspeed and Stem Displacement vs. Time (r8s3)

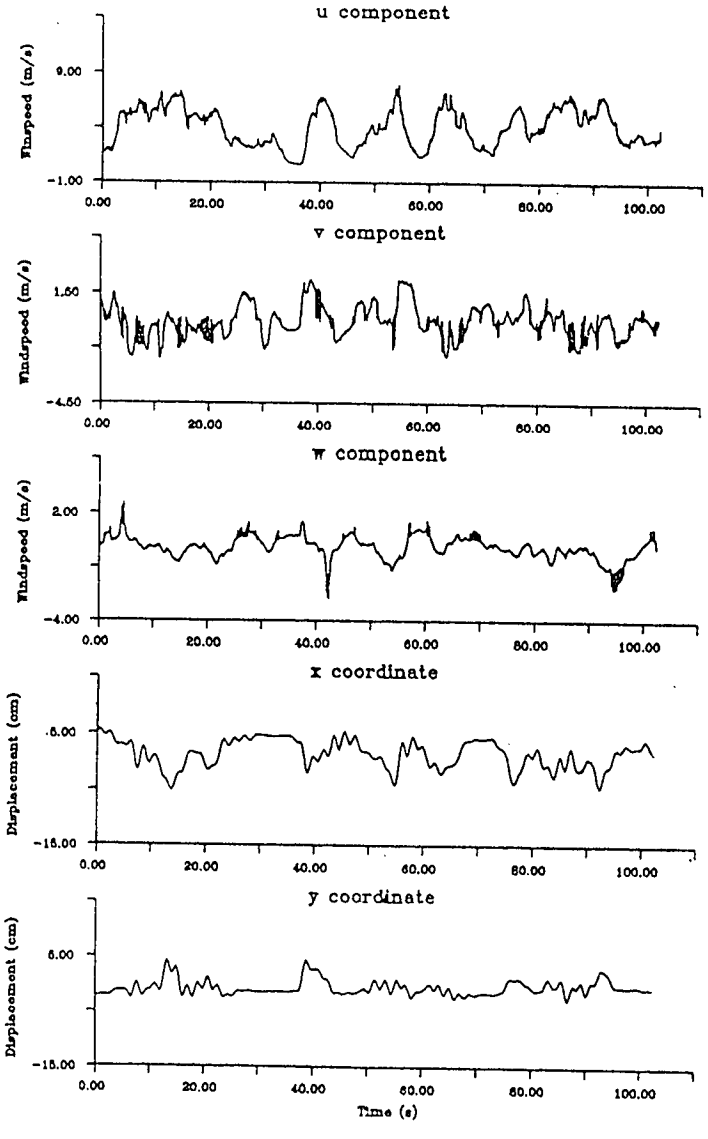

Windspeed and Stem Displacement vs. Time (r8s4)

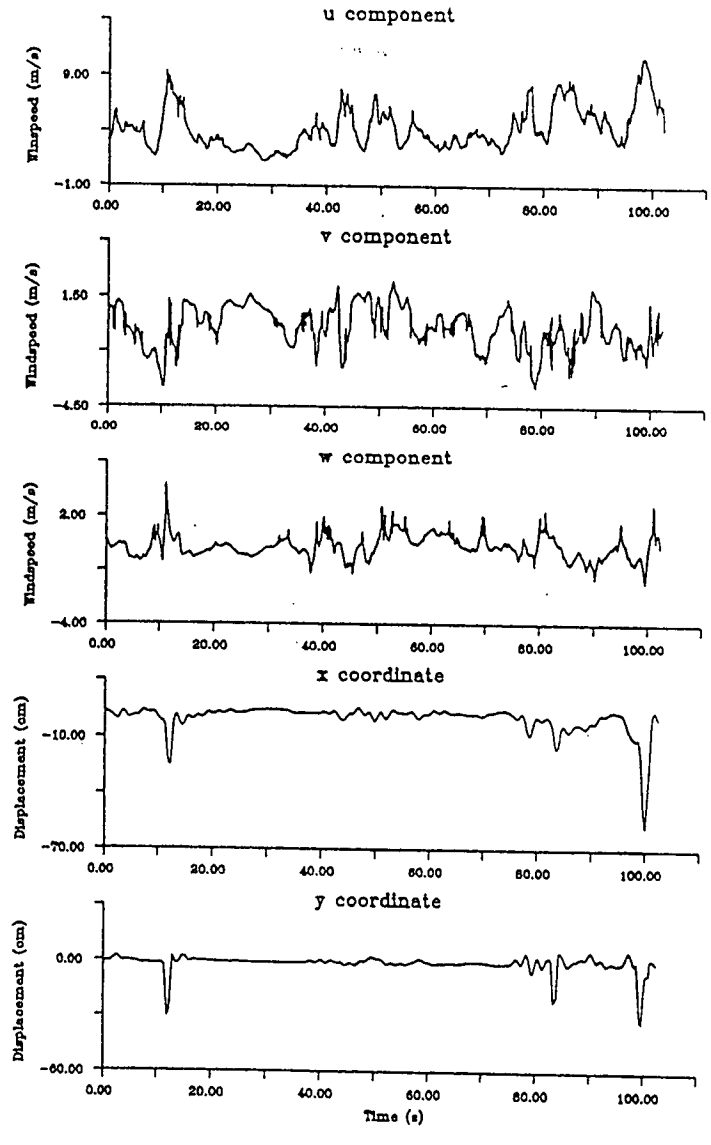

Windspeed and Stem Displacement vs. Time (r8s5)

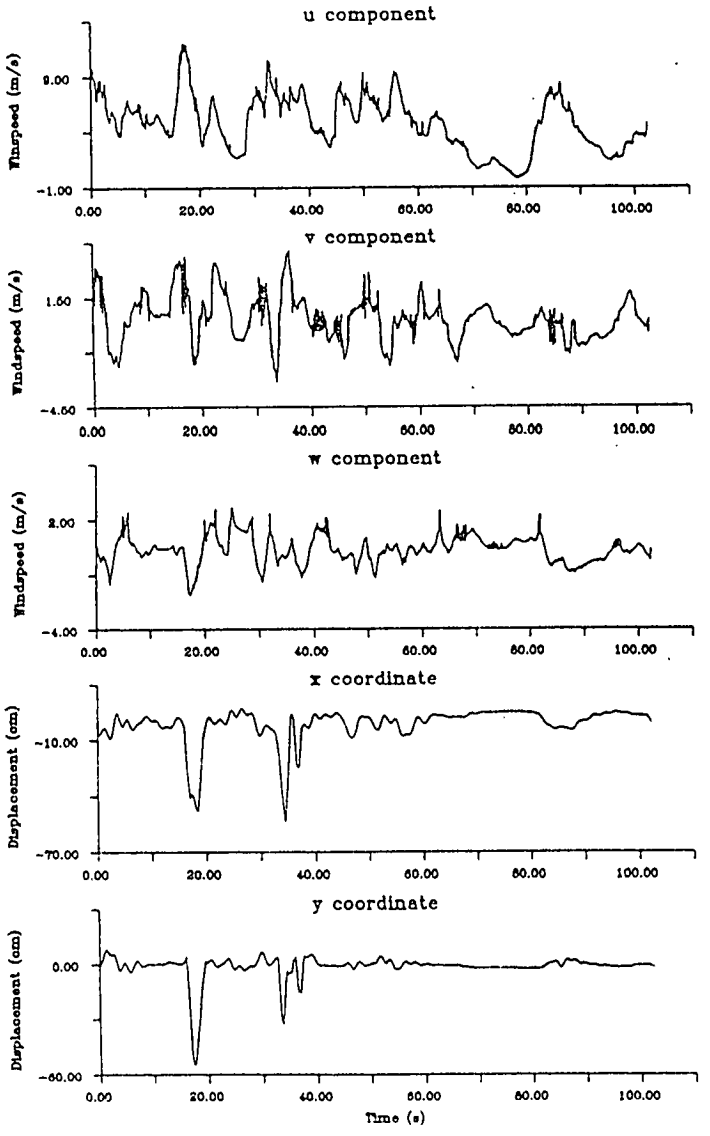

Windspeed and Stem Displacement vs. Time (r8s6)

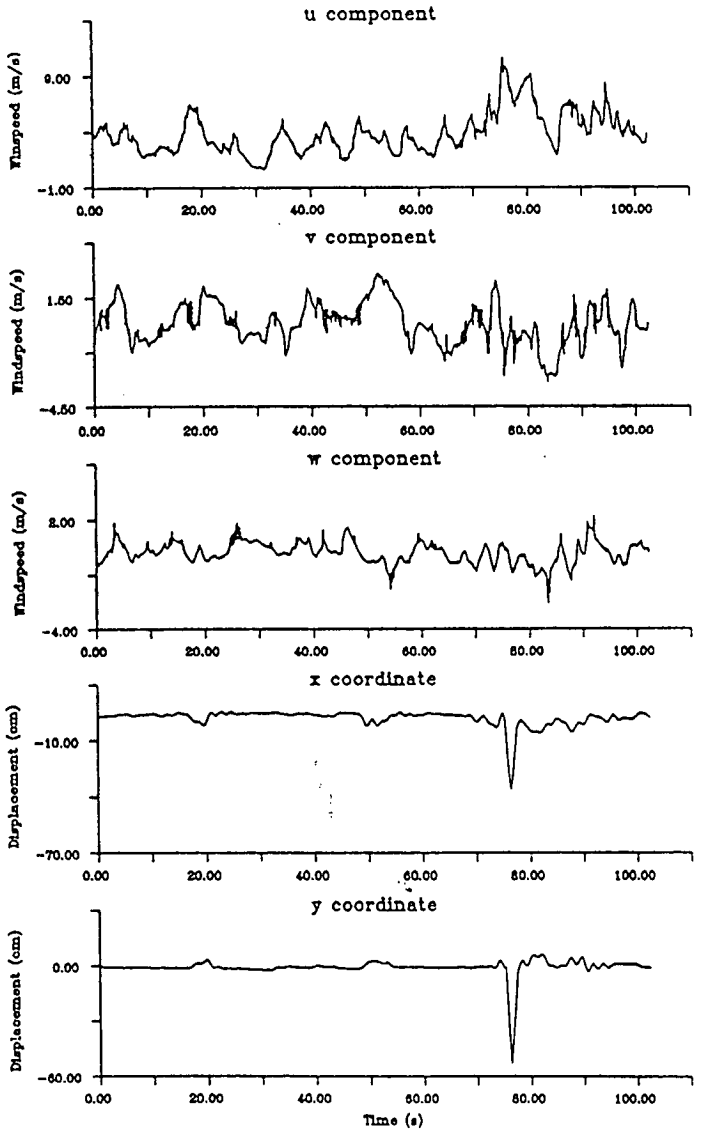

Windspeed and Stem Displacement vs. Time (r8s7)

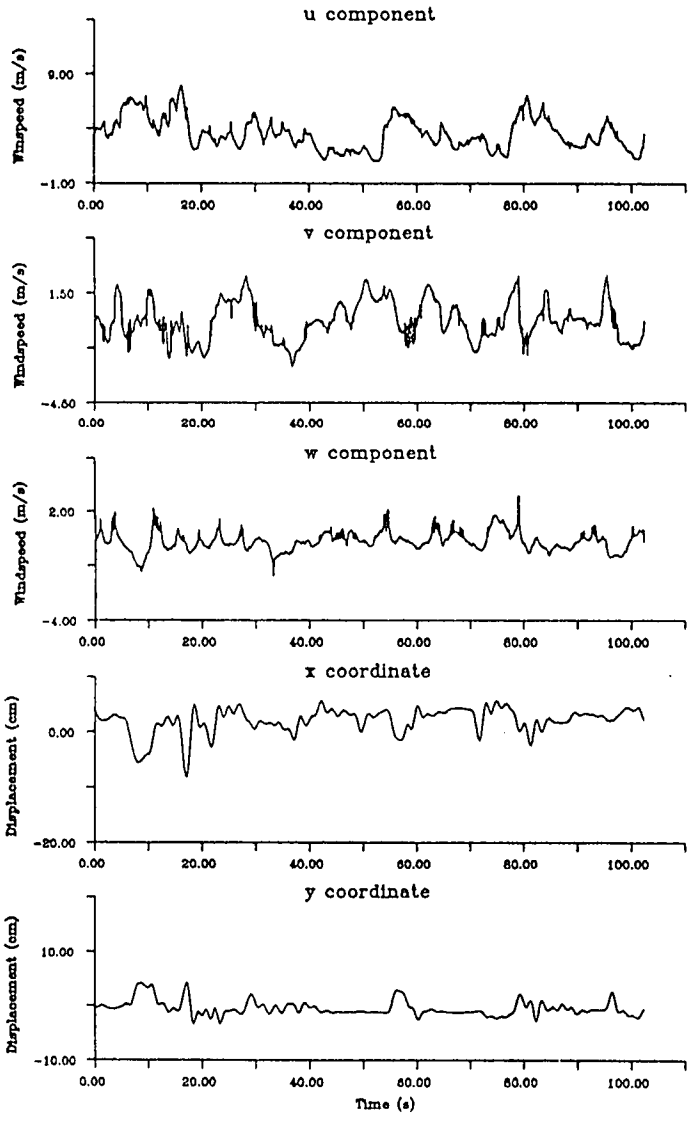

Windspeed and Stem Displacement vs. Time (r8s8)

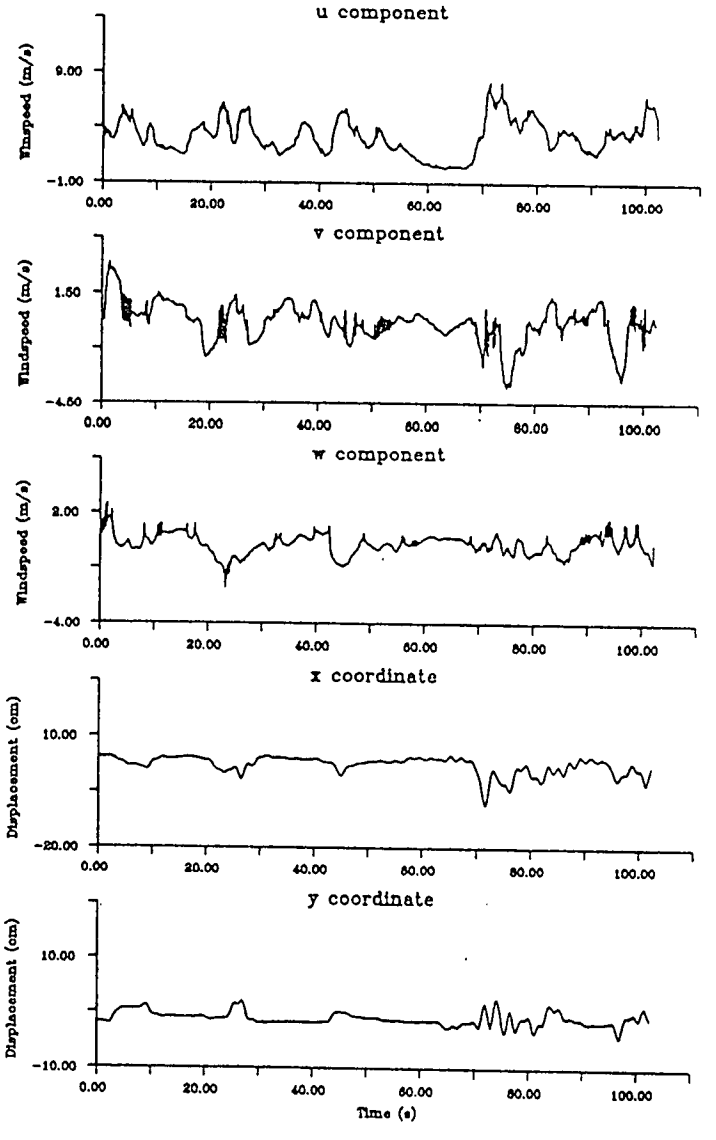

Windspeed and Stem Displacement vs. Time (r10s1)

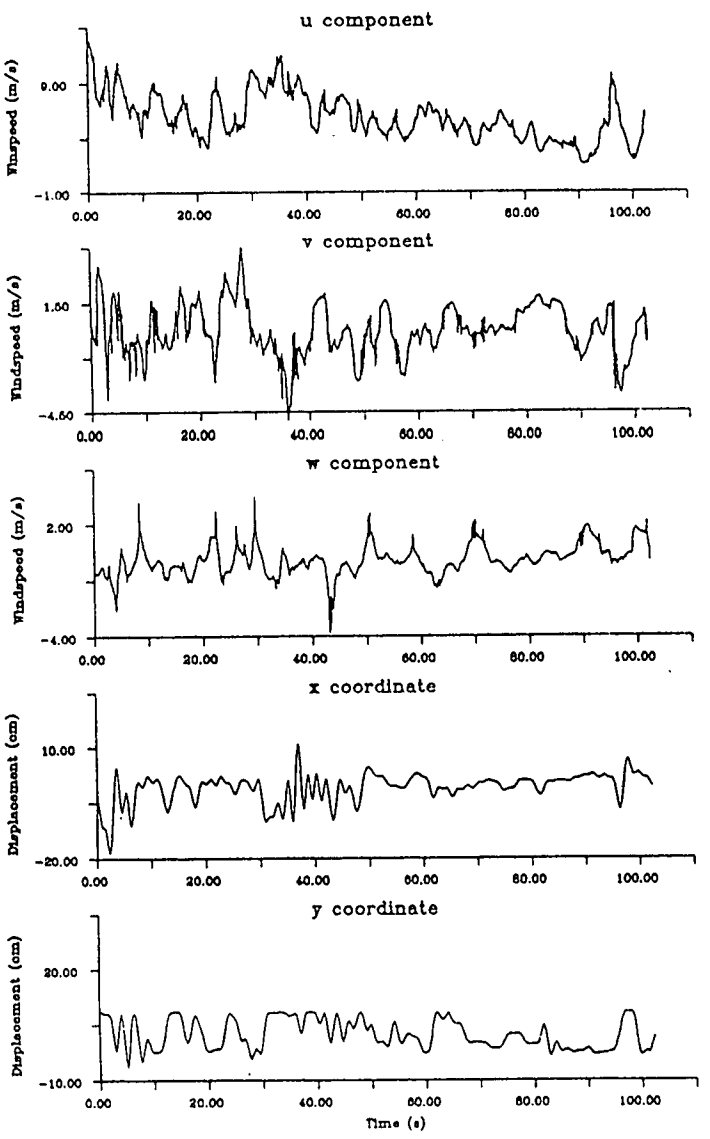

Windspeed and Stem Displacement vs. Time (r10s2)

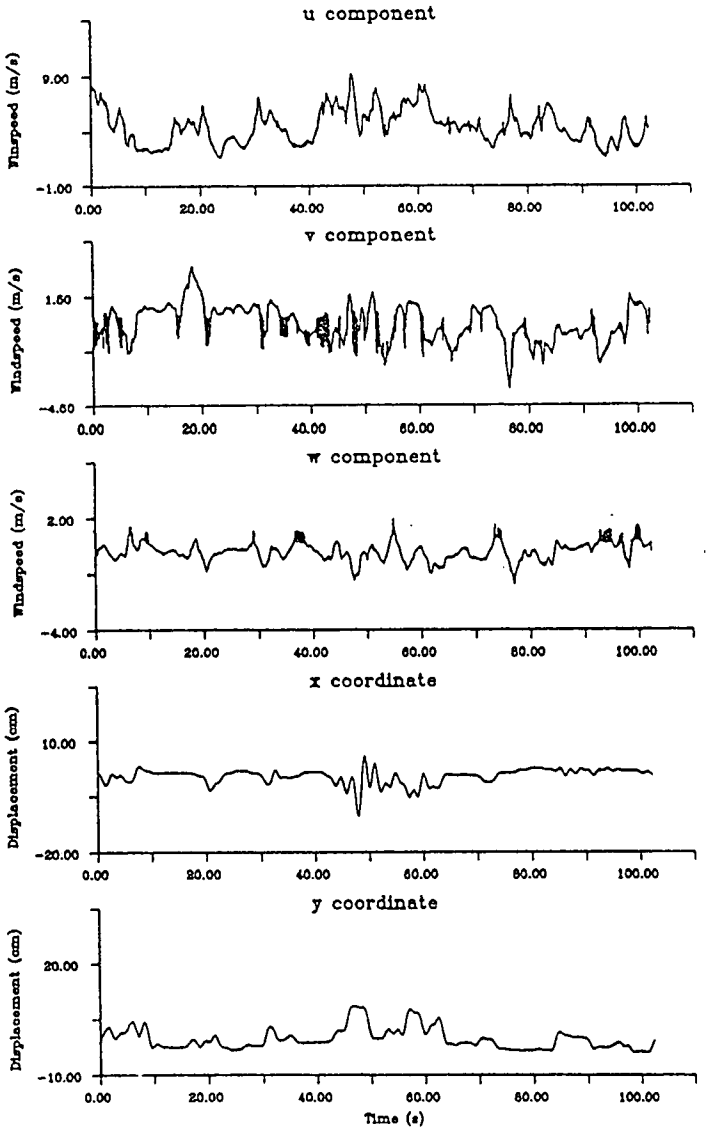

Windspeed and Stem Displacement vs. Time (r10s3)

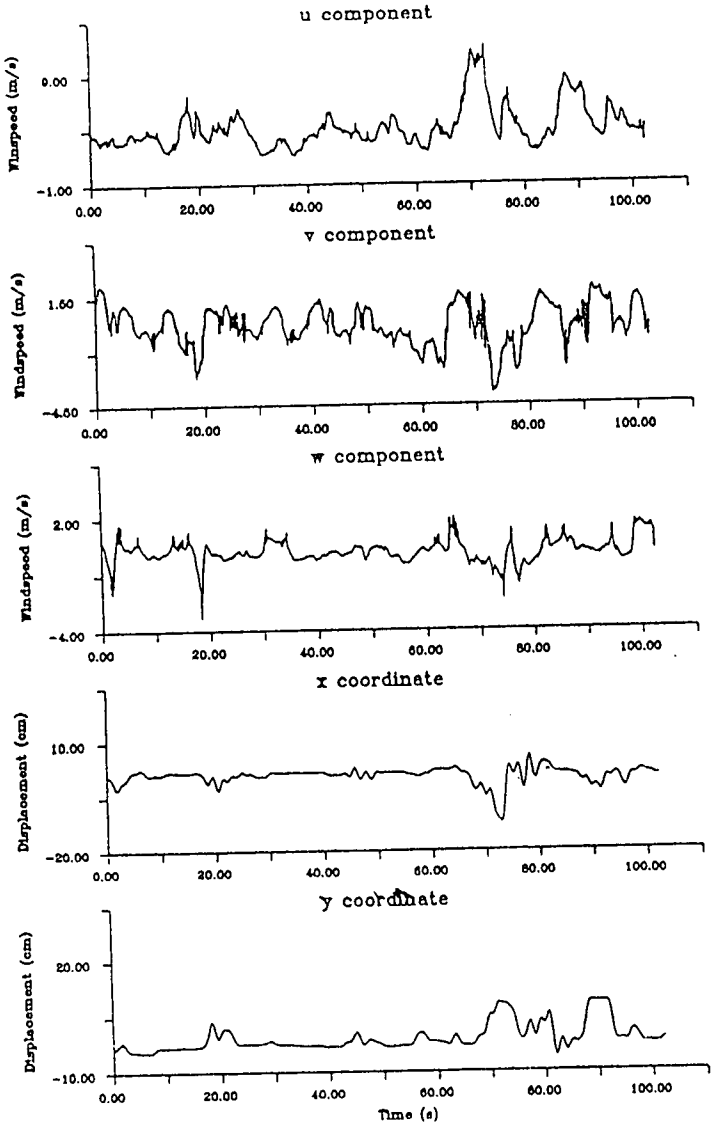

Windspeed and Stem Displacement vs. Time (r10s4)

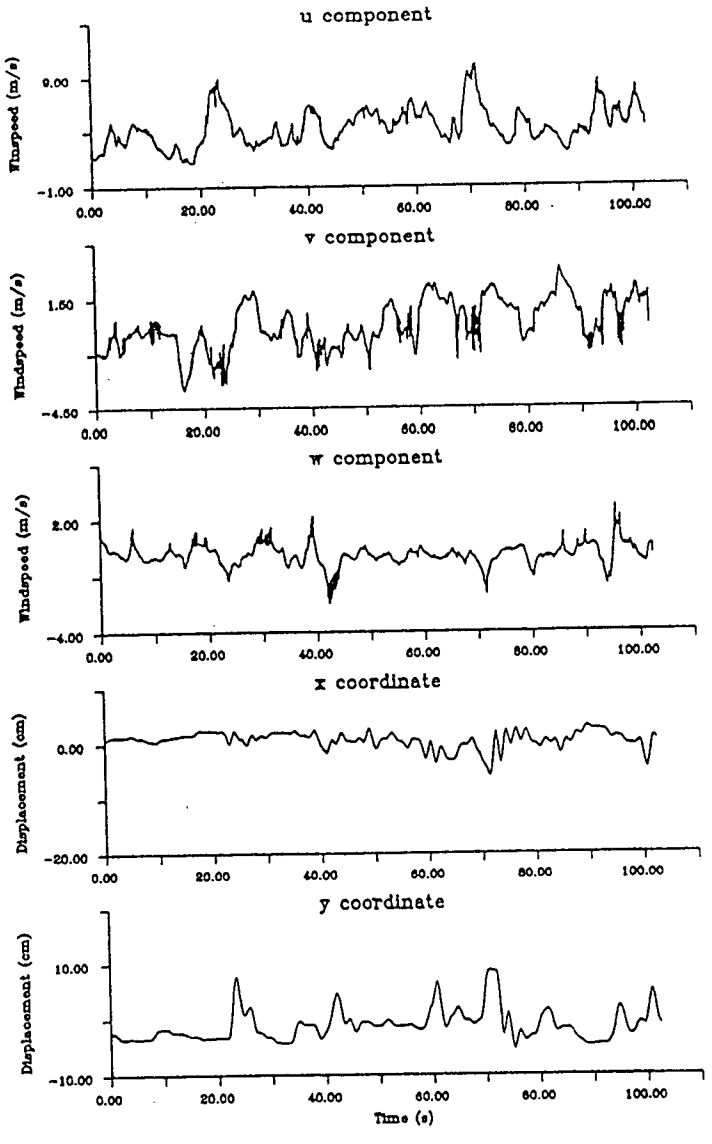

Appendix XVIII Computer program used to determine power spectra from time series data

Filename: SPECTRA

Language: Fortran

```
C     ------------------------------------------------------------------------------
C     Power spectrum program
C     ------------------------------------------------------------------------------

REAL*8 U(20000), UBAR, S2, S3, S4, WT(20000), UMIN, UMAX, WTSUM,
     * PX, PW, STA(4), UG(40000), ASP(20000), SR

INTEGER N, NANEMO, NCHAR, CHAN, IFAIL, KC, L, LG, MTX, MW, NX, VDU,
     * IOERR, NFLAG

      CHARACTER INFILE*21, OUTFILE*21, ANS*1

LOGICAL KEEPON

      IOERR = 0
200   FORMAT(A)
300   Call emas3prompt ('Enter filename containing time series: ')
      READ (5,200) infile
      OPEN (7,file = infile, status ='old', iostat  = inerr)
      IF (inerr.GT.0) THEN
      WRITE (6,*) 'File does not exist, try again'
      GOTO 300
      endIF

C     Set sample rate
      Call emas3prompt ('What was the sample rate (Hz)?: ')
      READ (5,*) sr

C     Read in data sets as a single column of velocities
      I = 1
      KEEPON = . TRUE.
      DO WHILE(KEEPON)
      READ (7,*,END=20) U(I)
      I = I + 1
      GOTO 30
20    KEEPON=. FALSE.
30    CONTINUE
      END DO
      N = I - 1
      WRITE (6,*) 'Number of raw data points = ', N

C     Calculate velocity statistics
      IFAIL = 1
      IWT = 0
```

```
      Call G01AAF(N, U, IWT, WT, UBAR, S2, S3, S4, UMIN, UMAX,
     * WTSUM, IFAIL)

      WRITE (6,301) UBAR, S2
      WRITE (6,302) S3, S4
301   FORMAT (1X, 'Mean = ', F8.2, ';Std. Devn =', F8.2)
302   FORMAT ('Skewness = ', F8.2,'; Kurtosis = ', F8.2)

C     Calculate power spectrum
DO 40 I = 1, N
      UG(I) = U(I) - UBAR
      UG(N+I) = 0.0
40    CONTINUE

C     Set parameters for call to routine G13CBF
      NX = 1024
      MTX = 1
      PXY = 0.10

C     Zero smoothing
      MW = NX

C     KC and L are order of FFT and frequency divicion of smoothed spectral
C     estimates as 2*PI/L
      KC = 4*N
      L = N
      IFAIL = 1

      Call G13CBF (N, MTX, PX, MW, PW, L, KC, LG, UG,
     * NG, STA, IFAIL)
      IF (IFAIL.EQ.0) GOTO 400
      WRITE (6,99400) IFAIL, INFILE
      GOTO 420

400 DO 410 I = 1, NG
      ASP(I) = UG(I)
      WRITE (6,99410) INFILE

      WRITE (6,*) 'Do you want the estimates of the spectral densities'
      Call emas3prompt ('Normalized by frequency/variance')
      READ (5,200) ANS

      IF (ANS.EQ.'Y'.OR.ANS.EQ.'y') THEN
      NFLAG = 1
      endIF
      IF (ANS.EQ.'N'.OR.ANS.EQ.'n') THEN
      NFLAG = 0
      endIF
```

```
C       Put results into an output file
        Call emas3prompt ('What is the name of the output file?: ')
        READ (5,200) OUTFILE
        OPEN (8, file = outfile, filetype = 'c')
        WRITE (8,99420) UBAR, S2, S3, S4


DO 1100  I  = 2, NG
        F  = REAL(I-1)*SR/REAL(L)
        IF (NFLAG.EQ.1) THEN
        IF (NFLAG.EQ.0) GOTO 1100
        ASP(I) = ASP(I)*F/(S2*S3)
        endIF


1100    WRITE (8,99420) F, ASP(I)


99400   FORMAT (SP, 'IFAIL = ',I2,' FAILED FOR: ',21A)
99410   FORMAT (SP,' Spectral estimate complete for: ',21A)
99420   FORMAT (1X,  7F10.5)
420     CONTINUE
        END
```

Appendix XIX Computer program used to determine the cross spectrum of Reynolds Stress

Filename: COSPECTRA

Language: Fortran

```
C     ------------------------------------------------------------------
C     Cross-spectru program
C     ------------------------------------------------------------------

REAL*8 U(20000), UBAR, S2, S3, S4, WT(20000), UMIN, UMAX, WTSUM,
     * W(20000), WBAR, WMIN, WMAX, ASP2(20000), WG(40000),
     * PX, PXY, PW, STA(4), UG(40000), ASP(20000), SR

INTEGER NXY, NANEMO, NCHAR, CHAN, IFAIL, KC, L, LG, MW, VDU,
     * IOERR, NFLAG, I, IS, J, MTXY, NG

      CHARACTER INFILE*21, OUTFILE*21, ANS*1

LOGICAL KEEPON

      IOERR = 0
200   FORMAT(A)
300   Call emas3prompt ('Enter filename containing time series: ')
      READ (5,200) infile
      OPEN (7,file = infile, status ='old', iostat  = inerr)
      IF (inerr.GT.0) THEN
      WRITE (6,*) 'File does not exist, try again'
      GOTO 300
      endIF

C     Set sample rate
      Call emas3prompt ('What was the sample rate (Hz)?: ')
      READ (5,*) sr

C     Read in data sets as a single column of velocities
      I = 1
25    READ (7,*) U(I), W(I)
      IF (I.EQ.1024) GOTO 30
      I = I + 1
      GOTO 25
30    NXY = I
      WRITE (6,*) 'Number of raw data points = ', NXY

C     Calculate velocity statistics
      IFAIL = 1
      IWT = 0
      Call G01AAF(NXY, U, IWT, WT, UBAR, S2, S3, S4, UMIN, UMAX,
     * WTSUM, IFAIL)
```

```
      WRITE (6,301) UBAR, S2
      WRITE (6,302) S3, S4
301   FORMAT (1X, 'Mean = ', F8.2, ';Std. Devn =', F8.2)
302   FORMAT ('Skewness = ', F8.2,'; Kurtosis = ', F8.2)

C     Calculate W Velocity Statistics
      IFAIL = 1
      IWT = 0
      Call G01AAF (NXY, W, IWT, WT, WBAR, S2, S3, S4, WMIN, WMAX,
     * WTSUM, IFAIL)
      WRITE (6,301) WBAR, S2
      WRITE (6,302) S3, S4

C     Calculate cross-spectrum
DO 40 I = 1, NXY
      UG(I) = U(I) - UBAR
      WG(I) = W(I) - WBAR
      UG(NXY+I) = 0.0
      WG(NXY+1) = 0.0
40    CONTINUE

C     Set parameters for call to routine G13CDF
      MTXY = 1
      PXY = 0.10

C     Zero smoothing
      MW = NXY
      PW = 1.0
      IS = 0

C     KC and L are order of FFT and frequency divicion of smoothed spectral
C     estimates as 2*PI/L
      KC = 4*NXY
      L = NXY
      IFAIL = -1

      WRITE (6,*) NXY, MTXY, PXY, MW, PW, L, IS
      Call G13CDF (NXY, MTXY, PXY, MW, IS, PW, L, KC, UG, WG,
     * NG, IFAIL)
      IF (IFAIL.EQ.0) GOTO 400
      WRITE (6,99400) IFAIL, INFILE
      GOTO 420

400 DO 410  I = 1, NG
      ASP(I) = UG(I)
      ASP2(I) = WG(I)
      WRITE (6,99410) INFILE

      WRITE (6,*) 'Do you want the estimates of the spectral densities'
      Call emas3prompt ('Normalized by frequency/variance')
      READ (5,200) ANS
```

```
      IF (ANS.EQ.'Y'.OR.ANS.EQ.'y') THEN
      NFLAG = 1
      endIF
      IF (ANS.EQ.'N'.OR.ANS.EQ.'n') THEN
      NFLAG = 0
      endIF

C     Put results into an output file
      Call emas3prompt ('What is the name of the output file?: ')
      READ (5,200) OUTFILE
      OPEN (9, file = outfile, filetype = 'c')
      WRITE (9,99420) UBAR, S2, S3, S4
      WRITE (9,99420) WBAR, S2, S3, S4

DO 1100  I = 2, NG
      F = REAL(I-1)*SR/REAL(L)
      IF (NFLAG.EQ.1) THEN
      IF (NFLAG.EQ.0) GOTO 1100
      ASP(I) = ASP(I)*F/(S2*S3)
      ASP2(I) = ASP2(I)*F/(S2*S3)
      endIF

1100  WRITE (9,99420) F, ASP(I), ASP2(I)

99420 FORMAT (SP, 'IFAIL = ',I2,' FAILED FOR: ',21A)
99410 FORMAT (SP,' Spectral estimate complete for: ',21A)
420   CONTINUE
      END
```

Appendix XX Power spectra of windspeed, Reynolds stress, mechanical transfer function and stem displacement for both plots
(R4 -7 Unthinned plot, R8 and R10 Thinned plot)

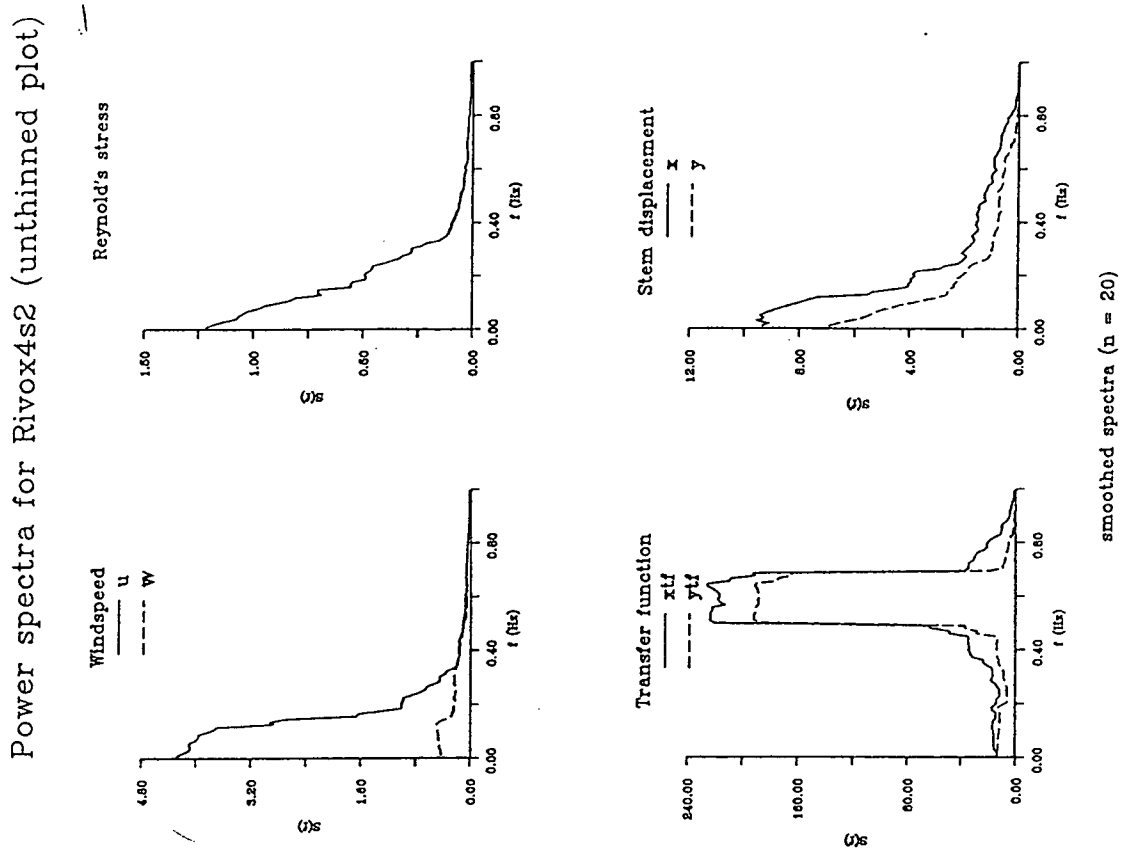

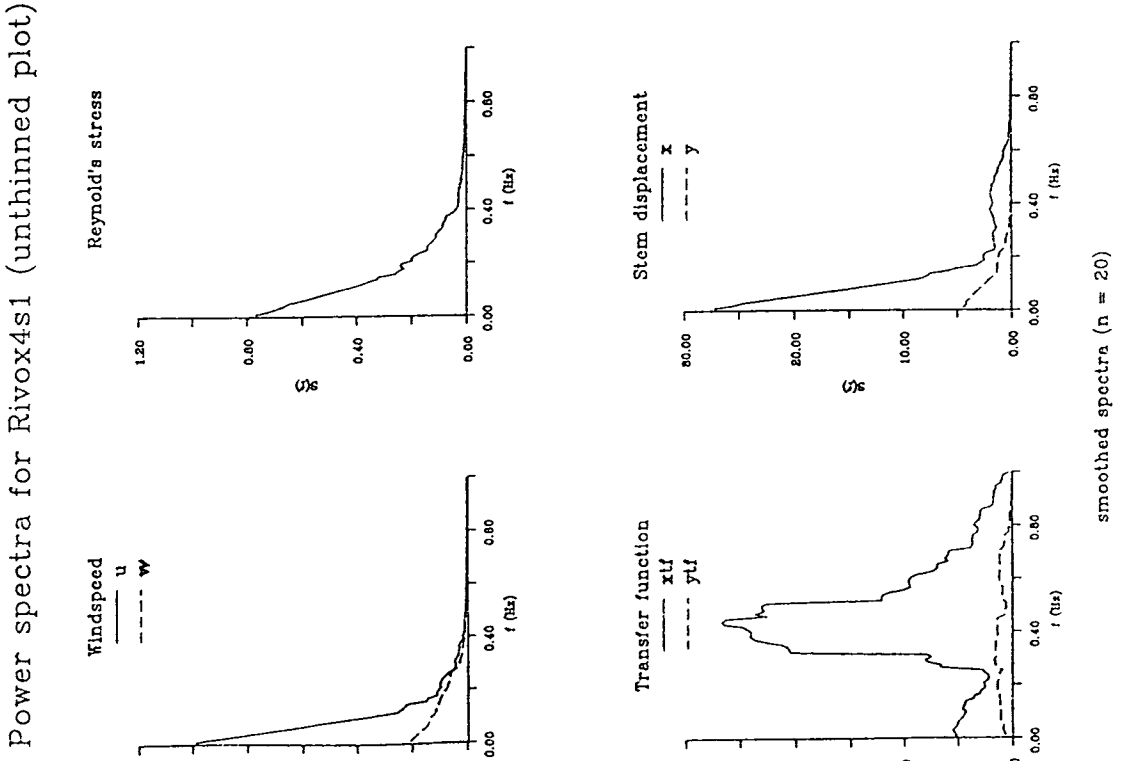

Power spectra for Rivox5s1 (unthinned plot)

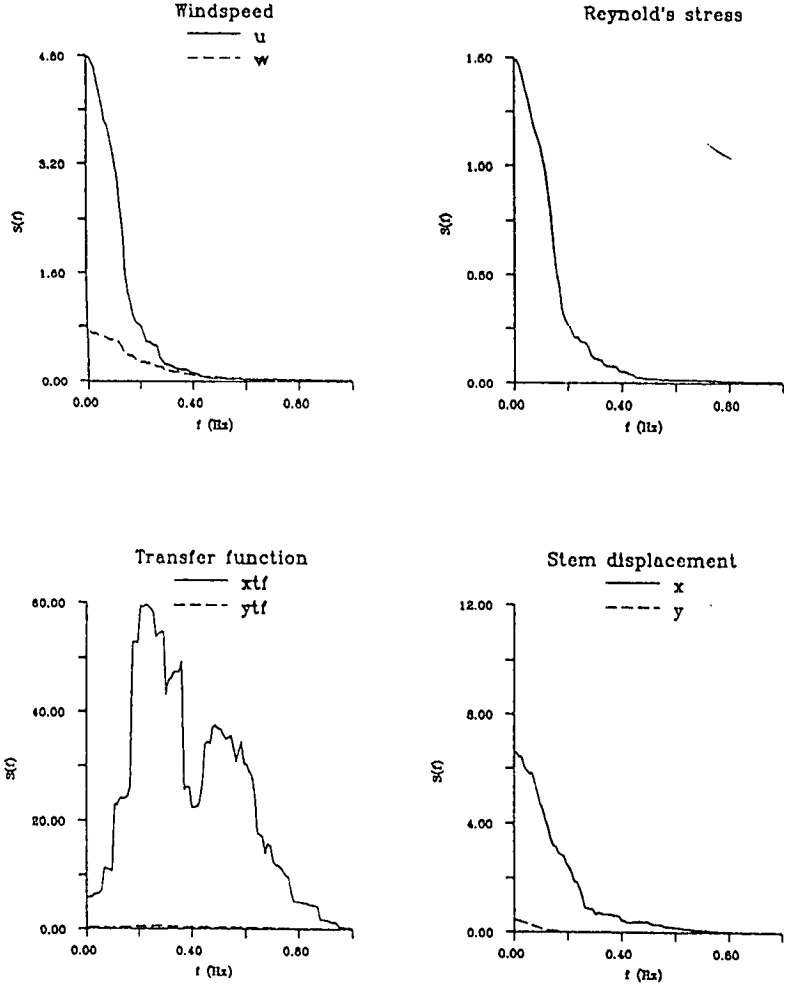

smoothed spectra (n = 20)

Power spectra for Rivox5s2 (unthinned plot)

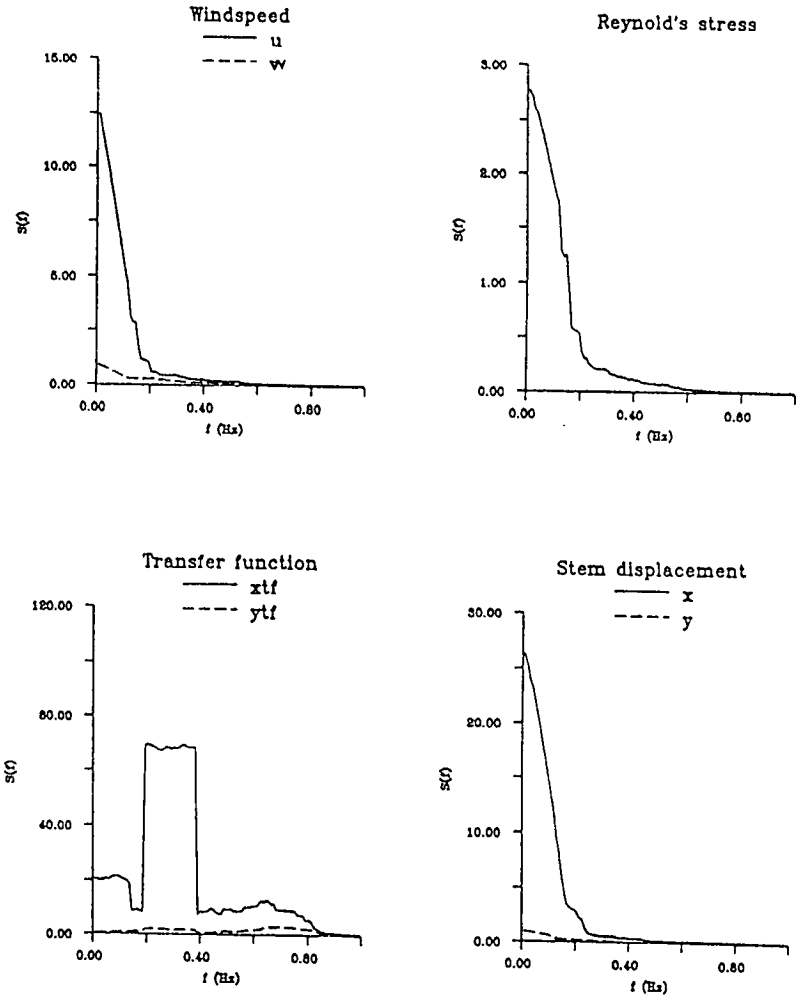

smoothed spectra (n = 20)

Power spectra for Rivox5s3 (unthinned plot)

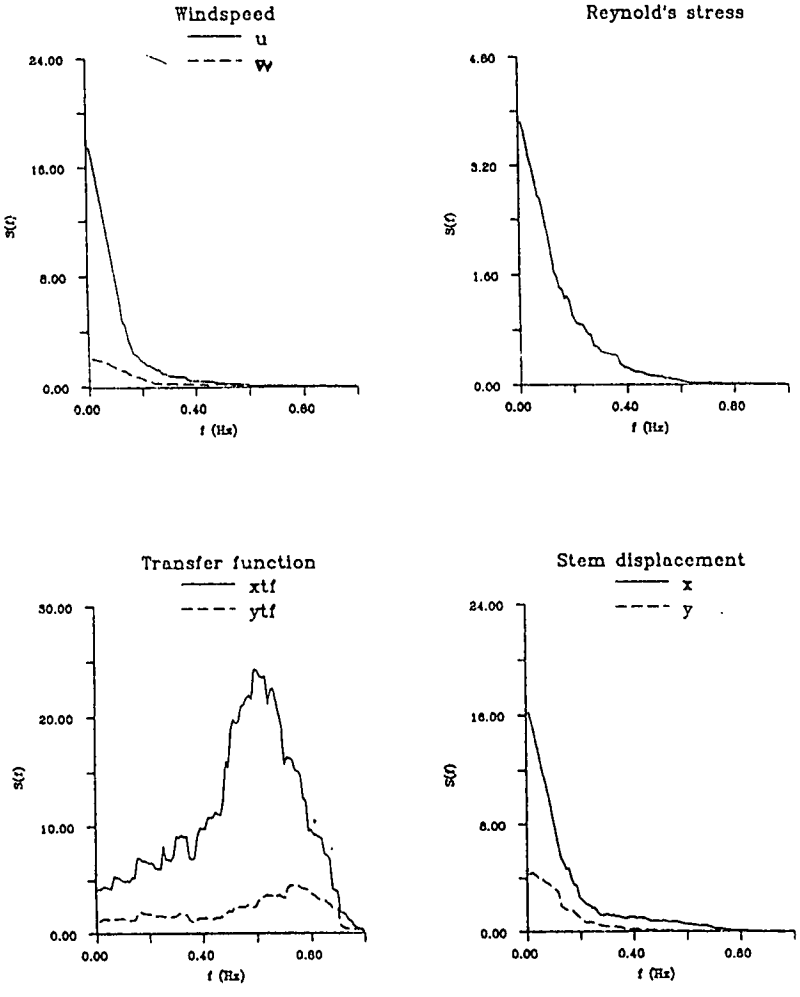

smoothed spectra (n = 20)

Power spectra for Rivox5s4 (unthinned plot)

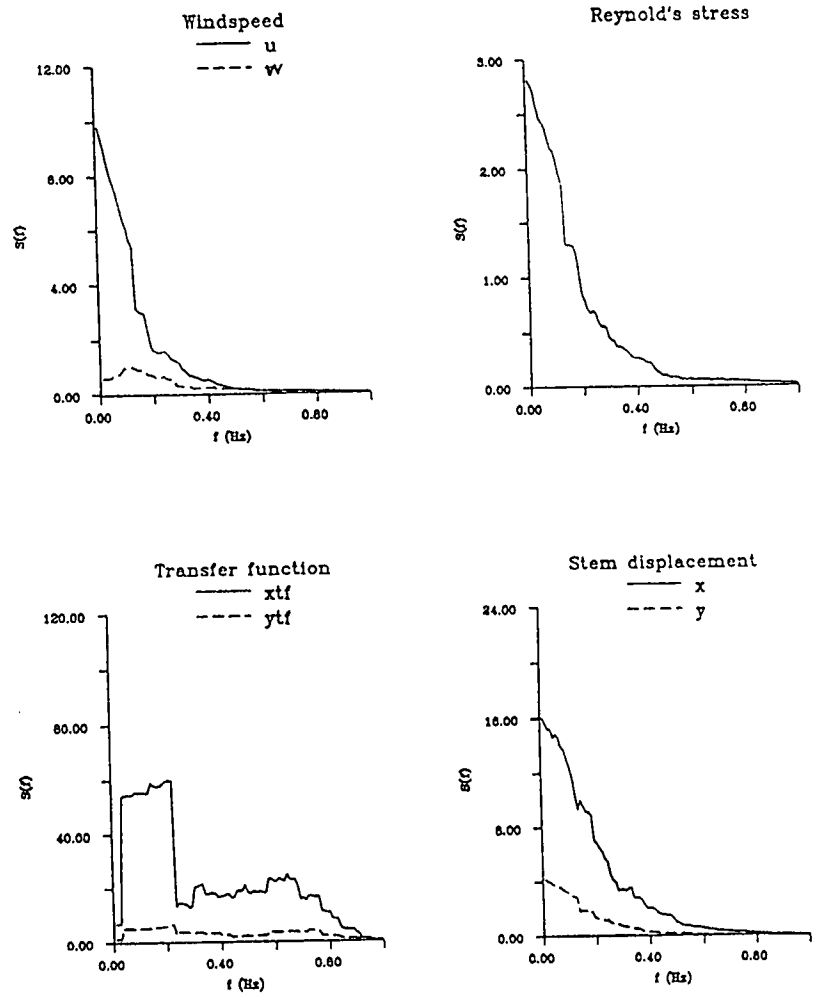

smoothed spectra (n = 20)

Power spectra for Rivox6s1 (unthinned plot)

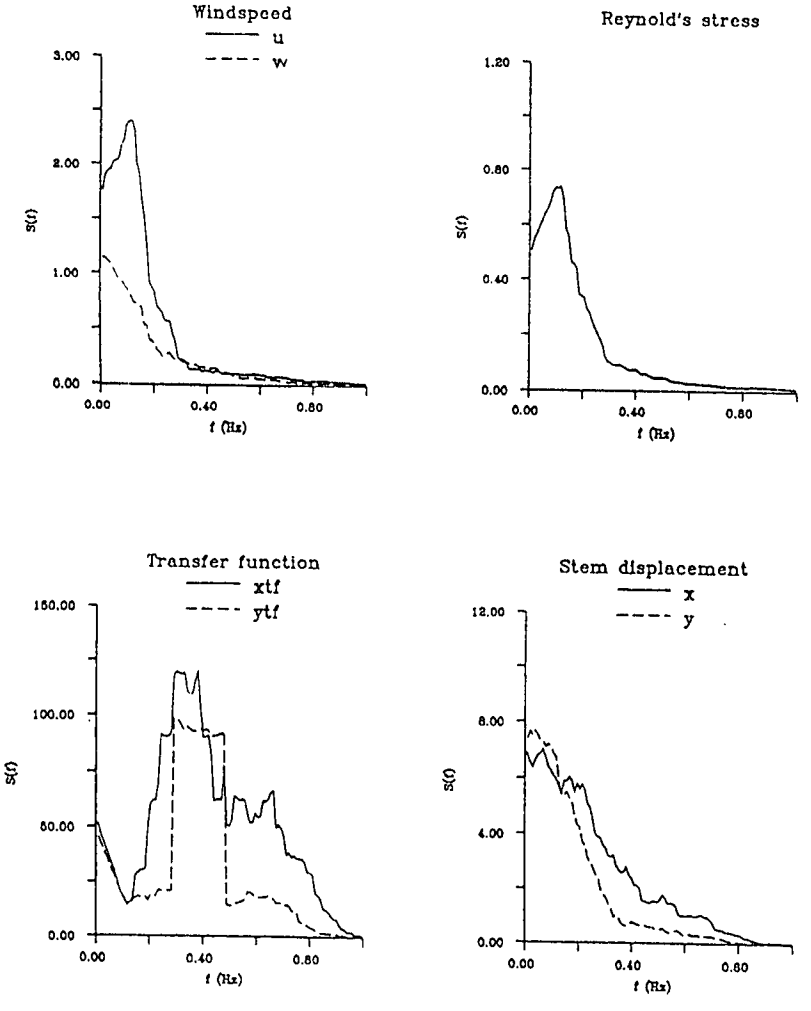

smoothed spectra (n = 20)

Power spectra for Rivox6s2 (unthinned plot)

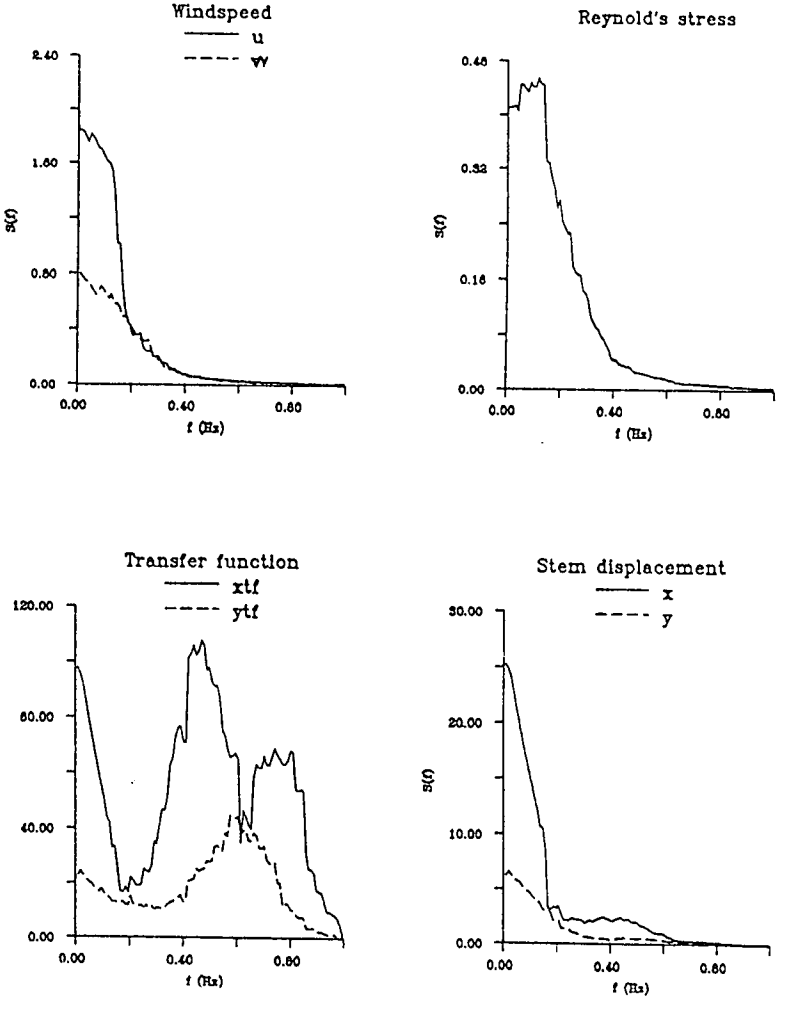

smoothed spectra (n = 20)

Power spectra for Rivox6s3 (unthinned plot)

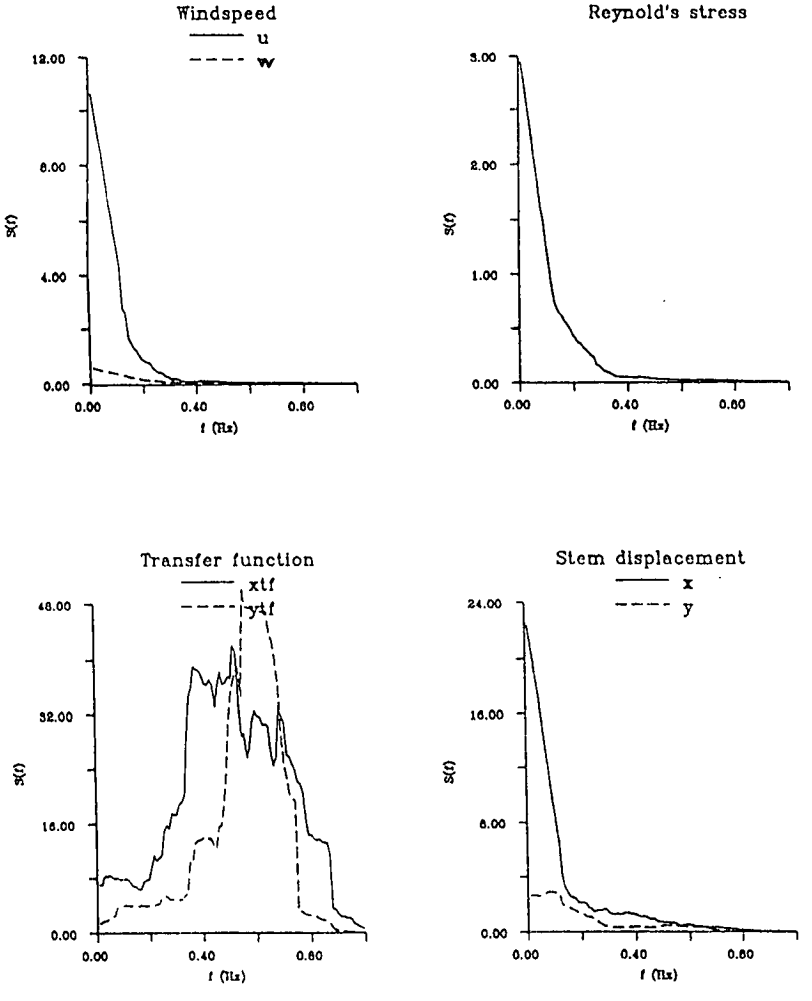

smoothed spectra (n = 20)

Power spectra for Rivox6s4 (unthinned plot)

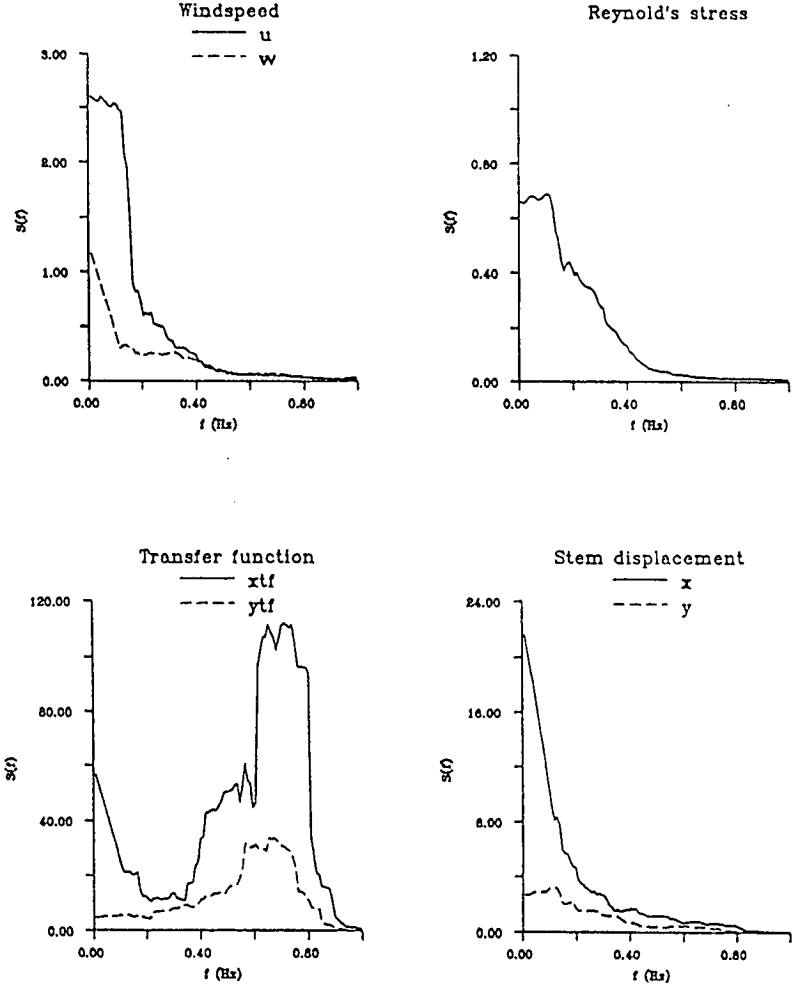

smoothed spectra (n = 20)

Power spectra for Rivox7s1 (unthinned plot)

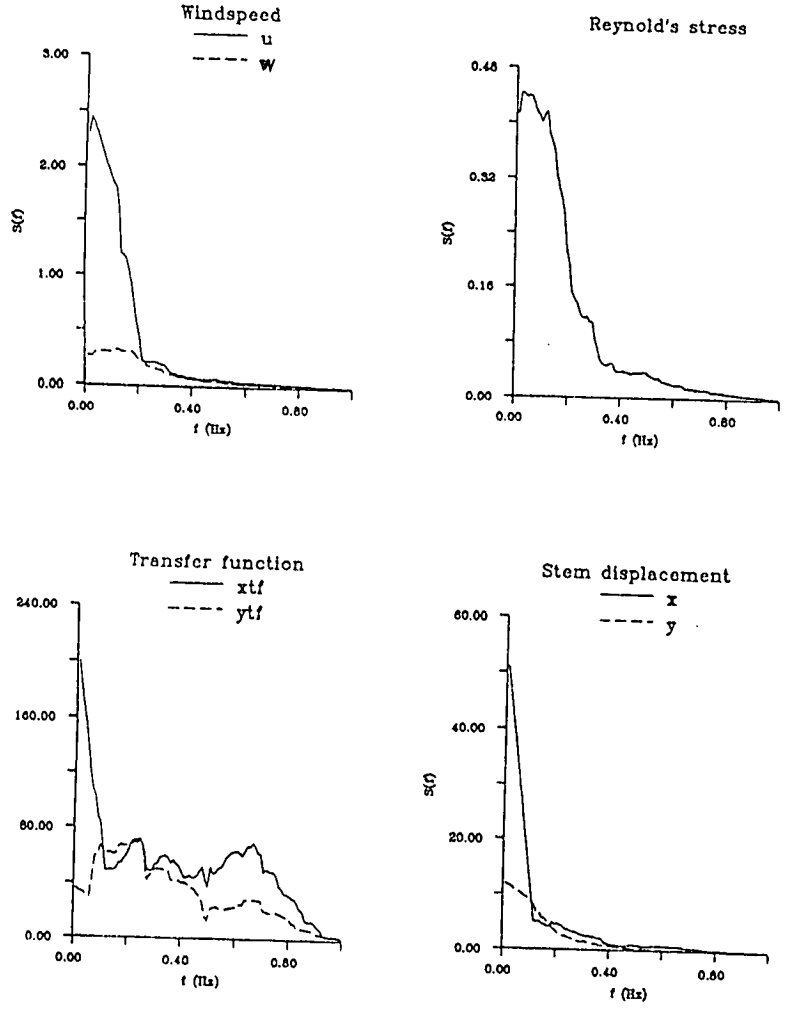

smoothed spectra (n = 20)

Power spectra for Rivox7s2 (unthinned plot)

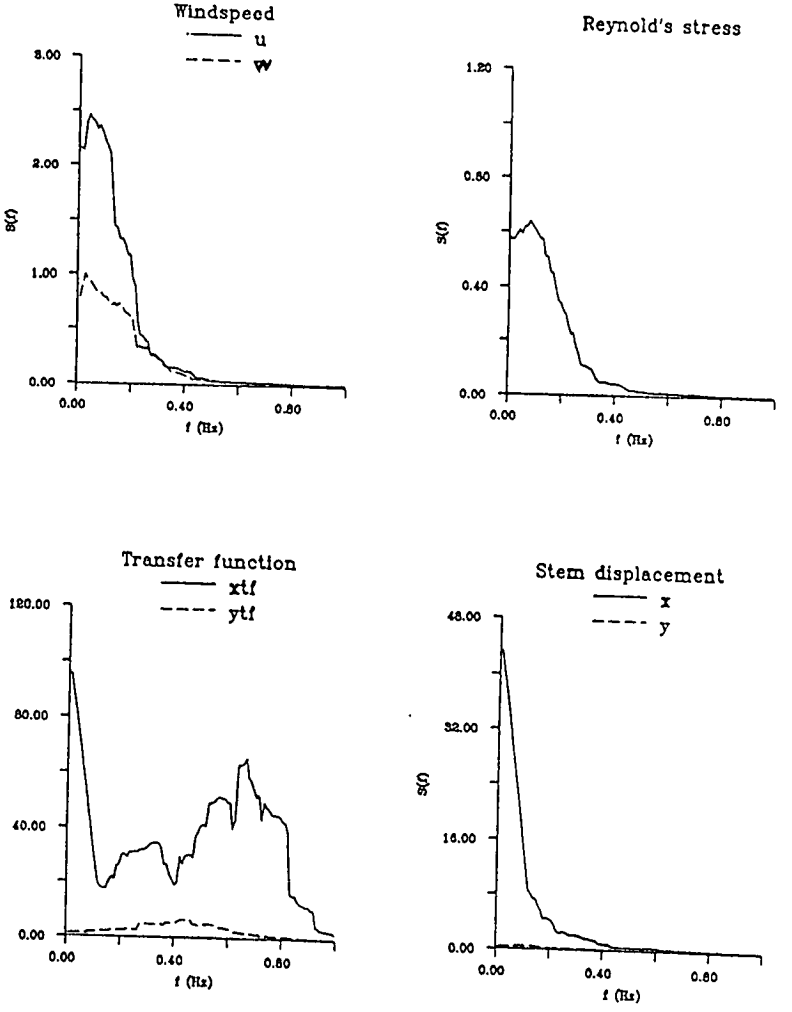

smoothed spectra (n = 20)

Power spectra for Rivox7s3 (unthinned plot)

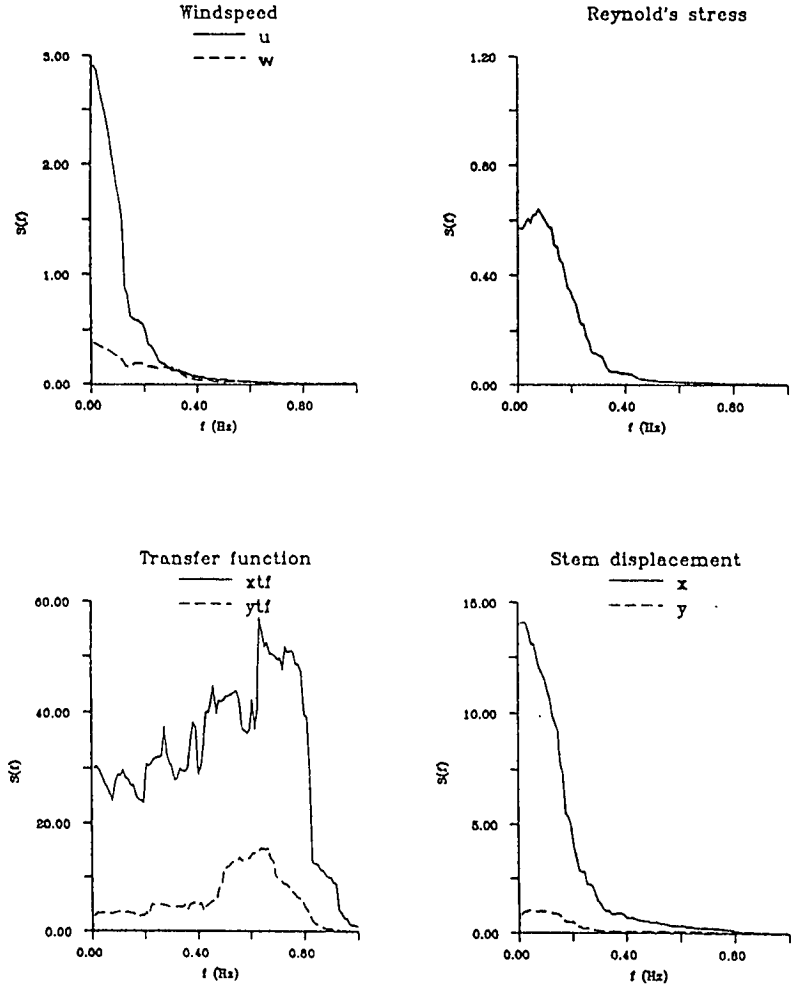

smoothed spectra (n = 20)

Power spectra for Rivox7s4 (unthinned plot)

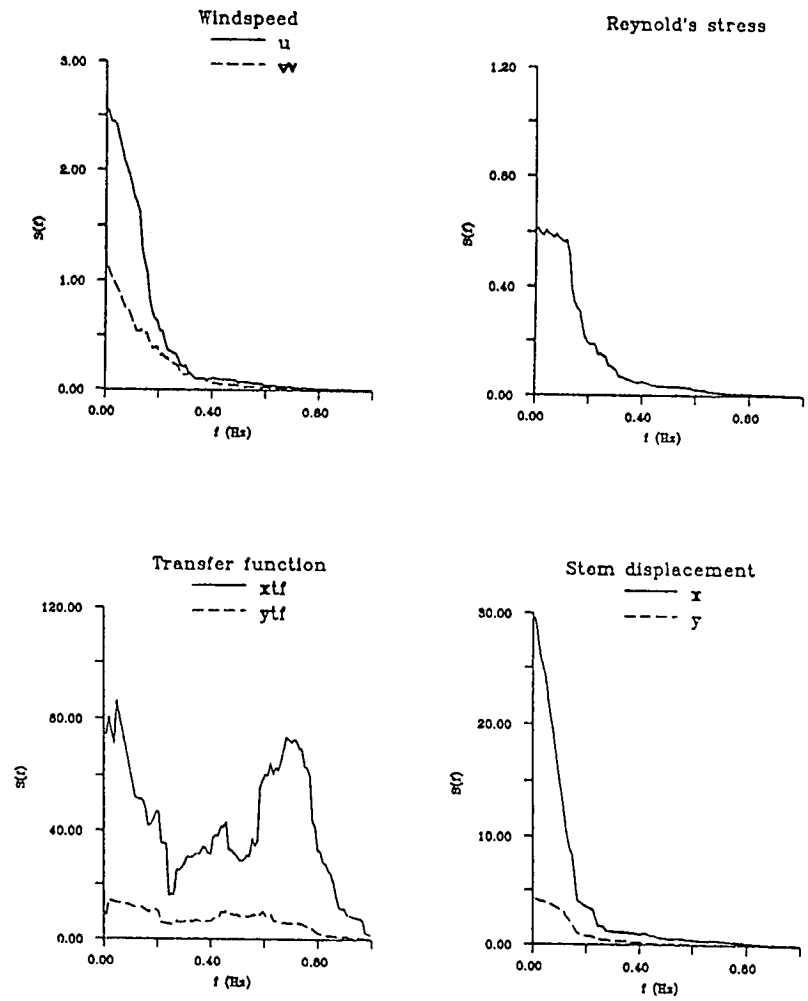

smoothed spectra (n = 20)

Power spectra for Rivox8s1 (thinned plot)

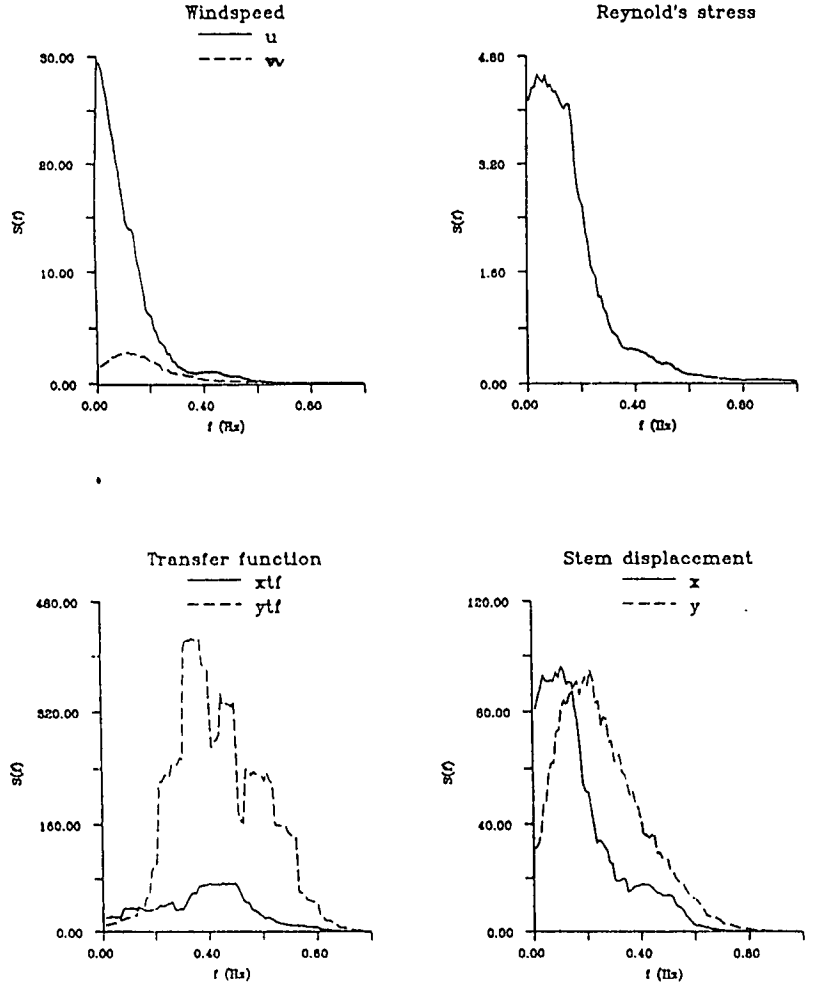

smoothed spectra (n = 20)

Power spectra for Rivox8s2 (thinned plot)

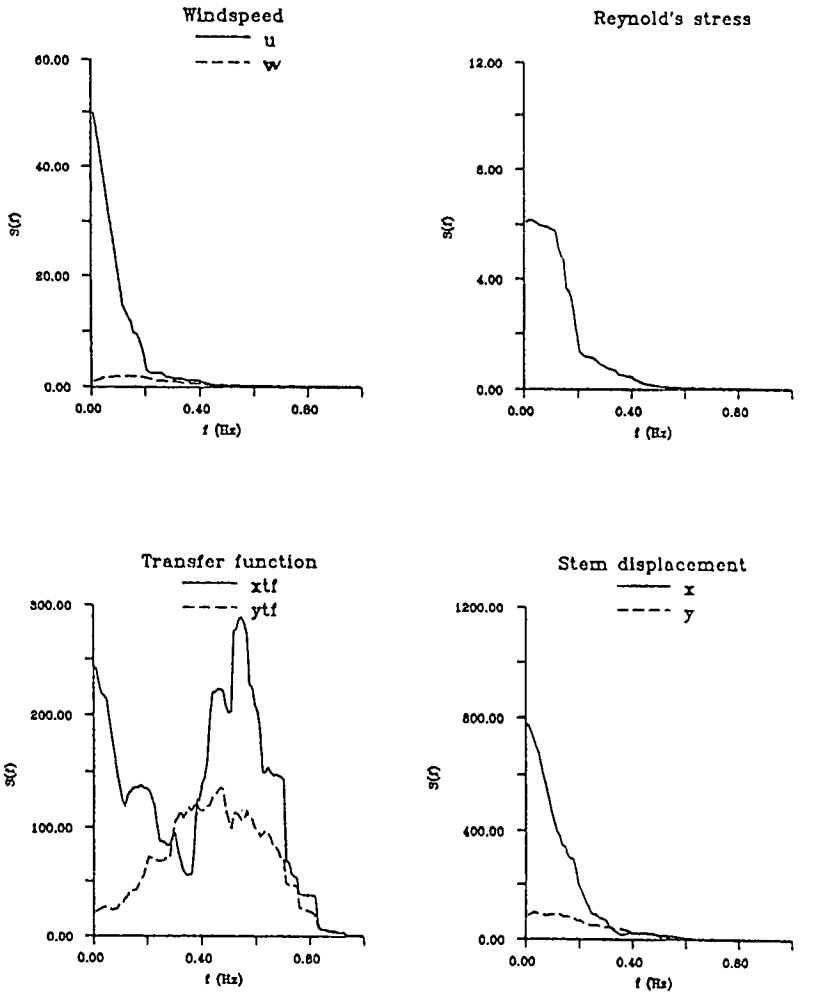

smoothed spectra (n = 20)

Power spectra for Rivox8s3 (thinned plot)

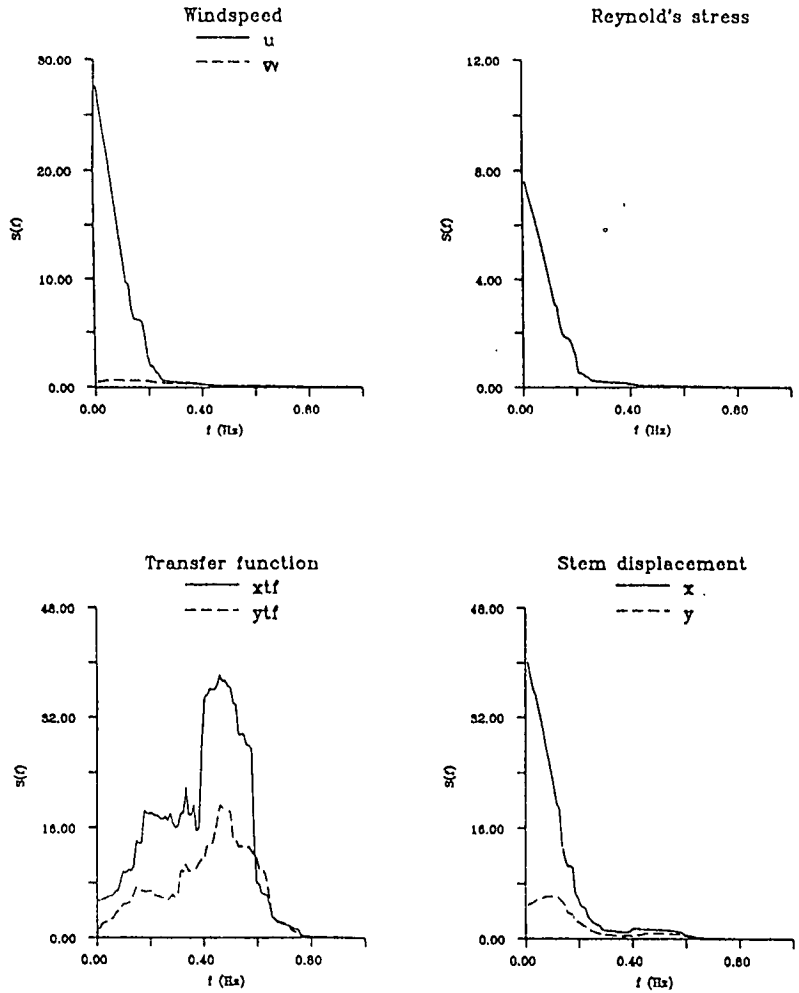

smoothed spectra (n = 20)

Power spectra for Rivox8s4 (thinned plot)

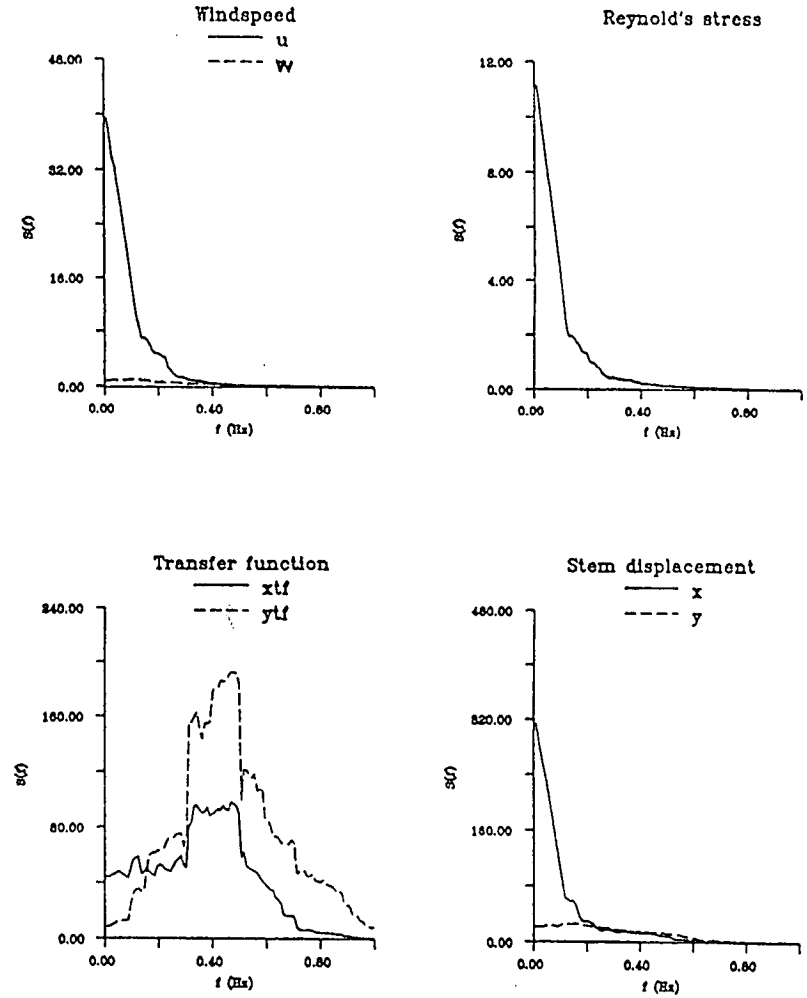

smoothed spectra (n = 20)

Power spectra for Rivox8s5 (thinned plot)

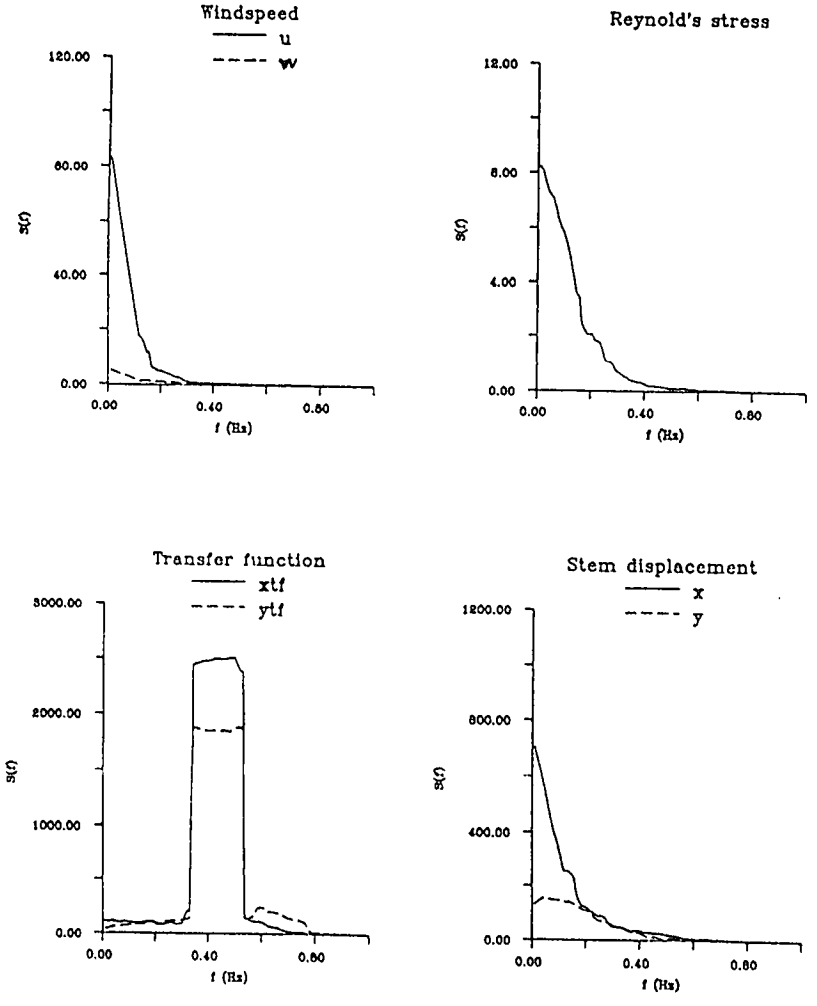

smoothed spectra (n = 20)

Power spectra for Rivox8s6 (thinned plot)

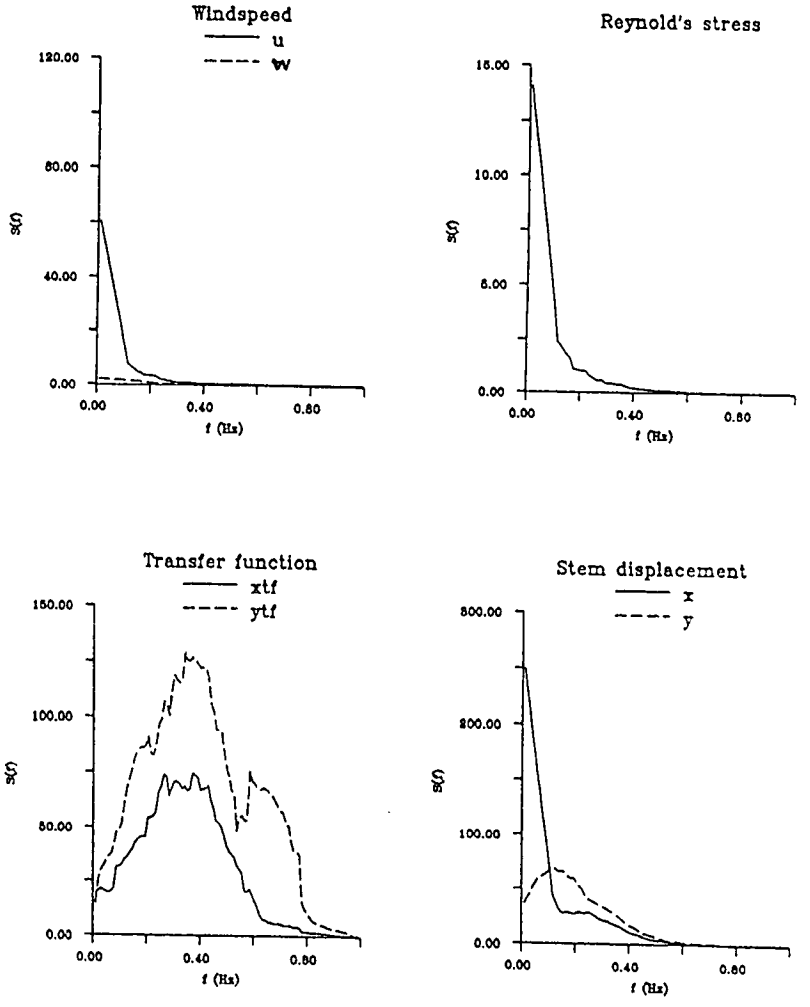

smoothed spectra (n = 20)

Power spectra for Rivox8s7 (thinned plot)

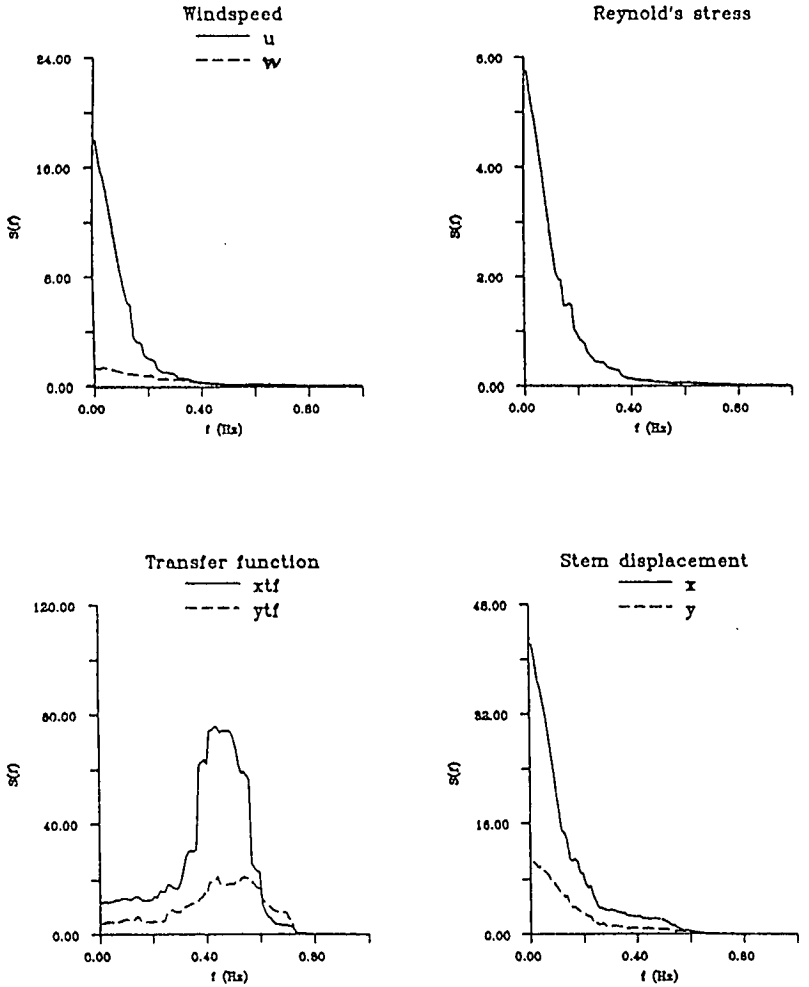

smoothed spectra (n = 20)

Power spectra for Rivox8s8 (thinned plot)

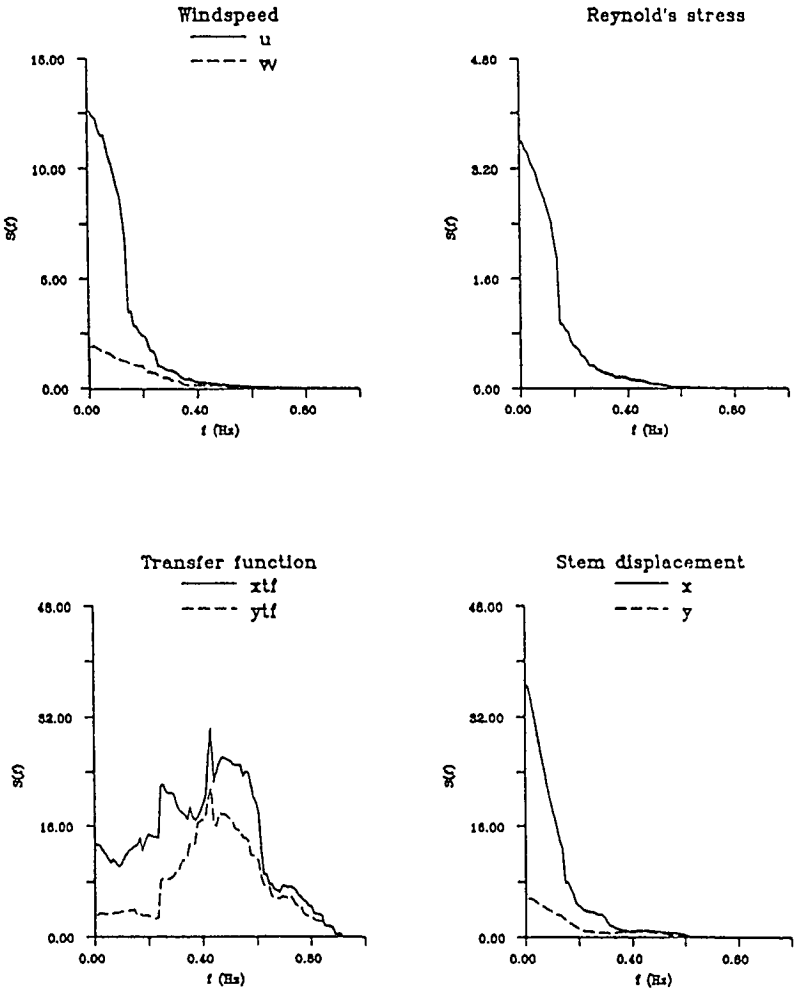

smoothed spectra (n = 20)

Power spectra for Rivox10s1 (thinned plot)

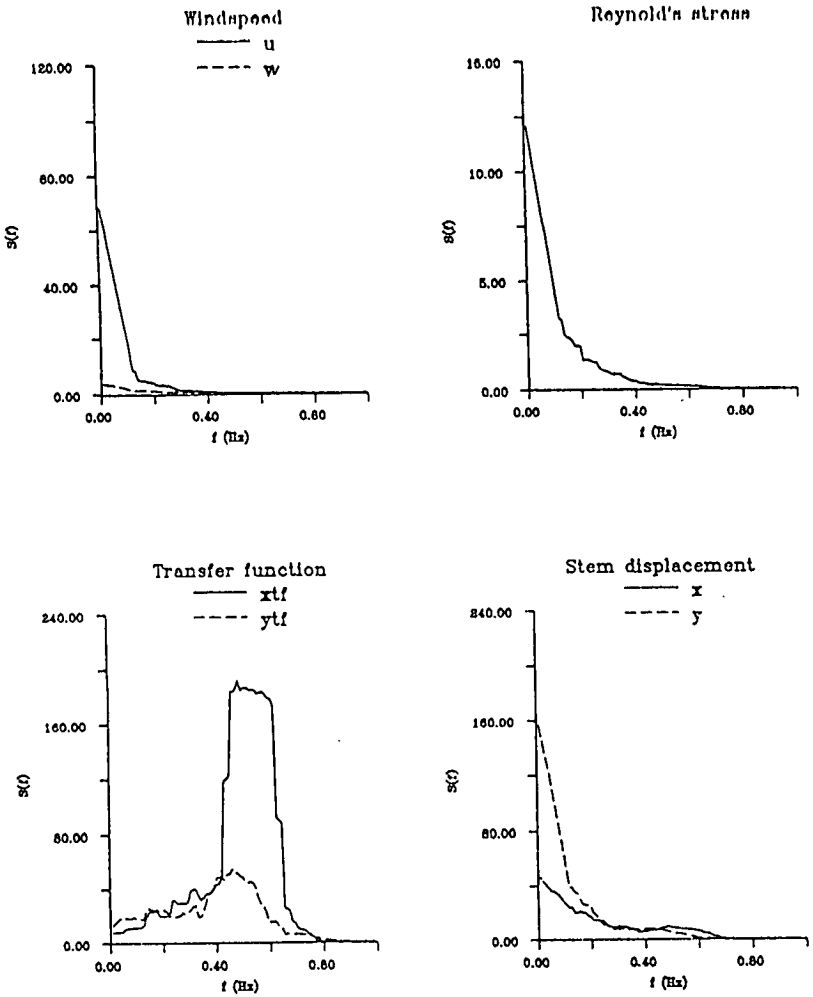

smoothed spectra (n = 20)

Power spectra for Rivox10s2 (thinned plot)

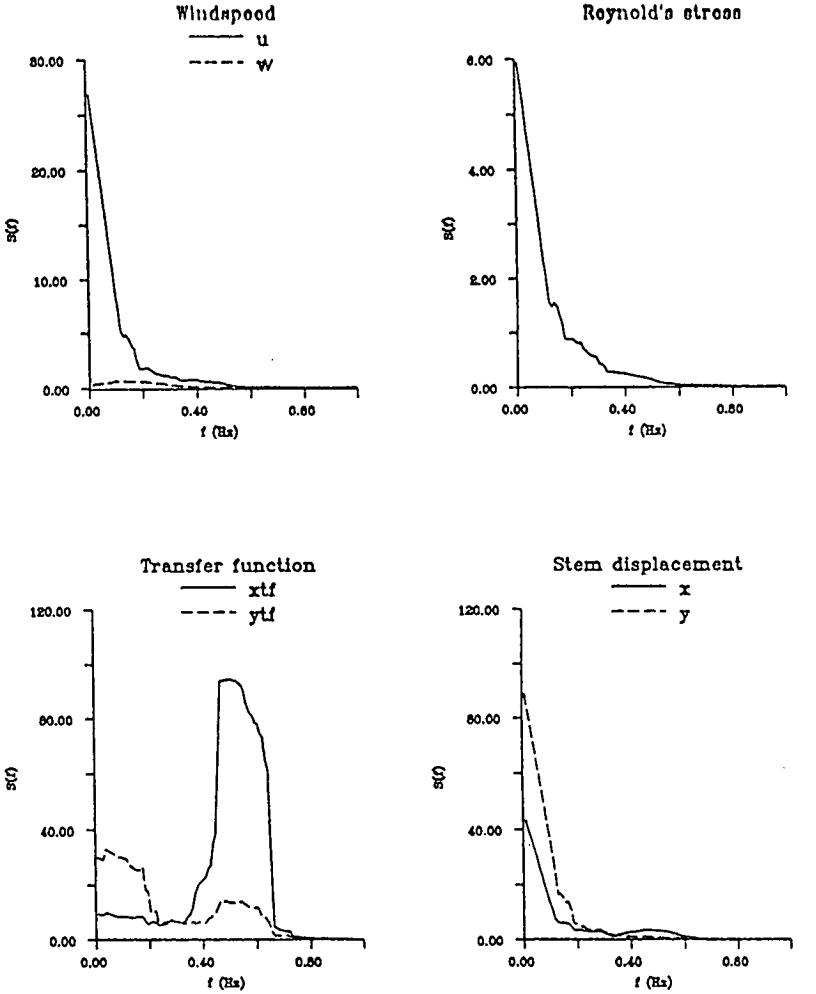

smoothed spectra (n = 20)

Power spectra for Rivox10s3 (thinned plot)

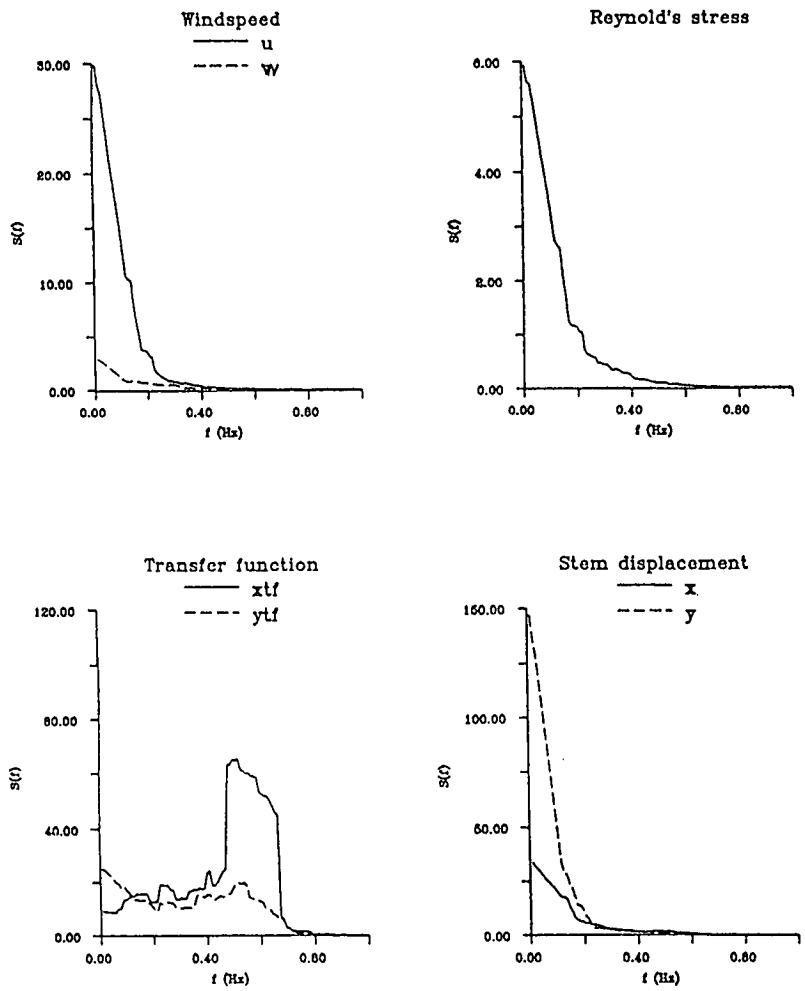

smoothed spectra (n = 20)

Power spectra for Rivox10s4 (thinned plot)

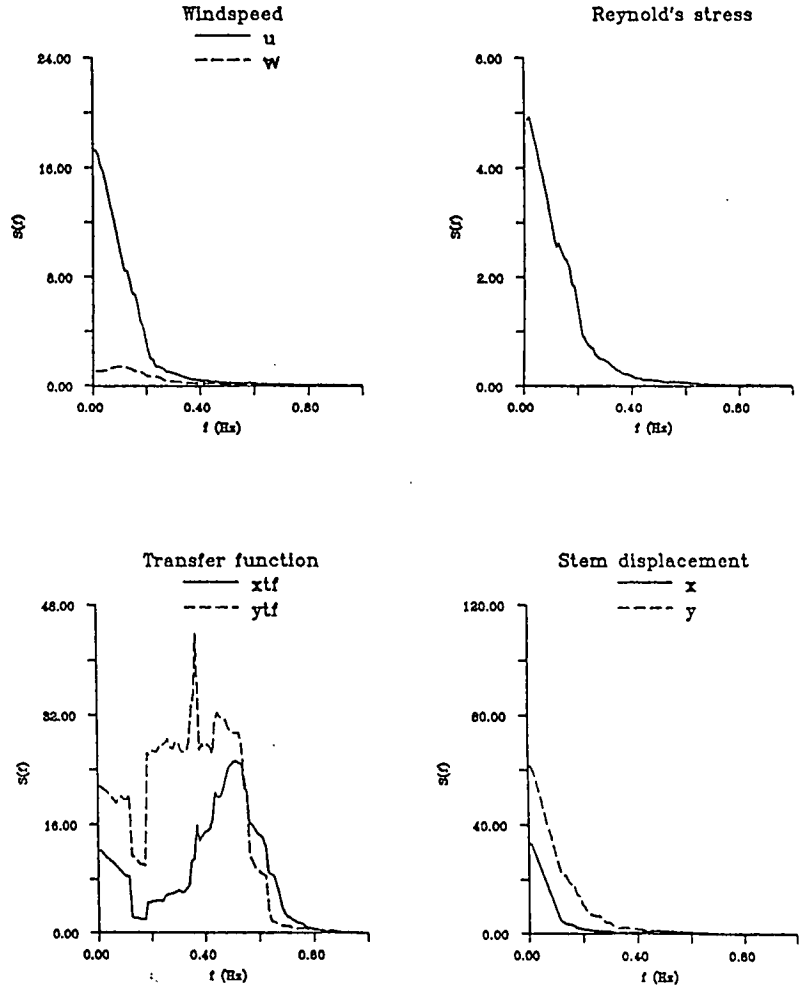

smoothed spectra (n = 20)